D 2023

U.PORTO
FEUP FACULDADE DE ENGENHARIA
UNIVERSIDADE DO PORTO

Nervous Tissue Response To Smart Nanomaterials for Deep Brain Stimulation: studies in In vitro and Ex vivo Brain Models of Different Complexity

MAURIZIO GULINO

TESE DE DOUTORAMENTO APRESENTADA
À FACULDADE DE ENGENHARIA DA UNIVERSIDADE DO PORTO EM
ENGENHARIA BIOMÉDICA

This thesis was supervised by:

-Doctor Ana Paula Pêgo, supervisor

INEB - Instituto de Engenharia Biomédica

i3S - Instituto de Investigação e Inovação em Saúde

ICBAS - Instituto de Ciências Biomédicas Abel Salazar

- Doctor Sofia Duque Santos, co-supervisor

INEB - Instituto de Engenharia Biomédica

i3S - Instituto de Investigação e Inovação em Saúde

The research described in this thesis was conducted at:

Nanobiomaterials for Targeted Therapies, nBTT. INEB-i3S, Instituto de Investigação e Inovação em Saúde, Universidade do Porto, Portugal

MSRL, Multi-scale Robotics Lab, Institute of Robotics and Intelligent Systems (IRIS), ETH Zurich, Zurich, Switzerland

The research described in this thesis was financially supported by:

The European Union's Horizon 2020 Research and Innovation Programme under the Marie Skłodowska-Curie grant agreement No. 764977, in the framework of the mCBEEs project (Advanced integrative solutions to corrosion problems beyond micro-scale: toward long-term durability of miniaturized biomedical, electronic, and energy systems).







ACKNOWLEDGMENTS

I am really happy to have spent these 4 years of work in Portugal: a country that I fell in love with since the beginning, thanks to the lovely and passionate people I had the pleasure to meet. Portugal has many similarities with my country, and I immediately felt at home, and this is thanks to all my wonderful lab mates, which became my real friends and whom I have been really lucky to have met.

First of all, I would like to acknowledge my supervisor Ana Paula Pêgo. During this experience, she has been always available to help me in work and to give me motivation and precious tips to face all the challenges of this Ph.D. It is thanks to her that I have grown as a researcher and if I gained experience in all the facets of this work. Moreover, we also shared a lot of enjoyable moments with all the group members outside the work environment. We participated in several social activities together, and I really appreciated that as it gave me the opportunity to improve my relationships with everyone. I will never thank her enough for this opportunity. I also would like to thank my co-supervisor Sofia Santos, for all the help she gave me in getting familiar with the different work environments, and for all the time and patience she dedicated to teaching new techniques and procedures. She has been always present with great optimism. she always supported me with professionalism, giving me valuable suggestions and making me feel absolutely without pressure.

A very special thank goes to all the members of the nBTT lab, and for all the help that I received since the very first time and for making me feel always welcome and part of this big family. In particular, a big thank goes to Ana Spencer, Eva Carvalho, Beatriz Custodio, Sofia Guimarães. They helped me a lot, and not only in work. We shared a lot of funny moments together and, as I always told them, I will never have desk mates/friends like them. I will always miss them.

Another special thank goes to my scientific and non-scientific friends: Pedro Mota, Paulo Gomes, Joao Cortinhas, Joao Freitas, Meghna Dabour, Emine Kahraman, Andrea Bortolin, Clive Jabangwe, Georgia Athanasapolou, Sara Zarza and many others, for having shared with them unforgettable moments, and several Italian and Portuguese dinners. Without them, this experience wouldn't have been so special. You will always be in my heart.

Finally, I want to thank my brother and my parents. There are no words to describe my gratitude for them. All that I am today, I owe it to them. It's all because of them that I managed to achieve all my

goals. Thank you for the support you gave me and the pride you showed me. Thank you for believing in me, and for having always supported me in my decisions.

And lastly, a very special thanks goes to you, for having always cheered me up, for having always been by my side in all the discouraging and happy moments, and for having been the most beautiful surprise of this journey. A big part of this achievement, I owe to you, Chiara.

ABSTRACT

Deep brain stimulation (DBS) is a rapidly expanding field of research with notable success in the clinics for treating neurological and neurodegenerative dysfunctions. The breakthroughs achieved in the last decades are the result of the contribution of several fields of research, such as neurophysiology, material sciences and brain-machine interface, which allowed to redefine the traditional therapeutic approaches and the design of new implantable microelectrodes with enhanced properties. Despite remarkable advances on improving their performance, target specificity and durability with the use of novel nanomaterials and microfabrication strategies, the process of nervous tissue response and glial scar formation remains a limitation to be further investigated and overcome.

The aim of this thesis was to explore in vitro and ex vivo biological models of increasing complexity for studying the biocompatibility of smart nanomaterials and coatings developed for microelectrode fabrication and the biochemical mechanisms at the basis of the process of nervous tissue response.

In the first part of the project, we explored rodent brain organotypic cultures in physiological and excitotoxic conditions, to mimic a pathological in vivo scenario. To do so, we faced hippocampus organotypic cultures with kainic acid, an agonist of glutamate receptors, which has been largely employed to induce epilepsy ex vivo and in vivo. We employed these organotypic cultures to evaluate the biocompatibility of commercially available sodium citrate-coated platinum nanoparticles (PtNPs, 50 nm). PtNPs have been already proposed as an excellent coating material for chronically implanted biomedical devices, including microelectrodes. We have shown that incubation of the brain slices with PtNPs for up to 24 hours does not severely impact neural cell viability in physiological and pathological conditions. Despite the overall biocompatibility, PtNPs were found to cause microglial cell activation and induce morphological alterations with cells acquiring an ameboid shape with loss of ramifications. Nevertheless, this did not worsen the tissue response to the PtNPs in the neuropathological induced scenario.

As second and related objective of the thesis, we have explored a novel coating of cobalt ferrite nanoparticles (CFO) with calcium/zirconium-doped barium titanate (CFO-BCZT) for non-invasive DBS in a collaborative work with our partners from the Multi-Scale Robotic Lab (MSRL-ETH Zurich). Magnetoelectric nanoparticles have already shown in vivo, to be a promising tool capable of

modulating neural circuits in a non-invasive way compared to traditional DBS approaches. The proposed nanoparticles exhibit magnetoelectric properties as a result of the coating of the CFO ferromagnetic core with a piezoelectric BCZT shell. In this study we first employed rodent primary cortical neurons and glial cell (microglia and astrocytes) cultures and exposed them for 24 hours to different concentrations of the developed materials, together with uncoated CFO nanoparticles and CFO nanoparticles coated with bismuth ferrite (BFO) for comparison. The latter is the most widely studied multiferroic coating material. Then, the impact of the nanoparticles on cell viability was evaluated through cytotoxicity assays, and cellular uptake by microscopy analysis. Our results show that astrocytes and neuronal cell viability was not affected after 24-hour exposure to the different nanoparticles, even when administered at high concentrations (100 μg/ml), while primary microglial cells' viability was significantly compromised when treated with CFO-BFO nanoparticles at these high concentrations. Uncoated CFO nanoparticles caused significant microglial cell shrinkage and detachment, while no effects were observed with CFONBCZT nanoparticles. Similarly, in organotypic hippocampal cultures, we reported microglial cell activation after 14 days of contact with CFO-BFO nanoparticles, characterized by a significant increase in Ionized calcium-binding adapter molecule 1 (IBA-1) fluorescence intensity and morphological alterations towards ameboid shape, while negligible effects were observed with CFO-BCZT and uncoated CFO nanoparticles. Subsequently, we also evaluated for the first time the behavior and impact of CFO-BCZT nanoparticles' motion through the brain tissue. Our results show that the application of a magnetic plate at the bottom of the brain slices for 30 minutes has resulted in magnetoelectric nanoparticles motion, occurring 30-40 um through the tissue, without causing any impact in tissue viability and cellular integrity after 24 hours. Preliminary works employing human SH-SY5Y neuronal cell lines showed that CFO-BCZT nanoparticles can induce neural differentiation when under magnetic stimulation. Overall, our novel CFO-BCZT nanoparticles have been shown to display excellent long-term biocompatibility, safety of motion through the brain tissue as well as successful neuronal electrical stimulation under magnetic field exposure. Owing to these characteristics, CFO-BCZT nanoparticles represent valuable candidates for minimally invasive DBS.

The presented works highlight the importance of using reliable and biological model systems with increasing complexity to satisfy the need for testing a constantly growing number of materials and coatings for neurostimulation devices. In these circumstances, relevant biological in vitro/ex vivo platforms constitute essential tools to accelerate the preclinical phase of material development before

clinical trials. We have in fact shown, throughout this work, the versatility of brain organotypic cultures as valuable tools to investigate the cytotoxicity of metallic nanoparticles in the central nervous tissue both in physiological conditions, as well as in the context of a pathologic scenario. Moreover, organotypic hippocampal cultures constitute a promising biological model for evaluating magnetoelectric nanoparticles' performance and impact on the brain tissue in terms of motion and neuronal electrical stimulation.

Additionally, these culture systems constitute an excellent tool to reduce the number of animal use and animal suffering, in compliance with the 3R's from Russell and Burch.

Finally, this work provides additional comprehension on the effects that certain metallic nanoparticles and smart nanomaterials with notable relevance display on the main effectors of the nervous tissue response and glial scar formation in the brain tissue. This is important considering the existent interest of the scientific community in exploring these materials and their promising application in the development of the next generations of smart microelectrodes for DBS.

RESUMO

A estimulação cerebral profunda (ECP) é um campo de investigação em rápida expansão, com notável sucesso na clínica relativa ao tratamento de disfunções neurológicas e neurodegenerativas. Os avanços alcançados nas últimas décadas são o resultado do contributo de várias áreas de investigação, como a neurofisiologia, as ciências dos materiais e a interface cérebro-máquina, que permitiram redefinir as abordagens terapêuticas tradicionais e o desenho de novos microeletrodos implantáveis com propriedades melhoradas. Apesar dos notáveis avanços na melhoria do seu desempenho, especificidade de alvo e durabilidade com o uso de novos nanomateriais e estratégias de microfabricação, o mecanismo de resposta do tecido nervoso e a formação de cicatriz glial continua como uma limitação a ser mais investigada e superada.

O objetivo desta tese foi explorar modelos biológicos in vitro e ex vivo com complexidade crescente para estudar a biocompatibilidade de nanomateriais e revestimentos inteligentes desenvolvidos para a fabricação de microeletrodos e os mecanismos bioquímicos na base do processo de resposta do tecido nervoso.

Na primeira parte do projeto, exploramos culturas organotípicas de cérebro de roedores em condições fisiológicas e excitotóxicas, para mimetizar um cenário patológico in vivo. Para isso, incubamos culturas organotípicas de hipocampo com ácido caínico, um agonista dos receptores de glutamato, que tem sido largamente empregado para induzir epilepsia ex vivo e in vivo. Em seguida, usamos este modelo para avaliar a biocompatibilidade de nanopartículas de platina revestidas com citrato de sódio, disponíveis comercialmente (PtNPs, 50 nm). As PtNPs foram já propostas como excelente material de revestimento para dispositivos biomédicos implantados cronicamente, incluindo microeletrodos. Mostramos que a incubação dos explantes de cérebro com PtNPs até 24 horas não afeta severamente a viabilidade das células neurais em condições fisiológicas e patológicas. Apesar da biocompatibilidade geral, verificou-se que as PtNPs causam ativação de células microgliais e induzem alterações morfológicas com células adquirindo uma forma ameboide com perda de ramificações. No entanto, isso não piorou a resposta do tecido no cenário neuropatológico induzido.

Como segundo e relacionado objetivo da tese, exploramos um novo revestimento de nanopartículas de ferrita de cobalto (CFO) com titanato de bário dopado com cálcio/zircónio (CFO-BCZT) para ECP não invasivo em um trabalho colaborativo com nossos parceiros da Multi -Scale Robotic Lab (MSRL-ETH Zurich). As nanopartículas magnetoelétricas já demonstraram in vivo, ser uma ferramenta promissora

capaz de modular circuitos neurais de forma não invasiva em comparação com as abordagens DBS tradicionais. As nanopartículas propostas exibem propriedades magnetoelétricas como resultado do revestimento do núcleo ferromagnético CFO com um invólucro piezoelétrico BCZT. Neste estudo, primeiro empregamos neurónios corticais primários de roedores e culturas de células gliais (micróglia e astrócitos) e os expusemos durante 24 horas a diferentes concentrações dos materiais desenvolvidos, juntamente com nanopartículas de CFO não revestidas e nanopartículas de CFO revestidas com ferrita de bismuto (BFO) para comparação. Este último é o material de revestimento multiferróico mais amplamente estudado. Em seguida, o impacto das nanopartículas na viabilidade celular foi avaliado por meio de ensaios de citotoxicidade, e a internalização celular por análise de microscopia. Nossos resultados mostram que a viabilidade dos astrócitos e das células neuronais não foi afetada após 24 horas de exposição às diferentes nanopartículas, mesmo em altas concentrações (100 μg/ml), enquanto que a viabilidade das células microgliais primárias foi significativamente comprometida quando tratadas com nanopartículas de CFO-BFO em altas concentrações. As nanopartículas de CFO não revestidas causaram contracção e descolamento significativo das células microgliais, enquanto que nenhum efeito foi observado com nanopartículas de CFO-BCZT. Da mesma forma, em culturas organotípicas de hipocampo, relatamos ativação de células microgliais após 14 dias de contacto com nanopartículas de CFO-BFO, caracterizada por um aumento significativo na intensidade de fluorescência da molécula adaptadora de ligação ao cálcio ionizado 1 (IBA-1) e alterações morfológicas em direção à forma amebóide, enquanto que efeitos insignificantes foram observados com nanopartículas de CFO-BCZT e CFO não revestidos. Posteriormente, também avaliamos pela primeira vez o comportamento e o impacto do movimento das nanopartículas CFO-BCZT através do tecido cerebral. Os nossos resultados mostram que a aplicação de um campo magnético na parte inferior das fatias do cérebro por 30 minutos resultou em movimento de nanopartículas magnetoelétricas de 30-40 um através do tecido, sem causar qualquer impacto na viabilidade do tecido e integridade celular após 24 horas. Trabalhos preliminares empregando linhas de células neuronais SH-SY5Y mostraram que nanopartículas CFO-BCZT podem induzir diferenciação neural quando sob estimulação magnética. No geral, as novas nanopartículas magnetoelétricas CFO-BCZT demonstraram exibir excelente biocompatibilidade a longo prazo, segurança de movimento através do tecido cerebral, bem como estimulação elétrica neuronal bem-sucedida sob exposição a campos magnéticos. Devido a essas características, as nanopartículas CFO-BCZT representam candidatos valiosos para ECP minimamente invasivo. Além disso, as culturas organotípicas do hipocampo constituem um modelo biológico ideal para avaliar o desempenho e o impacto das nanopartículas magnetoelétricas no tecido cerebral em termos de movimento e estimulação elétrica neuronal.

Os trabalhos apresentados destacam a importância do uso de sistemas de modelos biológicos fidedignos e com complexidade crescente para satisfazer a necessidade de testar um número cada vez maior de materiais e revestimentos para dispositivos de neuroestimulação. Nestas circunstâncias, plataformas biológicas relevantes in vitro/ex vivo constituem uma ferramenta essencial para acelerar a fase pré-clínica de desenvolvimento de material antes dos ensaios clinicos. De facto, demonstrámos, ao longo deste trabalho, a versatilidade das culturas organotípicas cerebrais como ferramentas valiosas para investigar a citotoxicidade de nanopartículas metálicas no tecido nervoso central, tanto em condições fisiológicas, como no contexto de um cenário patológico. Adicionalmente, estes sistemas de cultura constituem uma excelente ferramenta para reduzir o número de utilização e sofrimento animal, em conformidade com os 3R's de Russell e Burch.

Por fim, este trabalho fornece uma compreensão adicional sobre os efeitos que certas nanopartículas metálicas e nanomateriais inteligentes de notável relevância apresentam sobre os principais efetores da resposta do tecido nervoso e formação de cicatriz glial no tecido cerebral. Estes factos revestem-se de importância, considerando o interesse existente da comunidade científica em explorar esses materiais e a sua promissora aplicação no desenvolvimento das próximas gerações de microeletrodos inteligentes por ECP.

TABLE OF CONTENTS

ACKNOWLEDGEMENTS IV
ABSTRACT VI
RESUMO IX
LIST OF ABBREVIATIONS 6
AIM AND STRUCTURE OF THE THESIS 9

CHAPTER 1 **12**

INTRODUCTION **12**

1. HISTORY OF DEEP BRAIN STIMULATION 13
2. PRINCIPLES OF DEEP BRAIN STIMULATION 17
3. CONVENTIONAL ELECTRODES FOR DEEP BRAIN STIMULATION 21
4. CHALLENGES OF CONVENTIONAL ELECTRODES 25
5. THE NEW GENERATION OF DBS ELECTRODES 27
5.1 THIN METAL LAYER COATINGS FOR MICROELECTRODES 32
5.2 CONDUCTING POLYMER COATINGS FOR MICROELECTRODES 33
5.3 CARBON-BASED MATERIALS FOR MICROELECTRODES 36
5.4 HYDROGEL COATINGS FOR MICROELECTRODES 37
5.5 COATINGS WITH BIOACTIVE MOLECULES 42
5.6 MAGNETOELECTRIC NANOPARTICLES FOR NON-INVASIVE DEEP BRAIN STIMULATION 43
6. CONCLUDING REMARKS 46

REFERENCES 47

CHAPTER 2: ***TISSUE RESPONSE TO NEURAL IMPLANTS: THE USE OF MODEL SYSTEMS TOWARDS NEW DESIGN SOLUTIONS OF IMPLANTABLE MICROELECTRODES*** **61**

1. INTRODUCTION **62**

1.1 IMPLANTABLE ELECTRODES IN NEUROLOGICAL AND NEUROPSYCHIATRIC DISORDERS 62
1.2 CURRENT MATERIALS FOR MICROELECTRODE FABRICATION 64

2. FOREIGN BODY RESPONSE AS A CAUSE OF IMPLANT FAILURE **66**

3. EXPERIMENTAL MODELS TO STUDY FOREIGN BODY RESPONSE TO NEURAL IMPLANTS **72**

3.1 IN VITRO MODELS 73
3.1.1 IMMORTALIZED CELL LINE CULTURES 79
3.1.2 PRIMARY CELL CULTURES 80

3.1.3 3D PRIMARY CELL CULTURES 82
3.2 EX VIVO MODELS 83
3.2.1 ORGANOTYPIC CULTURES 83
3.3 IN VIVO MODELS 87

4. FUTURE PERSPECTIVES **90**

4.1 INCREASING COMPLEXITY 90
4.2 DESIGN SOLUTIONS AND NEW MATERIALS FOR THE IMPROVEMENT OF MICROELECTRODE DURABILITY AND BIOCOMPATIBILITY 94

5. CONCLUDING REMARKS **97**

6. ACKNOWLEDGMENTS **99**

REFERENCES 100

CHAPTER 3: ***BIOCOMPATIBILITY OF PLATINUM NANOPARTICLES IN BRAIN EX VIVO MODELS IN PHYSIOLOGICAL AND PATHOLOGICAL CONDITIONS*** **120**

ABSTRACT **121**

1. INTRODUCTION **122**

2. MATERIALS AND METHODS **123**

2.1 ANIMALS 123
2.2 ORGANOTYPIC HIPPOCAMPAL SLICE CULTURES 123
2.3 KAINIC ACID-INDUCED EXCITOTOXICITY AND PLATINUM NANOPARTICLES ADMINISTRATION 124
2.4 PROPIDIUM IODIDE UPTAKE 124
2.5 FLUORO-JADE STAINING 125
2.6 IMMUNOFLUORESCENCE 125
2.7 IMAGE ANALYSIS AND QUANTIFICATION 126
2.8 STATISTICS 127

3. RESULTS **127**

3.1 ORGANOTYPIC HIPPOCAMPAL SLICES ARE RESPONSIVE TO THE PATHOLOGICAL STIMULUS 127
3.2 PLATINUM NANOPARTICLES DO NOT NEGATIVELY IMPACT CELL VIABILITY IN NORMAL OR PATHOLOGICAL CONDITIONS 128
3.3 PLATINUM NANOPARTICLES CAUSE MICROGLIA ACTIVATION IN ORGANOTYPIC HIPPOCAMPAL SLICES 132

3.4 PLATINUM NANOPARTICLES CAUSE MORPHOLOGICAL ALTERATIONS OF MICROGLIA 135

4. DISCUSSION **137**

5. ACKNOWLEDGMENTS **139**

REFERENCES 139

CHAPTER 4: ***NOVEL MULTIFERROIC CORE-SHELL NANOPARTICLES DISPLAYING MAGNETOELECTRIC FEATURES FOR BRAIN STIMULATION: BIOCOMPATIBILITY AND ORGANOTYPIC CULTURES APPLICATIONS*** **146**

ABSTRACT **147**

1. INTRODUCTION **148**

2. MATERIALS AND METHODS **150**

2.1 SYNTHESIS OF CFO CORE NPS 150
2.2 SYNTHESIS OF CFO-BFO CORE-SHELL NPS 150
2.3 SYNTHESIS OF CFO-BCZT CORE-SHELL NPS 150
2.4 CHARACTERIZATION OF MENPS 151
2.5 ANIMALS 125
2.6 PRIMARY MICROGLIA AND ASTROCYTE CULTURES 125
2.7 CORTICAL NEURON CULTURES 123
2.8 LIVE-DEAD ASSAY 152
2.9 REACTIVE OXYGEN SPECIES (ROS) AND NITRITE OXIDE (NO) QUANTIFICATION 123
2.10 PRUSSIAN BLUE STAINING 123
2.11 ORGANOTYPIC HIPPOCAMPAL SLICE CULTURES 123
2.12 MOTION EXPERIMENTS OF MENPS IN ORGANOTYPIC HIPPOCAMPAL SLICE CULTURES 123
2.13 PROPIDIUM IODIDE ASSAY IN ORGANOTYPIC HIPPOCAMPAL SLICE CULTURES 125
2.14 IMMUNOFLUORESCENCE 125
2.15 TEM IMAGE ANALYSIS 123
2.16 NEURAL STIMULATION EXPERIMENTS USING MENPS ON IN VITRO SH-SY5Y CELLS 157
2.17 IMAGE ANALYSIS AND QUANTIFICATION 123
2.18 STATISTICS 160

3. RESULTS **160**

3.1 CFO-BCZT NPS DISPLAY APPROPRIATE MAGNETOELECTRIC PROPERTIES 125
3.2 CFO-BCZT NPS DO NOT IMPACT NEURAL CELL VIABILITY EVEN AT HIGH CONCENTRATIONS 162

3.3 CFO-BCZT NPS DO NOT COMPROMISE CELL VIABILITY AND NEURONAL CELL INTEGRITY IN ORGANOTYPIC HIPPOCAMPAL SLICE CULTURES 166
3.4 CFO-BCZT NPS MOTION DOES NOT IMPACT BRAIN TISSUE VIABILITY AND INTEGRITY 123
3.5 UNDER MAGNETIC FIELD CFO-BCZT NPS INDUCE CELL DIFFERENTIATION IN SH-SY5Y CELLS 176
3. DISCUSSION **122**

3. ACKNOWLEDGMENTS **180**

REFERENCES 181

CHAPTER 5: ***CONCLUSIONS AND FUTURE DIRECTIONS*** **186**

LIST OF ABBREVIATIONS

A	
A-549	Adenocarcinomic Human alveolar Basal Epithelial Cells
aCSF	Artificial Cerebrospinal fluid
ANOVA	Analysis of Variance
B	
BBB	Blood Brain Barrier
BCZT	Calcium/zirconium-doped Barium Titanate
BFO	Bismuth Ferrite
BTO	Barium Titanate
BSA	Bovine Serum Albumin
C	
C1q	Complement component 1q
CA1-3	Cornus Ammonis 1-3
CD14	Cluster of Differentiation 14
CFO	Cobalt Ferrite
CH	Conducting Hydrogel
CIC	Charge Injection Capacity
CNS	Central Nervous System
CNT	Carbon Nanotube
CP	Conducting Polymer
CSC	Charge Storage Capacity
D	
DBS	Deep Brain Stimulation
DG	Dentate Gyrus
DMEM	Dulbecco's Modified Eagle's Medium
E	
ECM	Extracellular Matrix
ECS	Embrionic Stem Cells
EDX	Energy Dispersive X-ray Spectroscopy
F	
FBS	Fetal Bovine Serrum
FDA	Food and Drug Administration
G	
GFAP	Glial Fibrillary Acidic Protein
GPi	Globus Pallidus
H	
HBMVC	Human Brain-derived Microvascular Endothelial Cells
HUVEC	Human Umbilical Vein Endothelial Cells
HAADF-STEM	High-angle Annular Dark-field Scanning Transmission Electron Microscopy

I

IBA-1	Ionized Calcium Binding Adaptor Molecule-1
Ig	Immunoglobulin
IL	Interleukin
IO	Iron Oxide
IPG	Implantable Pulse Generator
iPSC	Induced Ploripotent Stem Cells

K

KA	Kainic Acid

L

LPS	Lipopolysaccharides

M

MCP-1	Monocyte Chemoattractant Protein 1
MEMS	Microelectromechanical systems
MEAs	Microelectrode array
MENPs	Magnetoelectric Nanoparticles

N

NBM	Neurobasal Medium
NC	Neural Channel
NCCC	Neuronal Cortical Cell Cultures
NCI-H520	Human Lung squamous Carcinoma Cell Lines
NMDA	N-methyl-D-aspartate receptor
NG2	Neuron-glia antigen
NGF	Nerve Growth Factor
NVU	Neurovascular Unit
NO	Nitrite Oxide

O

6-OHDA	6-Hydroxydopamine

P

P/S	Penicillin/Streptomycin
PBS	Phosphate-Buffered Saline
PD	Parkinson Disease
PDL	Poly-D-**Lysine**
PDMS	Polydimethylsiloxane
PEDOT	Poly(3,4-ethylene dioxythiophene)
PEG	Poly(ethylene glycol)
PFA	Paraformaldehyde
PLGA	Poly(lactic-co-glycolic acid)
PLL	Poly-L-Lysine
PSS	Poly(styrene sulfonate)
PI	Propidium Iodide
PtNPs	Platinum Nanoparticles

PTH	Polypyrrole
PPY	Polythiophene
PVA	Poly(vinyl acetate)
S	
RGD	Arginylglycylaspartic Acid
ROS	Reactive Oxygen Species
RN	Reactive Nitrogen Species
S	
SNT	Subthalamic Nucleus
T	
TEM	Transmission Electron Microscopy
TNF-α	Tumor Necrosis Factor- α
THP-1	Human acute monocytic leukemia Cell Lines
TMS	Transcranial Magnetic Stimulation
TRPV1	Transient Receptor Potential Vanilloid 1
Y	
YIGSR	The laminin-derived peptide (Tyr–Ile–Gly–Ser–Arg)
V	
VTA	Volume of Tissue Activated

AIM AND STRUCTURE OF THE THESIS

Biomedical micro- and nano-devices have tremendously improved over the last decades in terms of performance and safety. New materials and fabrication approaches have revolutionized traditional biomedical devices, promoting the transition toward miniaturization. Huge strides have been made especially in the field of neuroscience and neurostimulation thanks to the progress in implantable electrode fabrication and design. Successful goals were achieved by their clinical applications for treating several neurological diseases and as fundamental components of neural prosthetics. However, new challenges have come to light for this industry, as miniaturizing these devices requires smaller components, new manufacturing processes and material manipulation. The electrochemical properties of metals and alloys drop down with the decrease in dimensions. Corrosion reactions occurring at the microscale can as well develop differently, also considering the integration of several materials in close contact that can lead to the degradation and dissolution of small components. Moreover, considering that implantable electrodes act as an interface between electronic devices and the brain tissue, the materials employed must display good biocompatibility to minimize nervous tissue deleterious responses, which represent a crucial aspect on contributing to device durability and the most important cause of failure of these devices in the clinics.

The mCBEEs project, supported by an European Commission funded Marie Curie Training Network, in which I was involved, had as one of its major goals to understand degradation, corrosion phenomena and biocompatibility of materials and coatings for micro and nanoelectronic devices, with a special focus on the events occurring at the microscale. The main aim of my project was in particular to provide significant contribution as bioengineers on investigating those phenomena from a biological perspective in the context of the nervous tissue. The first aspect that stands out from the state of the art is the huge number of new materials and coatings developed in recent years. However, most of these new materials are still in the first stages of testing. A possible explanation could be the "excessive" preference of the scientific community for in vivo studies, which must be the ultimate step before clinical testing. However, animal studies are not always ideal to investigate the cellular responses nor the molecular or biochemical events at the tissue-material interface. Moreover, in vivo studies are complex, costly and time-consuming, together with the legal and ethical enactments to which researchers must contend. These are important factors that can cause the slowdown of the arrival to the clinical trials of many of the new materials and devices that have been proposed in recent times.

In light of these observations, it is paramount to enrich the developmental phase with alternative approaches to satisfy the massive demand for material testing. The use of in vitro/ex vivo relevant biological platforms can represent an excellent approach to dissecting mechanisms of cell/tissue response, as well as for high throughput screening to speed up the testing processes, ultimately allowing an efficient progression of successful technologies.

For this purpose, we have initially conducted a thorough analysis of the state of the art of in vitro and ex vivo models available for the study of neural tissue response to implantable microelectrodes. Then, we have proposed rodent brain organotypic cultures as ideal platforms to study the biocompatibility of materials appropriate for microelectrode fabrication and microelectrode coatings for deep brain stimulation (DBS). These complex cultures were obtained by dissecting and slicing specific a brain area-the hippocampus from early-stage animals, followed by their establishment in culture plates, where they acquire an organ-like structure. The great advantages that these 3D models have are the preservation of the tissue architecture of the native tissue, the possibility to mimic different pathophysiological scenarios by external induction and to dissect the process of nervous tissue response in all its features.

This thesis is divided into five main chapters:

- Chapter 1 concerns an introductory part that covers the history of neurostimulation, the achievements reached in the clinic over the last century and the principles of DBS. Subsequently, a description of the conventional DBS electrodes and their related caveats and challenges for clinical use is presented. This is followed by the discussion of the electrode coating approaches that are currently under investigation to improve the performance of the conventional electrode and minimally invasive strategies under development for the next generation of DBS electrodes.

- Chapter 2 presents our review article focused on the description of the clinical applications of implantable electrodes for the treatment of neurological and neuropsychiatric disorders, the current materials employed for their fabrication, followed by a discussion on the known biological responses of the brain tissue to such devices and the challenges that need to be overcome. Then, a detailed description of the state-of-the-art of the most relevant in vitro/ex

vivo and in vivo models available for the study of the nervous tissue response to implantable electrodes is presented.

- Chapter 3 shows the experimental work, demonstrating the suitability of rodent brain organotypic cultures for assessing the short-term cellular responses of glial and neuronal cells to monodispersed citrate-coated platinum nanoparticles (PtNPs) in normal and excitotoxic conditions (pathological scenario).

- Chapter 4 displays the experimental work conducted in collaboration with our partners from the Multi-Scale Robotic Lab (MSRL-ETH Zurich). We explored a novel coating for cobalt ferrite nanoparticles (CFO) with calcium/zirconium-doped barium titanate (CFO-BCZT) intended for non-invasive DBS. We initially assessed their biocompatibility on in vitro primary glial and neuronal cultures and rodent brain organotypic cultures to assess the long-term cellular responses, as well as the impact of nanoparticles motion through the tissue, using an external magnetic field to initiate the motion. Finally, we conducted preliminary experiments employing SH-SY5Y cell lines to evaluate the potential of CFO-BCZT to induce neural differentiation under magnetic stimulation.

- Chapter 5 summarizes the overall analysis of the results presented in this thesis, headlining the most important findings and conclusions, together with the future directions for assessing the long-term biocompatibility of PtNPs (Chapter 3) and safety of magnetoelectric nanoparticles (Chapter 4).

Chapter 1

INTRODUCTION

1. HISTORY OF DEEP BRAIN STIMULATION

Deep brain stimulation (DBS) has drastically changed the clinical approach to the treatment of neurological dysfunctions (Harmsen et al., 2020). In the last years, we assisted to its rapid progression from a neurophysiological tool to the therapy of election for an increasing range of pathological conditions (Marín et al., 2022). Considering this recent exponential success, one may think that DBS and the use of implantable electrodes in biomedicine date to our century. Instead, it has very deep roots. The first scientists that conducted experiments on stimulating body regions with induced electrical fields were Luigi Galvani and his wife Lucia Galeazzi in the late 18th century, where they discovered the possibility to generate muscle contraction by electrical impulse into a nerve of a dead frog (**Fig.1**). Such experiments at that time paved the way to a new medical treatment based on nerve stimulation known as Galvanism.

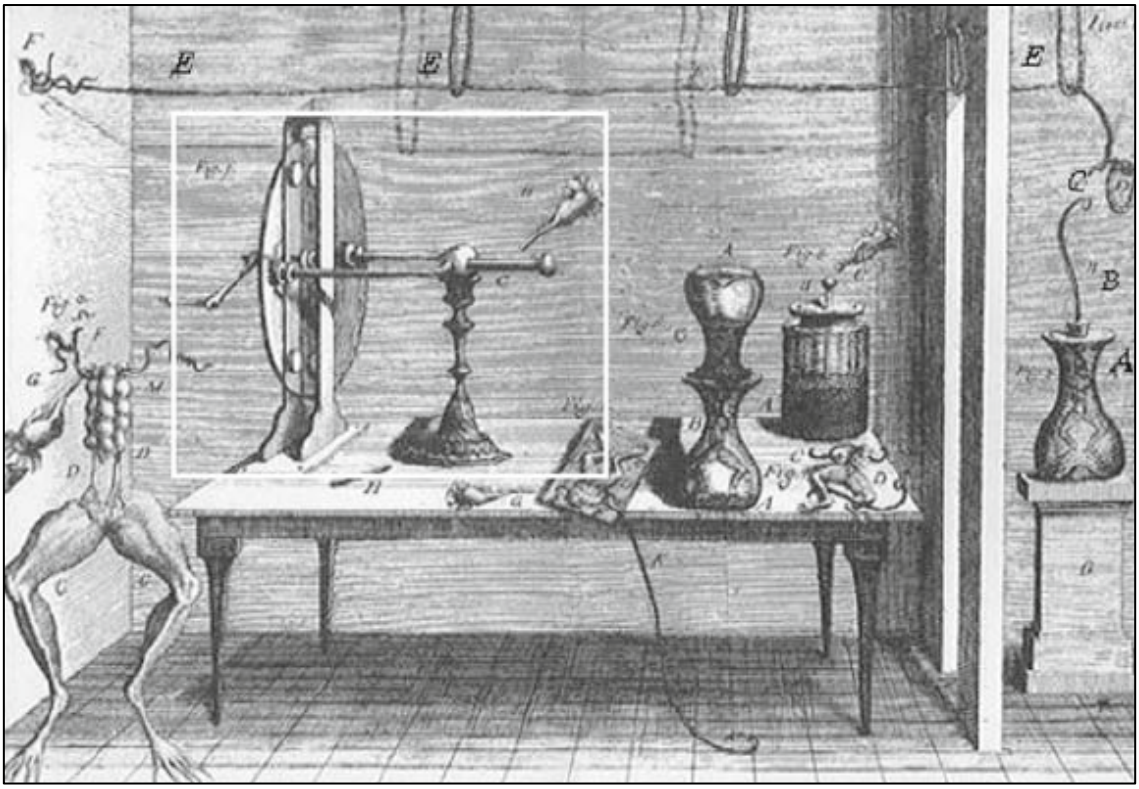


Figure 1. *Experimental apparatus of Luigi Galvani. The drawing on the left shows the preparation of the frog for the electrical stimulation. The white square indicates the electric machine employed for the experiments. Used with permission from* (Piccolino, 1997).

In the following century, scientists from different backgrounds ranging from physics to physiology based their research on those previous fascinating discoveries and employed animal models to

stimulate and record electrical activity in the brain and other body parts (Chandrasekaran et al., 2021). Moreover, ethically questionable experiments conducted by others following Galvani's observations were conducted on human dead corpses and revealed the possibility of electrically stimulating the cerebral cortex. These early findings supported the theory that electrical stimulation could become in the future a therapeutic strategy to treat neuropsychiatric conditions. Other smaller steps directed to brain electrical stimulation were given by several scientists around the globe at the end of the 19th century, such as the American physician Robert Bartholow, which is considered the first one to perform electrical stimulation of the cerebral cortex in an awakened human (Patra et al., 2019), or the British neurosurgeon Victor Horsley which gave important contributions on understanding and studying human brain topography thanks to his use of electrical stimulation on epileptic patients (Vilensky and Gilman, 2002). These types of approaches were only possible due to pre-existing pathological circumstances of the patients involved, which allowed them to have facilitated access to the dura mater surface to perform electrical stimulation. Several researchers at that time also explored the use of electrical stimulation of brain districts in animal models which allowed to add further tiles to the understanding of brain anatomy. The main advances in this context were achieved later, in the second half of the 20th century, in which fundamental studies on brain topography and stereotactic neurosurgery were conducted (Rahman et al., 2009) (**Fig.2**).

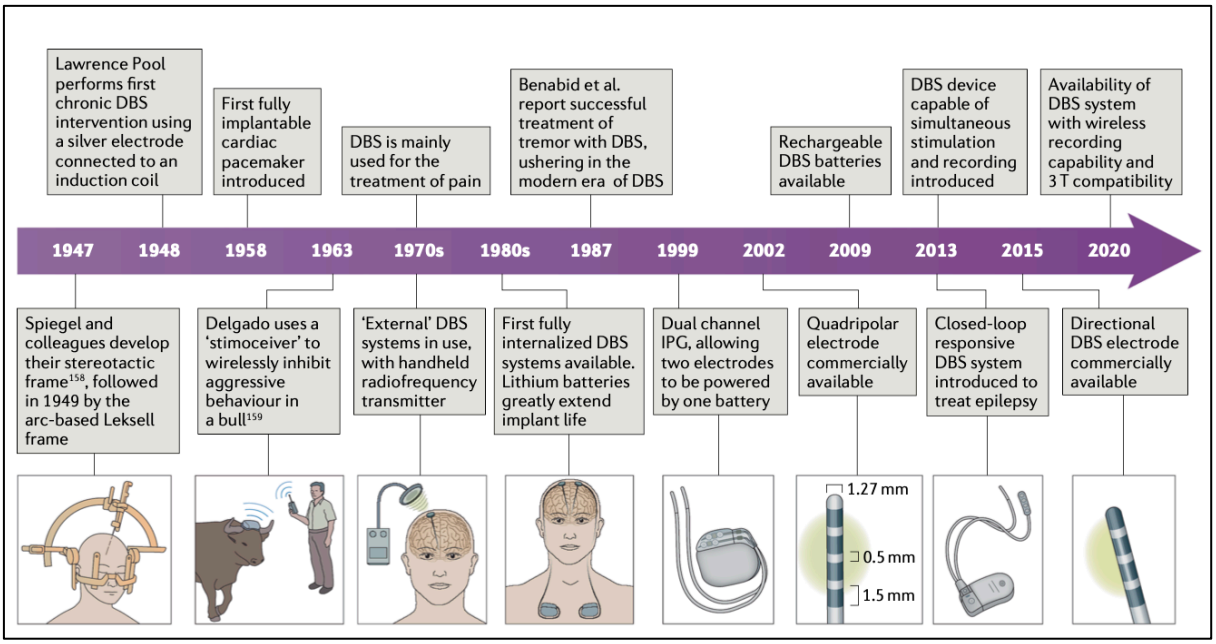


Figure 2. *Timeline of technology development for deep brain stimulation. DBS: deep brain stimulation; IPG: implantable pulse generator. Used with permissions from* (Krauss et al., 2021)

The roots of the modern techniques of DBS stretch back to the stereotactic neurosurgery treatments, consisting in the production of lesions in specific brain targets to disrupt the brain tissue irreversibly. The location designated to be ablated is selected using intraoperative stimulating electrodes.

This approach was employed to get beneficial effects in patients affected by tremors coming from motor disorders. The initial enthusiasm for the use of this therapeutic strategy emerged from positive outcomes in the reduction of dyskinesia and tremors in patients affected by Parkinson's disease (PD) where it was observed that the stereotactic ablation of deep brain areas was leading to a reduction of disease manifestations. It took additional years of clinical trials to understand that the use of high-frequency electrical stimulation to alter brain activity, which is the basis of DBS, rather than disrupting it with ablative techniques, was providing major clinical benefits in patients with neurological dysfunctions. Promising clinical results were achieved in patients affected by PD, epilepsy, dystonia and chronic pain with the high-frequency DBS of different brain targets such as the cerebellum, cerebral cortex and thalamus (Sironi, 2011). However, the exact therapeutic mechanism was unknown. The only certainty was that the application of high-frequency stimulation in those areas was related to a suppressive effect of local neuronal elements.

The introduction of pharmacological therapy and DBS caused the stagnation of ablative neurosurgery, although today is still practiced with minimally invasive techniques (Hariz and Hariz, 2013). However, despite the beneficial results achieved, some hesitation on the use of DBS remained in the scientific community, due to reported cases of failures of the therapy and to the presence of side effects in patients subjected to prolonged treatments. This was also caused by the advent of levodopa in the 70's and its relative success as a pharmacological strategy to treat PD. This period was characterized by a temporary decline in the use of neurosurgery for treating Parkinson-related symptoms and other conditions. In the following decade, the untimely enthusiasm for levodopa treatment has taken a turn for the worse due to the presence of cases of patients that were not responding or were intolerant to this pharmacological treatment (Gardner, 2013). In light of this, another opportunity opened up for DBS, supported by the onset of new neuroimaging and engineering tools as well as technological advances in peacemaker design that were translated into neurosurgery (Coffey, 2009). It is in fact from the modification of cardiac pacemakers that "modern" DBS electrodes arise.

The early clinical success of DBS was achieved in the 1980's, in which electrical stimulation of the ventral intermediate nucleus of the thalamus was employed to treat movement disorders in essential

tremors and PD. Technological advances in material sciences led to substantial improvements in these devices. The clinical use of fully internalized dual channel implantable pulse generators (IPG) for bilateral DBS was introduced at the end of the 20th century, followed by the use of rechargeable batteries and improved electrode design with multiple stimulating contact sites with different configurations to direct and shape electrical stimulation depending on the target area. Moreover, closed-loop systems employing electrodes capable of recording and stimulating capabilities were also introduced for better control of symptoms and side effects. Subsequently, the use of DBS was successfully employed to stimulate other target areas such as the subthalamic nucleus (STN), the globus pallidus (Gpi) receiving CE Mark and Food and Drug Administration (FDA) approval for treating Essential tremor, PD and epilepsy (Frey et al., 2022). The use of DBS was extended to other neuropsychological and neurodegenerative disorders such as depression, obsessive-compulsive disorders, and movement disorders, and its range of applications is still growing (de Koning et al., 2011; Laxton and Lozano, 2013; Kisely et al., 2018). The reason for such clinical success is due to the technological advances in the field of the electrode device industry, confirmed by the birth of manufacturing companies and the accelerated enlargement of the global market for neurostimulation and recording devices (Krauss et al., 2021). By virtue of this technological innovation, the neurosciences field progressed simultaneously, as neurophysiologists nowadays have at their disposal excellent tools not only to improve the stimulation therapy efficacy, but also to record and study brain activity in normal and pathological scenarios.

The concurrent progress from different fields of research has turned DBS therapy into a strategy of election for a vast number of neurological conditions, making implantable electrodes fundamental device components and key players in the complex relationship between electronic devices and brain tissue.

2. PRINCIPLES OF DEEP BRAIN STIMULATION

Although considered a relatively recent procedure, the modulation of brain activity dates back more than 2 centuries ago, as described in the previous section, where the first experiments conducted on animals and dead corpses showed that it was possible to induce motor movements by cortex electrical impulses. Huge strides have been done since that time when the relationship between electricity, brain functioning, and movement represented a fascinating topic for scientists.

Several efforts have been made to understand the multiplicity of effects behind neurostimulation and their application in a variety of pathologies. Nevertheless, some concepts are still under debate. The main reason for that lies in the intrinsic complexity of the human brain network, whose understanding requires the involvement of scientists from different scientific areas ranging from mathematics, physics and computer science, as well as their commitment to helping neuroscientists to answer to unresolved issues for far too long.

In general, electrical stimulation of neurons consists of the induction of transmembrane potential. When a neuron is subjected to an electric field, the membrane can be depolarized from its resting value (i.e., -70 mV), causing excitation or inhibition of the cell. When the depolarization reaches a certain threshold (~ -55/-50 mV) an action potential is generated, which involves the opening of voltage-gated ion channels such as sodium and potassium channels. This action potential then leads to the release of neurotransmitters in targeted pathways (McIntyre and Anderson, 2016).
Initially, DBS therapy showed similarities of effects with ablative neurosurgery, and therefore it was initially thought that the therapeutic effect was related to an inhibition of abnormal pathways in the target area. However, further studies, mainly focused on PD, reported also that high-frequency stimulation causes the excitation of neurons in the GPi, and that stimulation of STN can induce the firing of neurons in the GPi through excitatory projections. Vice versa, it was reported that stimulation of the GPi can also excite STN neurons. Although paradoxical, these data indicated the presence of overlapping neurochemical reactions as explanation for the variety of excitatory/inhibitory effects (Chiken and Nambu, 2015). It was in fact through consecutive studies that scientists reported the presence of other mechanisms that could explain those findings, such as a reversed direction (antidromic) from the axon to the cell body, or in a physiological direction (orthodromic) from the cell body to the axon of neurons in the vicinity of the electrode site (Kang and Lowery, 2014). The electrode positioning and the stimulation parameters can have in fact a direct influence on cortical

neurons and lead to an antidromic and orthodromic activation. These types of effects can excite/inhibit downstream patterns that can alter neuronal networks in basal ganglia or other districts. In conjunction with the alteration of the firing patterns, at the tissue material interface, there are other biochemical events such as altered neurotransmitter release and protein expression, which can induce afferent and efferent modulation in the long-term (Mohammadi and Mehdizadeh, 2016; Alosaimi et al., 2022). Taken together, these findings suggest that the effect of DBS is determined by an intricate number of neurochemical reactions overlapping with each other's and that is difficult to disclose into its small components (**Fig.3**).

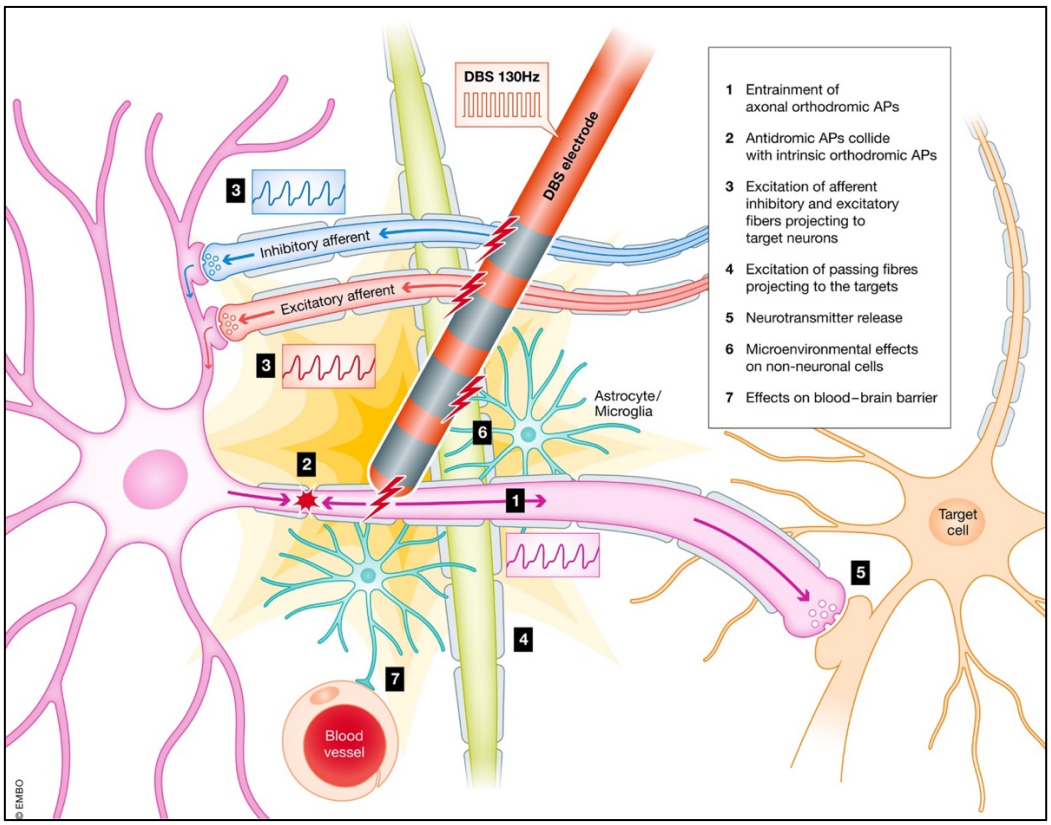


Figure 3. *Electrical effects of deep brain stimulation (DBS). When implanted in a selected brain region, high-frequency stimulation causes ortho- and antidromic axonal action potentials. Contact sites in the electrode determine excitation of afferent inhibitory and excitatory fibers, as well as excitation of passing fibers. Neurotransmitters release, biochemical alterations in surrounding non-neural cells such as astrocytes, microglia, endothelial cells and in the blood-brain barrier are also secondary reactions caused by DBS. Used with permission from* (Jakobs et al., 2019).

Hence, the exact mechanisms by which DBS suppresses abnormal neural activity in the various pathologies still needs to be further studied. This is also due to the different neurological effects of DBS in the clinical scenarios in which it is applied and the brain areas involved. Despite the unquestionable therapeutic effects, the expansion in the clinical application over the years arose

considerable inconsistencies and re-evaluations of DBS action mechanisms. Nevertheless, the scientific community is geared toward the following hypotheses to explain the therapeutic effects of DBS (Chiken and Nambu, 2015):

- the “inhibition” hypothesis sustains that DBS induces a reduction in abnormal firing patterns by inhibiting neural activity in stimulated neurons. This hypothesis is supported by the fact that electrical stimulation in some cases displays similar effects to ablative techniques;

- the “excitation” hypothesis, where the effects of DBS on the target site are a result of excitation of afferent and efferent axons that can normalize or inhibit abnormal firing patterns;

- the “disruption hypothesis”, where electrical stimulation generates a series of input and output signals through the target nucleus and thus disrupting abnormal information flow.

The most credited hypothesis is the disruption, where DBS is in fact the result of the combination of dissociating patterns of excitatory and inhibitory signals dissipating into the surrounding neural network (Miocinovic et al., 2013). The resulting effect is not only a stimulation, but a modulation of the neural circuitry by means of a multitude of combinatorial effects such as antidromic and orthodromic axonal action potentials, modulation of afferent and efferent fibers through neurotransmitters release in the vicinity of the electrode, and effects on non-neuronal cells in the 3D space around the electrode (Ashkan et al., 2017). The consecutive therapeutic effect consists in the disruption of abnormal information flow which leads to regulation and recovery of the neuronal patterns with a reduction of disease symptoms.

Additional aspects influence and make even more complex the deep understanding of these reactions and explain the heterogeneity of responses that have made it difficult for neuroscientists to shed light on the effects of DBS. The following aspects have a huge impact on the clinical response to DBS.

i) Anatomical target selected for stimulation. For the same disease, different brain districts are selected as targets for DBS to reduce symptoms. However, different neurological and biochemical effects can be obtained (Deli et al., 2011). This can be due to the different anatomy of the target, such as the proximity of white and grey matter (Mohan et al., 2020), tissue heterogeneity in pathological conditions (Young et al., 2018) and clinical differences in individuals with the same disease (Greenland et al., 2019).

ii) Proximity of the electrode to the target. Electrode positioning plays a fundamental role in ensuring the efficacy of DBS. It has been in fact shown that after the surgery electrodes can move due to operative subdural air invasion, which is formed because the brain returns to its original position (van den Munckhof et al., 2010). Moreover, the outflow of cerebrospinal fluid caused by surgery is another cause of brain sinking, which in turn leads to electrode displacement and loss of efficacy. In PD patients, for instance, the vicinity of the stimulation to the subthalamic nucleus is crucial to improve motor symptoms (Zhang et al., 2021a).

iii) Electrode contact design. A great number of electrode types with different configurations of electrode contacts exist in the market, offering the possibility to steer the stimulation based on the anatomy of the neural target (Alonso et al., 2016). Each electrode type can have a different impact in terms of the volume of neural tissue activated and consequently clinical outcomes (Slopsema et al., 2018) with an impact on foreign body response (discussed in the following chapter 2). Therefore, the use of imaging techniques and computational modeling software have been proposed to help clinicians to identify the best DBS orientation according to patient-specific tissue anisotropy and anatomical morphologies (Sitz et al., 2017; Zhang et al., 2020).

iv) Selection of the stimulation parameters. The selection of specific current amplitude, frequency and pulse width of stimulation can have a different impact on DBS effects. Although high-frequency stimulation is an effective DBS approach for treating motor symptoms in PD and movement disorders, also low-frequency stimulation can provide a better response to akinesia and freezing of gait (Su et al., 2018; Valldeoriola et al., 2019). Likewise, it was reported that DBS with different pulse widths can have an impact on the therapeutic window. DBS with short pulse widths has been in fact shown to have positive effects in the reduction of gait disturbance, improvement in speed of gait and perceptual speech in patients with essential tremors and PD (Dayal et al., 2018; Kroneberg et al., 2019).

Remarkable efforts are constantly done by scientists from different backgrounds to find optimal strategies to reduce these external aspects, which represent the still present caveats for the clinical use of DBS devices. A possible explanation is that while great improvements were achieved from the clinical application of DBS, the field of electrode fabrication and design did not undergo substantial changes until the last decades, generating a gap between clinics and electrode design. When these limitations, which are strictly related to the electrode itself and its placement, were more tangible, the need for reducing the invasiveness of electrode implantation and improving clinical outcomes became a priority. Nowadays, we are assisting to a continuous implementation of electrode devices. Advances

in microfabrication and in the production of smart materials are still evolving and it is expected to assist to the genesis of new technologies and approaches that in future years will be applied to the clinics and will pave the way to new frontiers of neurostimulation. Clinicians have already at their disposal a wide range of conventional DBS electrodes with improved performance and different designs that allow to select proper stimulation parameters and configurations depending on the neurological dysfunction of the patient and the brain district to be targeted, with the aim of providing improved treatment efficacy. In the following paragraph, conventional electrodes available in the market for DBS are presented.

3. CONVENTIONAL ELECTRODES FOR DEEP BRAIN STIMULATION

Neuronal implant devices have progressed substantially over the last years after long decades of stasis. The first trials with DBS in the 70's were conducted using "homemade" electrodes. The first electrodes described were composed of a Teflon (tetrafluoroethylene) coated stainless steel lead with different contact surface configurations. One decade later, the second generation of electrodes was composed of a platinum-iridium alloy as conductor, with 4 stimulation surfaces insulated with an epoxy resin (Coffey, 2009). These conductive materials were selected based on their electrochemical properties rather than the possible reactions to the tissue. Electrodes with these metals had to fulfill the following electrochemical properties:

i) high charge injection capacity (CIC), which represents the maximum charge density that can be injected without causing irreversible damage of the material;

ii) high charge storage capacity (CSC), strictly related to CIC, it indicates the maximum amount of charge that a material can store and predict how much charge can be injected reversibly;

iii) low electrode impedance, which is a measure of the opposition of the tissue-electrode interface to the flow of charges;

iv) inertness, as the materials employed needed to preserve their electrochemical stability in order to make electrodes durable and reliable for long-term implantations.

Subsequently, clinical concerns related to surface irregularity, tissue encapsulation and hemorrhages led to design improvements of the implantable electrodes, which are employed up to the present day.

Such electrodes are composed of a polyurethane smooth surface, with four platinum-iridium cylindrical surface contacts closed to the tip, which has a diameter of 1,27 mm and insulated with fluoropolymers. The core has a space for a tungsten stylet, which is placed to increase the stiffness of the lead during implantation and then removed afterward (Coffey, 2009; Frey et al., 2022). Different electrode configurations became most commonly employed in the clinic (**Fig.4A**). The quadripolar electrode with 4 electrode contacts is one of the first configurations largely employed in the clinic. This type of configuration has been extensively employed to stimulate the subthalamic nucleus and internal segment of globus pallidus in patients affected by PD (Kleiner-Fisman et al., 2006), and then extended to other diseases such as essential tremor and epilepsy. Conventional quadripolar electrodes have 1.5 mm contacts with a space of 0.5 or 1,5 mm between them, allowing the production of a spherical electric field along the z-axis of the lead. The presence of side effects due to the spreading of the stimulation outside the target area led to the design of electrodes with new configurations that allow shaping the electric fields in different modalities according to the anatomy of the target (**Fig.4B**).

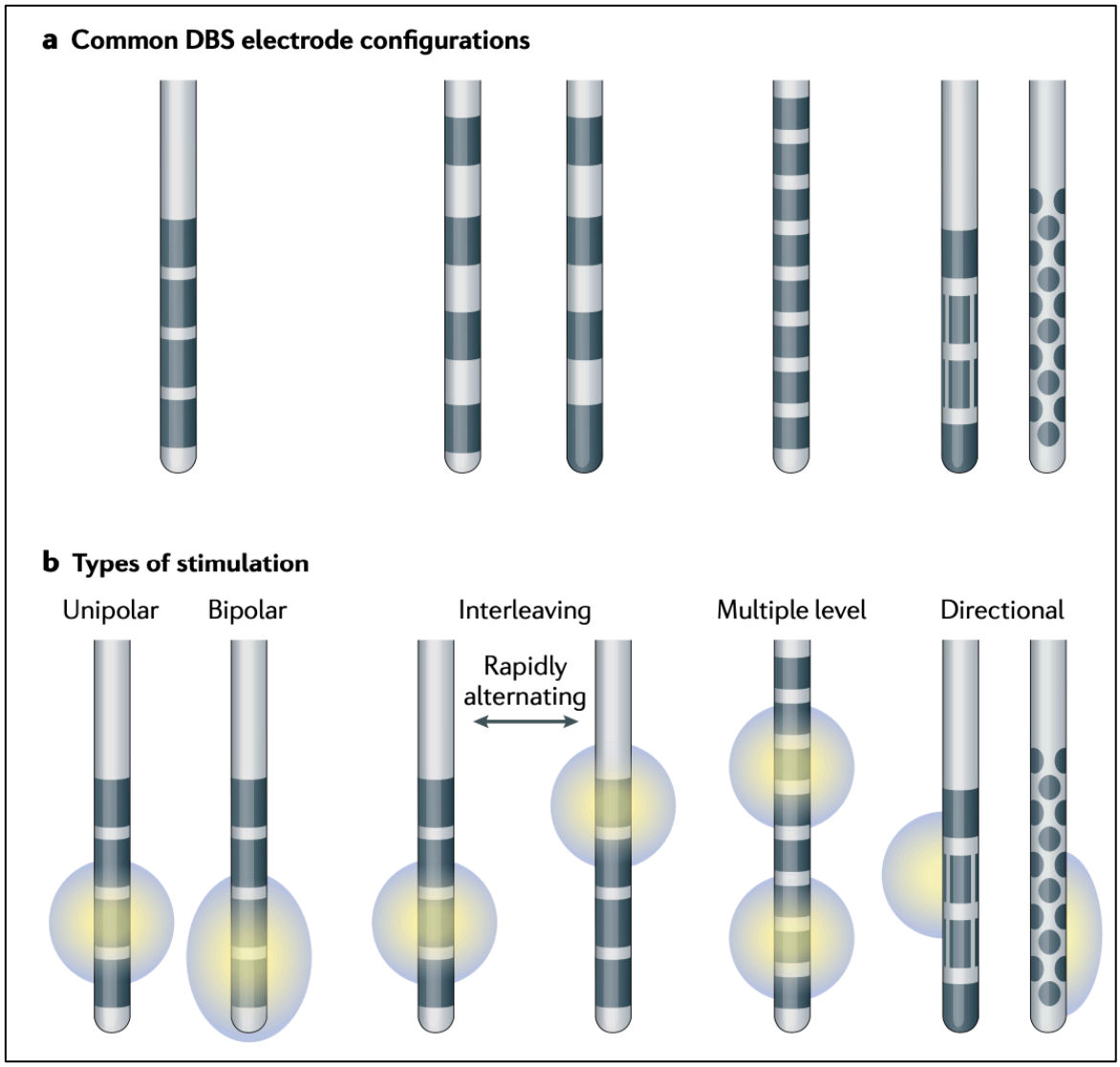


Figure 4. *Commercially available deep brain stimulation (DBS) electrodes.* ***A***. *Common electrode configurations for DBS. Dark grey regions represent the electrode contact sites that deliver current. The different configurations presented differ in the distance between contact sites, their number and their shape.* ***B***. *Types of stimulation, which depend on the type of DBS electrode used. Used with permissions from* (Krauss et al., 2021).

Commercially available electrodes produced by several companies differ by the number of contacts, lead diameter, length of contacts and space between them (Frey et al., 2022). The choice of the electrode design for specific target is based on the volume of tissue activated (VTA), a modeling technique that allows to assess the brain tissue that is stimulated (Devaluez et al., 2020). The VTA depends on several factors such as the characteristics of the tissue that must be stimulated, the stimulation settings and the electrode configuration. Depending on the system that is used, different types of stimulations can be obtained and, as consequence, different therapeutic effects. Unipolar stimulation is a type of stimulation in which only one electrode contact is activated, while bipolar

stimulation involves the activation of 2 contacts in which current flows between them. Unipolar stimulation generates radial current diffusion covering a spherical area around the contact, resulting in a higher VTA compared to bipolar stimulation, which generates a more restricted area around the contacts. It has been reported that unipolar stimulation of the STN provides better outcomes in PD patients. However, it also causes more side effects than bipolar stimulation (Deli et al., 2011). Interleaving stimulation is a recently developed type of stimulation that has been proposed with the aim of reducing side effects. It consists in the rapid switching of the current diffusion between the contacts singularly. This approach can be also explained as the alternation of 2 different programs in the same electrode, and it represents an effective alternative in patients in which conventional stimulation parameters were not adequate. The use of this type of stimulation in the STN of PD patients has been shown to be an effective strategy to maximize symptom control (Zhang et al., 2016). Multiple-level deep DBS is another type of stimulation that involves the use of electrodes with multiple contacts. With this configuration it is possible to activate contacts at different levels along the electrode, allowing the possibility to target one or more pathological targets with high precision (Contarino et al., 2014).

The last innovation in the context of conventional DBS electrodes is mainly represented by directional stimulation (Steigerwald et al., 2019). Directional electrodes are composed of 2 conventional contacts and 2 contacts in the middle segmented in 3 equal parts. A lead marker is also present on top for the control of orientation. Another configuration that is still under investigation consists in 40 small circular 0.8mm contacts distributed in the electrode surface. This type of configuration, unlike the previous ones, has the great advantage to avoid the formation of radial current diffusion around the electrode which is the main cause of the spreading of the stimulation from the target area. The innovation of this approach over standard methods is confirmed by recent clinical studies conducted in patients with PD and essential tremors, in which the effects of omnidirectional and directional DBS were compared. What emerged from these works was that directional DBS significantly widens the therapeutic window with a reduction of disability in the long term without the need of reprogramming visits (Pollo et al., 2014; Rebelo et al., 2018; Schnitzler et al., 2022).

Directional electrodes with increasing number of contacts are expected to become the new standard electrode design for DBS, not only for the clinical experience but also for the potential that could reach in combination with the technological improvement of programming devices. Clinicians today have at their disposition advanced diagnostic tools and therapeutic methods to ensure patient comfort and reliability of treatment. In recent years, innovative approaches have been implemented to reduce

the invasiveness of the implantation, the efficacy of electrode placement and delivery of current in the target area. Nevertheless, material failure and the chronic nervous tissue response still represent a threat for conventional electrodes. Hence, new material-based strategies have been proposed by engineers to overcome these limitations. A deeper understanding of the interplay between material response and biological response at the brain tissue-electrode interface is paramount to address the limitations of conventional electrodes, which will be discussed in more detail in the following section.

4. CHALLENGES OF CONVENTIONAL ELECTRODES

Electrodes for recording and stimulating applications became rapidly precious tools for neuroscientists to study the pathophysiological mechanisms at the basis of neurological disfunctions and for clinicians to provide reliable and effective DBS therapy. In the course of time, however, the frequent occurrence of failures of DBS therapy due to chronic tissue response (discussed in detail in Chapter 2, (Gulino et al., 2019)) and corrosion phenomena in both recording and stimulating electrodes led to the need for dissecting the physical and biochemical mechanisms responsible for the loss of device functionality over time.

Substantial efforts were made to understand the factors at play on the tissue-electrode interface, in order to develop more durable devices and minimize risks and discomfort of the patients. The observations coming from clinical experience indicate that a series of aspects attributable to the characteristics of the material and the tissue damage caused by implantation take part in the decline of device functionality (Gulino et al., 2019).

i) Mechanical mismatch. This is mainly caused by the different mechanical characteristics of brain tissue and the electrode materials (Sunwoo et al., 2020). Metals are employed for conventional electrode design as they can ensure the electrochemical performance for delivering/recording electric signals. However, metals have a much higher young modulus compared to brain tissue. This discrepancy generates tension forces at the tissue-material interface, leading to cytoskeletal alterations and cellular damage (Jorfi et al., 2015). Moreover, electrodes big in size, besides causing greater cellular damage and blood-brain barrier (BBB) disruption, display higher mechanical mismatch due to the proportional increase in the extent of tension forces at the tissue-electrode interface. These processes are key determinant of the nervous tissue response, but they also have a substantial impact on determining chronicity of the response. Due to the high young modulus of the

material, brain micromotion caused by breathing and vascular pulsation generates motion of the electrodes around the target site, which magnifies the tension forces at the interface and leads to additional tissue damage and immune response (Duncan et al., 2021). Another type of mechanical mismatch is caused by the different electrochemical properties of materials employed for electrode design. Different materials in physical contact generate strain forces at their interface on which cracking and delamination phenomena most often occur and can lead to electrode failure (Kozai et al., 2015a).

ii) Electrode design. Another aspect that increases the mechanical mismatch is the electrode size and geometry. To achieve low impedance and high charge storage and injection capacity, electrodes need to have a high surface area. Consequently, the bigger the surface area the higher the mechanical mismatch and neuroinflammation. Material surface topography also plays a critical role in determining cellular response (Rantataro et al., 2022). It is now common knowledge that cells are sensitive to physical and mechanical properties of materials. Different cell types can have different behavior. In the brain tissue neuronal cells retract their extensions when in contact with rigid materials, while glial cells and fibroblasts spread more, leading to the formation of the glial scar (Janmey et al., 2019). Materials with low young modulus as close as possible to the brain tissue are preferred to improve implant integration and provide safety.

iii) Chemical mismatch. Like mechanical mismatch, the chemical one is also observed due to the different chemical composition of electrode materials and brain tissue. The brain tissue is composed of a high content of water and ions. Metals used for electrode design, on the contrary, are hydrophobic and this amplifies blood-serum proteins adsorption (Visalakshan et al., 2019) In this scenario, neuronal cells are not able to attach to the electrode surface and this causes neuronal cell retraction and many times death. This in turn contributes to a progressive loss of electrical communication between electrodes and neurons, due to the impossibility to provide charge transfer. The cellular damage caused by both chemical and mechanical mismatch, triggers the mechanism of glial scar formation which consequently increases the distance between electrode and target site.

iv) Device implantation. Injury of the nervous tissue is an unavoidable reaction to any type of electrode implantation irrespective of its composition. The higher the electrode size, the higher the mechanical damage to the surrounding tissue, which consists in the initial injury of the tissue after insertion, BBB disruption, hemorrhage and edema. The neuroinflammation in the acute phase is characterized by neuronal cell death, activation of glial cells, release of pro-inflammatory cytokines,

(Kozai et al., 2015c) an exacerbation of the process over time leading to the formation of the glial scar, which in turn increases electrode impedance and hampers electrochemical performance. The glial scar becomes an insulating barrier that can contribute to the formation of corrosion phenomena on the electrode surface (Meijs et al., 2019).

v) Corrosion. Besides their electrochemical properties, metals for conventional electrodes are selected also based on their inertness. By inertness one means that the selected metals must preserve their integrity during their clinical use. Human tissues and fluids can lead to corrosion phenomena due to the presence of corrosive species such as inorganic ions and oxygenated saline electrolytes. These phenomena can be potentiated by the physiological conditions, namely pH (6.5-7.5) and body temperature (37°C). In this context, metals such as platinum, iridium, and gold are ideal because generally more resistant to corrosion. However, episodes of electrode failure during the stimulation therapy are common and often associated to chronic tissue response and material encapsulation. The glial scar around the electrodes increases the tension forces at the interface exacerbating the inflammatory reactions and further impacting the corrosion resistance.

While still a matter of study, in recent years a great number of studies involving the use of molecular, biochemical and imaging technologies allowed to highlight the intricacies of biological reactions involved at the tissue-electrode interface (Gulino et al., 2021). Consequently, additional design optimizations are expected to be translated in the clinic to overcome these limitations, while maintaining performance of implantable electrodes. The manufacturing process requires a drastic rearrangement not only to promote the transition towards small-scale electrodes, but also to provide automated alternatives to manual assembling reducing costs and time. Miniaturization is in fact the biggest challenge for engineers because, if on the one hand the use of flexible conductive microelectrodes may be advisable, ensuring the same conductive performance of conventional electrodes, on the other hand becomes the main challenge. Such developments are discussed in more detail in the next section.

5. THE NEW GENERATION OF DBS ELECTRODES

The most recent generation of DBS electrodes used in the clinic has had tremendous success as evidenced by the clinical experience and the vast number of new approaches for disease treatment and monitoring. However, as discussed above, conventional electrode design displays physical and electrochemical constraints related to the characteristics of the hard materials employed and its size.

Hard metals and their alloys were selected for their conductivity, inertness as well as for stiffness, which makes the manual production feasible and simplifies implantation procedure. However, these characteristics cause several biological constraints and represent key technical challenges to overcome. As previously explained, the most effective approach is the decrease in size, but with conventional materials this would be at the expense of the increase in impedance and decrease in charge injection capacity. With this purpose, other approaches employing microfabrication techniques were explored to develop miniaturized electrodes with enhanced spatial resolution. Nevertheless, the evolution towards miniaturized devices is accompanied by new challenges, but their clinical use may provide tremendous advancements in terms of target specificity, minimal invasiveness, and durability (Pancrazio et al., 2017).

Implantable electrodes have been traditionally divided in two main categories: microelectrodes for recording applications with an area below 0.0001 cm^2, and conventional electrodes for DBS, with an area above 0.001 cm^2. This difference in areas is because for recording purposes electrodes must record small amplitude signals, while for DBS therapy electrodes need higher electrode voltages and current densities to enable charge transfer. As time progressed, however, this distinction became less evident thanks to the improvements in microelectrode performance, paving the way for their use also for DBS.

Microelectrode technology dates back to the second half of the 20^{th} century, in which single metal microwires made of platinum, iridium, platinum-iridium alloys and stainless steel were used as neurophysiological tools for scientists to record single-unit neural activity. Over the years, microwire arrays with insulating materials such as glass, polypyrrole or Parylene C were introduced to improve recording performance and material stiffness (Tsai and Yen, 2003; Lu et al., 2007; Bae et al., 2008). A great variety of microwire arrays configurations integrated with printed circuit boards have been developed to be used for neurophysiological studies on animal models, as well as for intraoperative human recordings and brain-machine interfaces, offering the possibility to record simultaneously hundreds of neurons (**Fig.5A, B**) (Lehew and Nicolelis, 2008). Further improvements also in microfabrication capabilities led to the development of silicon-based multi electrode arrays (MEAs).

At the beginning of the 80's, researchers from the university of Michigan developed the Michigan-style microelectrodes (BeMent et al., 1986). A typical Michigan microelectrode array is composed by a 15 mm thick silicon wafer with one or more 2 mm shanks produced with diffusion-based etch stops technology, insulated by a dielectric. On the top of one side of the device, conductive traces are

placed to link the recording contacts to the signal process circuitry. Such contacts are composed of iridium or gold and have an area of around 100 mm^2. Traces are insulated with dielectrics such as silicon dioxide/silicon nitride through chemical vapor deposition, and dielectrics are then insulated with polymeric layers of Parylene C or epoxylite (**Fig.5C**) (Thompson et al., 2020; Wang and Guo, 2020). Michigan probes with higher number of contact sites have been also developed on larger planar shanks, but their performance is affected by higher tissue damage due to the big size and geometry (**Fig.5D**) (Karumbaiah et al., 2013; Kozai et al., 2015b). Different configurations have been developed, from the single or multiple shanks to 3D high-density MEAs with increased target sensitivity (**Fig.5E**) (Perlin and Wise, 2008; Ludwig et al., 2011; Zardini et al., 2021a). The great advantage of Michigan- style MEAs over microwire arrays is the presence of multiple recording sites in the same shank, allowing simultaneous recording of surrounding neuronal cells.

The Utah MEA is another type of MEA developed at the Utah University. Unlike the Michigan array, this MEA is composed by an array of penetrating silicon microelectrodes obtained by glass reflow technique. It is mainly employed as recording tool and in neuroprosthetics for sensory-motor deficits, and it received FDA and CE approval in the first years of the 21st century. The first Utah MEAs were composed of an array with 100-shank electrodes that extended 1.5 mm, with gold platinum at the tip as recording contact (**Fig.5F**). Adjustments were implemented to improve electrochemical performance and durability, such as the use of sputtered platinum or iridium oxide instead of gold and platinum in the recording sites and the insulation with parylene C coating to prevent material dissolution. Over the years, different alterations in the design were developed, such as the slanted Utah array which has shanks with varying length to record and stimulate many fibers for chronic rehabilitative applications (**Fig.5G**). Further optimization and etching techniques led to the development of additional designs with higher number of shanks and different surface shapes to fit to specific nerve geometries (Sharma et al., 2011; Zardini et al., 2021b). Clinical trials involving the use of Utah MEAs as interface device have shown promising results in chronic rehabilitative applications, in which it was possible to restore volitional control of external devices such as robotic arms and hands (Hochberg et al., 2006; Flesher et al., 2019). Despite the remarkable success, electrochemical instability has emerged as frequent drawback due to the microelectrode damage, corrosion reactions and nervous tissue response (Prasad et al., 2014; Nolta et al., 2015; Barrese et al., 2016).

One of the main causes for these limitations is the mechanical mismatch that silicon-based materials and metals display due to their high young modulus. Consequently, other flexible materials have been also employed as substrates for microelectrodes.

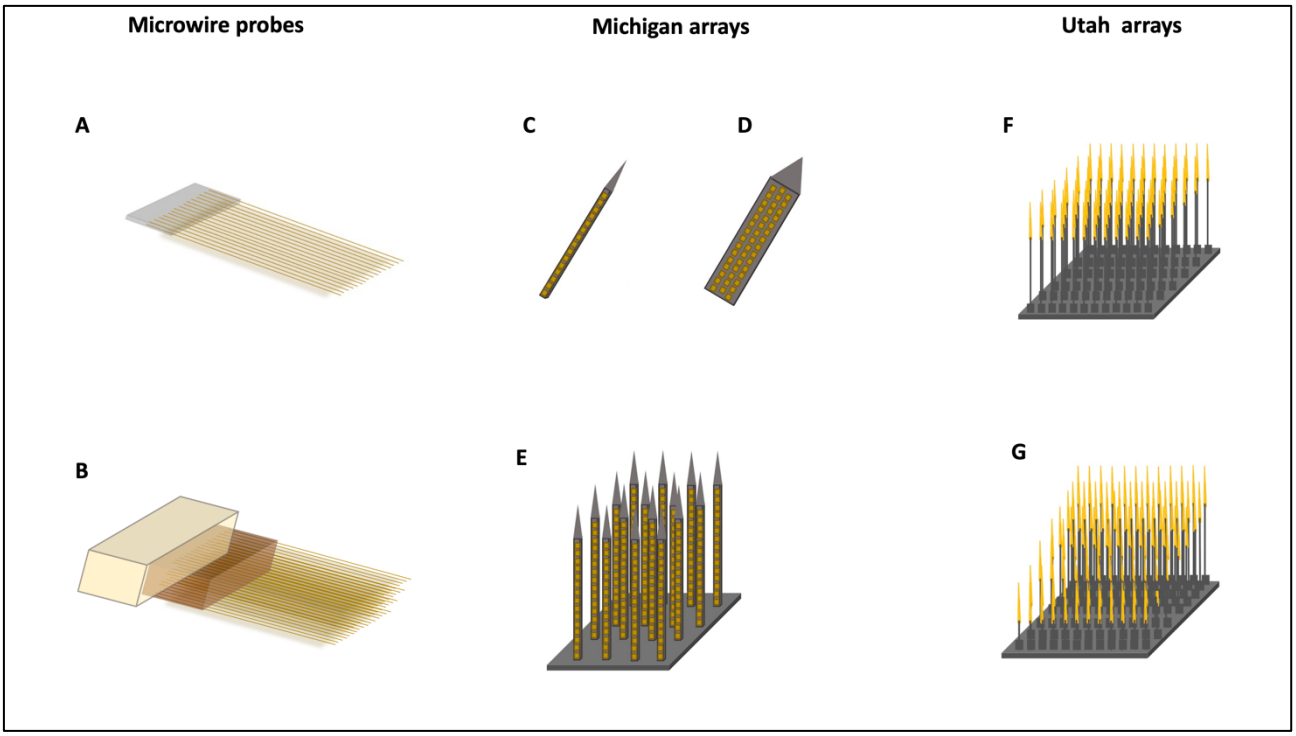


***Figure 5**. Microelectrode device configurations. **A**. Low density metal microwire bundles with insulating materials. **B**. High density metal microwire arrays connected with printed circuit boards. **C**. Single Michigan planar array with linear contact sites. **D** Michigan planar array with increased spatial coverage. **E** Michigan multielectrode array with 3D spatial coverage. **F**. Utah multielectrode array with 2D spatial coverage.100 contact sites at the tip of each shank. **G**. Slanted Utah array composed of 100 shanks with varying length.*

Polyimide is a synthetic polymer belonging to the class of plastics with interesting features for microelectrode design such as high flexibility, distinct biocompatibility and ease of manufacturing (Chen et al., 2009; Myllymaa et al., 2009). Parylene C is a thermoplastic polymer that has been largely employed as substrate material or coating for many biomedical implants. It displays good biocompatibility, chemical inertness and high dielectric strength (Golda-Cepa et al., 2020). Polydimethylsiloxane (PDMS) is a biocompatible silicon-based organic polymer with remarkable properties for several biomedical applications. It has low young modulus, excellent optical transparency, biocompatibility and resistance to biodegradation (Miranda et al., 2021). Thanks to these characteristics, these polymers have been employed for the production of flexible microelectrodes for recording and stimulating applications, not only for their use in the brain but also spinal cord as well as for neuroprosthetic devices (Lacour et al., 2010; Wang et al., 2010; Nandra et al., 2011). However, if on the one hand flexibility of these materials is attractive to reduce tissue damage and mechanical mismatch, on the other hand this has led to other problems related to their implantation. That is why these types of microelectrodes are often sandwiched with thin layers of

hard materials using photolithographic and deposition techniques to allow safe penetration and avoid displacement from the target site. Although very attractive, these polymers cannot entirely substitute hard metals and alloys as substrates for microelectrodes, especially due to their incomparable electrochemical properties for recording and stimulation applications. With this purpose, substantial research has been focused on proposing and developing innovative approaches to produce hard material-based devices with superior properties. These approaches involve the use of thin metal layers, soft conducting polymers (CPs), hydrogels, bioactive coatings and smart nanomaterials for the design of microelectrodes with improved softness and biocompatibility for long term performance.

The choice of the coating material and its properties determines the design, the application and the fabrication techniques, carrying the relative advantages and disadvantages. In the following chapters, the most promising materials as coating for the next generation of electrodes will be discussed (**Fig.6**).

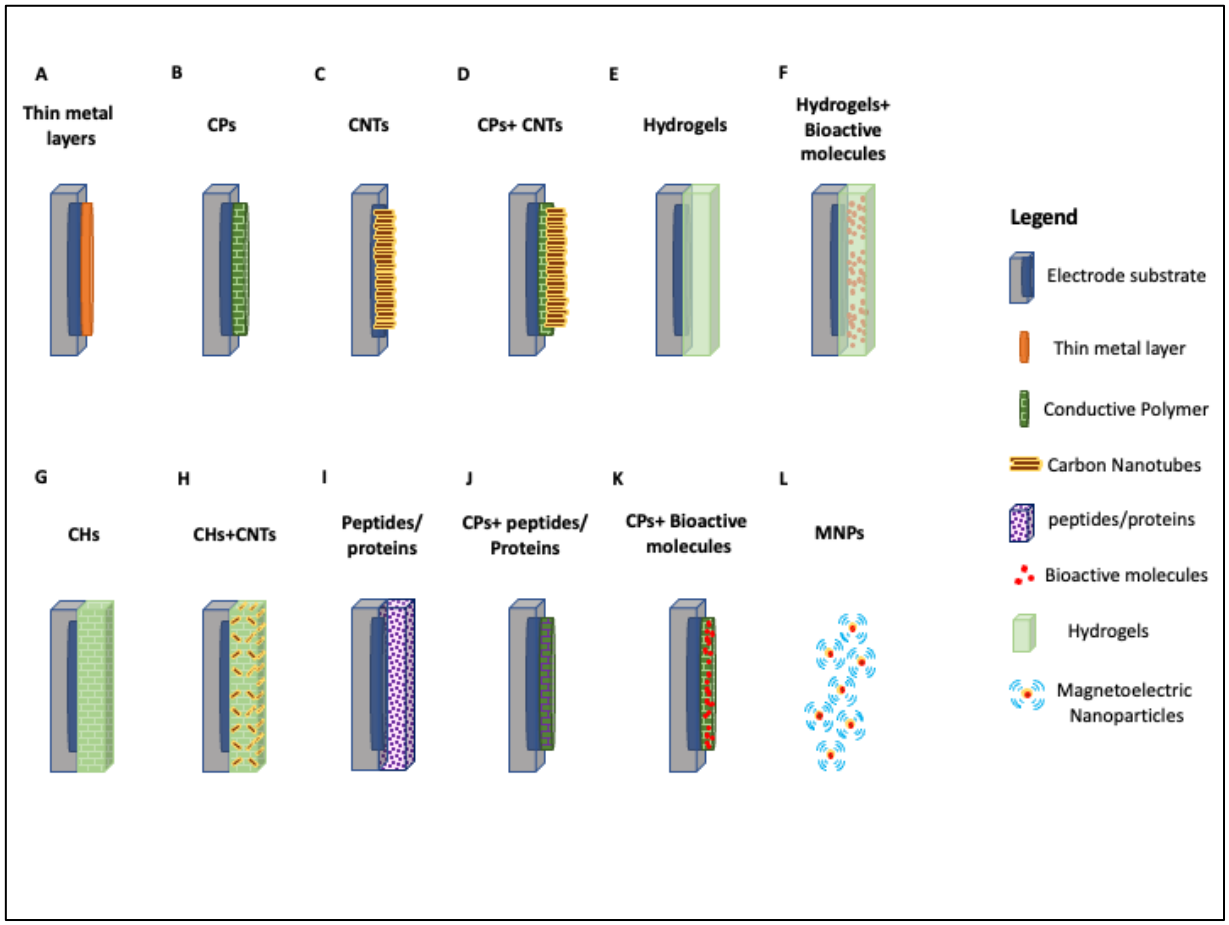


***Figure 6**. Scheme of the coating approaches and minimally invasive strategies employed to address the limitations of conventional deep brain stimulation (DBS) electrodes and caveats of microelectrodes. (**A**) Thin metal layer coatings on electrode substrates. (**B**) Conducting polymers (CPs) deposited on electrode substrates. (**C**) Carbon nanotubes (CNTs) deposited on electrode*

*substrates (**D**) CPs incorporating CNTs coatings deposited on electrode substrates. (**E**) Hydrogels as coatings deposited on electrode substrate (**F**) Hydrogels incorporating bioactive molecules deposited on electrode substrate (**G**) Conductive hydrogels (CHs) hybrid composites made of CPs and hydrogels deposited on electrode substrate. (**H**) CHs incorporating CNTs deposited on electrode substrate. (**I**) Cell adhesive peptides or proteins as coatings deposited on electrode substrates. (**J**) CPs incorporating peptides or proteins as dopants. (**K**) CPs incorporating bioactive molecules as dopants in deposited on electrode substrates. (**L**) Magnetoelectric nanoparticles (MNPs) for minimally invasive wireless DBS.*

5.1 THIN METAL LAYER COATINGS FOR MICROELECTRODES

As previously explained, the reduction in size of electrodes for DBS allows to decrease mechanical mismatch, glial cell activation, BBB injury and neuronal cell loss (Skousen et al., 2011). However, a smaller surface area reduces charge injection and storage capabilities. Moreover, this is inevitably accompanied by an increase in electrode impedance, leading to a non-efficient delivery of electric charge.

A strategy that is being adopted for microelectrode design with improved electrochemical properties for recording and stimulating application has been the use of metal ultrathin structures (**Fig.6A**). In this way, the reduction in thickness makes the metals more flexible and softer, displaying fewer mechanical differences compared to the brain tissue while maintaining the electrochemical properties.

Metals such as gold, platinum, iridium and their alloys were proposed as coatings for microelectrodes. Electrodeposition techniques have been proposed to produce metal nanostructured coatings in order to increase surface area. Particularly, electrodeposited platinum coatings have received remarkable attention for microelectrode design. This metal in the form of nanoparticles displays interesting surface physico-chemical properties to be used for several biomedical applications, such as remarkable electrical conductivity, high surface area, porosity and surface functionalization. The electrode deposition of nanostructured platinum coating has been shown to provide increase in surface roughness, with consequent drop in electrode impedance by two orders of magnitude on microelectrodes, offering the possibility to further reduce size and obtain superior spatial resolution (Boehler et al., 2015). Platinum-iridium-based coatings have been proposed to produce chronically implanted MEAs with improved electrochemical performance thanks to low impedance, reduced noise and increased signal-to-noise ratio (Petrossians et al., 2011; Cassar et al., 2019). Nanoporous gold has been also explored as coating for microelectrodes as it offers great advantages in terms of

design thanks to the high conductivity and surface area-to-volume ratio. The application of nanoporous gold with metal deposition techniques has been shown to provide lower impedance, higher charge injection capacity on MEAs for stimulating and recording applications (Seker et al., 2010; Kim et al., 2015). Moreover, gold surface nanotopography has been shown to reduce glial cell response while maintaining high neuronal cell adhesion (Chapman et al., 2015).

The use of metals as coating for microelectrodes represents a valuable method for taking advantage of the electrochemical properties of hard materials whose flexural rigidity has been reduced to minimize mechanical mismatch. However, additional improvements can be achieved to get even more closed to the young's modulus of the brain tissue. This aspect is really important in view of developing neural interfaces that maintain suitability during long-term applications. The use of soft, flexible conductive materials as coatings has been proposed and may represent the most effective alternative to provide the same electrochemical performance of metals while displaying enhanced biocompatibility and safe tissue integration.

5.2 *CONDUCTING POLYMER COATINGS FOR MICROELECTRODES*

Stiffness of conventional DBS materials is one of the principal causes of nervous tissue response and glial scar formation. The metals and alloys employed for electrode design are much stiffer than brain tissue and their surface morphology does not promote the most compatible and safe tissue integration (Chitrakar et al., 2022). With this purpose, substantial research has been focused on proposing a wide range of soft materials for the fabrication of miniaturized devices. Organic materials represent the most favored choice for next-generation neural interfaces. In this context, conducting polymers (CPs) have attracted substantial interest as coating materials for miniaturized devices (**Fig.6B**) (Green and Abidian, 2015). CPs are organic polymers that conduct electricity due to the presence of conjugate π-bonds. Conductivity can be obtained by the addition of dopants to the electrolytic solution during synthesis. They represent an ideal material for neural interfaces for several reasons. In the first place, their better flexibility and softness allow minimizing substantially tissue response. Because of this, impedance is also reduced, allowing their use for both stimulation and recording applications. The synthesis process, which is mainly electrochemical polymerization, has low processibility costs. Moreover, it is possible to tune physicochemical properties with doping techniques in course of synthesis and functionalize them to improve biocompatibility.

Among the CPs, polythiophene (PTh), poly-3,4-ethylene dioxythiophene (PEDOT) and polypyrrole (PPy) have been the most commonly used polymers for the development of neural interfaces. PTh is a CP with great potential as coating material for several biomedical applications (Mousavi et al., 2021). It is composed of polymerized sulfur heterocycles linked through the 2- and 5-positions. PTh has peculiar optical properties and great electrochemical stability. However, the most important characteristic is the high doping level, which allowed the design wide range of modified conjugates. Chen and colleagues developed a new strategy using an anionic surfactant to allow interaction of PTh chains with polyethylene glycol chains. This optimized composite showed higher conductivity, tensile strength and flexibility compared to PTh alone, paving the way to its use for flexible electronics (Chen et al., 2019). PEDOT, a derivative of PTh, is the most commercially successful polymer thanks to its high conductivity, chemical stability and excellent proven biocompatibility (Asplund et al., 2009; Starbird et al., 2013). However, due to its low mechanical stability and rigidity, PEDOT has been proposed in combination with other materials. In particular, sodium polystyrene sulfonate (PSS) has been employed as doping agent as it greatly enhances film-forming properties, transparency and flexibility, making it an excellent material for applications in biomedical devices and bioelectronics. PEDOT:PSS Coatings of PEDOT:PSS on metal microelectrodes has been shown to provide higher stability and stimulation capacity through improvement in charge injection capacity and reduction in impedance (Pranti et al., 2018). In the context of recording microelectrodes for neural prosthetics, PEDOT:PSS deposition on platinum-iridium microwires has been shown to provide higher signal-to-noise recordings in vivo and an extensive increase in charge injection capacity (Venkatraman et al., 2011). Recent investigations also reported a downregulating effect on glial cell activation while keeping intact the functional properties of the neuronal network (Cellot et al., 2016). PPy is another common CP that shares some characteristics with PEDOT:PSS. It is composed of five heterocyclic pyrrole rings and produced through electrochemical or chemical oxidation polymerization techniques. PPy displays good electrical conductivity, good stability in ambient conditions and biocompatibility. Similarly to PEDOT:PSS, it has been investigated as coating for neural electrodes for improving capacitance, reducing impedance while promoting neurite outgrowth (Lu et al., 2010).

The functionalization of CPs with biological or synthetic polymers has been further proposed for the development of coatings with improved mechanical properties and cellular interactions for neural interfaces (Hackett et al., 2017). Chitosan, a linear polysaccharide obtained by deacetylation of chitin extracted from the shell of shrimps and crustaceans among other sources, is a widely known material

with excellent mechanical properties and biocompatibility that has been employed for a great variety of biomedical applications including the development of nanomaterials, drug delivery systems and biomedical implant devices. The use of chitosan in combination with CPs has been explored for the design of electrically conductive scaffolds for neural tissue engineering and interfaces. Incorporation of PEDOT into chitosan/gelatin porous scaffolds has been shown to improve electrical conductivity, hydrophilicity, thermal and mechanical properties, as well as to promote adhesion, proliferation, and neurite outgrowth of rat pheocromocytoma PC12 cells (Wang et al., 2017). Similarly, Du and colleagues recently designed shell-core PEDOT/chitosan nanofibers for cell electrical stimulation. These nanofibers exhibited excellent biocompatibility low impedance, electrochemical stability, high charge storage capacity and piezoelectric properties. Thanks to these unique characteristics, these nanofibers have been shown to electrically and piezoelectrically stimulate brain neuroglioma cells promoting neurite outgrowth, proliferation and migration (Du et al., 2020)

Kim and co-workers developed a copolymer composed of PPy and polydopamine, a nature-inspired synthetic polymer with attractive properties for neural interface design (Kang et al., 2011), as coating to improve performance of microelectrodes for electromyography. The combination of these polymers has been shown to enhance electrochemical properties, promote neurite outgrowth and differentiation of PC12 neuronal cells, as well as successful in vivo recording of electromyography signals (Kim et al., 2018a). Moreover, the same group developed biomimetic PPy-based films incorporating low molecular weight hyaluronic acid, showing the ability to support fibroblast and neuronal cell growth in vitro as well as improved in vivo biocompatibility and recording performance (Kim et al., 2018b).

CPs provide countless options for improving biocompatibility, reliability and long-term performance of neural interfaces, and represent one of the most valuable tools to solve the limitations of miniaturized devices and finally actualize their translation to the clinics. Thanks to their ease of modulation and functionalization, and in consideration of the constantly growing variety of materials developed for neural applications, it is expected that future designs will involve more sophisticated polymer compositions for a more efficient management of mechanical, electrochemical and biological properties.

5.3 CARBON-BASED MATERIALS FOR MICROELECTRODES

An attractive strategy that was adopted to improve flexibility and electrochemical properties of miniaturized neural interfaces has been the use of carbon-based materials (**Fig.6C**). Graphene has emerged as one of the most studied materials for a multitude of biomedical applications such as drug delivery, cancer therapy, theranostic and neural interfaces (Kitko and Zhang, 2019; Song et al., 2020). It consists of a monolayer of carbon atoms organized into a hexagonal lattice structure (Kostarelos et al., 2017). This material displays interesting physical properties for microelectrode design such as flexibility, low resistance and optical transparency (Xu et al., 2021) as well as excellent biocompatibility, which is strictly dependent on the synthesis process (Reddy et al., 2019). Its use has been explored for the production of fully carbon electrode arrays and coatings for recording and stimulation applications (Apollo et al., 2015; Park et al., 2018; Bourrier et al., 2019). Besides the 2D forms of graphene, several types of 3D nanostructures have been developed and have attracted remarkable interest as they can provide additional characteristics for microelectrode design, such as improved mechanical properties, cell supportive characteristics and biocompatibility.

Among the variety of 3D structures, carbon nanotubes (CNTs) have been extensively employed as coating for microelectrodes thanks to their excellent conductivity, high surface area, mechanical strength and ease of functionalization (Voge and Stegemann, 2011) CNTs are cylindrical molecules composed of rolled-up sheets of a single layer of graphene. They can be in the form of single-walled or multi-walled, with diameters ranging from less than 1 nm to 100 nm respectively. Several techniques can be used for CNTs synthesis and can be divided into 2 main categories: the “growth-then-place” techniques, such as arc discharge and laser ablation, which consist in the synthesis of CNTs followed by their transfer on a substrate, and the “growth-in-place” technique, such as chemical vapor deposition, in which CNTs are directly synthesized in the substrate. Arc discharge consists of heating graphite at high temperatures close to its melting points, in absence of oxygen and with metals as catalysts. Laser ablation consists of the vaporization of graphite through pulsed lasers inside a high-temperature reactor filled with inert gas. The CNTs are produced when the vaporized carbon condenses. This technique has a higher yield compared to arc discharge. Chemical vapor deposition is considered the most suitable technique for CNTs synthesis in neural electronics, thanks to the possibility to grow them in predefined substrates. It consists of the catalytic decomposition of carbon-containing gases on transition metal catalysts (Nessim, 2010). Extensive studies were conducted to investigate the cell-supportive characteristics of CNTs. CNTs grown on silicon substrates through chemical vapor deposition technique have been shown to support primary neuronal cell growth and

to increase electrical activity of the neuronal network (Rago et al., 2019). CNT-multilayered nanocomposites have been also shown to promote neural differentiation, neurite outgrowth and electrophysiological maturation of neural stem cells-derived neurons (Shao et al., 2018). CNTs coatings have been recently employed as coating for microelectrodes for recording and stimulation applications, as well as for the detection of neurochemicals.

The use of CNTs in combination with CPs has emerged as a strategy to improve porosity and, consequently higher surface area of microelectrodes (**Fig.6D**). PPy and CNTs composites coatings for platinum/tungsten microelectrodes have been shown to reduce impedance while inducing superior signal to noise ratio during in vivo recordings (Baranauskas et al., 2011). Composite coatings composed of PEDOT and CNTs have been shown to provide higher capacitance and charge injection capacity compared to PEDOT coating alone on gold MEAs. The association of the two materials provided excellent biocompatibility in vitro. Moreover, the signal-to-noise ratio was improved during signal recording, as well as stability of charge injection capacity during long-term pulsing experiments (Gerwig et al., 2012). Carli and co-workers electrodeposited oxidized single-walled carbon nanohorns in conjunction with PEDOT:PSS on gold MEAs for recording and stimulation applications. In vitro and in vivo studies reported good biocompatibility, as well as higher charge storage and injection capacity thanks to increased electroactive surface area. Good recording performance and long-term material and impedance stability during electrical stimulation were reported, indicating that this composite coating can be ideal for designing microelectrodes capable of recording and stimulating neurons in vivo (Carli et al., 2018).

Despite the promising electrical, physical and biological properties of CNTs for neural interface applications, some concerns remain regarding their biocompatibility. In the literature there are contrasting results (Liu et al., 2008; Belyanskaya et al., 2009; Haniu et al., 2010; Galassi et al., 2020) and this can also be due to the several synthesis methods developed, the various nanostructures and their use as dispersion or attached to a substrate. This is mainly due to the lack of long-term in vivo studies, which will be necessary to provide new insights on their biosafety and toxicity profiles.

5.4 HYDROGEL COATINGS FOR MICROELECTRODES

Chemical inertness has been one of the principal characteristics for which hard metals were employed for conventional electrodes. However, it also represents one of the main causes of suboptimal in vivo

performance. On the one hand this characteristic brings the advantage of stability and resistance to degradation, on the other hand it is a factor of neuronal cell damage and glial cell activation in response to a detected “foreign body”. An ideal material interfacing with biological tissues must promote a stable neuronal cell interaction at the target site and minimize inflammatory cell activation. To achieve this, an important aspect on which it is pivotal to intervene is the reduction of the young modulus of the interfacing material that should be as similar as possible to the one of the nervous tissues. Thereby, the use of hydrogels has been proposed as coatings for microelectrodes (**Fig.6E**). Hydrogels are hydrophilic polymeric systems whose structure is held by physical or chemical crosslinks. These polymeric networks were extensively employed in several biomedical application fields, ranging from tissue engineering to drug delivery and regenerative medicine. More recently, the use of hydrogels has been investigated as coating for microelectrodes to achieve a great number of objectives, such as the minimization of the mechanical mismatch, biological functionalization for the delivery of bioactive molecules or drugs and improvement of microelectrode performance (Hyakumura et al., 2021).

Hydrogels can be fabricated from natural materials, synthetic materials or a combination of both. Natural derived materials display cell-supportive characteristics thanks to the presence of bioactive elements. Moreover, they are also biodegradable without release of toxic compounds, making them excellent candidates for providing long-term safety. Natural hydrogels composed of extracellular matrix (ECM) molecules such as collagen (Liu et al., 2011), hyaluronic acid (Yue et al., 2011), fibrin (Castagnola et al., 2013), laminin (Frick et al., 2017) have been explored as coatings for neural electrodes. The main aim of this approach is to promote physiological interactions between surrounding cells and material surface, stimulate neuronal cell attachment and reduce mechanical mismatch. In vivo studies on animal models were conducted to investigate the potential of biomimetic ECM coatings for neural electrodes. ECM components such as collagen I, fibronectin, laminin and mixtures containing other ECM constituents in the form of hydrogels showed to be beneficial on reducing astrogliosis and inflammation caused by intracortical microelectrodes without altering electrochemical properties and signal fidelity (Shen et al., 2018; Vitale et al., 2018; Bas et al., 2019).

Despite nature-derived hydrogels providing superior biocompatibility and safety for long-term applications, they lack long-term stability due to their high biodegradability. For this purpose, the use of synthetic hydrogel materials for neural interfaces has also been proposed. Synthetic materials such as polyethylene glycol (PEG)(Rao et al., 2012), poly(vinyl alcohol) (PVA)(Lu et al., 2009) and polyacrylamide (Shur et al., 2020) were extensively investigated for developing stable electrode

coatings. Although more stable and tunable, synthetic materials display lower biocompatibility than natural materials. However, the most important aspect is the possibility to functionalize them through chemical crosslinking groups and tunning the hydrogel network for better control of mechanical properties or biological functionalization with bioactive molecules to achieve higher biocompatibility (**Fig.6F**) (Mario Cheong et al., 2014; Mauri et al., 2018). As an example, synthetic hydrogels embedded with anti-inflammatory drugs were proposed as smart coatings to improve electrode biocompatibility and, at the same time, mitigate tissue inflammation (Zhang et al., 2015; Heo et al., 2016).

Although beneficial in providing softness and biocompatibility, natural and synthetic hydrogels do not directly improve electrode performance due to their poor conductivity. Another strategy that was recently advanced to improve hydrogel functionality is to combine them with CPs to produce hybrid composite materials called conductive hydrogels (CHs) (**Fig.6G**). This approach provides the opportunity to maintain the electrical characteristics of the CP coating and, contemporarily, include the beneficial properties of hydrogels necessary for excellent neural electrodes (Stejskal, 2017). Su and colleagues recently developed a PPy-heparin-collagen CH as film for neural scaffold. PPy was first conjugated with heparin and then collagen was crosslinked to PPy. The obtained film maintains conductivity while displaying improved mechanical stability and biocompatibility (Su et al., 2019). Similarly, Shur and co-workers developed a soft electrode coating composed of polyacrylamide and PEDOT:PSS deposited on a microelectrode array for electrocorticography. The CH coating confers softness to the microelectrode surface, promotes in vitro neural cell attachment and proliferation and electrochemical stability during in vivo recordings (Shur et al., 2020).

Alginate, a natural linear copolymer with excellent biocompatibility, low toxicity, ease of functionalization and structural similarities with the mammalian ECM, was recently employed in combination with PEDOT:PSS for the synthesis of a CH as coating for microelectrodes and for neuroregenerative applications. The CH has been shown to confer improved electrochemical properties, reduced signal-to-noise ratio for recording applications, it is non-toxic for neural cells and has a softness really close to the brain tissue (Ferlauto et al., 2018; Perkucin et al., 2022).

Wang and colleagues recently developed a similar hybrid CH composed of PEDOT:PSS, CNTs and alginate (**Fig.6H**). This composite material has been shown to display good biocompatibility in vitro. Moreover, it conferred high charge storage capacity (CSC) and lower electrochemical impedance to

metal microwires. These characteristics make it an excellent coating for microelectrodes for both recording and stimulating applications (Wang et al., 2019).

CHs have been shown to be candidate materials for promoting the transition towards small-scale neural electrodes, as they can mediate the mechanical properties and simultaneously enhance the electrochemical performance.

Engineers have today at their disposition a vast choice of CPs and hydrogels to test in order to address the limitations of conventional materials by reducing size, mechanical mismatch, young modulus and increasing biocompatibility. However, it is important to highlight that these results, despite promising, are not exhaustive and further research is required to investigate the mechanisms of incorporation of CPs with hydrogels, the most effective composites and the suitability for in vivo performance.

5.5 COATINGS WITH BIOACTIVE MOLECULES

To improve communication between neuronal cells and foreign materials, the use of biological molecules such as cell adhesion molecules, drugs and growth factors in some of the coating technologies employed has been proposed. The main strategy adopted in this perspective has been the use of extracellular matrix (ECM) proteins as temporary or resorbable coatings to stimulate neuronal cell attachment, improve biocompatibility and reduce glial scar formation (**Fig.6I**). In vivo studies reported that ECM-based coating design allows reduction of mechanical mismatch, with consequent reduction of inflammatory response while maintaining electrochemical performance of microelectrodes (Shen et al., 2015). The use of decellularized ECM harvested from animal tissues has been also investigated. Ceyssens and colleagues deposited thin films of ECM proteins extracted from porcine gut tissue to coat flexible microelectrocorticographic implants. The coating has been shown in vivo to ease the implantation procedure making the polyimide-based electrode arrays temporarily less flexible, without impacting glial cell activation and neuronal viability (Ceyssens et al., 2017). Another coating strategy that has been proposed is the use of cell-derived ECM. Oakes and colleagues developed an ECM coating derived from primary rat astrocytes that was employed as coating for silicon MEAs. The coating significantly reduced the level of astrogliosis in in vivo rat animal models 2 months after implantation and determined suppression of macrophage activation (Oakes et al., 2018).

Since glial cell activation and encapsulation are considered the most important factors on determining the decrease in microelectrode performance in vivo, several efforts have been done by scientists to identify other proteins capable of mitigating these reactions and ensuring effective integration with the surrounding neuronal tissue. Cell Adhesion Molecule L1 is a neuronal adhesion protein that emerged as a potential candidate for this purpose. This transmembrane protein is involved in several physiological processes including neuronal cell migration, neurite outgrowth, axonal integrity and differentiation (Sytnyk et al., 2017). Its use as coating for microelectrodes has been investigated. In vivo studies on rodent animal models in which microelectrodes were implanted in the spinal cord and dorsal root ganglion demonstrated its efficacy on promoting neuronal density and viability at the tissue-electrode interface (Kolarcik et al., 2012). Moreover, additional in vivo studies on rodent animal models reported reduction of surface adhesion of microglia in the vicinity of implanted silicon neural probes as well as reduced morphological activation of microglia far from the implantation site (Eles et al., 2017).

Single ECM components or peptides/proteins were also investigated as coating for microelectrodes such as laminin, fibronectin and collagen (Volkenstein et al., 2012; Ng and O'Hare, 2015; Sikder et al., 2021). The aim of these approaches is the promotion of neuronal attachment and neurite outgrowth with the simultaneous reduction of fibroblasts and glial cell attachment. Hyaluronic acid, a major ECM component, has attracted remarkable interest among other ECM proteins thanks to its hydrophilicity, biocompatibility and resistance to cell and plasma proteins adhesion. Its use in the context of microelectrodes has been employed in conjugation with CPs to reduce fibroblasts and astrocytes adhesion without hampering electrochemical properties both in vitro (Lee and Schmidt, 2010) and in vivo (Lee et al., 2015) (**Fig.6J**). By exploiting the possibility to functionalize coating materials proposed for microelectrodes in the course of synthesis, the incorporation of peptide sequences in CPs or CNTs has also been proposed. Covalent bonding of ECM peptide sequences such as the laminin-derived peptide (YIGSR) and Arginyl-glycyl-aspartic acid (RGD), or synthetic polypeptides such as poly(D-lysine) (PDL) have been employed to improve biocompatibility, neuronal cell adhesion and growing without modifying electrochemical performance of the neural interface (Wang et al., 2015; Ghane-Motlagh et al., 2016; Li and Yu, 2017).

Another approach that has been investigated is the incorporation of bioactive molecules in CPs as dopants during the CP synthesis (**Fig.6K**) for the production of CPs with superior biocompatibility, mechanical properties and cellular interactions. Co-incorporation of laminin peptide sequences as

dopants in PEDOT with entrapped nerve growth factor (NGF) during electrodeposition was proposed as a strategy to create a polymer capable of stimulating neurite outgrowth. The new polymer has been shown to display higher softness and preservation of NGF biofunctionality as confirmed by promotion of neurite outgrowth on in vitro PC12 cells. However, electrochemical stability and film adherence decreased (Green et al., 2010).

Another strategy to reduce inflammatory response is the incorporation of anti-inflammatory drugs. Dexamethasone is a potent glucocorticoid that has been investigated to attenuate the nervous tissue response to microelectrodes (Kozai et al., 2016; de la Oliva et al., 2018). CPs coatings embedded with dexamethasone have been developed to allow controlled release after implantation toward the mitigation of neuroinflammation. In vivo studies on rodent animal models reported that these multifunctional coatings consent effective drug release in the surrounding neuronal tissue, determine substantial decrease in nervous tissue response, improvements in charge storage capacity and impedance, as well as the potential to keep the glial scar formation to a low level in long term implantations (Mercanzini et al., 2010; Alba et al., 2015; Boehler et al., 2017).

Goding and colleagues developed a biofunctionalized PEDOT by co-doping with dexamethasone, and valproic acid, the latter being an anticonvulsant drug for epilepsy with evidenced neuroprotective and neuroregenerative properties (Biermann et al., 2010; Silva et al., 2018). Despite the polymers displayed minimal decrease in charge storage capacity and increase in impedance, the bioactivity of the two drugs was preserved and determined a decrease in the levels of the pro-inflammatory cytokine tumor necrosis factor-α (TNF-α) in in vitro primary mixed cultures of microglia and astrocytes (Goding et al., 2015).

Like dexamethasone, minocycline, an antibiotic with anti-inflammatory and neuroprotective properties, has been recently explored to produce controlled drug-release coatings with therapeutic effects. In vivo studies on rodent animals have reported its potential application for the reduction of nervous tissue response by minimizing microglial and astrocytic activation (Olczak et al., 2019; Holmkvist et al., 2020).

In light of the presented findings in the literature, the incorporation of bioactive molecules is emerging as a promising option to develop multifunctional coatings that ensure improved and stable performance and, at the same time, can further minimize the disparity between the implant and the brain tissue. Their integration can be attained in ways that do not interfere with the electrochemical

properties provided by the coating materials and, in addition, can potentially allow reduction in electrode impedance thanks to the mitigation of the formation of the glial scar and efficiency of recording/stimulation by promoting neuronal attachment.

However, this approach carries other challenges as the fabrication process may undergo drastic changes accompanied by additional costs to provide the scale-up for their broad use. Moreover, it is still uncertain if these strategies will be effective when translated to human patients. In the case of the use of drugs-releasing coatings, due to the small surface area it is still unknown if their amount will be enough in humans to exert the same positive effects that have been observed in rodent animal models. The studies conducted so far have shown positive improvements in short and long term (from days to months), but it is still unknown if they will persist in chronic (years) applications. Therefore, further experiments will be pivotal to assess which are the best strategies among the ones that have been proposed and concretize their suitability for the clinics.

5.6 MAGNETOELECTRIC NANOPARTICLES FOR NON-INVASIVE DEEP BRAIN STIMULATION

While in the last 10-20 years we assisted in substantial improvements in design, target specificity, biocompatibility and durability of conventional electrodes and microelectrodes, invasiveness of the neurosurgery remains a problem to solve in both cases. The use of microelectrodes for neuromodulation is not the only strategy that has been explored. Transcranial magnetic stimulation and transcranial direct current stimulation are non-invasive FDA-approved therapies for the treatment of psychiatric dysfunctions such as depression and schizophrenia. However, these therapies have poor spatial resolution and cannot reach deep brain areas as in DBS, which limit their clinical applications. Nevertheless, recent advances in nanotechnology provided revolutionary opportunities for neuroscientists to exert DBS in minimally invasive ways without the use of microelectrodes.

Magnetoelectric nanoparticles (MNPs) are a new class of smart nanomaterials that has been proposed as minimally invasive approach for DBS (**Fig.6L**). MNPs are composed of a ferromagnetic core and a ferroelectric shell. The core is usually composed of ferroic materials such as metallic oxides or ferrites that are magnetostrictive. Magnetostriction is a property of certain ferromagnetic materials consisting of a change in shape or dimensions in response to a magnetic field. Namely, magnetostrictive materials convert electromagnetic energy into mechanical energy and vice versa.

The shell is mainly composed by piezoelectric polymers or piezoceramics. Piezoelectricity is the conversion of mechanical energy into electrical energy and vice versa. The magnetoelectric coupling effect is obtained by the association of magnetostrictive and piezoelectric materials: when subjected to a magnetic field, the ferromagnetic core expands its area or shrinks. This mechanical strain occurring at the interface is converted into electric energy by the piezoelectric shell, generating an electric field (**Fig.7**). Thanks to this unique property, MNPs emerged as a potential solution to exploit remote control of neural activity in deep brain areas through the generation of localized electric fields in a minimally invasive way. Besides the magnetic and piezoelectric properties, an important requirement for these nanosystems is that they display good biocompatibility over time.

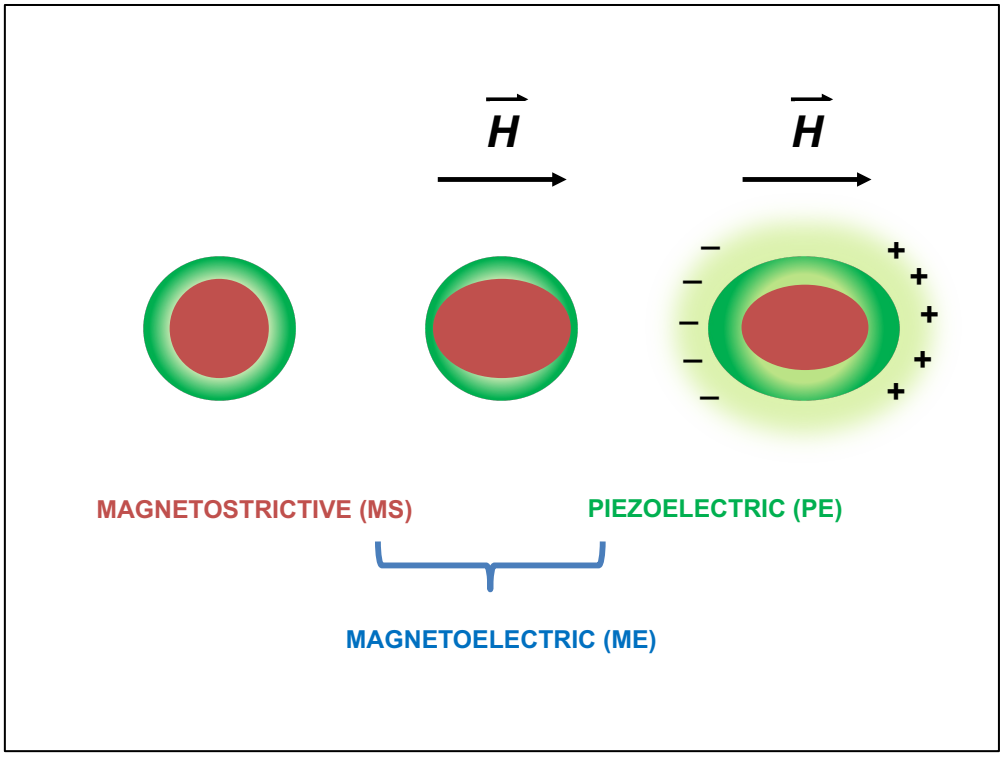


***Figure** 7. Schematic showing the structure of core-shell magnetoelectric nanoparticles composed of a magnetostrictive core and a piezoelectric shell. When subjected to an external magnetic field, the expansion of the core generates is converted into electrical energy from the piezoelectric shell. Redrawn with permission from (Kozielski et al., 2021)*

Various core-shell MNPs, differing in the type of magnetic and piezoelectric components employed were developed. Iron oxide (IO) has been widely explored for a wide range of biomedical applications (Maldonado-Camargo et al., 2017), and it was proposed as an ideal core for MNPs thanks to its good biocompatibility and high magnetostriction. Magnetoelectric IO NPs were proposed in association

with barium titanate (BTO) as shell for wireless electrical stimulation and regeneration. BTO arose great interest for this perspective thanks to remarkable piezoelectric properties other than biocompatibility. Zhang and colleagues developed a collagen hydrogel loaded with IO-BTO NPs capable of promoting neural differentiation in vitro and expression of differentiating proteins. Moreover, the hydrogel has demonstrated the ability to induce wireless electrical stimulation via magnetoelectric effect on in vivo rodent models of spinal cord injury and to promote recovery (Zhang et al., 2021b). However, IO NPs decrease their magnetic properties with a decrease in size, and their use in the CNS may cause iron accumulation, oxidative stress and protein aggregation in neural cells (Yarjanli et al., 2017).

Cobalt ferrite (CFO) NPs have also been widely employed as core for MNPs. Like IO NPs, CFO NPs display very attractive properties for biomedical applications. They have been in fact proposed for biosensing applications, drug delivery and diagnostic imaging (Srinivasan et al., 2018). Thanks to their high magnetic anisotropy, coercivity and magnetostriction, CFO NPs have been greatly employed as core for MNPs. Different groups explored the magnetoelectric coupling effect CFO and BTO for other applications such as drug delivery and cancer treatment (Rodzinski et al., 2016; Shahzad et al., 2021). CFO-BTO NPs demonstrated efficacy to achieve in vitro wireless neural stimulation with induction of calcium transients with a similar extent compared to traditional electrical stimulation using microelectrodes (Zhang et al., 2022). Moreover, studies employing in vivo rodent animal models reported the capability of CFO-BTO NPs to cross the BBB, to be moved to a specific brain district using a magnetic field gradient, and to finally evoke cortical neuronal activity wireless induced neural activity through evoked calcium spikes (Guduru et al., 2015; Nguyen et al., 2021).

Another interesting material with remarkable piezoelectric properties to be used as shell for MNPs is bismuth ferrite (BFO) (Hojo et al., 2018). CFO-BFO NPs have been shown to be capable of wirelessly stimulating neuronal-like cells in vitro promoting cell differentiation (Chen et al., 2019b), as well as enhancing bone cell proliferation (Mushtaq et al., 2019). Recent in vivo studies on rodent animal models reported efficient tumor therapy through wireless CFO-BFO NPs stimulation and generation of cytotoxic reactive oxygen species (ROS)(Ge et al., 2021). To the best of our knowledge, no in vivo studies exploring the potential of CFO-BFO NPs for neural stimulation were conducted. Besides the above-reported core-shell nanostructures, other materials with high piezoelectric coupling coefficient and biocompatibility such as piezoelectric ceramics (Poon et al., 2020), polymer-based materials

(Gonçalves et al., 2015) and their composites (Rosso et al., 2022) have attracted remarkable interest for biomedical applications and it is expected to see their use for MNPs design.

The studies so far reported on MNPs reveal the great potential that may provide in the clinics to finally overcome the problem of invasiveness of the therapy, which has always been the main caveat for implantable microelectrodes, improve efficacy and patient compliance. However, this technology is still in its infancy, and massive investigations are necessary to assess its suitability for clinical translation. Moreover, as for new classes of materials and technologies, robust biocompatibility screenings using more complex in vitro, ex vivo models followed by long-term in vivo studies must be conducted at the preclinical level to move forward with the most efficient materials and assess their safety and durability.

6. CONCLUDING REMARKS

DBS technology took its first steps in clinical practice at the end of the last century. Since then, technological innovations and updates have led to an unprecedented expansion, offering new treatment opportunities for a constantly increasing number of diseases and dysfunctions, as well as for improving patients' quality of life and clinical outcomes. Much of this success has been achieved by the substantial efforts invested in preclinical and neurophysiological studies to shed light on its mechanisms and on the characterization of the effects in the various pathological contexts in which DBS is applied. This wouldn't have been possible without the extraordinary progress in electrode technology. Advances in electrode design, software and hardware led to great improvements in the target specificity of neuromodulation with minimized side effects, as well as in the sensitivity and stability of recording brain activity in physiological and pathological contexts.

In the last decades, a constantly increasing number of materials have been developed and proposed to enhance electrochemical performance of electrodes and to promote the transition towards device miniaturization. However, to develop a neural interface that is reliable, durable and safe for long-term applications, it is paramount to establish the interplay between electrochemical and biological performance. A multitude of design approaches involving the use of thin metallic films, conductive polymers, carbon-based materials, hydrogels, bioactive coatings and minimally invasive approaches have been proposed and investigated, but their real potential is not completely understood and the majority of them has not been translated to the clinic. Accurate studies are still required to evaluate the different technologies and propose new directions on which these materials will provide the most

favorable characteristics for future devices. An important aspect on which it is imperative to focus the efforts is the process of nervous tissue response, whose complexity of biochemical and chemical events is not completely investigated, but that it is pivotal to uncover in order to develop new materials and technologies. Hence, the use of biological model systems and platform technologies with increased complexity represents a fundamental tool to provide advanced strategies to understand and counteract the process of nervous tissue response, accelerate electrode device development and promote their translation from the bench to the bedside.

REFERENCES

Alonso, F., Latorre, M. A., Göransson, N., Zsigmond, P., and Wårdell, K. (2016). Investigation into deep brain stimulation lead designs: a patient-specific simulation study. *Brain Sci* 6, 39. doi: 10.3390/brainsci6030039.

Alosaimi, F., Boonstra, J. T., Tan, S., Temel, Y., and Jahanshahi, A. (2022). The role of neurotransmitter systems in mediating deep brain stimulation effects in Parkinson's disease. *Front Neurosci*. doi: 10.3389/fnins.2022.998932.

Apollo, N. v, Maturana, M. I., Tong, W., Nayagam, D. A. X., Shivdasani, M. N., Foroughi, J., et al. (2015). Soft, Flexible Freestanding Neural Stimulation and Recording Electrodes Fabricated from Reduced Graphene Oxide. *Adv Funct Mater* 25, 3551–3559. doi: 10.1002/adfm.201500110.

Ashkan, K., Rogers, P., Bergman, H., and Ughratdar, I. (2017). Insights into the mechanisms of deep brain stimulation. *Nat Rev Neurol* 13, 548–554. doi: 10.1038/nrneurol.2017.105.

Asplund, M., Thaning, E., Lundberg, J., Sandberg-Nordqvist, A. C., Kostyszyn, B., Inganäs, O., et al. (2009). Toxicity evaluation of PEDOT/biomolecular composites intended for neural communication electrodes. *Biomedical Materials* 4, 045009. doi: 10.1088/1748-6041/4/4/045009

Bae, W. J., Ruddy, B. P., Richardson, A. G., Hunter, I. W., and Bizzi, E. (2008). Cortical recording with polypyrrole microwire electrodes. in *2008 30th Annual International Conference of the IEEE Engineering in Medicine and Biology Society*, 5794–5797. doi: 10.1109/IEMBS.2008.4650531.

Baranauskas, G., Maggiolini, E., Castagnola, E., Ansaldo, A., Mazzoni, A., Angotzi, G. N., et al. (2011). Carbon nanotube composite coating of neural microelectrodes preferentially improves the multiunit signal-to-noise ratio. *J Neural Eng* 8, 066013. doi: 10.1088/1741-2560/8/6/066013.

Barrese, J. C., Aceros, J., and Donoghue, J. P. (2016). Scanning electron microscopy of chronically implanted intracortical microelectrode arrays in non-human primates. *J Neural Eng* 13, 026003. doi: 10.1088/1741-2560/13/2/026003

Bas, E., Anwar, M. R., Goncalves, S., Dinh, C. T., Bracho, O. R., Chiossone, J. A., et al. (2019). Laminin-coated electrodes improve cochlear implant function and post-insertion neuronal survival. *Neuroscience* 410, 97–107. doi: 10.1016/j.neuroscience.2019.04.048.

Belyanskaya, L., Weigel, S., Hirsch, C., Tobler, U., Krug, H. F., and Wick, P. (2009). Effects of carbon nanotubes on primary neurons and glial cells. *Neurotoxicology* 30, 702–711. doi: 10.1016/j.neuro.2009.05.005.

BeMent, S. L., Wise, K. D., Anderson, D. J., Najafi, K., and Drake, K. L. (1986). Solid-State Electrodes for Multichannel Multiplexed Intracortical Neuronal Recording. *IEEE Trans Biomed Eng* BME-33, 230–241. doi: 10.1109/TBME.1986.325895.

Boehler, C., Stieglitz, T., and Asplund, M. (2015). Nanostructured platinum grass enables superior impedance reduction for neural microelectrodes. *Biomaterials* 67, 346–353. doi: 10.1016/j.biomaterials.2015.07.036.

Bourrier, A., Shkorbatova, P., Bonizzato, M., Rey, E., Barraud, Q., Courtine, G., et al. (2019). Monolayer Graphene Coating of Intracortical Probes for Long-Lasting Neural Activity Monitoring. *Adv Healthc Mater* 8, 1801331. doi: 10.1002/adhm.201801331.

Carli, S., Lambertini, L., Zucchini, E., Ciarpella, F., Scarpellini, A., Prato, M., et al. (2018). Single walled carbon nanohorns composite for neural sensing and stimulation. *Sens Actuators B Chem* 271, 280–288. doi: 10.1016/j.snb.2018.05.083.

Cassar, I. R., Yu, C., Sambangi, J., Lee, C. D., Whalen, J. J., Petrossians, A., et al. (2019). Electrodeposited platinum-iridium coating improves in vivo recording performance of chronically implanted microelectrode arrays. *Biomaterials* 205, 120–132. doi: 10.1016/j.biomaterials.2019.03.017.

Castagnola, E., Ansaldo, A., Maggiolini, E., Angotzi, G. N., Skrap, M., Ricci, D., et al. (2013). Biologically Compatible Neural Interface To Safely Couple Nanocoated Electrodes to the Surface of the Brain. *ACS Nano* 7, 3887–3895. doi: 10.1021/nn305164c.

Cellot, G., Lagonegro, P., Tarabella, G., Scaini, D., Fabbri, F., Iannotta, S., et al. (2016). PEDOT: PSS interfaces support the development of neuronal synaptic networks with reduced neuroglia response in vitro. *Front Neurosci* 9, 521. doi: 10.3389/fnins.2015.00521

Chandrasekaran, S., Fifer, M., Bickel, S., Osborn, L., Herrero, J., Christie, B., et al. (2021). Historical perspectives, challenges, and future directions of implantable brain-computer interfaces for sensorimotor applications. *Bioelectron Med* 7, 14. doi: 10.1186/s42234-021-00076-6.

Chapman, C. A. R., Chen, H., Stamou, M., Biener, J., Biener, M. M., Lein, P. J., et al. (2015). Nanoporous Gold as a Neural Interface Coating: Effects of Topography, Surface Chemistry, and Feature Size. *ACS Appl Mater Interfaces* 7, 7093–7100. doi: 10.1021/acsami.5b00410.

Chen, Q., Wang, X., Chen, F., Zhang, N., and Ma, M. (2019a). Extremely strong and tough polythiophene composite for flexible electronics. *Chemical Engineering Journal* 368, 933–940. doi: 10.1016/j.cej.2019.02.203.

Chen, X.-Z., Liu, J.-H., Dong, M., Müller, L., Chatzipirpiridis, G., Hu, C., et al. (2019b). Magnetically driven piezoelectric soft microswimmers for neuron-like cell delivery and neuronal differentiation. *Mater Horiz* 6, 1512–1516. doi: 10.1039/C9MH00279K

Chen, Y.-Y., Lai, H.-Y., Lin, S.-H., Cho, C.-W., Chao, W.-H., Liao, C.-H., et al. (2009). Design and fabrication of a polyimide-based microelectrode array: Application in neural recording and repeatable electrolytic lesion in rat brain. *J Neurosci Methods* 182, 6–16. doi: 10.1016/j.jneumeth.2009.05.010.

Chiken, S., and Nambu, A. (2015). Mechanism of Deep Brain Stimulation: Inhibition, Excitation, or Disruption? *The Neuroscientist* 22, 313–322. doi: 10.1177/1073858415581986.

Chitrakar, C., Hedrick, E., Adegoke, L., and Ecker, M. (2022). Flexible and Stretchable Bioelectronics. *Materials* 15. doi: 10.3390/ma15051664.

Coffey, R. J. (2009). Deep Brain Stimulation Devices: A Brief Technical History and Review. *Artif Organs* 33, 208–220. doi: 10.1111/j.1525-1594.2008.00620.x.

Contarino, M. F., Bour, L. J., Verhagen, R., Lourens, M. A. J., de Bie, R. M. A., van den Munckhof, P., et al. (2014). Directional steering: a novel approach to deep brain stimulation. *Neurology* 83, 1163–1169. doi: 10.1212/WNL.0000000000000823.

Dayal, V., Grover, T., Limousin, P., Akram, H., Cappon, D., Candelario, J., et al. (2018). The Effect of Short Pulse Width Settings on the Therapeutic Window in Subthalamic Nucleus Deep Brain Stimulation for Parkinson's disease. *J Parkinsons Dis* 8, 273–279. doi: 10.3233/JPD-171272.

de Koning, P. P., Figee, M., van den Munckhof, P., Schuurman, P. R., and Denys, D. (2011). Current Status of Deep Brain Stimulation for Obsessive-Compulsive Disorder: A Clinical Review of Different Targets. *Curr Psychiatry Rep* 13, 274–282. doi: 10.1007/s11920-011-0200-8.

Deli, G., Balas, I., Nagy, F., Balazs, E., Janszky, J., Komoly, S., et al. (2011). Comparison of the efficacy of unipolar and bipolar electrode configuration during subthalamic deep brain stimulation. *Parkinsonism Relat Disord* 17, 50–54. doi: 10.1016/j.parkreldis.2010.10.012.

Devaluez, M., Tir, M., Krystkowiak, P., Aubignat, M., and Lefranc, M. (2020). Selection of deep brain stimulation contacts using volume of tissue activated software following subthalamic nucleus stimulation. *Journal of Neurosurgery JNS*, 1–8. doi: 10.3171/2020.6.JNS192157.

Du, L., Li, T., Jin, F., Wang, Y., Li, R., Zheng, J., et al. (2020). Design of high conductive and piezoelectric poly (3,4-ethylenedioxythiophene)/chitosan nanofibers for enhancing cellular electrical stimulation. *J Colloid Interface Sci* 559, 65–75. doi: 10.1016/j.jcis.2019.10.003.

Duncan, J., Sridharan, A., Kumar, S., Iradukunda, D., and Muthuswamy, J. (2021). Biomechanical micromotion at the neural interface modulates intracellular membrane potentials in vivo. *J Neural Eng* 18. doi: 10.1088/1741-2552/ac0a56.

Ferlauto, L., D'Angelo, A. N., Vagni, P., Airaghi Leccardi, M. J. I., Mor, F. M., Cuttaz, E. A., et al. (2018). Development and characterization of PEDOT: PSS/alginate soft microelectrodes for application in neuroprosthetics. *Front Neurosci* 12, 648. doi: 10.3389/fnins.2018.00648

Flesher, S. N., Downey, J. E., Weiss, J. M., Hughes, C. L., Herrera, A. J., Tyler-Kabara, E. C., et al. (2019). Restored tactile sensation improves neuroprosthetic arm control. *bioRxiv*. doi: 10.1101/653428.

Frey, J., Cagle, J., Johnson, K. A., Wong, J. K., Hilliard, J. D., Butson, C. R., et al. (2022b). Past, present, and future of deep brain stimulation: hardware, software, imaging, physiology and novel approaches. *Front Neurol* 13. doi: 10.3389/fneur.2022.825178.

Frick, C., Müller, M., Wank, U., Tropitzsch, A., Kramer, B., Senn, P., et al. (2017). Biofunctionalized peptide-based hydrogels provide permissive scaffolds to attract neurite outgrowth from spiral ganglion neurons. *Colloids Surf B Biointerfaces* 149, 105–114. doi: 10.1016/j.colsurfb.2016.10.003.

Galassi, T. v, Antman-Passig, M., Yaari, Z., Jessurun, J., Schwartz, R. E., and Heller, D. A. (2020). Long-term in vivo biocompatibility of single-walled carbon nanotubes. *PLoS One* 15, e0226791. doi: 10.1371/journal.pone.0226791

Gardner, J. (2013). A history of deep brain stimulation: Technological innovation and the role of clinical assessment tools. *Soc Stud Sci* 43, 707–728. doi: 10.1177/0306312713483678.

Ge, M., Xu, D., Chen, Z., Wei, C., Zhang, Y., Yang, C., et al. (2021). Magnetostrictive-Piezoelectric-Triggered Nanocatalytic Tumor Therapy. *Nano Lett* 21, 6764–6772. doi: 10.1021/acs.nanolett.1c01313.

Gerwig, R., Fuchsberger, K., Schroeppel, B., Link, G. S., Heusel, G., Kraushaar, U., et al. (2012). PEDOT–CNT composite microelectrodes for recording and electrostimulation applications: fabrication, morphology, and electrical properties. *Front Neuroeng* 5, 8. doi: 10.3389/fneng.2012.00008

Golda-Cepa, M., Engvall, K., Hakkarainen, M., and Kotarba, A. (2020). Recent progress on parylene C polymer for biomedical applications: A review. *Prog Org Coat* 140, 105493. doi: 10.1016/j.porgcoat.2019.105493.

Gonçalves, R., Martins, P., Correia, D. M., Sencadas, V., Vilas, J. L., Leon, L. M., et al. (2015). Development of magnetoelectric CoFe 2 O 4/poly (vinylidene fluoride) microspheres. *RSC Adv* 5, 35852–35857. doi: 10.1039/C5RA04409J

Green, R., and Abidian, M. R. (2015). Conducting polymers for neural prosthetic and neural interface applications. *Advanced Materials* 27, 7620–7637. doi: 10.1002/adma.201501810

Greenland, J. C., Williams-Gray, C. H., and Barker, R. A. (2019). The clinical heterogeneity of Parkinson's disease and its therapeutic implications. *European Journal of Neuroscience* 49, 328–338. doi: 10.1111/ejn.14094.

Guduru, R., Liang, P., Hong, J., Rodzinski, A., Hadjikhani, A., Horstmyer, J., et al. (2015). Magnetoelectric 'spin'on stimulating the brain. *Nanomedicine* 10, 2051–2061. doi: 10.2217/nnm.15.52

Gulino, M., Kim, D., Pané, S., Santos, S. D., and Pêgo, A. P. (2019). Tissue Response to Neural Implants: The Use of Model Systems Toward New Design Solutions of Implantable Microelectrodes. *Front Neurosci* 13, 689. doi: 10.3389/fnins.2019.00689.

Gulino, M., Santos, S. D., and Pêgo, A. P. (2021). Biocompatibility of Platinum Nanoparticles in Brain ex vivo Models in Physiological and Pathological Conditions. *Front Neurosci* 15. doi: 10.3389/fnins.2021.787518.

Hackett, A. J., Malmström, J., and Travas-Sejdic, J. (2017). Functionalization of conducting polymers for biointerface applications. *Prog Polym Sci* 70, 18–33. doi: 10.1016/j.progpolymsci.2017.03.004.

Haniu, H., Matsuda, Y., Takeuchi, K., Kim, Y. A., Hayashi, T., and Endo, M. (2010). Proteomics-based safety evaluation of multi-walled carbon nanotubes. *Toxicol Appl Pharmacol* 242, 256–262. doi: 10.1016/j.taap.2009.10.015.

Harmsen, I. E., Elias, G. J. B., Beyn, M. E., Boutet, A., Pancholi, A., Germann, J., et al. (2020). Clinical trials for deep brain stimulation: Current state of affairs. *Brain Stimul* 13, 378–385. doi: 10.1016/j.brs.2019.11.008.

Heo, D. N., Song, S.-J., Kim, H.-J., Lee, Y. J., Ko, W.-K., Lee, S. J., et al. (2016). Multifunctional hydrogel coatings on the surface of neural cuff electrode for improving electrode-nerve tissue interfaces. *Acta Biomater* 39, 25–33. doi: 10.1016/j.actbio.2016.05.009.

Hochberg, L. R., Serruya, M. D., Friehs, G. M., Mukand, J. A., Saleh, M., Caplan, A. H., et al. (2006). Neuronal ensemble control of prosthetic devices by a human with tetraplegia. *Nature* 442, 164–171. doi: 10.1038/nature04970.

Hojo, H., Oka, K., Shimizu, K., Yamamoto, H., Kawabe, R., and Azuma, M. (2018). Development of Bismuth Ferrite as a Piezoelectric and Multiferroic Material by Cobalt Substitution. *Advanced Materials* 30, 1705665. doi: 10.1002/adma.201705665.

Hyakumura, T., Aregueta-Robles, U., Duan, W., Villalobos, J., Adams, W. K., Poole-Warren, L., et al. (2021). Improving Deep Brain Stimulation Electrode Performance in vivo Through Use of Conductive Hydrogel Coatings. *Front Neurosci* 15. doi: 10.3389/fnins.2021.761525.

Jakobs, M., Fomenko, A., Lozano, A. M., and Kiening, K. L. (2019). Cellular, molecular, and clinical mechanisms of action of deep brain stimulation—a systematic review on established indications and outlook on future developments. *EMBO Mol Med* 11, e9575. doi: 10.15252/emmm.201809575.

Janmey, P. A., Fletcher, D. A., and Reinhart-King, C. A. (2019). Stiffness Sensing by Cells. *Physiol Rev* 100, 695–724. doi: 10.1152/physrev.00013.2019.

Jorfi, M., Skousen, J. L., Weder, C., and Capadona, J. R. (2015). Progress towards biocompatible intracortical microelectrodes for neural interfacing applications. *J Neural Eng* 12. doi: 10.1088/1741-2560/12/1/011001.

Kang, G., and Lowery, M. M. (2014). Effects of antidromic and orthodromic activation of STN afferent axons during DBS in Parkinson's disease: a simulation study. *Front Comput Neurosci* 8, 32. doi: 10.3389/fncom.2014.00032.

Kang, K., Choi, I. S., and Nam, Y. (2011). A biofunctionalization scheme for neural interfaces using polydopamine polymer. *Biomaterials* 32, 6374–6380. doi: 10.1016/j.biomaterials.2011.05.028.

Karumbaiah, L., Saxena, T., Carlson, D., Patil, K., Patkar, R., Gaupp, E. A., et al. (2013). Relationship between intracortical electrode design and chronic recording function. *Biomaterials* 34, 8061–8074. doi: 10.1016/j.biomaterials.2013.07.016.

Kim, S., Jang, L. K., Jang, M., Lee, S., Hardy, J. G., and Lee, J. Y. (2018a). Electrically Conductive Polydopamine–Polypyrrole as High Performance Biomaterials for Cell Stimulation in Vitro and Electrical Signal Recording in Vivo. *ACS Appl Mater Interfaces* 10, 33032–33042. doi: 10.1021/acsami.8b11546.

Kim, S., Jang, Y., Jang, M., Lim, A., Hardy, J. G., Park, H. S., et al. (2018b). Versatile biomimetic conductive polypyrrole films doped with hyaluronic acid of different molecular weights. *Acta Biomater* 80, 258–268. doi: 10.1016/j.actbio.2018.09.035.

Kim, Y. H., Kim, G. H., Kim, A. Y., Han, Y. H., Chung, M.-A., and Jung, S.-D. (2015). In vitro extracellular recording and stimulation performance of nanoporous gold-modified multi-electrode arrays. *J Neural Eng* 12, 066029. doi: 10.1088/1741-2560/12/6/066029.

Kisely, S., Li, A., Warren, N., and Siskind, D. (2018). A systematic review and meta-analysis of deep brain stimulation for depression. *Depress Anxiety* 35, 468–480. doi: 10.1002/da.22746.

Kitko, K. E., and Zhang, Q. (2019). Graphene-based nanomaterials: From production to integration with modern tools in neuroscience. *Front Syst Neurosci* 13, 26. doi: 10.3389/fnsys.2019.00026

Kleiner-Fisman, G., Herzog, J., Fisman, D. N., Tamma, F., Lyons, K. E., Pahwa, R., et al. (2006). Subthalamic nucleus deep brain stimulation: summary and meta-analysis of outcomes. *Mov Disord* 21, S290–S304. doi: 10.1002/mds.20962.

Kostarelos, K., Vincent, M., Hebert, C., and Garrido, J. A. (2017). Graphene in the design and engineering of next-generation neural interfaces. *Advanced Materials* 29, 1700909. doi: 10.1002/adma.201700909

Kozai, T. D. Y., Catt, K., Li, X., Gugel, Z. v, Olafsson, V. T., Vazquez, A. L., et al. (2015a). Mechanical failure modes of chronically implanted planar silicon-based neural probes for laminar recording. *Biomaterials* 37, 25–39. doi: 10.1016/j.biomaterials.2014.10.040.

Kozai, T. D. Y., Jaquins-Gerstl, A. S., Vazquez, A. L., Michael, A. C., and Cui, X. T. (2015b). Brain tissue responses to neural implants impact signal sensitivity and intervention strategies. *ACS Chem Neurosci* 6, 48–67. doi: 10.1021/cn500256e.

Kozai, T. D. Y., Jaquins-Gerstl A. S., Vazquez A. L., Michael A. C., Cui X.T. (2016) Dexamethasone retrodialysis attenuates microglial response to implanted probes in vivo, *Biomaterials*, 87, 157-169. doi: 10.1016/j.biomaterials.2016.02.013.

Kozielski, K. L., Jahanshahi, A., Gilbert, H. B., Yu, Y., Erin, Ö., Francisco, D., et al. (2023). Nonresonant powering of injectable nanoelectrodes enables wireless deep brain stimulation in freely moving mice. *Sci Adv* 7, eabc4189. doi: 10.1126/sciadv.abc4189.

Krauss, J. K., Lipsman, N., Aziz, T., Boutet, A., Brown, P., Chang, J. W., et al. (2021). Technology of deep brain stimulation: current status and future directions. *Nat Rev Neurol* 17, 75–87. doi: 10.1038/s41582-020-00426-z.

Kroneberg, D., Ewert, S., Meyer, A.-C., and Kühn, A. A. (2019). Shorter pulse width reduces gait disturbances following deep brain stimulation for essential tremor. *Journal of Neurology, Neurosurgery & Psychiatry* 90, 1046. doi: 10.1136/jnnp-2018-319427.

Lacour, S. P., Benmerah, S., Tarte, E., FitzGerald, J., Serra, J., McMahon, S., et al. (2010). Flexible and stretchable micro-electrodes for in vitro and in vivo neural interfaces. *Med Biol Eng Comput* 48, 945–954. doi: 10.1007/s11517-010-0644-8.

Laxton, A. W., and Lozano, A. M. (2013). Deep Brain Stimulation for the Treatment of Alzheimer Disease and Dementias. *World Neurosurg* 80, S28.e1-S28.e8. doi: 10.1016/j.wneu.2012.06.028.

Lehew, G., and Nicolelis, M. A. L. (2008). State-of-the-art microwire array design for chronic neural recordings in behaving animals. *Methods for neural ensemble recordings* 2, 361–371.

Liu, X., Yue, Z., Higgins, M. J., and Wallace, G. G. (2011). Conducting polymers with immobilised fibrillar collagen for enhanced neural interfacing. *Biomaterials* 32, 7309–7317. doi: 1016/j.biomaterials.2011.06.047.

Liu, Z., Davis, C., Cai, W., He, L., Chen, X., and Dai, H. (2008). Circulation and Long-Term Fate of Functionalized, Biocompatible Single-Walled Carbon Nanotubes in Mice Probed by Raman Spectroscopy. *Proc Natl Acad Sci U S A* 105, 1410–1415. doi: 10.1073/pnas.0707654105

Lu, P.-L., Fan, C.-L., Yang, L.-J., Lin, C.-W., Yang, Y.-J., and Jaw, F.-S. (2007). Completely Parylene-Coated Neuroprobe for Chronic Recording. in *2007 2nd IEEE International Conference on Nano/Micro Engineered and Molecular Systems*, 223–226. doi: 10.1109/NEMS.2007.352267.

Lu, Y., Li, T., Zhao, X., Li, M., Cao, Y., Yang, H., et al. (2010). Electrodeposited polypyrrole/carbon nanotubes composite films electrodes for neural interfaces. *Biomaterials* 31, 5169–5181. doi: 10.1016/j.biomaterials.2010.03.022.

Lu, Y., Wang, D., Li, T., Zhao, X., Cao, Y., Yang, H., et al. (2009). Poly (vinyl alcohol)/poly (acrylic acid) hydrogel coatings for improving electrode–neural tissue interface. *Biomaterials* 30, 4143–4151. doi: 10.1016/j.biomaterials.2009.04.030

Ludwig, K. A., Langhals, N. B., Joseph, M. D., Richardson-Burns, S. M., Hendricks, J. L., and Kipke, D. R. (2011). Poly(3,4-ethylenedioxythiophene) (PEDOT) polymer coatings facilitate smaller neural recording electrodes. *J Neural Eng* 8, 014001. doi: 10.1088/1741-2560/8/1/014001.

Maldonado-Camargo, L., Unni, M., and Rinaldi, C. (2017). Magnetic characterization of iron oxide nanoparticles for biomedical applications. *Methods Mol Biol.* 1570:47-71. doi: 10.1007/978-1-4939-6840-4_4.

Marín, G., Castillo-Rangel, C., Salomón-Lara, L., Vega-Quesada, L. A., Zarate Calderon, C. J., Borda-Low, C. D., et al. (2022). Deep brain stimulation in neurological diseases and other pathologies. *Neurology perspectives* 2, 151–159. doi: 10.1016/j.neurop.2022.03.001.

Mario Cheong, G. L., Lim, K. S., Jakubowicz, A., Martens, P. J., Poole-Warren, L. A., and Green, R. A. (2014). Conductive hydrogels with tailored bioactivity for implantable electrode coatings. *Acta Biomater* 10, 1216–1226. doi: 10.1016/j.actbio.2013.12.032.

Mauri, E., Sacchetti, A., Vicario, N., Peruzzotti-Jametti, L., Rossi, F., and Pluchino, S. (2018). Evaluation of RGD functionalization in hybrid hydrogels as 3D neural stem cell culture systems. *Biomater Sci* 6, 501–510. doi: 10.1007/978-1-4939-6840-4_4

McIntyre, C. C., and Anderson, R. W. (2016). Deep brain stimulation mechanisms: the control of network activity via neurochemistry modulation. *J Neurochem* 139, 338–345. doi: 10.1111/jnc.13649.

Meijs, S., Rechendorff, K., Sørensen, S., and Rijkhoff, N. J. M. (2019). Corrosion Study of Implanted Tin Electrodes Using Excessive Electrical Stimulation in Minipigs. *Metals* 9(4), 389. doi: 10.3390/met9040389

Miocinovic, S., Somayajula, S., Chitnis, S., and Vitek, J. L. (2013). History, Applications, and Mechanisms of Deep Brain Stimulation. *JAMA Neurol* 70, 163–171. doi: 10.1001/2013.jamaneurol.45.

Miranda, I., Souza, A., Sousa, P., Ribeiro, J., Castanheira, E. M. S., Lima, R., et al. (2021). Properties and applications of PDMS for biomedical engineering: A review. *J Funct Biomater* 13, 2. doi: 10.3390/jfb13010002

Mohammadi, A., and Mehdizadeh, A. R. (2016). Deep brain stimulation and gene expression alterations in parkinson's disease. *J Biomed Phys Eng* 6, 47–50.

Mohan, U. R., Watrous, A. J., Miller, J. F., Lega, B. C., Sperling, M. R., Worrell, G. A., et al. (2020). The effects of direct brain stimulation in humans depend on frequency, amplitude, and white-matter proximity. *Brain Stimul* 13, 1183–1195. doi: 10.1016/j.brs.2020.05.009.

Mousavi, S. M., Hashemi, S. A., Bahrani, S., Yousefi, K., Behbudi, G., Babapoor, A., et al. (2021). Recent advancements in polythiophene-based materials and their biomedical, geno sensor and DNA detection. *Int J Mol Sci* 22, 6850. doi: 10.3390/ijms22136850.

Mushtaq, F., Torlakcik, H., Vallmajo-Martin, Q., Siringil, E. C., Zhang, J., Röhrig, C., et al. (2019). Magnetoelectric 3D scaffolds for enhanced bone cell proliferation. *Appl Mater Today* 16, 290–300. doi: 10.1016/j.apmt.2019.06.004

Myllymaa, S., Myllymaa, K., Korhonen, H., Töyräs, J., Jääskeläinen, J. E., Djupsund, K., et al. (2009). Fabrication and testing of polyimide-based microelectrode arrays for cortical mapping of evoked potentials. *Biosens Bioelectron* 24, 3067–3072. doi: 10.1016/j.bios.2009.03.028.

Nandra, M. S., Lavrov, I. A., Edgerton, V. R., and Tai, Y.-C. (2011). A parylene-based microelectrode array implant for spinal cord stimulation in rats. in *2011 IEEE 24th International Conference on Micro Electro Mechanical Systems* (IEEE), 1007–1010. doi: 10.1109/MEMSYS.2011.5734598

Nessim, G. D. (2010). Properties, synthesis, and growth mechanisms of carbon nanotubes with special focus on thermal chemical vapor deposition. *Nanoscale* 2, 1306–1323. doi: 10.1039/B9NR00427K.

Nguyen, T., Gao, J., Wang, P., Nagesetti, A., Andrews, P., Masood, S., et al. (2021). In Vivo Wireless Brain Stimulation via Non-invasive and Targeted Delivery of Magnetoelectric Nanoparticles. *Neurotherapeutics* 18, 2091–2106. doi: 10.1007/s13311-021-01071-0.

Nolta, N. F., Christensen, M. B., Crane, P. D., Skousen, J. L., and Tresco, P. A. (2015). BBB leakage, astrogliosis, and tissue loss correlate with silicon microelectrode array recording performance. *Biomaterials* 53, 753–762. doi: 10.1016/j.biomaterials.2015.02.081.

Pancrazio, J. J., Deku, F., Ghazavi, A., Stiller, A. M., Rihani, R., Frewin, C. L., et al. (2017). Thinking Small: Progress on Microscale Neurostimulation Technology. *Neuromodulation: Technology at the Neural Interface* 20, 745–752. doi: 10.1111/ner.12716.

Park, D.-W., Ness, J. P., Brodnick, S. K., Esquibel, C., Novello, J., Atry, F., et al. (2018). Electrical Neural Stimulation and Simultaneous in Vivo Monitoring with Transparent Graphene Electrode Arrays Implanted in GCaMP6f Mice. *ACS Nano* 12, 148–157. doi: 10.1021/acsnano.7b04321.

Patra, D. P., Hess, R. A., Abi-Aad, K. R., Muzyka, I. M., and Bendok, B. R. (2019). Roberts Bartholow: the progenitor of human cortical stimulation and his contentious experiment. *Neurosurgical Focus FOC* 47, E6. doi: 10.3171/2019.6.FOCUS19349.

Perkucin, I., Lau, K. S. K., Chen, T., Iwasa, S. N., Naguib, H. E., and Morshead, C. M. (2022). Facile Fabrication of Injectable Alginate and Poly(3,4-ethylenedioxythiophene)-Based Soft Electrodes toward the Goal of Neuro-Regenerative Applications. *Adv Healthc Mater* n/a, 2201164. doi: 10.1002/adhm.202201164.

Perlin, G. E., and Wise, K. D. (2008). A compact architecture for three-dimensional neural microelectrode arrays. in *2008 30th Annual International Conference of the IEEE Engineering in Medicine and Biology Society* (IEEE), 5806–5809. doi: 10.1109/IEMBS.2008.4650534

Petrossians, A., Whalen, J. J., Weiland, J. D., and Mansfeld, F. (2011). Surface modification of neural stimulating/recording electrodes with high surface area platinum-iridium alloy coatings. in *2011 Annual International Conference of the IEEE Engineering in Medicine and Biology Society*, 3001–3004. doi: 10.1109/IEMBS.2011.6090823.

Piccolino, M. (1997). Luigi Galvani and animal electricity: two centuries after the foundation of electrophysiology. *Trends Neurosci* 20, 443–448. doi: 10.1016/S0166-2236(97)01101-6.

Pollo, C., Kaelin-Lang, A., Oertel, M. F., Stieglitz, L., Taub, E., Fuhr, P., et al. (2014). Directional deep brain stimulation: an intraoperative double-blind pilot study. *Brain* 137, 2015–2026. doi: 10.1093/brain/awu102.

Poon, K. K., Wurm, M. C., Evans, D. M., Einarsrud, M.-A., Lutz, R., and Glaum, J. (2020). Biocompatibility of (Ba,Ca)(Zr,Ti)O3 piezoelectric ceramics for bone replacement materials. *J Biomed Mater Res B Appl Biomater* 108, 1295–1303. doi: 10.1002/jbm.b.34477.

Pranti, A. S., Schander, A., Bödecker, A., and Lang, W. (2018). PEDOT: PSS coating on gold microelectrodes with excellent stability and high charge injection capacity for chronic neural interfaces. *Sens Actuators B Chem* 275, 382–393. doi: 10.1016/j.snb.2018.08.007.

Prasad, A., Xue, Q.-S., Dieme, R., Sankar, V., Mayrand, R. C., Nishida, T., et al. (2014). Abiotic-biotic characterization of Pt/Ir microelectrode arrays in chronic implants. *Front Neuroeng* 7, 2. doi: 10.3389/fneng.2014.00002.

Rago, I., Rauti, R., Bevilacqua, M., Calaresu, I., Pozzato, A., Cibinel, M., et al. (2019). Carbon nanotubes, directly grown on supporting surfaces, improve neuronal activity in hippocampal neuronal networks. *Adv Biosyst* 3, 1800286. doi: 10.1002/adbi.201800286

Rahman, M., Murad, G. J. A., and Mocco, J. (2009). Early history of the stereotactic apparatus in neurosurgery. *Neurosurgical Focus FOC* 27, E12. doi: 10.3171/2009.7.FOCUS09118.

Rantataro, S., Parkkinen, I., Pande, I., Domanskyi, A., Airavaara, M., Peltola, E., et al. (2022). Nanoscale geometry determines mechanical biocompatibility of vertically aligned nanofibers. *Acta Biomater* 146, 235–247. doi: 10.1016/j.actbio.2022.04.032.

Rao, L., Zhou, H., Li, T., Li, C., and Duan, Y. Y. (2012). Polyethylene glycol-containing polyurethane hydrogel coatings for improving the biocompatibility of neural electrodes. *Acta Biomater* 8, 2233–2242. doi: 10.1016/j.actbio.2012.03.001.

Rebelo, P., Green, A. L., Aziz, T. Z., Kent, A., Schafer, D., Venkatesan, L., et al. (2018). Thalamic Directional Deep Brain Stimulation for tremor: Spend less, get more. *Brain Stimul* 11, 600–606. doi: 10.1016/j.brs.2017.12.015.

Reddy, S., He, L., Ramakrishana, S., and Luo, H. (2019). Graphene nanomaterials for regulating stem cell fate in neurogenesis and their biocompatibility. *Curr Opin Biomed Eng* 10, 69–78. doi: 10.1016/j.cobme.2019.04.002.

Rodzinski, A., Guduru, R., Liang, P., Hadjikhani, A., Stewart, T., Stimphil, E., et al. (2016). Targeted and controlled anticancer drug delivery and release with magnetoelectric nanoparticles. *Sci Rep* 6, 20867. doi: 10.1038/srep20867.

Rosso, J. M., Volnistem, E. A., Santos, I. A., Bonadio, T. G. M., and Freitas, V. F. (2022). Lead-free NaNbO3-based ferroelectric perovskites and their polar polymer-ceramic composites: Fundamentals and potentials for electronic and biomedical applications. *Ceram Int* 48, 19527–19541. doi: 10.1016/j.ceramint.2022.04.089.

Schnitzler, A., Mir, P., Brodsky, M. A., Verhagen, L., Groppa, S., Alvarez, R., et al. (2022). Directional Deep Brain Stimulation for Parkinson's Disease: Results of an International Crossover Study With Randomized, Double-Blind Primary Endpoint. *Neuromodulation: Technology at the Neural Interface* 25, 817–828. doi: 10.1111/ner.13407.

Seker, E., Berdichevsky, Y., Begley, M. R., Reed, M. L., Staley, K. J., and Yarmush, M. L. (2010). The fabrication of low-impedance nanoporous gold multiple-electrode arrays for neural electrophysiology studies. *Nanotechnology* 21, 125504. doi: 10.1088/0957-4484/21/12/125504.

Shahzad, K., Mushtaq, S., Rizwan, M., Khalid, W., Atif, M., Din, F. U., et al. (2021). Field-controlled magnetoelectric core-shell CoFe2O4@BaTiO3 nanoparticles as effective drug carriers and drug release in vitro. *Materials Science and Engineering: C* 119, 111444. doi: 10.1016/j.msec.2020.111444.

Shao, H., Li, T., Zhu, R., Xu, X., Yu, J., Chen, S., et al. (2018). Carbon nanotube multilayered nanocomposites as multifunctional substrates for actuating neuronal differentiation and functions of neural stem cells. *Biomaterials* 175, 93–109. doi: 10.1016/j.biomaterials.2018.05.028.

Sharma, R., Tathireddy, P., Lee, S., Rieth, L., Bamberg, E., Dorval, A., et al. (2011). Application-specific customizable architectures of Utah neural interfaces. *Procedia Eng* 25, 1016–1019. doi:.1016/j.proeng.2011.12.250.

Shen, W., Das, S., Vitale, F., Richardson, A., Ananthakrishnan, A., Struzyna, L. A., et al. (2018). Microfabricated intracortical extracellular matrix-microelectrodes for improving neural interfaces. *Microsyst Nanoeng* 4, 30. doi: 10.1038/s41378-018-0030-5.

Shur, M., Fallegger, F., Pirondini, E., Roux, A., Bichat, A., Barraud, Q., et al. (2020). Soft Printable Electrode Coating for Neural Interfaces. *ACS Appl Bio Mater* 3, 4388–4397. doi: 10.1021/acsabm.0c00401.

Sironi, V. A. (2011). Origin and evolution of deep brain stimulation. *Front Integr Neurosci* 5, 42.
Sitz, A., Hoevels, M., Hellerbach, A., Gierich, A., Luyken, K., Dembek, T., et al. (2017). Determining the orientation angle of directional leads for deep brain stimulation using computed tomography and digital x-ray imaging: A phantom study. *Med Phys* 44. doi: 10.1002/mp.12424.

Skousen, J., Merriam, S., Srivannavit, O., Perlin, G., Wise, K., and Tresco, P. (2011). Reducing surface area while maintaining implant penetrating profile lowers the brain foreign body response to chronically implanted planar silicon microelectrode arrays. *Prog Brain Res* 194, 167–180. doi: 10.1016/B978-0-444-53815-4.00009-1.

Slopsema, J. P., Peña, E., Patriat, R., Lehto, L. J., Gröhn, O., Mangia, S., et al. (2018). Clinical deep brain stimulation strategies for orientation-selective pathway activation. *J Neural Eng* 15, 056029. doi: 10.1088/1741-2552/aad978.

Song, S., Shen, H., Wang, Y., Chu, X., Xie, J., Zhou, N., et al. (2020). Biomedical application of graphene: From drug delivery, tumor therapy, to theranostics. *Colloids Surf B Biointerfaces* 185, 110596. doi: 10.1016/j.colsurfb.2019.110596.

Srinivasan, S. Y., Paknikar, K. M., Bodas, D., and Gajbhiye, V. (2018). Applications of cobalt ferrite nanoparticles in biomedical nanotechnology. *Nanomedicine* 13, 1221–1238. doi: 10.2217/nnm-2017-0379.

Starbird, R., Krautschneider, W., Blume, G., and Bauhofer, W. (2013). In vitro biocompatibility study and electrical properties of the PEDOT, PEDOT collagen-coat, PEDOT nanotubes and PEDOT aerogels for neural electrodes. *Mat. Science* doi: 10.2316/P.2013.791-072.

Steigerwald, F., Matthies, C., and Volkmann, J. (2019). Directional Deep Brain Stimulation. *Neurotherapeutics* 16, 100–104. doi: 10.1007/s13311-018-0667-7.

Stejskal, J. (2017). Conducting polymer hydrogels. *Chemical Papers* 71, 269–291. doi: 10.1007/s11696-016-0072-9.

Su, D., Chen, H., Hu, W., Liu, Y., Wang, Z., Wang, X., et al. (2018). Frequency-dependent effects of subthalamic deep brain stimulation on motor symptoms in Parkinson's disease: a meta-analysis of controlled trials. *Sci Rep* 8, 14456. doi: 10.1038/s41598-018-32161-3.

Su, D., Zhou, J., Ahmed, K. S., Ma, Q., Lv, G., and Chen, J. (2019). Fabrication and characterization of collagen-heparin-polypyrrole composite conductive film for neural scaffold. *Int J Biol Macromol* 129, 895–903. doi: 10.1016/j.ijbiomac.2019.02.087.

Sunwoo, S.-H., Han, S. I., Joo, H., Cha, G. D., Kim, D., Choi, S. H., et al. (2020). Advances in soft bioelectronics for brain research and clinical neuroengineering. *Matter* 3, 1923–1947. doi: 10.1016/j.matt.2020.10.020

Thompson, C. H., Ti'Air, E. R., Patel, P. R., Chestek, C. A., Li, W., and Purcell, E. (2020). Toward guiding principles for the design of biologically-integrated electrodes for the central nervous system. *J Neural Eng* 17, 021001. doi: 10.1088/1741-2552/ab7030.

Tsai, M.-L., and Yen, C.-T. (2003). A simple method for fabricating horizontal and vertical microwire arrays. *J Neurosci Methods* 131, 107–110. doi: 10.1016/S0165-0270(03)00235-8.

Valldeoriola, F., Muñoz, E., Rumià, J., Roldán, P., Cámara, A., Compta, Y., et al. (2019). Simultaneous low-frequency deep brain stimulation of the substantia nigra pars reticulata and high-frequency stimulation of the subthalamic nucleus to treat levodopa unresponsive freezing of gait in Parkinson's disease: A pilot study. *Parkinsonism Relat Disord* 60, 153–157. doi: 10.1016/j.parkreldis.2018.09.008.

van den Munckhof, P., Contarino, M. F., Bour, L. J., Speelman, J. D., de Bie, R. M. A., and Schuurman, P. R. (2010). Postoperative curving and upward displacement of deep brain stimulation electrodes caused by brain shift. *Neurosurgery* 67, 49–54. doi: 10.1227/01.NEU.0000370597.44524.6D.

Venkatraman, S., Hendricks, J., King, Z. A., Sereno, A. J., Richardson-Burns, S., Martin, D., et al. (2011). In Vitro and In Vivo Evaluation of PEDOT Microelectrodes for Neural Stimulation and Recording. *IEEE Transactions on Neural Systems and Rehabilitation Engineering* 19, 307–316. doi: 10.1109/TNSRE.2011.2109399.

Vilensky, J. A., and Gilman, S. (2002). Horsley was the first to use electrical stimulation of the human cerebral cortex intraoperatively. *Surg Neurol* 58, 425–426. doi: 10.1016/S0090-3019(02)00920-5.

Visalakshan, R. M., MacGregor, M. N., Sasidharan, S., Ghazaryan, A., Mierczynska-Vasilev, A. M., Morsbach, S., et al. (2019). Biomaterial surface hydrophobicity-mediated serum protein adsorption and immune responses. *ACS Appl Mater Interfaces* 11, 27615–27623. doi: 10.1021/acsami.9b09900.

Vitale, F., Shen, W., Driscoll, N., Burrell, J. C., Richardson, A. G., Adewole, O., et al. (2018). Biomimetic extracellular matrix coatings improve the chronic biocompatibility of microfabricated subdural microelectrode arrays. *PLoS One* 13, e0206137-. doi: 10.1371/journal.pone.0206137.

Voge, C. M., and Stegemann, J. P. (2011). Carbon nanotubes in neural interfacing applications. *J Neural Eng* 8, 011001. doi: 10.1088/1741-2560/8/1/011001.

Wang, K., Tian, L., Wang, T., Zhang, Z., Gao, X., Wu, L., et al. (2019). Electrodeposition of alginate with PEDOT/PSS coated MWCNTs to make an interpenetrating conducting hydrogel for neural interface. *Compos Interfaces* 26, 27–40. doi: 10.1080/09276440.2018.1465766

Wang, M., and Guo, L. (2020). "Intracortical Electrodes," in *Neural Interface Engineering: Linking the Physical World and the Nervous System*, ed. L. Guo (Cham: Springer International Publishing), 67–94. doi: 10.1007/978-3-030-41854-0_4.

Wang, R., Huang, X., Liu, G., Wang, W., Dong, F., and Li, Z. (2010). Fabrication and characterization of a parylene-based three-dimensional microelectrode array for use in retinal prosthesis. *Journal of Microelectromechanical Systems* 19, 367–374. doi: 10.1109/JMEMS.2009.2039773

Wang, S., Sun, C., Guan, S., Li, W., Xu, J., Ge, D., et al. (2017). Chitosan/gelatin porous scaffolds assembled with conductive poly(3,4-ethylenedioxythiophene) nanoparticles for neural tissue engineering. *J. Mater. Chem. B* 5, 4774–4788. doi: 10.1039/C7TB00608J.

Xu, B., Pei, J., Feng, L., and Zhang, X.-D. (2021). Graphene and graphene-related materials as brain electrodes. *J. Mater. Chem. B* 9, 9485–9496. doi: 10.1039/D1TB01795K.

Yarjanli, Z., Ghaedi, K., Esmaeili, A., Rahgozar, S., and Zarrabi, A. (2017). Iron oxide nanoparticles may damage to the neural tissue through iron accumulation, oxidative stress, and protein aggregation. *BMC Neurosci* 18, 51. doi: 10.1186/s12868-017-0369-9.

Young, A. L., Marinescu, R. v, Oxtoby, N. P., Bocchetta, M., Yong, K., Firth, N. C., et al. (2018). Uncovering the heterogeneity and temporal complexity of neurodegenerative diseases with Subtype and Stage Inference. *Nat Commun* 9, 4273. doi: 10.1038/s41467-018-05892-0.

Yue, Z., Liu, X., Molino, P. J., and Wallace, G. G. (2011). Bio-functionalisation of polydimethylsiloxane with hyaluronic acid and hyaluronic acid – Collagen conjugate for neural interfacing. *Biomaterials* 32, 4714–4724. doi: 10.1016/j.biomaterials.2011.03.032.

Zardini, A. S., Rostami, B., Najafi, K., Hetrick, V. L., and Ahmed, O. J. (2021a). Sea of Electrodes Array (SEA): Extremely Dense and High-Count Silicon-Based Electrode Array Technology for High-Resolution High-Bandwidth Interfacing with 3D Neural Structures. *bioRxiv*. doi: 10.1101/2021.01.24.427975.

Zhang, D., Di, F., Zhu, Y., Xiao, Y., and Che, J. (2015). Electroactive hybrid hydrogel: Toward a smart coating for neural electrodes. *J Bioact Compat Polym* 30, 600–616. doi: 10.1177/0883911515591647.

Zhang, E., Abdel-Mottaleb, M., Liang, P., Navarrete, B., Yildirim, Y. A., Campos, M. A., et al. (2022). Magnetic-field-synchronized wireless modulation of neural activity by magnetoelectric nanoparticles. *Brain Stimul* 15, 1451–1462. doi: 10.1016/j.brs.2022.10.004.

Zhang, F., Wang, F., Li, W., Wang, N., Han, C., Fan, S., et al. (2021a). Relationship between electrode position of deep brain stimulation and motor symptoms of Parkinson's disease. *BMC Neurol* 21, 122. doi: 10.1186/s12883-021-02148-1.

Zhang, S., Tagliati, M., Pouratian, N., Cheeran, B., Ross, E., and Pereira, E. (2020). Steering the Volume of Tissue Activated With a Directional Deep Brain Stimulation Lead in the Globus Pallidus Pars Interna: A Modeling Study With Heterogeneous Tissue Properties. *Front Comput Neurosci*, doi: 10.3389/fncom.2020.561180.

Zhang, S., Zhou, P., Jiang, S., Wang, W., and Li, P. (2016). Interleaving subthalamic nucleus deep brain stimulation to avoid side effects while achieving satisfactory motor benefits in Parkinson disease: A report of 12 cases. *Medicine* 95. doi: 10.1097/MD.0000000000005575

Zhang, Y., Chen, S., Xiao, Z., Liu, X., Wu, C., Wu, K., et al. (2021b). Magnetoelectric Nanoparticles Incorporated Biomimetic Matrix for Wireless Electrical Stimulation and Nerve Regeneration. *Adv Healthc Mater* 10, 2100695. doi: 10.1002/adhm.202100695.

Chapter 2

TISSUE RESPONSE TO NEURAL IMPLANTS: THE USE OF MODEL SYSTEMS TOWARDS NEW DESIGN SOLUTIONS OF IMPLANTABLE MICROELECTRODES

Maurizio Gulino[1,2,3]; Donghoon Kim[4]; Salvador Pané[4]; Sofia Duque Santos[1,2]; Ana Paula Pêgo[1,2,3,5,*]

[1]i3S - Instituto de Investigação e Inovação em Saúde, Universidade do Porto, Porto, Portugal

[2]INEB - Instituto de Engenharia Biomédica, Universidade do Porto, Porto, Portugal

[3]FEUP - Faculdade de Engenharia, Universidade do Porto, Porto, Portugal

[4]Multi-scale Robotics Lab (MSRL), Institute of Robotics and Intelligent Systems (IRIS), ETH Zurich, Zurich, Switzerland

[5]ICBAS - Instituto de Ciências Biomédicas Abel Salazar, Universidade do Porto, Porto, Portugal

Published in Frontiers in Neuroscience, Volume 13 - 2019

ABSTRACT

The development of implantable neuroelectrodes is advancing rapidly as these tools are becoming increasingly ubiquitous in clinical practice, especially for the treatment of traumatic and neurodegenerative disorders. Electrodes have been exploited in a wide number of neural interface devices, such as deep brain stimulation, which is one of the most successful therapies with proven efficacy in the treatment of diseases like Parkinson or epilepsy. However, one of the main caveats related to the clinical application of electrodes is the nervous tissue response at the injury site, characterized by a cascade of inflammatory events, which culminate in chronic inflammation, and, in turn, result in the failure of the implant over extended periods of time. To overcome current limitations of the most widespread macroelectrode based systems, new design strategies and the development of innovative materials with superior biocompatibility characteristics are currently being investigated.
This review describes the current state of the art of in vitro, ex vivo and in vivo models available for the study of neural tissue response to implantable microelectrodes. We particularly highlight new models with increased complexity that closely mimic in vivo scenarios and that can serve as promising alternatives to animal studies for investigation of microelectrodes in neural tissues. Additionally, we also express our view on the impact of the progress in the field of neural tissue engineering on neural implant research.

1. IMPLANTABLE ELECTRODES IN NEUROLOGICAL AND NEUROPSYCHIATRIC DISORDERS

1.1 CLINICAL APPLICATIONS

Recent technological progress in the field of brain-machine interfaces boosted the development of innovative tools and electrodes for neurophysiological research and neurostimulation applications to treat neuro disability-related conditions.
Deep brain stimulation (DBS) is an invasive neurosurgical operation consisting in the delivery of electrical impulses to specific areas of the brain by means of implantable electrodes connected to a pulse generator. The concept of DBS is the generation of action potentials resulting in beneficial

neurochemical effects, such as the recovery of disrupted neural circuits and physiological brain function. For specific applications, DBS is a U. S. “Food and Drug Administration” (FDA) approved technique which is already applied in the clinic for a vast number of neurological dysfunctions (Revell, 2015; Dougherty, 2018). In patients affected by Parkinson’s disease, DBS at the level of the globus pallidus or subthalamic nucleus is able to reduce bradykinesia, dystonia, as well as walking problems, allowing for substantial improvements in the quality of life (Ramirez-Zamora and Ostrem, 2018). In patients affected by dystonia, globus pallidus DBS has been shown to reduce tremors and involuntary motor contraction, with persistent effects after several years (Meoni et al., 2017). For essential tremors, the principal targets for DBS to reduce tremors with lower stimulation amplitudes and fewer side effects than previous treatments are the posterior subthalamic area and the zona incerta (Holslag et al., 2017; Barbe et al., 2018). In patients with medically refractory epilepsy, long-term DBS at the level of the anterior nucleus of the thalamus is an U. S. FDA-approved therapy that is able to reduce epileptic episodes and ensure perdurable improvements in the quality of life for years (Salanova, 2018). For the treatment of chronic and neuropathic pain, DBS is a supported therapy in Europe, although not currently approved by the U. S. FDA. Several clinical studies report a reduction of pain in patients with amputations, post-stroke pain, cranial and facial pain (Farrell et al., 2018). DBS was also found to be a valid therapeutic approach for the treatment of psychiatric disorders. Ventral capsule/ventral striatum DBS is another U. S. FDA-approved treatment under a humanitarian device exemption for patients affected by obsessive-compulsive disorder (Dougherty, 2018). A relevant efficacy of DBS has been also observed for the treatment of refractory depression. Clinical application of DBS in patients non-responsive to anti-depressant treatments reported a remission of depression after chronic stimulation of various brain targets, with a decrease in negativity and sadness, reduction of cerebral blood flow at the level of the limbic-cortical circuitry, and improvements in memory and motor function (Dandekar et al., 2018; Drobisz and Damborská, 2019). Spinal cord stimulation (SCS) has shown to be an effective strategy for the treatment of different diseases. SCS is being successfully used to treat angina pectoris pain, low back, and leg pain and peripheral limb ischemia (Song et al., 2014). Clinical studies reported beneficial effects of SCS combined with activity-based training in the recovery of motor function and muscle activation patterns in patients that suffered spinal cord injury (Rejc et al., 2017).

Besides the applications described above, the use of implantable electrodes for neurostimulation therapy is continuing to expand towards many other medical conditions. DBS has been recently proposed for the treatment of pain, dystonia and motor symptoms in post-stroke, although additional investigations are necessary to identify specific brain districts to improve the effectiveness of the treatment (Elias et al., 2018). In a study involving patients affected by Tourette syndrome, DBS of

the anterior and posterior globus pallidus, centromedian thalamus and anterior limb of internal capsule showed common positive results after one year of treatment in the reduction of motor tic symptoms (Martinez-Ramirez et al., 2018). Partial improvements have been described in clinical trials involving patients affected by Alzheimer's disease, with positive effects in cognition, reversal of memory and reduction of altered glucose metabolism (Mao et al., 2018).

As seen above, the progress in neurostimulation technology and the increased knowledge of the neurophysiology of the central nervous system (CNS) opened the way to new therapeutic approaches for the treatment of a vast number of neurological disorders and neuropsychiatric conditions. Although well established and approved for some diseases, additional trials and experimental work need to be conducted to better define the ideal brain targets, stimulation variables, and electrode design in order to ameliorate the clinical outcomes. Due to the impact of the inflammatory response and tissue encapsulation elicited by traditional DBS macroelectrodes, the field of neuroengineering is progressing towards the employment of implantable microelectrodes (Daniele et al., 2014). Traditional DBS electrodes present several drawbacks such as the rigidity of the materials employed for fabrication as well as a high size which exacerbate the neuroinflammatory response and tissue damage. Although they have a higher activation radius compared to microelectrodes, macroelectrode implantation is often associated to a wrong positioning in the interested area causing a decrease in therapeutic efficacy of DBS (Kloc et al., 2017; Morishita et al., 2017). In the case of small target areas, the reduced dimensions of microelectrodes can provide a better targeting accuracy ensuring an increased therapeutic efficacy of DBS and tissue integration for chronic applications (Desai et al., 2012; Du et al., 2017; Ganji et al., 2017). These miniaturized devices offer additional advantages such as reduced tissue damage and impedance, increased signal-to-noise ratio and neuronal activation compared to traditional electrodes (Desai et al., 2014). A key component contributing to microelectrode design and, ultimately, to clinical performance is the selection of the materials for the device. Such materials should not only satisfy the mechanical and the structural requirements for the efficient electrochemical performance but also provide a durable and biocompatible interface with the brain tissue. In the following section, the current materials used in microelectrode fabrication are presented.

1.2 CURRENT MATERIALS FOR MICROELECTRODE FABRICATION

For the long-lasting efficient microelectrodes, the material should not only function properly in vivo but also be biocompatible and durable for the protection of both the patient and the device (Williams, 2008; Szostak et al., 2017). As different materials show dissimilar behavior in the tissue environment

the choice of the implant material is crucial. To mitigate foreign body reactions and corrosion/degradation of the structures, electrical, chemical and mechanical properties of materials, such as chemical composition, crystallinity, surface morphology, the electrode microstructure, and Young's modulus (a measurement of elasticity) need to be carefully considered (Cogan, 2008; Williams, 2008, 2009). With the advance of the micro-fabrication techniques, silicon and polymers have been widely employed as the substrate materials, while metals, carbon nanotubes, conductive polymers as electrode site materials (Samba et al., 2015; Yi et al., 2015; Antensteiner and Abidian, 2017).

Typical microelectrodes are designed to have either an array of microwires or micro-electromechanical system (MEMS) arrays. Microwires are generally composed of metals such as gold, tungsten, and stainless-steel, coated with insulators. Two different types of silicon substrate-based MEMS micro-machined electrodes, i.e. the Utah array (Normann and Fernandez, 2016; Wendelken et al., 2017) and the Michigan array (Kipke et al., 2008; Kiss et al., 2015), have been significantly exploited for decades. However, a huge mechanical mismatch between hard metals/silicon (E ~ 10 to 100 GPa) and soft brain tissue (0.4-15 kPa) results in substantial strain at the tissue-electrode interface, causing local physical damage that result in inflammation and neural degeneration (Polikov et al., 2005; Harris et al., 2011; Merrill, 2014). The inflammatory process may hinder the stimulation of neuronal cells, as well as it may contribute to device failure as a result of electrode degradation (Kozai et al., 2015b; McCreery et al., 2016). However, it must be highlighted that not all the microelectrode types exhibit the same degradation profile or that there is a direct correlation between electrode failure and the acute inflammatory response (Gaire et al., 2018b). Several efforts have been reported to overcome the drawbacks from the mechanical mismatch between electrode and tissue by implementing materials with lower Young's modulus, e.g. flexible and biocompatible polymer substrates (Trevathan et al., 2019). Polyimide- (Lai et al., 2012) and parylene-based MEMS (Hess et al., 2011) electrodes have been heavily investigated for their improved mechanical properties, easy access to fabricate, and capability to introduce bioactive molecules at the interface to facilitate long-term interaction with the tissue. As chronic stimulation electrode site materials, metals including tungsten, platinum, iridium, tantalum pentoxide, and titanium nitride have been extensively used for their electrical charge-injection properties and biocompatibility (Cogan, 2008; Fattahi et al., 2014; Meijs et al., 2015). For its remarkably increased charge storage and injection capacity and high corrosion resistivity, iridium oxide has been also widely utilized as a coating material (Meyer et al., 2001; Hasenkamp et al., 2009) to enhance the performance and the durability of the electrode. Carbon nanotubes (Jiang et al., 2011; Schmidt et al., 2013) and conducting polymers such as poly(3,4-ethylene dioxythiophene) (PEDOT) and

poly(styrene sulfonate) (PSS) (Cui and Martin, 2003; Pranti et al., 2018b) are attracting considerable attention as alternatives to the metal electrodes and coatings for their biocompatibility and tunable electrical properties.

An important challenge in microelectrode fabrication for neural stimulation is the identification of smart materials that are able to provide enhanced biocompatibility. So far, all the current microelectrodes are recognized, in the long run, as foreign bodies by the nervous tissue. As the difference in Young's modulus between the electrode and tissue is the the main factor that causes damage and inflammation, most research is focused on using materials with low Young's modulus for both substrates and electrode sites. However, it should be also taken into account that mechanical strain from the motion artifacts, such as bending of conducting material, can cause changes in resistance or capacitance of materials. As a result, this can affect the electrical signals of the electrode and can result in unintended performance (Michelson et al., 2019). Thus, the balance between Young's modulus and the electrical properties need to be carefully considered in designing microelectrodes for neural stimulation.

2. FOREIGN BODY RESPONSE AS A CAUSE OF IMPLANT FAILURE

The nervous tissue response to implantable microelectrodes is a complex process characterized by a cascade of biochemical alterations and chemical reactions occurring at the level of the tissue-material interface. These biochemical and chemical alterations may culminate in an undesired foreign body response. Additionally, changes in the inherent properties of the electrode after long-term implantation, for example due to corrosion, may further impair its tissue compatibility and durability. Body fluids and tissues are highly corrosive environments characterized by an elevated presence of oxygen, saline electrolytes, macromolecules and dissolved ions that can cause the electrochemical detachment of microelectrode surface. Once surgically implanted, microelectrodes must remain intact for several years to ensure the efficacy of the therapy and device functionality. To provide successful integration, reliability, and durability once implanted in the brain tissue, microelectrodes must fulfill the following requirements:

- **Biocompatibility**: the surface of the microelectrode must be non-toxic for neural cells without causing any adverse effects to the surrounding tissues.

- **Biomimicry**: the surface has to mimic the physicochemical and mechanical characteristics of the extracellular matrix (ECM) in order to promote neurite outgrowth towards the electrode surface and to avoid activation and recruitment of glial cells and fibroblasts that can contribute to the encapsulation of the electrodes.

- **Biostability**: microelectrodes need to maintain their physical integrity, electrochemical stability, and functionality, and resist the highly corrosive tissue microenvironment without undergoing any structural modification.

Microelectrode implantation causes unavoidable damage to the tissue, triggering a series of neuroinflammatory reactions, which are part of the natural wound healing process that can seriously affect the stimulating site integrity and hamper the electrochemical performance in long-term implantations (Salatino et al., 2018). The complexity of such a process can be described by dividing it into two coupled factors: biotic factors, represented by the effects of cells and tissue reactions occurring at the surface; and the abiotic factors, related to the characteristic of the material itself.
Biotic factors include the blood-brain barrier (BBB) rupture, protein absorption at the material surface, immune cells and fibroblast recruitment, increased production of radical ions, cell death and the formation of the insulating glial scar around the electrode surface, which hampers blood supply and ionic equilibrium at the injury site. The abiotic factors are represented by the physicochemical surface modifications such as the dissolution of passive films, material-related impedance, the failure of the stimulating site integrity, the formation of electrochemical cells at the level of the surface that can evolve in crevices or pits. Biotic and abiotic factors cannot be considered as two separated processes, as they are strictly dependent and occur simultaneously interacting in different manners during the lifetime of the electrode. The complexity of such a process is not totally understood and further research is needed to clarify whether the contributions of these interrelated factors occur and what are the most effective intervention strategies.
In this section, we will provide a description of the main cascade of biochemical and cellular events occurring upon brain microelectrode implantation with a focus on the biotic reactions.
The process that leads to glial scar formation due to implantation and can culminate in the encapsulation of an implant can be divided into two phases (**Fig.1**). An acute phase that starts immediately after device implantation and characterized by BBB dysfunction and glial cell activation, followed by a chronic phase characterized by an immune response and the development of a glial scar around the implant.

The first and one of the most critical events occurring during device implantation is the rupture of the BBB. The implantation causes a break at the level of the endothelial vessels, with a reduction of blood flow and oxygen supply, accumulation of plasma proteins and pro-inflammatory factors, and myeloid cell infiltration (Kozai et al., 2015a). Cell membrane damage by mechanical stress causes an increase in Ca^{2+} concentration either by its release through the pores in the cell membrane and by disturbances in the electrochemical potential of Na^{+} channels, which lead to membrane depolarization (Eles et al., 2018; Salatino et al., 2019). Membrane depolarization, in turn, leads to the increase in intracellular Ca^{2+}, neurotransmitters release from presynaptic terminations (Eles et al., 2018), resulting in excessive production of reactive oxygen species (ROS) due to mitochondrial damage (Potter-baker et al., 2015; Ereifej et al., 2018). The BBB breach has been shown to be crucial in the triggering of biochemical pathways responsible for neuronal degeneration and glial activation (Saxena et al., 2013). Some plasma proteins such as globulins, fibrinogen, thrombin, plasmin, and albumin can accumulate at the injury site through the BBB gap and can be adsorbed at the electrode surface.

2.1 MICROGLIA

Glial activation represents the main cellular event involved in the neuroinflammatory response. As the resident macrophage cells of the brain, microglia are ubiquitous in the CNS, and they become activated to carry out their neuroprotective functions immediately after electrode implantation. Once activated, they act as principal effectors of the neuroinflammatory response and can orchestrate the process through cross-talk with astrocytes and oligodendrocytes. It is already been accepted that microglia exist in “pro-inflammatory” and “anti-inflammatory” phenotypes. The former is the “classical activation” phenotype, in which cells secrets pro-inflammatory cytokines and contribute to neuronal injury; in the case of the latter phenotype cells secret anti-inflammatory cytokines and contribute to tissue remodeling and repair, phagocytosis of cell debris, as well as antagonize pro-inflammatory activity. In the early hours post-implantation, pro-inflammatory microglia secrete pro-inflammatory cytokines and chemokines such as interleukins IL-1α, IL-1β, IL-6, tumor necrosis factor (TNF-α), monocyte chemoattractant protein 1 (MCP-1) (Sawyer et al., 2014), ROS and reactive nitrogen species (RNS), determining massive immune cell recruitment and additional cytokine production (Hermann et al., 2018a). The lack of oxygen redox homeostasis acts directly on microglia, astroglia and endothelial cells causing activation of metalloproteinase, downregulation of tight junctions and adherens junction genes in the first hours after BBB injury (Bennett et al., 2018), facilitating the entrance of infiltrating macrophages, which will also have a crucial role in neurodegeneration (Ravikumar et al., 2014).

2.2 ASTROCYTES

Astrocytes are another type of neuroglia that is very affected after implantation. Astrocytes perform many functions, including biochemical support of endothelial cells that form the BBB, supplying of nutrients to the nervous tissue, maintenance of extracellular ion balance, having a key role in the repair and scarring process of the brain. In analogy to microglia, astrocytes exist in a pro-inflammatory phenotype and an anti-inflammatory phenotype. Pro-inflammatory astrocytes are activated by pro-inflammatory microglia and secret neurotoxins creating a hostile environment for neuronal and oligodendrocytes regeneration. Pro-inflammatory astrocytes are activated by Il-1β, TNF-α and complement component 1q (C1q) from microglia, responding immediately to electrode implantation and changes in neuronal activity, accumulating in the vicinity of the microelectrode during the first week after implantation (Liddelow et al., 2017). At this level, astrocytes alter the neuronal viability causing neuronal loss, reduction of fiber density and overexpression of glial fibrillary protein (GFAP) and vimentin, which are critical for their change in morphology and extension of the protrusions at the injury site (Woolley et al., 2013; Moeendarbary et al., 2017).

2.3 NEURONS

The neuronal loss also occurs immediately after implantation. The mechanical stress caused by electrode entry into the tissue leads to axonal morphological changes, neuronal membrane disruption with the formation of axonal blebs as an indication of neuronal damage. Oxidative stress in neurons is caused by the increase in intracellular calcium through glutamate-N-methyl-D-aspartate receptor (NMDA) activation, as well as by ROS and RNS produced by microglia and astrocytes, causing mitochondrial dysfunction. Neuronal degeneration and neuroinflammation are exacerbated by the persistent secretion of proinflammatory cytokines and glial fibrillary proteins deposition by microglia and astrocytes, finally forming the glial scar (**Fig.1**). As a consequence of this neuronal death at the tissue-electrode interface, the distance between electrode and synapses grows in time, hampering electrical stimulation performance.

2.4 OLIGODENDROCYTES

Oligodendrocyte cell death will also occur at the implantation site. Either due to cell membrane damage or as a result of neuronal cell death or axonal degeneration. Oligodendrocytes play the important function of ensuring axonal support and myelin production and maintenance. In the acute phase of foreign body reaction, oligodendrocytes become highly sensitive to oxidative stress by ROS and RNS as well as excitotoxic damage by glutamate oversignaling. Apoptosis of oligodendrocytes leads to demyelination and can also culminate in neuronal death depending on the extent of the event. In the adult brain, one can find not only myelinating oligodendrocytes but also cells in the form of neuron-glia antigen 2-expressing glial cells (NG2) precursors, which are present from development to the adult phase, denominated oligodendrocyte progenitor cells. In vivo studies showed that new NG2 precursors become activated by proinflammatory factors secreted by reactive microglia and can be seen migrating to the injury site 12 hours post-implantation (Wellman and Kozai, 2018). But there, NG2 precursors preferentially differentiate to astrocytes and further move towards the implant participating in the formation of the glial scar, not contributing to the turnover of new myelinating oligodendrocytes (Wellman et al., 2018a).

2.5 THE GLIAL SCAR

Over two weeks post-implantation, in the chronic phase of the process, it has been observed that astrocytes and microglia have their protrusions extended towards the material surface creating a non-permeable barrier between the implant and the tissue over two weeks post-implantation (Wellman and Kozai, 2017). At this stage, fibroblasts have reached the inflammation core from meninges and secret ECM proteins such as fibronectin, type IV collagen, laminin, and chondroitin sulfate proteoglycans, also contributing to the formation of the glial scar and the encapsulation of the microelectrode at the parenchymal level (Dias and Göritz, 2018). This insulating barrier constitutes a hostile environment that hampers electrophysiological performance due to the absence of contact between microelectrode and neurons, leading to the failure of the implant over extended periods of time (**Fig.1**).

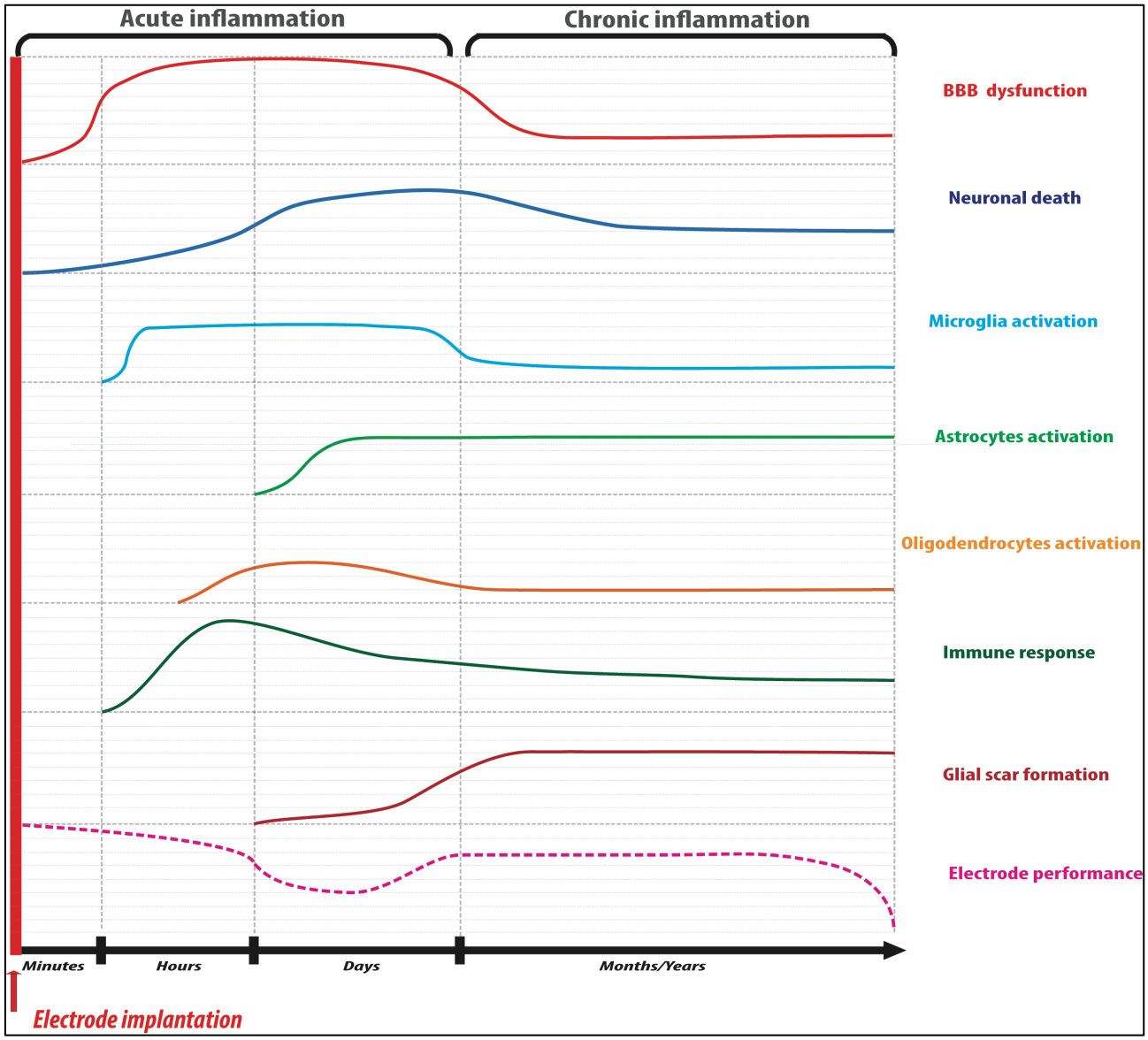


Figure 1. *Schematic timeline representation of the reactions involved in the process of neural tissue response to implantable microelectrodes. The acute phase of inflammation is characterized by BBB disruption and neuronal death due to mechanical insult followed by glial activation and immune cell recruitment at the injury site. Microelectrode performance may be hampered at this level due to mechanical mismatch with the tissue accompanied by a temporary recovery. In the chronic phase of inflammation, a glial fibrotic scar surrounds the microelectrode impeding material and stimulating site integrity that, ultimately, may result in implant failure.*

Despite all the efforts that have been carried out to study the dynamics of glial scar in injury and disease, additional investigations are required to understand the specificities of the foreign body response in the context of electrode implantation, to uncover the most effective intervention strategies to promote microelectrode integration in the CNS (Salatino et al., 2018). Besides, it is important to take in consideration that other aspects can influence glial scar heterogeneity, such as the type of microelectrode material used, the cerebral anatomical district of implantation, as well as the pathological context in which it is applied. Hence, the use of modeling systems that can mimic specific in vivo pathological conditions is a great opportunity to move towards the establishment of innovative approaches on which to base future microelectrode design.

3. EXPERIMENTAL MODELS TO STUDY FOREIGN BODY RESPONSE TO NEURAL IMPLANTS

Despite the great advances achieved in neural interface technology, some questions related to the molecular and cellular events involved in nervous tissue response to implantable microelectrodes remain unanswered. Several in vivo studies have been performed to identify critical aspects and design solutions to inhibit glial encapsulation in chronic applications. However, due to their cost, time consumption and complexity in vivo models are not ideal systems to investigate the detailed cues of tissue-electrode interactions. With this purpose, substantial research has been focused on the development of relevant in vitro biological platforms of increased complexity to test new materials and biosurfaces, which can offer a controlled and reproducible platform for high-throughput screenings. In the following paragraphs, we provide an overview of the current in vitro/ex vivo/in vivo models employed in microelectrode research, as well as a description of new promising 3D in vitro technologies with increased complexity that can be of added value to future investigations in this field (**Fig.2**).

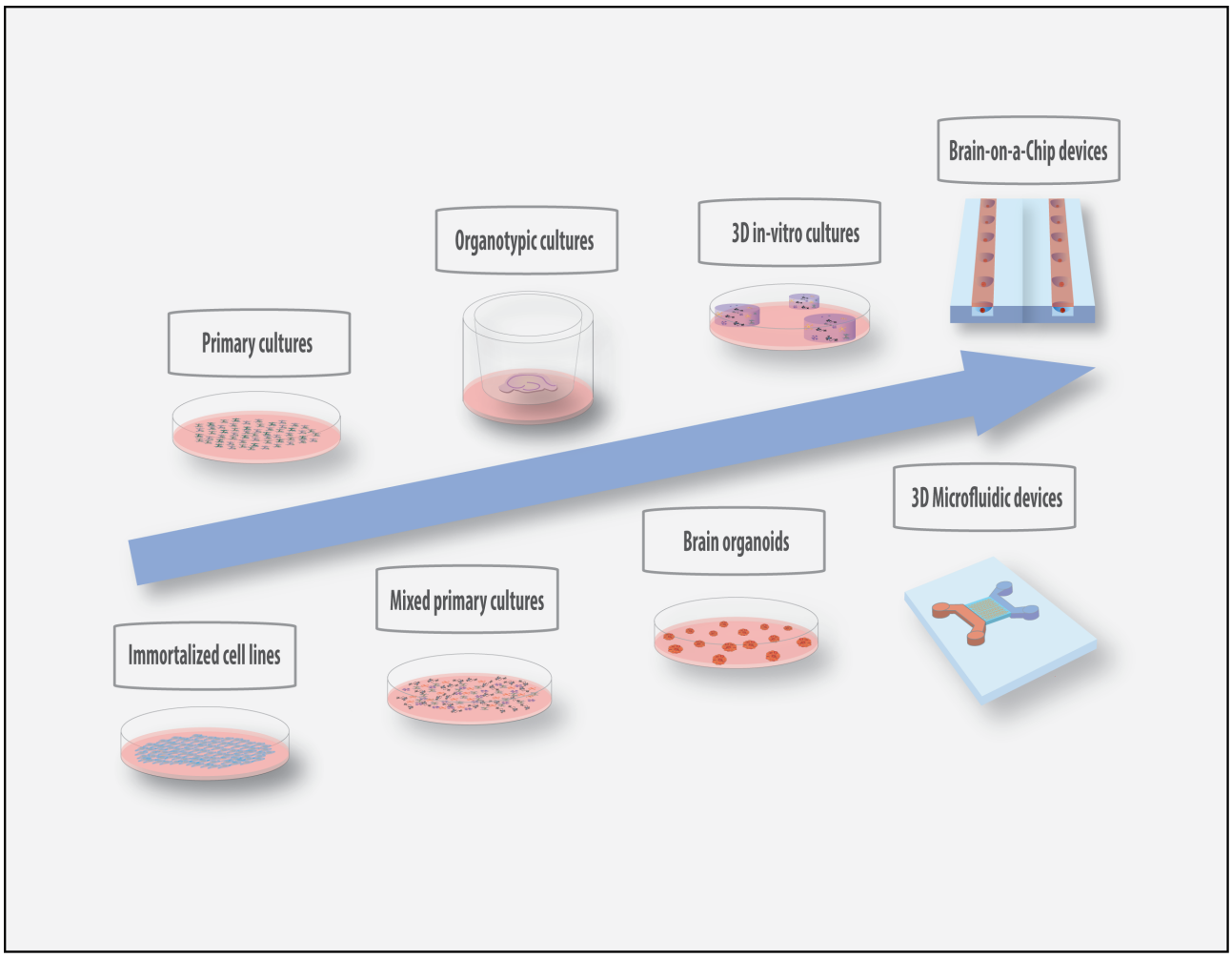


***Figure 2**. Schematic representation of the current and promising in vitro/ex vivo models with increased physiological relevance for the screening of materials and coatings for the development of implantable microelectrodes.*

3.1 IN VITRO MODELS

One of the main goals in the design and testing of new materials as well as coatings for microelectrodes is to reduce glial cell activation while allowing/inducing neuronal synaptic activity. In vitro 2D cultures represent the simplest model to investigate the impact of materials properties on the cellular response (**Table 1**).

Table 1. *Current and novel models explored for the study of biocompatibility of materials for neural applications and assessment of electrochemical performance and durability of implantable microelectrodes.*

Model	Specifics	Purpose of the study	Reference
Immortalized cell cultures	BV-2 mouse microglia cell line	Cellular responses to nanotextured silicon surfaces	(Persheyev et al., 2011)
	C6 rat astrocytoma cell line	Effect of nanopatterned poly(methyl methacrylate) surfaces on astrocyte reactivity	(Ereifej et al., 2013b)
	PC-12 rat pheochromocytoma cell line	Biocompatibility of polyurethane/poly(vinyl alcohol) hydrogel coatings	(Li et al., 2015)
	SH-SY5Y human neuroblastoma cell line	Cytotoxicity of nanostructured Pt-coatings	(Boehler et al., 2015b)
	NIH/3T3 mouse embryonic fibroblast cell line	Cytocompatibility of polyaniline surfaces	(Rejmontová et al., 2016)
	L929 mouse fibroblast cell line	Cytotoxicity of poly(3,4-ethylenedioxythiophene): glycosaminoglycan (PEDOT:GAG)	(Mantione et al., 2016)
	NIH/3T3 mouse embryonic fibroblast cell line	Biocompatibility of hydrophilic copolymers	(Hadler et al., 2017)
Primary cell cultures	Primary microglia	Cellular responses to nanostructured titanium oxide surfaces	(De Astis et al., 2013)
	Primary rat microglia	Response of microglia to P(TMC-CL))	(Pires et al., 2015)
	Primary mouse hippocampal neurons	Effects of nanotopography on neuronal cell signaling	(Onesto et al., 2017)

	Primary rat hippocampal neurons	Biocompatibility of poly(3,4-ethylenedioxythiophene) doped with poly(styrene sulfonate) MEAs	(Koutsouras et al., 2017);
	Primary human dermal fibroblasts	Study of surface nano-topography and chemistry on collagen I and III production	(Bachhuka et al., 2017)
	Primary rat cortical neurons	Development of a MEA-based *in vitro* model for drug screening	(Bradley et al., 2018)
	Primary rat cortical and spinal cord Astrocytes	Response of astrocytes to fiber surface nanotopography	(Johnson et al., 2018)
2D mixed cell cultures	Primary rat mixed microglia, astrocytes and oligodendrocytes	2D *in vitro* glial scar assay to test biocompatibility of insulating silicone polymer coatings	(Achyuta et al., 2010)
	Primary rat astrocytes derived from neurospheres and rat embryonic spinal cord cells	2D *in vitro* model of spinal cord injury for drug screening	(Boomkamp et al., 2012)
	Primary rat mixed neurons, microglia, astrocytes and oligodendrocytes	2D *in vitro* glial scar assay to test cellular responses of dip-coated PEG films	(Sommakia et al., 2014)
	Rat primary astrocytes and dorsal root ganglia neurons	2D *in vitro* model of spinal cord injury to study isotropic-to-anisotropic cellular transitions	(Zuidema et al., 2015)
	Primary cortical neurons and astrocytes	Cellular responses to nanoporous gold surfaces	(Chapman et al., 2016)

3D *in vitro* cultures	Primary rat microglia and astrocytes	Hyaluronic-based hydrogel as a 3D model to test electrode biocompatibility	(Jeffery et al., 2014)
	Primary mouse mixed neurons, microglia, astrocytes and oligodendrocytes	Alvetex membrane scaffold as a 3D culture for high-throughput screening	(Smith et al., 2015)
	Primary rat cortical neurons and astrocytes	Alginate-based hydrogel as a 3D model of glial scar	(Rocha et al., 2015)
	Primary rat mixed neurons, microglia, astrocytes and oligodendrocytes	Type I collagen-based hydrogel as a 3D model of glial scar	(Spencer et al., 2017a)
	Primary rat mixed microglia, astrocytes and oligodendrocytes	Hyaluronic acid-based hydrogel as a 3D model of glial scar	(Koss et al., 2017)
	PC-12, C6, human iPSC and rat primary dorsal root ganglia neurons	Type I collagen-based 3D hydrogel for high-throughput study of neurodegeneration	(O'Rourke et al., 2017)
Organotypic cultures	Rat organotypic hippocampal slices	Biocompatibility of silicon-based electrode arrays	(Kristensen et al., 2001)
	Rat organotypic brain slices	Biocompatibility of nanopatterned polydimethylsiloxane	(Ereifej et al., 2013a)
	Mouse organotypic spinal cord slices	Characterization of the ability of 3D meshed-carbon nanotubes to support neurite regrowth	(Usmani et al., 2016)
	Chicken embryo organotypic brain and liver slices	Cyto-biocompatibility of thin-film transistors	(Leclerc et al., 2017)

Brain Organoids	Human induced pluripotent stem cells (hiPSC) derived organoids	Model of autosomal recessive primary microcephaly	(Gabriel and Gopalakrishnan, 2017)
	Human embryonic stem cells (hESCs) derived organoids	Testing functionalized borosilicate glass capillaries for glutamate detection	(Nasr et al., 2018);
	Human primary microvascular endothelial cells, perycites, and astrocytes, mixed iPSC derived oligodendrocytes, microglia and neural stem cells	3D spheroid model of BBB for High-Throughput neurotoxicity screening and disease modeling	(Nzou et al., 2018)
Microfluidics	hiPSC-derived neurons and astrocytes	High-throughput screening of neurotoxic compounds	(Wevers et al., 2016)
	Ventral spinal cord motoneurons, rat primary meningeal fibroblasts and astrocytes	*In vitro* model of glial scar	(Li et al., 2017)
	Pre-differentiated hiPSC lines derived from skin fibroblasts	Brain organoids on chip for the study of impaired neurogenesis induced by cadmium	(Yin et al., 2018)
***In vivo* models**	Unilateral 6-OHDA injection in adult rats to model nigrostriatal	Analysis of c-fos expression after DBS of the pedunculopontine tegmental nucleus	(Saryyeva et al., 2011);

	degeneration of Parkinson's disease		
	Unilateral 6-OHDA injection Adult rats to model nigrostriatal degeneration of Parkinson's disease	Analysis of subthalamic nucleus-DBS on behavioral performance	(Badstuebner et al., 2017)
	Rat model of retinitis pigmentosa	Analysis of a fully organic retinal prosthesis to treat degenerative blindness	(Maya-vetencourt et al., 2017)
	Induction of status epilepticus through injection of pilocarpine in adult rats	Study of long-term DBS of the anterior thalamic nucleus	(Ferreira et al., 2018)

BV-2: mouse microglia cell line (CVCL_0182). C6: rat astrocytoma cell line (CVCL_0194). DBS: deep brain stimulation. C-fos: transcription factor subunit (OMIM: 164810). hESCs: human embryonic stem cells. hiPSC: human induced pluripotent stem cells. L929: mouse fibroblast cell line (CVCL_AR58). MEA: multi-electrode array. NIH/3T3: mouse embryonic fibroblast cell line (CVCL_0594). 6-OHDA: 6-hydroxidopamine (5-(2-aminoethyl)benzene-1,2,4-triol). PEDOT:GAG: poly(3,4-ethylenedioxythiophene): glycosaminoglycan. PEG: poly(ethylene glycol). PC-12: rat pheochromocytoma cell line (CVCL_F659). P(TMC-CL): poly(trimethylene carbonate-co-epsilon-caprolactone). SH-SY5Y: human neuroblastoma cell line (CVCL_0019).

3.1.1 IMMORTALIZED CELL LINE CULTURES

The use of relevant immortalized cell lines can provide significant insights regarding material biocompatibility and can contribute to the study of cell-microelectrode material interactions. The experimental conditions are controlled in terms of cell identity, adaptability, and reproducibility. Immortalized cell lines are simple to culture, can be grown for indefinite periods of time, maintaining genotypic stability and allowing the readily generation of large amounts of cells for analysis. Fibroblasts are one of the most well-characterized cell types to study the biocompatibility and the cell-adhesion properties of metals and coatings for biomedical devices. These cells play a critical role in the formation of the fibrotic scar in the late phases of inflammation. The modulation of their adhesion and interactions with the implants is crucial for ensuring a stable device performance. Fibroblast cell lines such as L929 and NIH/3T3 have been widely used to conduct standard material biocompatibility and cytotoxicity testing in accordance with the International Organization for Standardization (ISO) norm 10993-5. The latter defines a series of test methods employing cell monolayers in contact with the material or with material extracts to assess toxicity. In particular, the mouse embryonic NIH/3T3 fibroblasts are a well-characterized cell type used by FDA for biocompatibility testing of materials and coatings for neural devices. Namely, these were employed to assess surface properties of various preparations of polymeric conductive materials for neural devices applications (Bae et al., 2012; Mantione et al., 2016; Rejmontová et al., 2016; Hadler et al., 2017; Morin and He, 2017; Wang et al., 2018a).

Given their central role in orchestrating nervous tissue response to microelectrodes, glial cell were also employed to investigate the effects of new surfaces and designs on cell adhesion, morphology and activation (Persheyev et al., 2011; Ereifej et al., 2013b; Lee et al., 2014). Bérces and colleagues employed the immortalized murine microglial cell line BV-2 to investigate the effects of nanotopography on silica and platinum surfaces and compared their behavior with neural stem cells. They showed that while BV-2 cells grew indifferently on nanostructured and non-coated samples, neural stem cells grown on nanostructured surfaces displayed a decrease in cell viability, adhesion and a tendency to adhere to each other instead of to the surface (Bérces et al., 2018). C6 glioma cells were employed to investigate the biocompatibility of Pt-grown carbon nanofibers coatings for enzymatic glutamate biosensors and compared to Ni-grown nanofibers, showing that cells exhibit different cell adhesion and morphology at different dimensions of nanofibers (Isoaho et al., 2018).

Several studies have been conducted to investigate the biocompatibility and the effect of surface properties, like roughness and topography, on neuronal cells. Rat pheochromocytoma PC12 neuronal cell lines are the most used to study the ability of new biomaterials to promote neuronal adhesion and

neurite outgrowth (Arsiwala et al., 2014; Klymov et al., 2015; Li et al., 2015). Wandiyanto and colleagues have recently shown that PC12 cells grown on anti-bactericidal titanium nanostructures displayed enhanced proliferation, differentiation and neurite outgrowth compared to non-nanostructured surfaces (Wandiyanto et al., 2018). Tasnim and colleagues recently investigated, using the SH-SY5Y cell line, the biocompatibility of graphene oxide coating for commercially available 316 stainless steel. They showed that graphene oxide coating enables cell adhesion, proliferation and viability, as well as reduces ROS production compared to bare 316 stainless steel (Tasnim et al., 2018). Nissan and co-workers also employed SH-SY5Y to investigate the nanotopographical effects of silver nanoline coatings, showing that cells positively respond by increasing neurite outgrowth and branching points compared to unmodified silica wafers (Nissan et al., 2017).

While immortalized cell lines are a versatile and readily available tool in the early phases of material testing (**table 1**), these do not have the same biological relevance and response of their primary counterparts or even. Immortalized cell lines display evident phenotypic and physiological differences from the cell type of origin. These differences can be due to the cell source (many times tumor samples), immortalization process, the propagation and differentiation protocols, as well as the culture conditions and medium composition (Kaur and Dufour, 2012; Lorsch et al., 2014). Consequently, despite being from a similar cell type, immortalized cells can display different viability, metabolic and adhesive properties, as well as different expression profiles and cytotoxic responses to materials. In the context of neurophysiological investigations, they can display different electrophysiological responses to stimulations/recordings, thus they are not the best candidates to serve as models to recapitulate the pathophysiology of diseases (Xicoy et al., 2017). Therefore, results obtained with these cells require validation and comparison with more relevant experimental models. Primary cell lines are a more reliable cell type as they do not have a tumor origin or were not manipulated, and, therefore, more closely recapitulate the characteristics of neural cells in vivo.

3.1.2 PRIMARY CELL CULTURES

Primary cells represent the most used and reliable cell type for in vitro studies because they are similar to cells involved in the tissue response in vivo (**Table 1**). These cultures are not always the first choice due to experimental constraints, like ethics and economic issues. However, they are an excellent tool to study cell behavior prior to in vivo studies. CNS neural primary cells are obtained by dissociation of excised CNS tissue explants and subsequent isolation and plating. For in vitro studies, CNS primary cells are most commonly obtained from animal models like rat and mouse, as one has very

limited access to human CNS biopsies. With the recent advances in neuronal cell derivation from (human) pluripotent stem cells, neuronal cultures derived from these cell sources are emerging as a powerful tool for in vitro modeling (Song et al., 2016; Chen et al., 2018b).

In vitro primary neuronal cultures are widely employed in microelectrode research for the testing of new surface modified materials with improved biocompatibility and to investigate the effects of surface topographies in the enhancement of neuronal adhesion, neurite outgrowth and electrochemical performance (Chapman et al., 2016; Catt et al., 2017; Davoust et al., 2017; Seyock et al., 2017; Zöndör and Thoumine, 2017).

The use of single isolated cell types, despite being useful for the investigation of specific biochemical and morphological responses once in contact with a surface, excludes the possibility to study cell interaction with the material in the presence of the glial and neuronal cells crosstalk. A common approach to improve the in vitro assays is the use of mixed glial cultures with neuronal cells, obtained in a single isolation procedure, as a strategy to mimic the environmental characteristics and cellular events involved in astrogliosis. The use of mixed glial cells allowed to increase the physiological relevance of in vitro testing and to monitor the neuroinflammatory process and microelectrode modifications under manageable and reproducible conditions. Mixed glial and neuronal cultures were used as an efficient in vitro glial scar model for the screening of new design coatings for microelectrodes (Achyuta et al., 2010; Sommakia et al., 2014) (see **table 1** for examples). However, despite useful and cost-effective if compared to in vivo studies, primary neural cell cultures also present limitations. The isolation procedures are challenging and require appropriate expertise (Uysal et al., 2018). In addition, primary cell lines do not divide (as in the case on neurons) or do not divide indefinitely as immortalized cell lines, hence the number of cells obtained for each isolation is substantially reduced, limiting the number of experiments and the amount of sample for molecular studies (Gordon et al., 2014). Besides the difficulty in their manipulation, primary neural cells, are isolated in early stages of development, therefore they can result unapt for the study of processes that are only observed in the adult or lead to unaccurate results, as some cellular responses can only be observed in early stages of development. The neural differentiation protocols, including for embryonic stem cells (ESCs) or induced pluripotente stem cells (iPSCs), are also laborious and expensive and can lead to different maturation properties (Verpelli et al., 2013; Engel et al., 2016).

Common to conventional immortalized and primary cell cultures conducted in 2D substrates, is the loss of the ECM composition and structure, cell-ECM and cell-cell interactions (namely, the neuronal network), and cell mechanics of the tissue of origin, which, inevitably, results in a different cell behavior compared to in vivo (Tekin et al., 2018). Thus, conventional cell cultures cannot provide detailed information about the interactions of electrode materials with the neural tissue in the initial

phases of acute injury or the process of foreign body response in pathological environments. Whence, the necessity of developing complementary models in order to properly study the host reaction to microelectrodes.

3.1.3 3D PRIMARY CELL CULTURES

With progress in the field of tissue engineering, one is observing an increase in the number of reports of mixed culture systems conducted in 3D scaffolds (**Table 1**). The use of 3D matrices provides additional dynamics to the application of in vitro platforms for glial scar modeling, offering a valid and reproducible system to implement microelectrode research prior to in vivo studies. Several types of 3D scaffolds for neural cultures have been developed. These engineered scaffolds can be based on natural or synthetic materials (mostly polymers). These constitute a great improvement for in vitro studies in terms of increase in complexity and open the way to a vast window of applications in nervous system modeling (Ko and Frampton, 2016). Jeffery and colleagues developed a photocrosslinkable and tunable hyaluronic acid-based hydrogel scaffold for mixed glial cultures and high throughput screening of microelectrode materials (Jeffery et al., 2014). A commercially available synthetic polystyrene scaffold was shown to support neuronal cell growth and differentiation. It has been already tested for the development of a 3D model of neuroinflammation employing embryonic primary cortical neurons that are able to grow, interact and form networks possessing electrical activity in the presence of mixed glial cultures (Smith et al., 2015). We have proposed the use of a alginate-based simple and reproducible astrocyte 3D culture system that mimics many features of astrogliosis (Rocha et al., 2015). Using this platform, we established the ECM mechanical properties as a key modulator of astrogliosis. Spencer and coworkers developed a type-1 collagen gel with mixed primary embryonic neural cultures as an in vitro model of glial scar to investigate the effects of micromotion around neural implants (Spencer et al., 2017a). Koss et al. recently developed a hyaluronic acid-based 3D hydrogel model to study the process of glial scar formation in response to implantable microelectrodes. The biocompatibility of this system allows the encapsulation of primary oligodendrocytes, microglia and astrocytes and has shown to reproduce the typical features of the in vivo glial scar process (Koss et al., 2017).

The additional advantage of using 3D systems is the possibility to manipulate and tune scaffold composition through the incorporation of different matrix components and bioactive factors to promote cell survival, migration, and differentiation in a 3D context. The objective is to generate 3D structures with mechanical and structural properties as similar as possible to the ones of the CNS tissue (see **table 1** for examples). Despite the great advances in this field, these systems still present

some constraints. Some biomaterials used for scaffold production are characterized by a high modulus compared to the neural tissue and can lead to altered cell viability, proliferation, and differentiation. Conversely, soft biomaterials are more difficult to handle. The design of matrices with a nanosized microstructure and topographical cues that fully mimic the one found in the nervous tissue was still not attained. The procedures of cell extraction for molecular analysis after testing, scaffold processing, and imaging become more challenging in 3D, limiting high-throughput studies. Additional complications are related to the cell culture conditions: 3D scaffolds can constitute a physical barrier that limits oxygen perfusion, nutrient supply and accumulation of toxic compounds that can cause cellular alterations or apoptosis. Optimizations are still required to ensure a versatile cell encapsulation for different cell types and controlled culture conditions as close as possible to the in vivo environment. This is even more challenging in the context of disease modeling, where cells must be induced to display specific pathological profiles.

It is expectable in the future that the continuous progresses attained in the tissue engineering field, particularly related to improved scaffolds/matrices development, will allow the development of better in vitro systems that recapitulate neural tissue architecture, in an effort to minimize the gap between in vitro and in vivo experiments.

3.2 EX VIVO MODELS

The development of 3D in vitro models of brain tissue, as stated above, represents an attractive tool for researchers working in the neurosciences field and their use in microelectrode research would have a great impact on the screening of new biomaterials for biomedical applications. However, additional optimizations are still required to allow a consistent application in neuroscientific research. A potential alternative that enables researchers to get closer to in vivo conditions is the use of ex vivo excised brain/spinal cord tissues.

3.2.1 ORGANOTYPIC CULTURES

Tissue explants can be extracted from euthanized animals or obtained from human biopsies and cultured in vitro. The great advantage of organotypic cultures compared to artificial in vitro systems is the preservation of the native cytoarchitecture with the maintenance of intact neuronal networks. Although several types of ex vivo models have been described in literature (Mii et al., 2013; Nery et al., 2015; Jones et al., 2016; Neville et al., 2018), brain slice cultures from rodents are the most established and widely used as a system of election for neurophysiological investigations,

neuropharmacology and as a model of disease. The procedure consists in the isolation of specific districts from the whole brain, their dissection in slices and incubation under controlled conditions. The possibility to obtain several slices from a single animal constitutes an additional advantage in terms of reduction of the number of animals for experiment and of related costs.

Brain slice cultures have been well established from different brain regions (**Table 2**). Two types of brain slices preparations exist: acute slices from the adult brain, with a short life and mainly used for electrophysiological recordings, and organotypic slices from neonatal animals. The latter are the most diffused ex vivo platforms for the study of many physiological and pathological conditions, thanks to the possibility to reproduce, by external intervention, the hallmarks of diseases that occur in vivo (Magalhães et al., 2018). The great success of this system is due to the simplicity of the procedure and manipulation by mechanical or pharmacological treatment, as well as the possibility to perform electrophysiological recordings on bioelectric activity. Based on these features, organotypic cultures can constitute an ideal model for the long-term assessment of the complex host reaction to microelectrodes or for high-throughput biocompatibility studies of new materials and surfaces. Nevertheless, few works can be found in the open literature (Kristensen et al., 2001; Huuskonen et al., 2005; Ereifej et al., 2013a; Usmani et al., 2016; Leclerc et al., 2017). A possible explanation for this fact could be related to the preferential use of in vivo models as the gold standard for microelectrode testing. Although necessary for the translation of new materials to the clinic, in vivo experiments have ethical issues, they are expensive, time-consuming and unapt for screening studies due to their complexity. The great advances achieved by in vitro/ex vivo systems can be the successful strategy to accelerate microelectrode research prior to in vivo testing. The controllable and reproducible conditions make them suitable to identify strategies to mitigate neuroinflammation, to prevent the early biochemical and corrosion-related events at the interface electrode-neural tissue and to impair foreign body response. Nevertheless, although organotypic cultures maintain the 3D cytoarchitecture, slice preparation causes an unavoidable axotomy of the brain tissue and neuronal death. This physical damage is accompanied by loss of blood flow, and consequently jeopardize oxygen perfusion and nutrient supply. As occurs in primary neural cultures, organotypic cultures are derived from animals in early stages of development and require extensive periods of culture for their maturation for use in post-developmental studies and assessment of pathophysiological processes. Another important caveat is the lack of the BBB and circulating immune cells. In the context of testing materials for neural devices, we previously showed that these factors play a crucial role in the process of foreign body response. BBB dysfunction and cell infiltration are also associated with several neuropathological processes. This can limit the physiological relevance of organotypic cultures for disease modeling (Humpel, 2016). Hence, researchers are developing innovative approaches

combining microfluidic technologies with cellular vascular structures to mimic BBB microarchitecture and improve culture conditions for long term studies (Xu et al., 2016). These authors proposed a new and dynamic in vivo-like three-dimensional microfluidic system to replicate the the BBB in vivo. Despite these limitations, organotypic cultures are still one of the most relevant models and can represent a fascinating tool to reduce the differences between in vitro and in vivo studies (some examples are present in **table 1** and **2**).

Table 2. *Organotypic cultures as a model of neurological and neurodegenerative diseases.*

Disease	Type of organotypic slice	Induction of disease	Reference
Parkinson´s disease	Parasagittal nigrostriatal slices	Slices incubation with 6-hydroxydopamine (6-OHDA)	(Kearns et al., 2006)
	Organotypic midbrain slices	Transfection with truncated α-synuclein (A53T)	(Zach et al., 2007)
	Nigrostriatal organotypic slices	Mechanical cutting of dopaminergic fibers from substantia nigra to striatum	(Cavaliere et al., 2010)
	Ventral mesencephalon organotypic slices	Unilateral microinjection of 6-hydroxydopamine (6-OHDA)	(Stahl et al., 2011)
	Sagittal nigrostriatal slices	mechanical transection of the medial forebrain bundle	(Daviaud et al., 2014)
	Coronal nigrostriatal slices	Injection of rotenone	(Testa et al., 2005; Ullrich and Humpel, 2009)
	Cerebellar nigrostriatal slices	Slices incubation with 1-methyl-4-phenylpyridinium (MPP+)	(Chong et al., 2015)
Epilepsy	Organotypic hippocampal slices	Slices incubation with Kainic acid	(Järvelä et al., 2011; Jung et al., 2013a)

	Organotypic hippocampal slices	Slices incubation with kainic acid or n-methyl di-aspartate	(Prasad Tripathi and Ayyannan, 2017)
	Organotypic hippocampal slices	Slices incubation in a Neurobasal/B27 serum-free medium	(Magalhães et al., 2018)
Alzheimer disease	Organotypic hippocampal slices	P301S Alzheimer disease mouse model	(Mewes et al., 2012)
	Organotypic coronal brain slices	Co-transfection with amyloid precursor protein cDNA or human tau4R0N cDNA	(Kanegan et al., 2016)
	Organotypic hippocampal slices	APPsdl mouse model	(Penazzi et al., 2017)
	Organotypic hippocampal slices	3xTg-AD mouse model	(Croft and Noble, 2018; Jang et al., 2018)
Traumatic brain injury	Organotypic hippocampal slices	Focal mechanical trauma at the CA1 region	(Schoeler et al., 2012; Krings et al., 2016)
	Organotypic hippocampal slices	Tissue deformation by mechanical stretching	(Choo et al., 2013; Lamprecht et al., 2017)
Stroke	Organotypic coronal brain slices	Exposure to oxygen glucose deprivation	(Wang et al., 2006);
	Organotypic hippocampal slices	Exposure to oxygen glucose deprivation	(Hall et al., 2009)
Spinal cord injury	Organotypic spinal cord slices	Exposure to hypoxic condition	(Kim et al., 2010b)
	Organotypic spinal cord slices	Slices incubation with kainic acid	(Mazzone and Nistri, 2014)
	Organotypic spinal cord slices	Mechanical damage using weight drop model of injury	(Labombarda et al., 2013; Pandamooz et al., 2019)

APPsdl: amyloid precursor protein gene mutation. A53T: point mutation human α-synuclein protein. CA1: "Cornu Ammonis" 1 hippocampal region. MPP+: (1-Methyl-4-phenylpyridin-1-ium). 6-OHDA: 6-hydroxidopamine (5-(2-aminoethyl)benzene-1,2,4-triol). P301S: microtubule associated protein Tau (OMIM 157140 genetic mutation). tau4R0N: human microtubule associated protein tau, transcript variant 3, mRNA. 3xTg-AD: transgenic Alzheimer Disease mouse model.

Finally, as a duty of each and every scientist, the use of in vitro/ex vivo models must be encouraged in order to improve the ethical acceptability of research in the fulfillment of the principles of Replacement, Reduction, and Refinement (3R's) (Lossi and Merighi, 2018).

3.3 IN VIVO MODELS

Different types of in vivo studies have been carried out in microelectrode research to evaluate therapeutic efficacy, durability and safety of microelectrodes. In this type of studies rats and mice are the most common model of choice. The animal disease models that are used to assess the efficacy of neurostimulation therapies are several (Table 1). The main categories are represented by animal models of neurodegenerative disease such as Parkinson's disease (Badstuebner et al., 2017; Musacchio et al., 2017), Alzheimer's disease (Leplus et al., 2018), epilepsy (Desai et al., 2016), sensory-motor deficits due to spinal cord injury (Capogrosso et al., 2018), blindness (Tang et al., 2018), hearing loss conditions (Allitt et al., 2016) and ischemic models (Yang et al., 2017). Large animals such as cats, dogs, sheep, pigs, and non-human primates, are used for chronic studies on the efficacy and safety of neural stimulators. They concern the analysis of both biotic and abiotic reactions on the tissue-electrode interface in long-term experiments (Shepherd et al., 2018). The employment of large animals for these types of investigations is recommended because their anatomy perfectly mimics the environment in which microelectrodes will be applied, allowing the use of all the device components in their real size. Moreover, the full inflammatory component is present in vivo as opposed to in vitro/ex-vivo models. The surgical procedure in in vivo experiments generally consists in the exposition of the skull in a deeply anesthetized animal, the production of one or more drills in the vicinity of the target region, the insertion of the neural implant in a specific site and fixation of the plugs with dental cement, followed by continuous monitoring to assess the recovery of the animal, integrity of device and/or efficacy of the therapy (Fluri et al., 2015). Besides the damage caused by electrode implantation, the majority of in vivo experiments are carried out by tethering the animal to an external component through cables, causing severe discomfort. To overcome this, new

wireless microstimulation technologies were developed to ensure better freedom of movement, allowing the reduction of distress (Fluri et al., 2017; Pinnell et al., 2018). Besides the use of animal models of disease, chimeric mice models have found great utility for answering important biological questions concerning the role of different cell types in the process of foreign body response. Chimeras are animal models with two or more different genotypes experimentally obtained by transplanting cells or organs from another organism. Bone marrow chimeric mice were employed to investigate the contributions of different cells in the mechanism of foreign body response (Ravikumar et al., 2014). Sawyer and colleagues generated chimera mice between wild type and MCP-1 knock out mice, assessed the key-role of MCP-1 in the enhancement of neuronal loss and showed that its inhibition can be an effective strategy to prolong the lifetime of implantable microelectrodes (Sawyer et al., 2014). Bedell and co-workers recently developed chimeric mice lacking cluster of differentiation 14 (CD-14) genes in myelinating cells and blood-derived macrophages. They demonstrated that targeting CD-14 in blood-derived macrophages improved microelectrode performance in long term experiments (Bedell et al., 2018a). Genetically engineered animal models are another successful tool in microelectrode research. Mice lacking specific genes involved in neuroinflammation and immunity were employed to investigate the biochemical pathways involved in the foreign body response, the identification of pharmacological targets (Kozai et al., 2014; Bedell et al., 2018b; Hermann et al., 2018b, 2018a) and material testing (Lee et al., 2017; Mols et al., 2017). Mice carrying cell specific fluorescent tags have been shown to provide great advantages in the study of the contribution of different cells in a single animal as well as a valuable alternative to immunostaining steps (Sunshine et al., 2018; Eles et al., 2019). Gaire and colleagues recently developed a quadruple-labelled mouse with specific fluorescent tags for oligodendrocytes, microglia, neurons, and astrocytes and investigate the process of nervous tissue response to “Michigan” array silicon microelectrodes (Gaire et al., 2018).

Substantial improvements have been implemented in the quality and quantity of in vivo investigations: new bio-imaging tools were applied in microelectrode research to make in vivo works more explanatory. Two-photon laser scanning microscopy allows imaging of living animals with elevated resolution. It has been used to investigate the nervous tissue response to new electrode coatings (Eles et al., 2017a), glial cells characterization (Wellman and Kozai, 2018) or live calcium imaging (Kondo et al., 2017). Optical coherence tomography is a minimally invasive technique that has been proposed to be used in combination with two-photon laser scanning microscopy to provide high resolution angiography of damaged tissues around microelectrodes (Hammer et al., 2016). As an alternative to laborious histological and staining procedures on sectioned brains, x-ray micro CT scanning has been proposed as a high-resolution, time and cost saving procedure that allows a 3D x-

ray scanning of the entire brain to quantify and characterize the lesions caused by electrode implantation (Masís et al., 2018).

The growing scientific interest in neural interfaces in the last decades is confirmed by the multitude of in vivo works focused on the testing of new and fully biocompatible coatings (Du et al., 2017b; Spencer et al., 2017b; Shen et al., 2018b; Vitale et al., 2018b), less invasive implantation strategies (Tawakol et al., 2016; Shoffstall et al., 2018b) and new designs with improved electrical performance (Ferlauto et al., 2018b; Xu et al., 2018) and with longer durability.

Despite being considered the ultimate model to test microelectrode prior clinical tests, in vivo models present some important drawbacks as previously mentioned. An important aspect to consider is the elevated costs and time required for animal experiments, as well as the resulting ethical constraints. In vivo experiments are complex and demand adequate facilities and technical expertise. As discussed above, transgenic mice offer great advantages, however, they have an extremely high cost due to their production and maintenance. More importantly, the effects of such modifications can lead to altered phenotypes that depart from the real scenario. In the context of device testing, in vivo experiments are quite laborious and require long periods of time to assess the long-term performance of microelectrodes or the biological and behavioral effects of specific neurostimulation therapies. The complexity and invasiveness of the experimental techniques do not always enable scientists to identify the early biochemical and material-related events at the interface electrode-neural tissue and the strategies to mitigate neuroinflammation.

Despite these weaknesses, in vivo studies constitute the gold-standard for the investigations on neural implants, where the results obtained by previous in vitro testing find their effective validation. They represent the final step in the long process of microelectrode design and testing before the application in the clinic. A rigorous progression along all the steps determines the success of new technologies. This is even more important in the case of new materials or designs, where a careful preclinical assessment is necessary to minimize the risk of failure once applied to human patients.

4. FUTURE PERSPECTIVES

4.1 INCREASING COMPLEXITY

Preclinical studies are paramount in the development and testing of new materials for neural implants. As a consequence, the demand for more reliable in vitro/ex vivo models is growing to satisfy the need for assessing of the increasing number of new materials being proposed for this application, improve the quality of device testing and reduce the time between prototyping and commercialization of new products. As discussed in the previous section, several in vitro models and new platforms have been described in the literature (**Table 1**), but they still need to be explored, tested and eventually adapted for microelectrode research.

The use of ex vivo platforms from tissue explants can represent a valuable solution that fits perfectly these purposes. Brain organotypic cultures have been widely used in the last years as an excellent model for a great number of applications. They were employed to study physiological (Svensson and Chen, 2018), and pathological conditions (Tan et al., 2017) or for the screening of new therapeutics (Minami et al., 2017). Furthermore, several organotypic cultures have been established as models of neurological and neurodegenerative diseases (**Table 2**), for which neural implants have been proposed as therapeutic strategies. This places organotypic models that mimic a pathological environment in a privileged position to serve as platforms for microelectrode testing and a potential strategy to move closer to the in vivo scenario. Moreover, thanks to the preservation of intact neural circuitry, organotypic cultures are particularly suitable to perform electrophysiological studies, analyze microelectrode performance and assess astrogliosis.

Developments in the stem cell biology field have also contributed to the establishment of new in vitro models of human disease, aiming at an increase of complexity to reach the relevance of the in vivo environment, while maintaining the controllability and manageability of in vitro systems. Organoids, self-organized 3D tissue cultures derived from stem cells, are currently leading these technologies and have already been developed for the majority of human tissues, including the brain. More recently, the advances in hiPSC reprogramming techniques are also contributing to a better performance of organoid platforms in mimicking human disease and serve as testing platforms for personalized medicine (Perkhofer et al., 2018). Lancaster and Knoblich, described in 2014 the preparation of cerebral organoids prepared from hiPSC (Lancaster and Knoblich, 2014). The described methodology allows cell aggregates cultured in Matrigel to mimic native brain tissue, originating different developing brain regions, namely, cerebral cortex, ventral telencephalon and

retinal, among others, within one to two months. iPSC derived organoids represent an innovation in the field of in vitro disease modeling, offering a great opportunity to investigate pathophysiological mechanisms of neurological diseases with elevated reliability (Ho et al., 2018; LaMarca et al., 2018; Sun et al., 2018) and can also contribute to the field of implantable microelectrodes. In fact, Ormel and colleagues demonstrated that organoids can innately develop microglia and have a response to inflammatory stimuli that recapitulates neurons-glia interactions in vivo (Ormel et al., 2018). This is an important aspect since glial cells, particularly microglia, are involved in a great variety of pathophysiological mechanisms.

Great advances in in vitro modeling have been also achieved thanks to the application of microfluidics combined with 3D in vitro cultures (Rocha et al., 2016). Microfluidic platforms consist of polymer-based platforms for in vitro culture of cells that allow control and manipulation of microenvironment and fluids (see **Fig.3** for relevant examples). The use of these microdevices brings in vitro models to a whole new level, thanks to the possibility of modifying spatial organization by isolating specific districts and simulate 3D tissue architecture of the native tissue. These systems allow the continuous control of external conditions, conferring an added value to in vitro technology, and giving the possibility to reproduce new biological features that are not possible to achieve with conventional culture systems (as discussed in section 3.2.1 for the case of the BBB). Wang and colleagues developed an organ-on-a-chip system for long-term culture of brain organoids under controlled conditions. Brain organoids were cultured on Matrigel scaffolds with a sided channel for the culture medium supply and a central perfusion channel, allowing a continuous culture medium flow and providing an improved proliferation and neural differentiation compared to static culture conditions (Wang et al., 2018b). Liu and co-workers combined multielectrode array technology with a microfluidic perfusion system for organotypic hippocampal slices as a platform for high throughput drug discovery (Liu et al., 2018). Microfluidic vascular models have been developed and applied to brain-on-a-chip platforms, enabling scientists to improve the quality of culture conditions and get even more close to in vivo dynamics (Osaki et al., 2018; Wang, 2018). New microfluidic devices that model the BBB were fabricated and tested on 2D and 3D cultures, showing that BBB integrity and permeability simulates in vivo characteristics (Chin and Goh, 2018). Adriani and collaborators developed a 3D neurovascular chip composed by a central hydrogel co-culture of rat primary neurons and astrocytes, and two lateral channels hosting human umbilical vein endothelial cells and human cerebral microvascular endothelial cells (Adriani et al., 2017). Bang and colleagues developed a 3D microfluidic BBB platform with a vascular channel composed by a co-culture of human umbilical vein endothelial cells and primary human lung fibroblasts directly interfacing with a neural channel composed by a co-culture of primary rat neurons and astrocytes to simulate the neurovascular unit.

They showed that this platform displayed permeability, cellular contacts and synaptic structures comparable to the in vivo BBB, suggesting its great potential for the drug screening for neurological diseases (Bang et al., 2017). Microfluidic technology can conduct in vitro culture system to a more complex and realistic level providing many advantages and details that cannot be extracted with conventional in vivo models, such as the easy manipulation, low cost, and the possibility to investigate more intimately key mechanisms of diseases. These characteristics perfectly fit with ideal biological platforms for the testing of microelectrode materials developed in the last decades. 3D microfluidic systems can eliminate some of the limitations of 3D in vitro technology, creating new high-fidelity throughput systems that can improve the testing performance and reduce the cost and time for pre-clinical assessment. An additional advantage is the possibility to induce specific pathological features by external treatment for long-term experiments, offering the possibility to investigate in advance microelectrode performance and nervous tissue response under disease conditions.

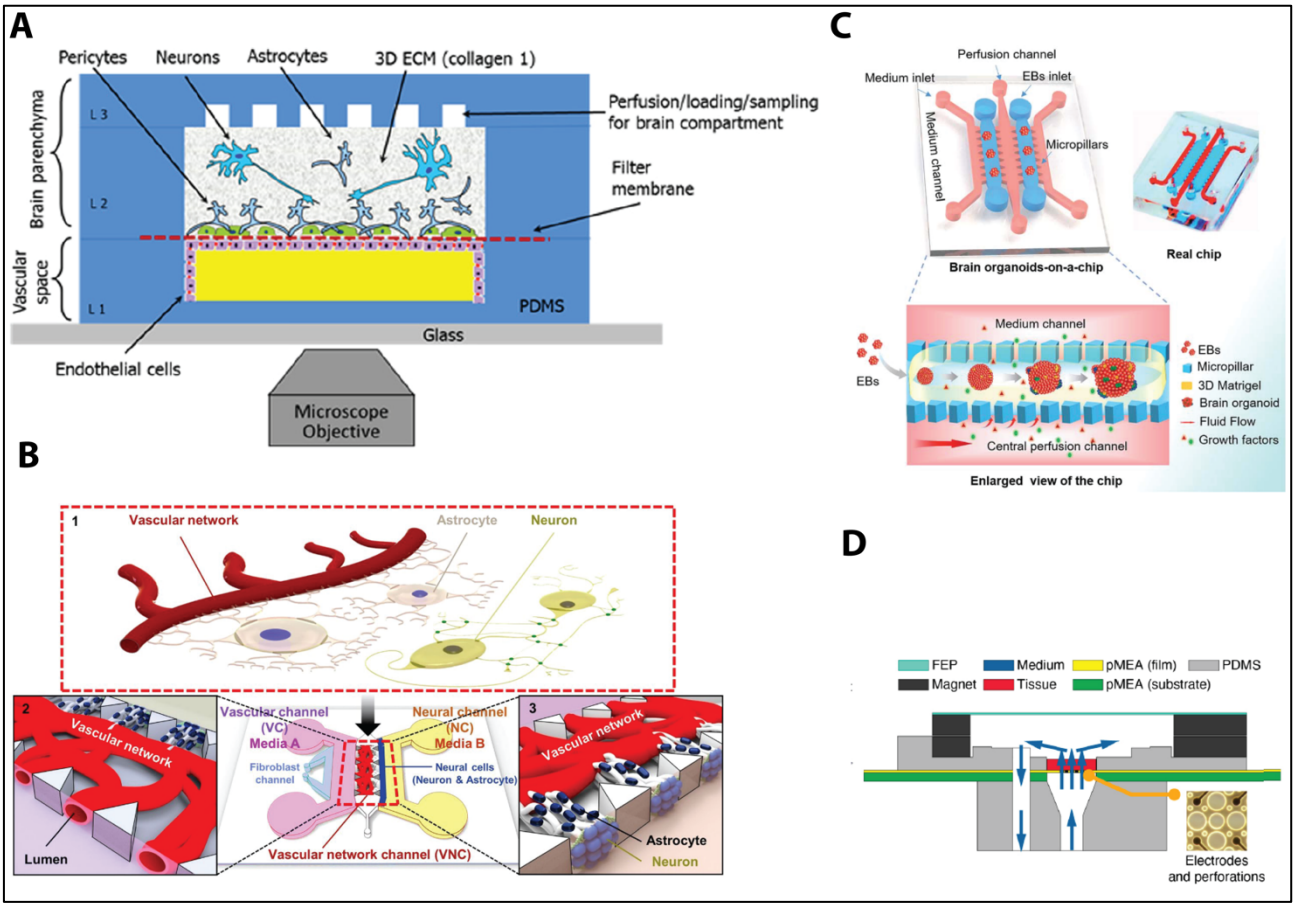


Figure 3. *Schematic representations of 3D microfluidic systems. (A) Schematic view of a microfluidic device for 3D cell culture composed by a vascular channel for primary human brain-derived microvascular endothelial cells (hBMVEC), and a brain chamber for primary cell-derived human neurons, pericytes and astrocytes culture in a type I collagen matrix. Reprinted from (Brown et al., 2015) with the permission of AIF publishing. (B) 3D microfluidic platform for the establishment of a neurovascular unit (NVU) including blood-brain barrier (BBB). The NVU is characterized by a vascular channel (VC) composed by a co-culture of HUVEC and Primary human lung fibroblasts, and a secondary neural channel (NC) composed by a co-culture of neurons and astrocytes. Adapted with permission from (Bang et al., 2017). (C) Organ-on-a-chip device for 3D culture and differentiation of brain organoids, showing an enlarged view of the component parts and a flow chart showing the development stages of hiPSCs-derived brain organoids (Wang et al., 2018b) published by the Royal Society of Chemistry. (D) Vertical cross-section view of a perforating multi-electrode array (MEA) integrated in a PDMS device for long-term culture, live imaging, recording and stimulation of brain tissues and 3D cultures (Killian et al., 2016).*

4.2 DESIGN SOLUTIONS AND NEW MATERIALS FOR THE IMPROVEMENT OF MICROELECTRODE DURABILITY AND BIOCOMPATIBILITY

Despite remarkable developments in implantable microelectrodes for neuroprosthetics and DBS, additional investigations are still required to address the biocompatibility and the long-term durability issues. A critical issue is reducing the physical stress, local inflammation and electrode degradation caused by the reaction between electrode and tissue interface while maintaining the electrical sensitivity of the electrode (Prodanov and Delbeke, 2016). To tackle these issues, multiple material-based strategies regarding this problem have been suggested, including (i) chemical modification of the electrode materials, (ii) new design of electrode structures, and (iii) non-invasive and wireless approach using functional nanoparticles.

Biological and non-biological electrode modifications, especially through the surface coating of substrates and electrode sites, are the most commonly used strategies to improve interfacial mechanical mismatch (Aregueta-Robles et al., 2014). Advances in fabrication approaches for integrating conductive polymers (Kim et al., 2018c), shape-memory polymers (Shoffstall et al., 2018a), hydrogels (Crompton et al., 2007; Frampton et al., 2007) and carbon nanotubes (Baranauskas et al., 2011b; Bareket-Keren and Hanein, 2012) onto complex electrode structures, provide not only a chronically stable neural interface, but also an improvement in the electrode performance. The reduced surface area combined with low impedance and sensitivity provided by such materials make them suitable for either stimulation and recording applications (Vitale et al., 2015; Du et al., 2017a; Pancrazio et al., 2017b; Wang et al., 2019a).

The additional advantage is that the bioactive molecules can be attached to the coating surfaces to increase stimulating/recording sensitivity. Employing composite materials for electrodes and coatings has also emerged as a promising strategy for upgrading electrode functionalities and biocompatibility. Heo et al. have reported improved biocompatibility in polyimide-based microelectrodes by coating them with PEG hydrogels containing Poly lactic-glycol acid (PLGA) microspheres loaded with the anti-inflammatory drug (Heo et al., 2016a). On the other hand, Zhou et al. proposed a carbon nanotube doped PEDOT composite coating material onto the Pt electrode. They showed that this coating makes the electrode more stable with enhanced charge transfer capacity and tissue-electrode interaction (Zhou et al., 2013). While chemical modification of materials is still being suggested as an efficient way of protecting both electrode and brain tissue, the long-term stability issue caused by the degradation and delamination of coating materials still remains as the challenge that needs to be overcome (Green et al., 2008).

Another attempt to reduce the immune response while enhancing functionality is to introduce new microelectrode designs. The development of the fabrication techniques of soft materials has enabled the production of ultrasoft and ultrathin electrodes with complex designs that minimize the mechanical mismatch of the electrode-tissue interface (Weltman et al., 2016). Recently, Kim et al. have fabricated ultrathin polyimide-based polymer electrodes covered by bioresorbable silk film. They successfully demonstrated the integration of the ultrathin electrodes with a complex structure by allowing the silk to be dissolved and resorbed. This procedure encouraged the spontaneous wrapping process driven by the capillary effect at the material-tissue interface, generating greatly improved biocompatibility (Kim et al., 2010a). Carbon nanotube-based soft fiber microelectrodes have also proved to have low impedance and effective therapeutic stimulation along with single-neuronal-unit signal detectable resolution, owing to their high surface area and electrical conductivity (Vitale et al., 2015). Compared to the similar dimension and surface environment, ultra-soft and ultra-thin electrodes have a great potential to significantly reduce inflammatory tissue response in the long-term scale (Du et al., 2017b). However, as mentioned earlier, the balance between flexibility/softness and the electrical performance should be carefully considered when designing these type of electrodes (Wellman et al., 2018b). Implementing functional nanoparticles are attracting increasing attention as a non-invasive and remotely controllable method. Chen R. et al. succeeded in utilizing the magnetothermal effect of nanoparticles for DBS (**Fig.4A** and **B**). They injected Fe_3O_4 magnetic nanoparticles in the ventral tegmental area of mice and exposed them to the external magnetic field. When magnetic nanoparticles are exposed to the AC magnetic field, stimulation of neurons at the targeted brain region was triggered by the dissipated heat from the magnetothermal effect. Wireless neural stimulation was successfully performed one month after injection. Moreover, lower glial activation, less macrophage accumulation and neuronal loss have been reported compared to a stainless steel implant (Chen et al., 2015). Chen S. et al. recently proposed optogenetic treatment by shining near infrared light to molecular tailored upconversion nanoparticles (**Fig.4C-E**). They injected nanoparticles into the ventral tegmental area of the brain to stimulate deep neurons and successfully demonstrated that light treatment on upconversion nanoparticles can induce dopamine release from dopaminergic neurons, activation of inhibitory neurons, inhibition of hippocampal excitatory cells, and memory recall. (Chen et al., 2018a). Magnetoelectric nanoparticles are another great candidate for neural stimulation. It has been already proven that the piezoelectric materials can generate electric signals under the acoustic wave and can induce neural cell differentiation (Chen et al., 2019c). As ferromagnetism and ferroelectricity are coupled to each other, applied external magnetic field can induce variation in electric polarization of nanoparticles, causing a change of the electronic structure at the particle surface and therefore facilitating stimulation of the tissue deep

inside the brain (Kargol et al.; Guduru et al., 2015a). As a non-invasive stimulating method, implementing magnetoelectric material is attracting significant attention. While these approaches using nanoparticles have great potential, biocompatibility and cellular uptake of these functional particles still remain as a problem to be solved (Adjei et al., 2014; Behzadi et al., 2017).

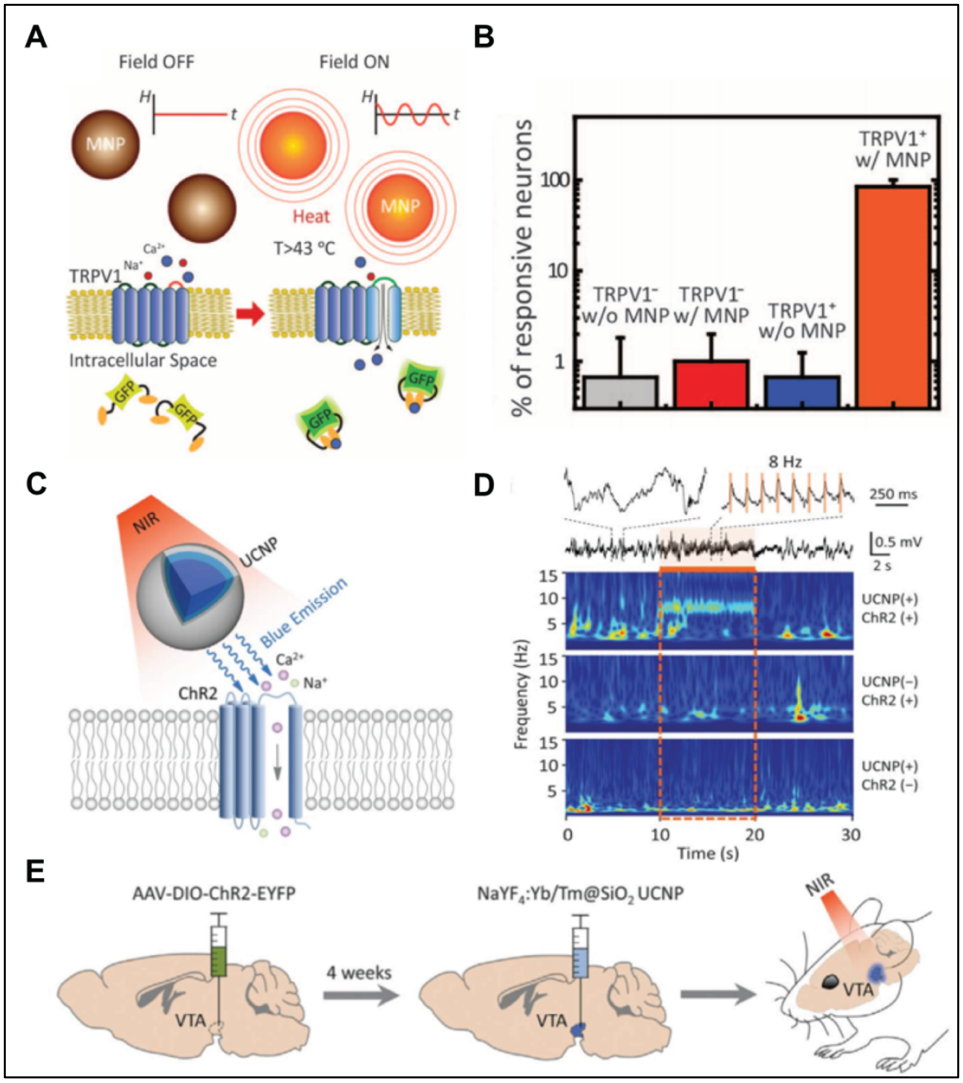


Figure 4. *New strategies for deep brain stimulation using functional nanoparticles. (A) A schematic description of magnetothermal effect on transient receptor potential cation channel subfamily V member 1 (TRPV1) cells. (B) Comparison of the neuron reactivity under different conditions. Figures from (Chen et al., 2015), reprinted with permission from AAAS. (C) A schematic description of nanoparticle-mediated near infrared (NIR) upconversion optogenetics. (D) Hippocampal local field potential response under NIR stimulation under different conditions. (E) In vivo experimental description of NIR stimulation of the ventral tegmental area of mice. Figures from (Chen et al., 2018a), reprinted with permission from AAAS.*

5. CONCLUDING REMARKS

The field of the brain-machine interface is exponentially growing and comprises an important source of progress in many aspects of neurosciences. The application of bionic systems, neural prosthetics and neurostimulation for restoring/treating severe neuro-debilitating conditions and neurological diseases has attracted the interest of many researchers and clinicians. All these technologies require the use of implantable microelectrodes to interface with the CNS. They represent an essential tool that serves as a link between the electronic components and the neuronal networks, in order to ensure a stable electrochemical communication over time. Great success has been achieved by the clinical application of neural prosthetics in the improvement of the quality of life of patients that suffer from sensory-motor deficits. DBS has become a treatment of choice for movement disorders and neuropsychiatric diseases and is proving to be a relevant alternative for a multitude of other pathological conditions.

The recent progress in microfabrication techniques made possible the development of microelectrodes capable of simultaneous recording and stimulation with improved cell selectivity and spatial resolution. Despite the improvements in device fabrication, biocompatibility and electrochemical performance for long-term applications, unfavorable nervous tissue response and microelectrode failure are still significant limitations. The process of nervous tissue response to microelectrodes has been described by an acute and chronic phase. The acute phase represents the most critical step characterized by a series of pathological reactions triggered by BBB dysfunction and glial activation. The persistence of this neuroinflammation is responsible for the immune response and the formation of the glial scar in the chronic phase, which may lead to microelectrode failure. A better understanding of the signaling pathways involved in the acute and chronic responses is required in order to develop new design strategies to mitigate neuroinflammation and promote a successful integration.

Several surface modified microelectrodes have been designed to provide minimal damage and establish a minimally reactive interaction with the brain tissue. However, additional studies are necessary to comprehend some of the key-cellular mechanisms implicated in the process of the glial scar formation around microelectrodes that remain to be elucidated. An important aspect in which research must be focused on is the binary role of the glial scar: several studies report a neuroprotective function of the glial scar in many pathological conditions, and its modulation has been suggested as a therapeutic approach to improve neuronal recovery and tissue regeneration. In the case of chronically implanted microelectrodes, the participation of the various glial subtypes to the nervous

tissue response and how their activation states can be influenced to soften tissue damage and avoid rejection are still unclear aspects. Towards this end, the use of appropriate experimental models can provide significant advantages in the development and testing of biocompatible and durable neural devices.

In this review, we provide an overview of the current and potential experimental in vitro, ex vivo and in vivo models to investigate the mechanisms of foreign body response to implantable microelectrodes. The progress in 3D tissue engineering and disease modeling opened the way towards the development of in vitro biological platforms with increased complexity and physiological relevance to be used for high-throughput studies before moving to in vivo animals. Organotypic culture systems are widely established ex vivo platforms which offer the possibility to simulate several pathological conditions and to isolate specific cerebral regions, ensuring the preservation of tissue architecture and synaptic organization for electrophysiological studies. While the use of organotypic culture systems as screening platforms for novel microelectrodes is still limited, their application is expected to grow in the near future, not only for the reasons mentioned earlier but also because these systems can contribute to significantly minimize the use of animal models. Additional implementations have been also achieved in in vivo studies. Despite being considered the gold-standard for microelectrode safety and efficacy studies, the principal limitation of in vivo experiments is the difficulty to monitor tissue response in the initial phases of injury. New advanced neuroimaging techniques open a new window of opportunities to improve the relevance of in vivo assessment thanks to the possibility to study biochemical processes, cell behavior and structural modifications in real time with elevated resolution. The advent of iPSC technology has enabled to simulate more closely the pathophysiological cues that occur in human diseases, offering the relevant advantage to recapitulate molecular and biological characteristics of the human brain. Success is also being achieved by the use of microfluidic systems combined with 3D cell cultures and/or iPSC-derived organoids, which allowed for integrating mechanical and physiological dynamics to simulate organ-like functions and responses. They represent a cost-effective compromise between the versatility of in vitro models and physiological relevance of in vivo models, offering the possibility to model pathophysiological cues under simulated conditions.

In conclusion, researchers have now a great variety of relevant models that can be adopted to improve microelectrode research in all the phases of development and to address the scientific unknowns related to the nervous tissue response to microelectrodes. Ultimately, with further improvements of these in vitro models, one can expect the creation of optimal milieus, which can substantially replace animal experimentation for large scale studies.

6. ACKNOWLEDGMENTS

This work was financially supported by Projects NORTE-01-0145-FEDER-000008 and NORTE-01-0145-FEDER-000012, supported by Norte Portugal Regional Operational Programme (NORTE 2020), under the PORTUGAL 2020 Partnership Agreement, through the European Regional Development Fund (ERDF) and FEDER - Fundo Europeu de Desenvolvimento Regional funds through the COMPETE 2020 - Operacional Programme for Competitiveness and Internationalisation (POCI), Portugal 2020, and by Portuguese funds through FCT/MCTES in the framework of the project "Institute for Research and Innovation in Health Sciences" (POCI-01-0145-FEDER-007274).
S.Pané acknowledges funding from a Consolidator Grant from the European Research Council (ERC) under the European Union's Horizon 2020 research and innovation programme (Grant Agreement No. 771565).
M. Gulino and D. Kim acknowledge their Ph.D. grants in the framework of the project mCBEEs funded by the European Union's Horizon 2020 research and innovation programme under the Marie Skłodowska-Curie grant agreement No 764977.
S.D. Santos would like to acknowledge national funds through FCT – Fundação para a Ciência e a Tecnologia , I.P., provided by the contract-program and according to numbers 4, 5 and 6 of art. 23 of Law no. 57/2016 of 29th August, as amended by Law no. 57/2017 of 19th July
A.P. Pêgo and S. Pané would like to acknowledge the contribution of the COST Action CA16122.

REFERENCES

Achyuta, A. K. H., Polikov, V. S., White, A. J., Pryce Lewis, H. G., and Murthy, S. K. (2010). Biocompatibility assessment of insulating silicone polymer coatings using an in vitro glial scar assay. Macromol. Biosci. 10, 872–880. doi:10.1002/mabi.200900451.

Adjei, I., Sharma, B., and Labhasetwar, V. (2014). Nanoparticles: cellular uptake and cytotoxicity. Adv Exp Med Biol 811, 73–91. doi:10.1007/978-94-017-8739-0_5.

Adriani, G., Ma, D., Pavesi, A., Kamm, R. D., and Goh, E. L. K. (2017). A 3D neurovascular microfluidic model consisting of neurons, astrocytes and cerebral endothelial cells as a blood–brain barrier-. Lab Chip 17, 448–459. doi:10.1039/c6lc00638h.

Allitt, B. J., Harris, A. R., Morgan, S. J., Clark, G. M., and Paolini, A. G. (2016). Thin-film micro-electrode stimulation of the cochlea in rats exposed to aminoglycoside induced hearing loss. Hear. Res. 331, 13–26. doi: 10.1016/j.heares.2015.10.003.

Antensteiner, M., and Abidian, M. R. (2017). Tunable Nanostructured Conducting Polymers for Neural Interface Applications. Conf Proc IEEE Eng Med Biol Soc. 2017, 1881–1884. doi:10.1109/EMBC.2017.8037214.Tunable.

Aregueta-Robles, U. A., J.Woolley, A., Poole-Warren, L. A., Lovell, N. H., and Green, R. A. (2014). Organic electrode coatings for next-generation neural interfaces. Front. Neuroeng. 7:15. doi:10.3389/fneng.2014.00015.

Bachhuka, A., Hayball, J. D., Smith, L. E., and Vasilev, K. (2017). The Interplay between Surface Nanotopography and Chemistry Modulates Collagen I and III Deposition by Human Dermal Fibroblasts. ACS Appl. Mater. Interfaces 9, 5874–5884. doi:10.1021/acsami.6b15932.

Badstuebner, K., Gimsa, U., Weber, I., Tuchscherer, A., and Gimsa, J. (2017). Deep Brain Stimulation of Hemiparkinsonian Rats with Unipolar and Bipolar Electrodes for up to 6 Weeks: Behavioral Testing of Freely Moving Animals. Park. Dis 5693589. doi:10.1155/2017/5693589.

Bang, S., Lee, S., Ko, J., Son, K., and Tahk, D. (2017). A Low Permeability Microfluidic Blood-Brain Barrier Platform with Direct Contact between Perfusable Vascular Network and Astrocytes. Sci. Rep. 7, 8083. doi:10.1038/s41598-017-07416-0.

Baranauskas, G., Maggiolini, E., Castagnola, E., Ansaldo, A., Mazzoni, A., Angotzi, G. N., et al. (2011). Carbon nanotube composite coating of neural microelectrodes preferentially improves the multiunit signal-to-noise ratio. J Neural Eng. 8:066013. doi:10.1088/1741-2560/8/6/066013.

Barbe, M. T., Reker, P., Hamacher, S., Franklin, J., Kraus, D., Dembek, T. A., et al. (2018). DBS of the PSA and the VIM in essential tremor. Neurology 91, e543–e550. doi:10.1212/WNL.0000000000005956.

Bareket-Keren, L., and Hanein, Y. (2012). Carbon nanotube-based multi electrode arrays for neuronal interfacing : progress and prospects. Front. Neural Circuits 6:122. doi:10.3389/fncir.2012.00122.

Bedell, H. W., Hermann, J. K., Ravikumar, M., Lin, S., Rein, A., Li, X., et al. (2018a). Targeting CD14 on blood derived cells improves intracortical microelectrode performance. Biomaterials 163, 163–173. doi:10.1016/j.biomaterials.2018.02.014.

Bedell, H. W., Song, S., Li, X., Molinich, E., Lin, S., Stiller, A., et al. (2018b). Understanding the Effects of Both CD14-Mediated Innate Immunity and Device / Tissue Mechanical Mismatch in the Neuroinflammatory Response to Intracortical Microelectrodes. Front. Neurosci. 12:772. doi:10.3389/fnins.2018.00772.

Behzadi, S., Serpooshan, V., Tao, W., Hamaly, M. A., Alkawareek, M. Y., Dreaden, E. C., et al. (2017). Cellular uptake of nanoparticles: journey inside the cell. Chem. Soc. Rev. 46, 4113–4376. doi:10.1039/c6cs00636a.

Bennett, C., Samikkannu, M., Mohammed, F., Dietrich, W. D., Rajguru, S. M., and Prasad, A. (2018). Blood brain barrier (BBB)-disruption in intracortical silicon microelectrode implants. Biomaterials 164, 1–10. doi:10.1016/j.biomaterials.2018.02.036.

Bérces, Z., Pomothy, J., Horváth, Á. C., Kőhidi, T., Benyei, É., Fekete, Z., et al. (2018). Effect of nanostructures on anchoring stem cell-derived neural tissue to artificial surfaces. J. Neural Eng. 15, 056030. doi:10.1088/1741-2552/aad972.

Boehler, C., Stieglitz, T., and Asplund, M. (2015). Nanostructured platinum grass enables superior impedance reduction for neural microelectrodes. Biomaterials 67, 346–353. doi:10.1016/j.biomaterials.2015.07.036.

Boomkamp, S. D., Riehle, M. O., Wood, J., Olson, M. F., and Barnett, S. C. (2012). The Development of a Rat In Vitro Model of Spinal Cord Injury Demonstrating the Additive Effects of Rho and ROCK Inhibitors on Neurite Outgrowth and Myelination. Glia 60, 441–456. doi:10.1002/glia.22278.

Bradley, J. A., Luithardt, H. H., Metea, M. R., and Strock, C. J. (2018). In vitro screening for seizure liability using microelectrode array technology. Toxicol. Sci. 163, 240–253. doi:10.1093/toxsci/kfy029.

Brown, J. A., Pensabene, V., Markov, D. A., Allwardt, V., Neely, M. D., Shi, M., et al. (2015). Recreating blood-brain barrier physiology and structure on chip: A novel neurovascular microfluidic bioreactor. Biomicrofluidics 9, 054124. doi:10.1063/1.4934713.

Capogrosso, M., Wagner, F. B., Gandar, J., Moraud, E. M., Wenger, N., Milekovic, T., et al. (2018). Configuration of electrical spinal cord stimulation through real-time processing of gait kinematics. Nat. Protoc. 13, 2031–2061.

Catt, K., Li, H., and Cui, X. T. (2017). Poly (3,4-ethylenedioxythiophene) graphene oxide composite coatings for controlling magnesium implant corrosion. Acta Biomater 48, 530–540. doi:10.1016/j.actbio.2016.11.039.

Cavaliere, F., Vicente, E. S., and Matute, C. (2010). An organotypic culture model to study nigro-striatal degeneration. J. Neurosci. Methods 188, 205–212. doi:10.1016/j.jneumeth.2010.02.008.

Chapman, C. A. R., Chen, H., Stamou, M., Lein, P. J., and Seker, E. (2016). Mechanisms of Reduced Astrocyte Surface Coverage in Cortical Neuron-Glia Co-cultures on Nanoporous Gold Surfaces. Cell Mol Bioeng. 9, 433–442. doi:10.1007/s12195-016-0449-4.

Chen, R., Romero, G., Christiansen, M. G., Mohr, A., and Anikeeva, P. (2015). Wireless magnetothermal deep brain stimulation. Science. 347, 1477–80. doi:10.1126/science.1261821.

Chen, S., Weitemier, A. Z., Zeng, X., He, L., Wang, X., Tao, Y., et al. (2018a). Near-infrared deep brain stimulation via upconversion nanoparticle – mediated optogenetics. Science. 359, 679–684. doi:10.1126/science.aaq1144.

Chen, W., Han, S., Qian, W., Weng, S., Yang, H., Sun, Y., et al. (2018b). Nanotopography regulates motor neuron differentiation of human pluripotent stem cells. Nanoscale 10, 3556–3565. doi:10.1039/c7nr05430k.

Chen, X.-Z., Liu, J.-H., Dong, M., Müller, L., Chatzipirpiridis, G., Hu, C., et al. (2019). Magnetically driven piezoelectric soft microswimmers for neuron-like cell delivery and neuronal differentiation. Mater. Horiz. doi:10.1039/C9MH00279K.

Chin, E., and Goh, E. (2018). Blood–brain barrier on a chip. Methods Cell Bio 146, 159–182. doi:10.1016/bs.mcb.2018.06.003.

Chong, C., Ma, D., Zhao, C., Franklin, R. J. M., Zhou, Z., Ai, N., et al. (2015). Discovery of a novel neuroprotectant, BHDPC, that protects against MPP+/ MPTP-induced neuronal death in multiple experimental models. Free Radic. Biol. Med. 89, 1057–1066. doi:10.1016/j.freeradbiomed.2015.08.013.

Choo, A. M., Miller, W. J., Chen, Y., Nibley, P., Patel, T. P., Goletiani, C., et al. (2013). Antagonism of purinergic signalling improves recovery from traumatic brain injury. Brain. 136, 65–80. doi:10.1093/brain/aws286.

Coenen, V. A., Amtage, F., Volkmann, J., and Schläpfer, T. E. (2015). Deep Brain Stimulation in Neurological and Psychiatric Disorders. Dtsch. Arztebl. Int. 112, 519–526. doi:10.3238/arztebl.2015.0519.

Cogan, S. F. (2008). Neural Stimulation and Recording Electrodes. Annu Rev Biomed Eng 10, 275–308. doi:10.1146/annurev.bioeng.10.061807.160518.

Croft, C. L., and Noble, W. (2018). Preparation of organotypic brain slice cultures for the study of Alzheimer's disease. F1000Research 7, 592. doi:10.12688/f1000research.14500.2.

Crompton, K. E., Goud, J. D., Bellamkonda, R. V, Gengenbach, T. R., Finkelstein, D. I., Horne, M. K., et al. (2007). Polylysine-functionalised thermoresponsive chitosan hydrogel for neural tissue engineering. Biomaterials 28, 441–449. doi:10.1016/j.biomaterials.2006.08.044.

Cui, X., and Martin, D. C. (2003). Electrochemical deposition and characterization of poly (3,4-ethylenedioxythiophene) on neural microelectrode arrays. Sensors Actuators B 89, 92–102. doi:10.1016/S0925-4005(02)00448-3.

Dandekar, M. P., Fenoy, A. J., Carvalho, A. F., Soares, J. C., and Quevedo, J. (2018). Deep brain stimulation for treatment-resistant depression: an integrative review of preclinical and clinical findings and translational implications. Mol Psychiatry 23, 1094–1112. doi:10.1038/mp.2018.2.

Daniele, S., and Bragato, C. (2014). From Macroelectrodes to Microelectrodes: Theory and Electrode Properties BT - Environmental Analysis by Electrochemical, in, eds. L. M. Moretto and K. Kalcher, 373–401. doi:10.1007/978-1-4939-0676-5_15.

Daviaud, N., Garbayo, E., Lautram, N., Franconi, F., Lemaire, L., Perez-Pinzon, M., et al. (2014). Modeling nigrostriatal degeneration in organotypic cultures, a new ex vivo model of Parkinson's disease. Neuroscience 256, 10–22. doi:10.1016/j.neuroscience.2013.10.021.

De Astis, S., Corradini, I., Morini, R., Rodighiero, S., Tomasoni, R., Lenardi, C., et al. (2013). Nanostructured TiO2 surfaces promote polarized activation of microglia, but not astrocytes, toward a proinflammatory profile. Nanoscale 5, 10963–74. doi:10.1039/c3nr03534d.

Desai, S. A., Rolston, J. D., Mccracken, C. E., Potter, S. M., and Gross, R. E. (2016). Asynchronous Distributed Multielectrode Microstimulation Reduces Seizures in the Dorsal Tetanus Toxin Model of Temporal Lobe Epilepsy. Brain Stimul. 9, 86–100. doi:10.1016/j.brs.2015.08.008.

Desai, S. A., Gutekunst, C., Potter, S. M., and Gross, R. E. (2014). Deep brain stimulation macroelectrodes compared to multiple microelectrodes in rat hippocampus. Front. Neuroeng. 7:16. doi:10.3389/fneng.2014.00016.

Desai, S. A., Gutekunst, C. A., Potter, S. M., and Gross, R. E. (2012). Analyzing neuronal activation with macroelectrode vs. microelectrode array stimulation. Conf Proc IEEE Eng Med Biol Soc. 2012, 4144–4147. doi:10.1109/EMBC.2012.6346879.

Dias, D. O., and Göritz, C. (2018). Fibrotic scarring following lesions to the central nervous system. Matrix Biol. 68–69, 561–570. doi:10.1016/j.matbio.2018.02.009.

Dougherty, D. D. (2018). Deep Brain Stimulation: Clinical Applications. Psychiatr Clin North Am 41, 385–394. doi:10.1016/j.psc.2018.04.004.

Drobisz, D., and Damborská, A. (2019). Deep brain stimulation targets for treating depression. Behav. Brain Res. 359, 266–273. doi:10.1016/j.bbr.2018.11.004.

Du, Z. J., Kolarcik, C. L., Kozai, T. D. Y., Luebben, S. D., Sapp, S. A., Sally, X., et al. (2017). Ultrasoft microwire neural electrodes improve chronic tissue integration. Acta Biomater. 53, 46–58. doi:10.1016/j.actbio.2017.02.010.

Eles, J. R., Vazquez, A. L., Kozai, T. D. Y., and Cui, X. T. (2018). In vivo imaging of neuronal calcium during electrode implantation: Spatial and temporal mapping of damage and recovery. Biomaterials 174, 79–94. doi:10.1016/j.biomaterials.2018.04.043.

Eles, J. R., Vazquez, A. L., Kozai, T. D. Y., and Cui, X. T. (2019). Meningeal inflammatory response and fibrous tissue remodeling around intracortical implants: An in vivo two-photon imaging study. Biomaterials 195, 111–123. doi:10.1016/j.biomaterials.2018.12.031.

Eles, J. R., Vazquez, A. L., Snyder, N. R., Lagenaur, C., Matthew, C., Kozai, T. D. Y., et al. (2017). Neuroadhesive L1 coating attenuates acute microglial attachment to neural electrodes as revealed by live two-photon microscopy. Biomaterials 113, 279–292. doi:10.1016/j.biomaterials.2016.10.054.

Elias, G. J. B., Namasivayam, A. A., and Lozano, A. M. (2018). Deep brain stimulation for stroke: Current uses and future directions. Brain Stimul. 11, 3–28. doi:10.1016/j.brs.2017.10.005.

Engel, M., Do-Ha, D., Munoz, S. S., and Ooi, L. (2016). Common pitfalls of stem cell differentiation: a guide to improving protocols for neurodegenerative disease models and research. Cell. Mol. Life Sci. 73, 3693–3709. doi:10.1007/s00018-016-2265-3.

Ereifej, E. S., Cheng, M. M., Mao, G., and Vandevord, P. J. (2013a). Examining the inflammatory response to nanopatterned polydimethylsiloxane using organotypic brain slice methods. J. Neurosci. Methods 217, 17–25. doi:10.1016/j.jneumeth.2013.04.023.

Ereifej, E. S., Matthew, H. W., Newaz, G., Mukhopadhyay, A., Auner, G., Salakhutdinov, I., et al. (2013b). Nanopatterning effects on astrocyte reactivity. J Biomed Mater Res A 101, 1743–57. doi:10.1002/jbm.a.34480.

Ereifej, E. S., Rial, G. M., Hermann, J. K., Smith, C. S., Meade, S. M., Rayyan, J. M., et al. (2018). Implantation of Neural Probes in the Brain Elicits Oxidative Stress. Front. Bioeng. Biotechnol. 6. doi:10.3389/fbioe.2018.00009.

Farrell, S. M., Green, A., and Aziz, T. (2018). The Current State of Deep Brain Stimulation for Chronic Pain and Its Context in Other Forms of Neuromodulation. Brain Sci 8, 158. doi:10.3390/brainsci8080158.

Fattahi, P., Departments, C. E., State, P., Yang, G., and Kim, G. (2014). A Review of Organic and Inorganic Biomaterials for Neural Interfaces. Adv Mater. 26, 1846–1885. doi:10.1002/adma.201304496.A.

Ferlauto, L., D'Angelo, A. N., Vagni, P., Leccardi, M. J. I. A., Mor, F. M., Cuttaz, E. A., et al. (2018). Development and characterization of PEDOT:PSS/alginate soft microelectrodes for application in neuroprosthetics. Front. Neurosci. 12: 648. doi:10.3389/fnins.2018.00648.

Ferreira, E. S., Vieira, G., Moraes, D. M., Amorim, B. O., Malheiros, J. M., Hamani, C., et al. (2018). Long-Term Effects of Anterior Thalamic Nucleus Deep Brain Stimulation on Spatial Learning in the Pilocarpine Model of Temporal Lobe Epilepsy. Neuromodulation 21, 160–167. doi:10.1111/ner.12688.

Fluri, F., Bieber, M., Volkmann, J., and Kleinschnitz, C. (2015). Microelectrode Guided Implantation of Electrodes into the Subthalamic Nucleus of Rats for Long-term Deep Brain Stimulation. J. Vis. Exp. doi:10.3791/53066.

Fluri, F., Mützel, T., Schuhmann, M. K., Krstić, M., Endres, H., and Volkmann, J. (2017). Development of a head-mounted wireless microstimulator for deep brain stimulation in rats. J. Neurosci. Methods 291, 249–256. doi:10.1016/j.jneumeth.2017.08.024.

Frampton, J. P., Hynd, M. R., Williams, J. C., Shuler, M. L., and Shain, W. (2007). Three-dimensional hydrogel cultures for modeling changes in tissue impedance around microfabricated neural probes. J Neural Eng. 4, 399–409. doi:10.1088/1741-2560/4/4/006.

Gabriel, E., and Gopalakrishnan, J. (2017). Generation of iPSC-derived Human Brain Organoids to Model Early Neurodevelopmental Disorders. J Vis Exp (122). doi:10.3791/55372.

Gaire, J., Lee, H. C., Ward, R., Currlin, S., Woolle, A. J., Coleman, J. E., et al. (2018a). PrismPlus: a mouse line expressing distinct fluorophores in four different brain cell types. Sci. Rep. 8: 7182. doi:10.1038/s41598-018-25208-y.

Gaire, J., Lee, H. C., Hilborn, N., Ward, R., Regan, M., and Otto, K. J. (2018b). The role of inflammation on the functionality of intracortical microelectrodes. J. Neural Eng. 15:066027. doi:10.1088/1741-2552/aae4b6.

Ganji, M., Tanaka, A., Gilja, V., Halgren, E., and Dayeh, S. A. (2017). Scaling Effects on the Electrochemical Stimulation Performance of Au, Pt, and PEDOT:PSS Electrocorticography Arrays. Adv. Funct. Mater. 27, 1703019. doi:10.1002/adfm.201703019.

Gordon, J., Amini, S., and White, M. K. (2014). General overview of neuronal cell culture. Methods Mol Biol 1078: 1–8. doi:10.1007/978-1-62703-640-5.

Green, R. A., Lovell, N. H., Wallace, G. G., and Poole-warren, L. A. (2008). Conducting polymers for neural interfaces: Challenges in developing an effective long-term implant. Biomaterials 29, 3393–3399. doi:10.1016/j.biomaterials.2008.04.047.

Guduru, R., Liang, P., Hong, J., Rodzinski, A., Hadjikhani, A., Horstmyer, J., et al. (2015). Magnetoelectric 'spin' on stimulating the brain. Nanomedicine 10, 2051–2061. doi:10.2217/nnm.15.52.

Hadler, C., Wissel, K., Brandes, G., Dempwolf, W., Reuter, G., Lenarz, T., et al. (2017). Photochemical coating of Kapton ® with hydrophilic polymers for the improvement of neural implants. Mater. Sci. Eng. C 75, 286–296. doi:10.1016/j.msec.2017.02.020.

Hall, A. A., Leonardo, C. C., Collier, L. A., Rowe, D. D., Willing, A. E., and Pennypacker, K. R. (2009). Delayed treatments for stroke influence neuronal death in rat organotypic slice cultures subjected to oxygen glucose deprivation. Neuroscience 164, 470–477. doi:10.1016/j.neuroscience.2009.08.051.

Hammer, D. X., Kim, D.-H., Lozzi, A., Boretsky, A., Ye, M., and Welle, C. (2016). Imaging the response to long-term neural implants. SPIE Newsroom. doi:10.1117/2.1201601.006321.

Harris, J. P., Capadona, J. R., Miller, R. H., Healy, B. C., Shanmuganathan, K., Rowan, S. J., et al. (2011). Mechanically adaptive intracortical implants improve the proximity of neuronal cell bodies. J Neuroeng Rehabil. 8:066011. doi:10.1088/1741-2560/8/6/066011.

Hasenkamp, W., Musa, S., Alexandru, A., Eberle, W., and Bartic, C. (2009). Electrodeposition and characterization of iridium oxide as electrode material for neural recording and stimulation. IFMBE Proc. 25, 472–475. doi:10.1007/978-3-642-03889-1.

Heo, D. N., Song, S., Kim, H., Jae, Y., Ko, W., Jin, S., et al. (2016). Multifunctional hydrogel coatings on the surface of neural cuff electrode for improving electrode-nerve tissue interfaces. Acta Biomater. 39, 25–33. doi:10.1016/j.actbio.2016.05.009.

Hermann, J. K., Lin, S., Soffer, A., Wong, C., Srivastava, V., Chang, J., et al. (2018a). The Role of Toll-Like Receptor 2 and 4 Innate Immunity Pathways in Intracortical Microelectrode-Induced Neuroinflammation. Front. Bioeng. Biotechnol. 6:113. doi:10.3389/fbioe.2018.00113.

Hermann, J. K., Ravikumar, M., Shoffstall, A., Ereifej, E., Kovach, K., Chang, J., et al. (2018b). Inhibition of the cluster of differentiation 14 innate immunity pathway with IAXO-101 improves chronic microelectrode performance. J. Neural Eng. 15: 025002.

Hess, A. E., Capadona, J. R., Shanmuganathan, K., Hsu, L., Rowan, S. J., Weder, C., et al. (2011). Development of a stimuli-responsive polymer nanocomposite toward biologically optimized, MEMS-based neural probes. J. Micromech. Microeng 21, 054009. doi:10.1088/0960-1317/21/5/054009.

Ho, B. X., Pek, N. M. Q., and Soh, B. S. (2018). Disease modeling using 3D organoids derived from human induced pluripotent stem cells. Int. J. Mol. Sci. 19. doi:10.3390/ijms19040936.

Holslag, J. A. H., Neef, N., Beudel, M., Drost, G., Oterdoom, D. L. M., Kremer, N. I., et al. (2017). Deep Brain Stimulation for Essential Tremor: A Comparison of Targets. World Neurosurg. 110, e580–e584. doi:10.1016/j.wneu.2017.11.064.

Humpel, C. (2016). Organotypic brain slice cultures: A review. Neuroscience 305, 86–98. doi:10.1016/j.neuroscience.2015.07.086.

Huuskonen, J., Suuronen, T., Miettinen, R., Groen, T. Van, and Salminen, A. (2005). A refined in vitro model to study inflammatory responses in organotypic membrane culture of postnatal rat hippocampal slices. J Neuroinflammation 2, 25. doi:10.1186/1742-2094-2-25.

Isoaho, N., Peltola, E., Sainio, S., Koskinen, J., and Laurila, T. (2018). Pt-grown carbon nanofibers for enzymatic glutamate biosensors and assessment of their biocompatibility. RSC Adv 8, 35802–35812. doi:10.1039/c8ra07766e.

Jang, S., Kim, H., Kim, H. J., Lee, S. K., Kim, E. W., Namkoong, K., et al. (2018). Long-term culture of organotypic hippocampal slice from old 3xTg-AD mouse: An ex vivo model of alzheimer's disease. Psychiatry Investig. 15, 205–213. doi:10.30773/pi.2017.04.02.

Järvelä, J. T., Ruohonen, S., Kukko-Lukjanov, T. K., Plysjuk, A., Lopez-Picon, F. R., and Holopainen, I. E. (2011). Kainic acid-induced neurodegeneration and activation of inflammatory processes in organotypic hippocampal slice cultures: Treatment with cyclooxygenase-2 inhibitor does not prevent neuronal death. Neuropharmacology 60, 1116–1125. doi:10.1016/j.neuropharm.2010.09.024.

Jeffery, A. F., Churchward, M. A., Mushahwar, V. K., Todd, K. G., and Elias, A. L. (2014). Hyaluronic acid-based 3D culture model for in vitro testing of electrode biocompatibility. Biomacromolecules 15, 2157–2165. doi:10.1021/bm500318d.

Jiang, C., Li, L., and Hao, H. (2011). Carbon Nanotube Yarns for Deep Brain Stimulation Electrode. IEEE Trans Neural Syst Rehabil Eng 19, 612–616. doi:10.1109/TNSRE.2011.2165733.

Johnson, C. D., D'Amato, A. R., Puhl, D. L., Wich, D. M., Vesperman, A., and Gilbert, R. J. (2018). Electrospun fiber surface nanotopography influences astrocyte-mediated neurite outgrowth. Biomed. Mater 13, 054101. doi:10.1088/1748-605X/aac4de.

Jones, R. S. G., da Silva, A. B., Whittaker, R. G., Woodhall, G. L., and Cunningham, M. O. (2016). Human brain slices for epilepsy research: Pitfalls, solutions and future challenges. J. Neurosci. Methods 260, 221–232. doi:10.1016/j.jneumeth.2015.09.021.

Jung, N. Y., Lee, K. H., Won, R., and Lee, B. H. (2013). Neuroprotective effects of α-tocotrienol on kainic acid-induced neurotoxicity in organotypic hippocampal slice cultures. Int. J. Mol. Sci. 14, 18256–18268. doi:10.3390/ijms140918256.

Kanegan, M. J. Van, Dunn, D. E., Kaltenbach, L. S., Shah, B., He, D. N., Mccoy, D. D., et al. (2016). Dual activities of the anti-cancer drug candidate PBI-05204 provide neuroprotection in brain slice models for neurodegenerative diseases and stroke. Nat. Publ. Gr. 6, 25626. doi:10.1038/srep25626.

Karas, P. J., Lee, S., Jimenez-Shahed, J., Goodman, W. K., Viswanathan, A., & Sheth, S. A. (2019). Deep Brain Stimulation for Obsessive Compulsive Disorder: Evolution of Surgical Stimulation Target Parallels Changing Model of Dysfunctional Brain Circuits. Front. neurosci, 12, 998. doi:10.3389/fnins.2018.00998

Kargol, A., Malkinski, L., and Caruntu, G. (2012) Biomedical Applications of Multiferroic Nanoparticles. Advanced Magnetic Materials, doi:10.5772/39100.

Kaur, G., and Dufour, J. M. (2012). Cell lines: Valuable tools or useless artifacts. Spermatogenesis 2, 1–5. doi: 10.4161/spmg.19885.

Kearns, S. M., Scheffler, B., Goetz, A. K., Lin, D. D., Baker, H. D., Roper, S. N., et al. (2006). A method for a more complete in vitro Parkinson's model: Slice culture bioassay for modeling maintenance and repair of the nigrostriatal circuit. J. Neurosci. Methods 157, 1–9. doi:10.1016/j.jneumeth.2006.03.020.

Killian, N. J., Vernekar, V. N., Potter, S. M., and Vukasinovic, J. (2016). A Device for Long-Term Perfusion, Imaging, and Electrical Interfacing of Brain Tissue In vitro. Front. Neurosci. 10:135. doi:10.3389/fnins.2016.00135.

Kim, D., Viventi, J., Amsden, J. J., Xiao, J., Vigeland, L., Kim, Y., et al. (2010a). Dissolvable Films of Silk Fibroin for Ultrathin, Conformal Bio-Integrated Electronics. Nat Mater. 9, 511–517. doi:10.1038/nmat2745.

Kim, H. M., Lee, H. J., Lee, M. Y., Kim, S. U., and Kim, B. G. (2010b). Organotypic Spinal Cord Slice Culture to Study Neural Stem/Progenitor Cell Microenvironment in the Injured Spinal Cord. Exp Neurobiol 19, 106–113. doi:10.5607/en.2010.19.2.106.

Kim, S., Kim, N., Kim, Y., Baik, M., Yoo, M., Kim, D., et al. (2018). High-performance, polymer-based direct cellular interfaces for electrical stimulation and recording. NPG Asia Mater. 10, 255–265. doi:10.1038/s41427-018-0014-9.

Kipke, D. R., Shain, W., Buzsaki, G., Fetz, E., Henderson, J. M., Hetke, J. F., et al. (2008). Advanced Neurotechnologies for Chronic Neural Interfaces: New Horizons and Clinical Opportunities. J. Neurosci. 28, 11830–11838. doi:10.1523/JNEUROSCI.3879-08.2008.

Kiss, M., Foldesy, P., and Fekete, Z. (2015). Optimization of a Michigan-type silicon microprobe for infrared neural stimulation. Sensors Actuators B Chem. 224, 676–682. doi:10.1016/j.snb.2015.10.084.

Klymov, A., Rodrigues Neves, C. T., te Riet, J., Agterberg, M. J. H., Mylanus, E. A. M., Snik, A. F. M., et al. (2015). Nanogrooved Surface-Patterns induce cellular organization and axonal outgrowth in neuron-like PC12-Cells. Hear. Res. 320, 11–17. doi:10.1016/j.heares.2014.12.009.

Kloc, M., Kosutzka, Z., Steno, J., and Valkovic, P. (2017). Prevalent placement error of deep brain stimulation electrode in movement disorders (technical considerations). Bratisl Med J 118, 647–653. doi:10.4149/BLL.

Ko, K. R., and Frampton, J. P. (2016). Developments in 3D neural cell culture models: the future of neurotherapeutics testing? Expert Rev. Neurother. 16, 739–741. doi:10.1586/14737175.2016.1166053.

Kondo, M., Kobayashi, K., Ohkura, M., Nakai, J., and Matsuzaki, M. (2017). Two-Photon calcium imaging of the medial prefrontal cortex and hippocampus without cortical invasion. Elife 6, e26839. doi:10.7554/eLife.26839.

Koss, K. M., Churchward, M. A., Jeffery, A. F., Mushahwar, V. K., Elias, A. L., and Todd, K. G. (2017). Improved 3D Hydrogel Cultures of Primary Glial Cells for In Vitro Modelling of Neuroinflammation. J. Vis. Exp. doi:10.3791/56615.

Koutsouras, D. A., Hama, A., Pas, J., Gkoupidenis, P., Hivert, B., Faivre-Sarailh, C., et al. (2017). PEDOT:PSS microelectrode arrays for hippocampal cell culture electrophysiological recordings. MRS Commun. 7, 259–265. doi:10.1557/mrc.2017.34.

Kozai, T. D. Y., Jaquins-Gerstl, A. S., Vazquez, A. L., Michael, A. C., and Cui, X. T. (2015a). Brain tissue responses to neural implants impact signal sensitivity and intervention strategies. ACS Chem. Neurosci. 6, 48–67. doi:10.1021/cn500256e.

Kozai, T. D. Y., Catt, K., Li, X., Gugel, Z. V., Olafsson, V. T., Vazquez, A. L., et al. (2015b). Mechanical failure modes of chronically implanted planar silicon-based neural probes for laminar recording. Biomaterials 37, 25–39. doi:10.1016/j.biomaterials.2014.10.040.

Kozai, T. D. Y., Li, X., Bodily, L. M., Caparosa, E. M., Zenonos, G. A., Carlisle, D. L., et al. (2014). Effects of caspase-1 knockout on chronic neural recording quality and longevity: Insight into cellular and molecular mechanisms of the reactive tissue response. Biomaterials 35, 9620–9634. doi:10.1016/j.biomaterials.2014.08.006.Effects.

Krings, M., Höllig, A., Liu, J., Grüsser, L., Rossaint, R., and Coburn, M. (2016). Desflurane impairs outcome of organotypic hippocampal slices in an in vitro model of traumatic brain injury. Med. Gas Res. 6, 3–9. doi:10.4103/2045-9912.179338.

Kristensen, B. W., Noraberg, J., Thiébaud, P., Koudelka-Hep, M., and Zimmer, J. (2001). Biocompatibility of silicon-based arrays of electrodes coupled to organotypic hippocampal brain slice cultures. Brain Res. 896, 1–17. doi:10.1016/S0006-8993(00)03304-7.

Labombarda, F., Ghoumari, M. A., Liere, P., De Nicola, A. F., Schumacher, M., and Guennoun, R. (2013). Neuroprotection by steroids after neurotrauma in organotypic spinal cord cultures: A key role for progesterone receptors and steroidal modulators of GABA(A) receptors. Neuropharmacology 71, 46–55. doi:10.1016/j.neuropharm.2013.03.010.

Lai, H., Liao, L., Lin, C., Hsu, J., He, X., Chen, Y.-Y., et al. (2012). Design, simulation and experimental validation of a novel flexible neural probe for deep brain stimulation and multichannel recording. J. Neural Eng. 9:036001. doi:10.1088/1741-2560/9/3/036001.

LaMarca, E. A., Powell, S. K., Akbarian, S., and Brennand, K. J. (2018). Modeling Neuropsychiatric and Neurodegenerative Diseases with Induced Pluripotent Stem Cells. FrontPediatr 6;82. doi:10.3389/fped.2018.00082.

Lamprecht, M. R., Elkin, B. S., Kesavabhotla, K., and Crary, J. F. (2017). Strong Correlation of Genome-Wide Expression after Traumatic Brain Injury In Vitro and In Vivo Implicates a Role for SORLA. J Neurotrauma 34, 97–108. doi:10.1089/neu.2015.4306.

Lancaster, M. A., and Knoblich, J. A. (2014). Generation of cerebral organoids from human pluripotent stem cells. Nat Protoc. 9, 2329–2340. doi:10.1038/nprot.2014.158.

Leclerc, E., Duval, J. L., Egles, C., Ihida, S., Toshiyoshi, H., and Tixier-Mita, A. (2017). In vitro cyto-biocompatibility study of thin-film transistors substrates using an organotypic culture method. J. Mater. Sci. Mater. Med. 28, 0–1. doi:10.1007/s10856-016-5815-1.

Lee, C., Cheng, Y., and Huang, G. S. (2014). Topographical control of cell-cell interaction in C6 glioma by nanodot arrays. Nanoscale Res Lett 9, 250. doi:10.1186/1556-276X-9-250.

Lee, H. C., Ejserholm, F., Gaire, J., Currlin, S., Schouenborg, J., Wallman, L., et al. (2017). Histological evaluation of flexible neural implants; flexibility limit for reducing the tissue response? J. Neural Eng. 14: 036026.

Leplus, A., Lauritzen, I., Melon, C., Kerkerian-Le Goff, L., Fontaine, D., and Checler, F. (2018). Chronic fornix deep brain stimulation in a transgenic Alzheimer's rat model reduces amyloid burden, inflammation, and neuronal loss. Brain Struct. Funct. 224, 363-372. doi:10.1007/s00429-018-1779-x.

Li, M., Zhou, H. H., Li, T., Li, C. Y., Xia, Z. Y., and Duan, Y. Y. (2015). Polyurethane/poly(Vinyl alcohol) hydrogel coating improves the cytocompatibility of neural electrodes. Neural Regen. Res. 10, 2048–2053. doi:10.4103/1673-5374.172325.

Li, Y., Chen, Y., Tan, L., Lin, J. P. W., Wu, J., Hu, W., et al. (2017). RNAi-mediated ephrin-B2 silencing attenuates fibrotic scar formation and improves spinal cord axon growth. CNS Neurosci Ther 23, 779–789. doi:10.1111/cns.12723.

Liddelow, S. A., Guttenplan, K. A., Clarke, L. E., Bennett, F. C., Bohlen, C. J., Schirmer, L., et al. (2017). Neurotoxic reactive astrocytes are induced by activated microglia. Nature. 541, 481–487. doi:10.1038/nature21029.

Liu, J., Sternberg, A. R., Ghiasvand, S., and Berdichevsky, Y. (2018). Epilepsy-on-a-chip System for Antiepileptic Drug Discovery. IEEE Trans Biomed Eng. doi:10.1109/TBME.2018.2871415.

Lorsch, B. J. R., Collins, F. S., and Lippincott-schwartz, J. (2014). Fixing problems with cell lines.Technologies and policies can improve authentication. Science. 346, 1452–1453.

Lossi, L., and Merighi, A. (2018). The Use of ex Vivo Rodent Platforms in Neuroscience Translational Research With Attention to the 3Rs Philosophy. Front. Vet. Sci. 5, 164. doi:10.3389/fvets.2018.00164.

Magalhães, D. M., Pereira, N., Rombo, D. M., Beltrão-Cavacas, C., Sebastião, A. M., and Valente, C. A. (2018). Ex vivo model of epilepsy in organotypic slices – a new tool for drug screening. J. Neuroinflammation 15:203. doi:10.1186/1742-2094-4-18.

Mantione, D., del Agua, I., Schaafsma, W., Diez-garcia, J., Castro, B., Sardon, H., et al. (2016). Poly(3,4-ethylenedioxythiophene):GlycosAmino-Glycan Aqueous Dispersions: Toward Electrically Conductive Bioactive Materials for Neural Interfaces. Macromol. Biosci. 16, 1227–38. doi:10.1002/mabi.201600059.

Mao, Z. Q., Wang, X., Xu, X., Cui, Z. Q., Pan, L. S., Ning, X. J., et al. (2018). Partial improvement in performance of patients with severe Alzheimer's disease at an early stage of fornix deep brain stimulation. Neural Regen. Res. 13, 2164–2172. doi:10.4103/1673-5374.241468.

Martinez-Ramirez, D., Jimenez-Shahed, J., Leckman, J. F., Porta, M., Servello, D., Meng, F. G., et al. (2018). Efficacy and safety of deep brain stimulation in tourette syndrome: The international tourette syndrome deep brain stimulation public database and registry. JAMA Neurol. 75, 353–359. doi:10.1001/jamaneurol.2017.4317.

Masís, J., Mankus, D., Wolff, S. B. E., Guitchounts, G., Joesch, M., and Cox, D. D. (2018). A micro-CT-based method for quantitative brain lesion characterization and electrode localization. Sci. Rep. 8, 5184. doi:10.1038/s41598-018-23247-z.

Maya-vetencourt, J. F., Ghezzi, D., Antognazza, M. R., Colombo, E., Mete, M., Feyen, P., et al. (2017). A fully organic retinal prosthesis restores vision in a rat model of degenerative blindness. Nat Mater 16, 681–689. doi:10.1038/nmat4874.A.

Mazzone, G., and Nistri, A. (2014). S100β as an early biomarker of excitotoxic damage in spinal cord organotypic cultures. J. Neurochem. 130, 598–604. doi:10.1111/jnc.12748.

McCreery, D., Cogan, S., Kane, S., and Pikov, V. (2016). Correlations between histology and neuronal activity recorded by microelectrodes implanted chronically in the cerebral cortex. J. Neural Eng. 13:036012. doi:10.1088/1741-2560/13/3/036012.

Meijs, S., Fjorback, M., Jensen, C., Sørensen, S., Rechendorff, K., and Rijkhoff, N. J. M. (2015). Electrochemical properties of titanium nitride nerve stimulation electrodes: an in vitro and in vivo study. Front. Neurosci. 9:268. doi:10.3389/fnins.2015.00268.

Meoni, S., Fraix, V., Castrioto, A., Benabid, A. L., Seigneuret, E., Vercueil, L., et al. (2017). Pallidal deep brain stimulation for dystonia: a long term study. J Neurol Neurosurg Psychiatry 88, 960–967. doi:10.1136/jnnp-2016-315504.

Merrill, D. R. (2014). Materials considerations of implantable neuroengineering devices for clinical use. Curr. Opin. Solid State Mater. Sci. 18, 329–336. doi:10.1016/j.cossms.2014.07.002.

Mewes, A., Franke, H., and Singer, D. (2012). Organotypic Brain Slice Cultures of Adult Transgenic P301S Mice — A Model for Tauopathy Studies. PLoS One 7, e45017. doi:10.1371/journal.pone.0045017.

Meyer, R. D., Cogan, S. F., Nguyen, T. H., and Rauh, R. D. (2001). Electrodeposited Iridium Oxide for Neural Stimulation and Recording Electrodes. IEEE Trans Neural Syst Rehabil Eng 9, 2–11. doi:10.1109/7333.918271.

Michelson, N. J., Eles, J. R., Vazquez, A. L., Ludwig, K. A., and Kozai, T. D. Y. (2019). Calcium activation of cortical neurons by continuous electrical stimulation: Frequency dependence, temporal fidelity, and activation density. J Neurosci Res 97, 620–638. doi:10.1002/jnr.24370.

Mii, S., Uehara, F., Yano, S., Tran, B., Miwa, S., Hiroshima, Y., et al. (2013). Nestin-Expressing Stem Cells Promote Nerve Growth in Long-Term 3-Dimensional Gelfoam®-Supported Histoculture. PLoS One 8. doi:10.1371/journal.pone.0067153.

Minami, N., Maeda, Y., Shibao, S., Arima, Y., Ohka, F., Kondo, Y., et al. (2017). Organotypic brain explant culture as a drug evaluation system for malignant brain tumors. Cancer Med. 11, 2635–2645. doi:10.1002/cam4.1174.

Moeendarbary, E., Weber, I. P., Sheridan, G. K., Koser, D. E., Soleman, S., Haenzi, B., et al. (2017). The soft mechanical signature of glial scars in the central nervous system. Nat. Commun. 8:14787. doi:10.1038/ncomms14787.

Morin, E. A., and He, W. (2017). In vitro study of central nervous system foreign body response towards hydrogel particle modified planar substrate. J Biomed Mater Res A 105, 3242–3250. doi:10.1002/jbm.a.36180.

Morishita, T., Hilliard, J. D., Okun, M. S., Neal, D., Nestor, K. A., Peace, D., et al. (2017). Postoperative lead migration in deep brain stimulation surgery: Incidence, risk factors, and clinical impact. PLoS One 12, 1–22. doi:10.1371/journal.pone.0183711.

Musacchio, T., Rebenstorff, M., Fluri, F., Brotchie, J. M., Volkmann, J., Koprich, J. B., et al. (2017). Subthalamic nucleus deep brain stimulation is neuroprotective in the A53T α-synuclein Parkinson's disease rat model. Ann. Neurol. 81, 825–836. doi:10.1002/ana.24947.

Nasr, B., Chatterton, R., Yong, J. H. M., Jamshidi, P., D'Abaco, G. M., Bjorksten, A. R., et al. (2018). Self-organized nanostructure modified microelectrode for sensitive electrochemical glutamate detection in stem cells-derived brain organoids. Biosensors 8. doi:10.3390/bios8010014.

Nery, F. C., da Hora, C. C., Yaqub, U., Zhang, X., McCarthy, D. M., Bhide, P. G., et al. (2015). New methods for investigation of neuronal migration in embryonic brain explants. J. Neurosci. Methods 239, 80–84. doi:10.1016/j.jneumeth.2014.09.028.

Neville, K. E., Bosse, T. L., Klekos, M., Mills, J. F., Weicksel, S. E., Waters, J. S., et al. (2018). A novel ex vivo method for measuring whole brain metabolism in model systems. J. Neurosci. Methods 296, 32–43. doi:10.1016/j.jneumeth.2017.12.020.

Nissan, I., Schori, H., Kumar, B., Passig, A., Shefi, O., and Gedanken, A. (2017). Topographical impact of silver nanolines on the morphology of neuronal SH-SY5Y Cells. J. Mater. Chem. B 5, 9346–9353. doi:10.1039/c7tb02492d.

Normann, R. A., and Fernandez, E. (2016). Clinical applications of penetrating neural interfaces and Utah Electrode Array technologies. J. Neural Eng. 13 061003. doi:10.1088/1741-2560/13/6/061003.

Nzou, G., Wicks, R. T., Wicks, E. E., Seale, S. A., Sane, C. H., Chen, A., et al. (2018). Human Cortex Spheroid with a Functional Blood Brain Barrier for High-Throughput Neurotoxicity Screening and Disease Modeling. Sci. Rep. 8, 7413. doi:10.1038/s41598-018-25603-5.

O'Rourke, C., Lee-reeves, C., Drake, R. A. L., Cameron, G. W. W., Loughlin, A. J., and Phillips, J. B. (2017). Adapting tissue-engineered in vitro CNS models for high-throughput study of neurodegeneration. J Tissue Eng 8, 1–9. doi:10.1177/2041731417697920.

Onesto, V., Cancedda, L., Coluccio, M. L., Nanni, M., Pesce, M., Malara, N., et al. (2017). Nano-topography Enhances Communication in Neural Cells Networks. Sci. Rep. 7, 9841. doi:10.1038/s41598-017-09741-w.

Ormel, P., Vieira de Sa, R., Hol, E., and Pasterkamp, R. J. (2018). Microglia innately develop within cerebral organoids. Nat. Commun. 9, 4167. doi:10.1038/s41467-018-06684-2.

Osaki, T., Sivathanu, V., and Kamm, R. D. (2018). Vascularized microfluidic organ-chips for drug screening , disease models and tissue engineering. Curr Opinin Biotechnol 52, 116–123. doi:10.1016/j.copbio.2018.03.011.

Pancrazio, J. J., Deku, F., Ghazavi, A., Stiller, A. M., Rihani, R., Frewin, C. L., et al. (2017). Thinking Small: Progress on Microscale Neurostimulation Technology. Neuromodulation 20, 745–752. doi:10.1111/ner.12716.

Pandamooz, S., Saied, M., Ismail, M., and Safari, A. (2019). Tissue and Cell Modeling traumatic injury in organotypic spinal cord slice culture obtained from adult rat. Tissue Cell 56, 90–97. doi:10.1016/j.tice.2019.01.002.

Penazzi, L., Lorengel, J., Sündermann, F., Golovyashkina, N., Marre, S., Mathis, C. M. B., et al. (2017). DMSO modulates CNS function in a preclinical Alzheimer's disease model. Neuropharmacology 113, 434–444. doi:10.1016/j.neuropharm.2016.10.020.

Perkhofer, L., Frappart, P.-O., Muller, M., and Kleger, A. (2018). Importance of organoids for personalized medicine. Per Med 15, 461–465. doi:10.2217/pme-2018-0071.

Persheyev, S., Fan, Y., Irving, A., and Rose, M. J. (2011). BV-2 microglial cells sense micro-nanotextured silicon surface topology. J. Biomed. Mater. Res. - Part A 99, 135–40. doi:10.1002/jbm.a.33159.

Pinnell, R. C., de Vasconcelos, A. P., Cassel, J. C., and Hofmann, U. G. (2018). A Miniaturized, Programmable Deep-Brain Stimulator for Group-Housing and Water Maze Use Richard. Front. Neurosci. 12:231. doi:10.3389/fnins.2018.00231.

Pires, L. R., Rocha, D. N., Ambrosio, L., Pe, A. P., and Pe, A. P. (2015). The role of the surface on microglia function: implications for central nervous system tissue engineering. J R Soc Interface 12, 20141224. doi:10.1098/rsif.2014.1224.

Polikov, V. S., Tresco, P. A., and Reichert, W. M. (2005). Response of brain tissue to chronically implanted neural electrodes. J. Neurosci. Methods 148, 1–18. doi:10.1016/j.jneumeth.2005.08.015.

Pranti, A. S., Schander, A., Bödecker, A., and Lang, W. (2018). PEDOT: PSS coating on gold microelectrodes with excellent stability and high charge injection capacity for chronic neural interfaces. Sensors Actuators B. Chem. 275, 382–393. doi:10.1016/j.snb.2018.08.007.

Prasad Tripathi, R. K., and Ayyannan, S. R. (2017). Anticonvulsant activity, organotypic hippocampal neuroprotection assay and in-silico sodium channel blocking potential of 2-amino-6-nitrobenzothiazole derived semicarbazones. Biomed. Pharmacother. 95, 1451–1460. doi:10.1016/j.biopha.2017.09.070.

Prodanov, D., and Delbeke, J. (2016). Mechanical and Biological Interactions of Implants with the Brain and Their Impact on Implant Design. Front. Neurosci. 10:11. doi:10.3389/fnins.2016.00011.

Ramirez-Zamora, A., and Ostrem, J. L. (2018). Globus Pallidus Interna or Subthalamic Nucleus Deep Brain Stimulation for Parkinson Disease: A Review. JAMA Neurol. 75, 367–372. doi:10.1001/jamaneurol.2017.4321.

Ravikumar, M., Sunil, S., Black, J., Barkauskas, D. S., Haung, A. Y., Miller, R. H., et al. (2014). The roles of blood-derived macrophages and resident microglia in the neuroinflammatory response to implanted Intracortical microelectrodes. Biomaterials 35, 8049–8064. doi:10.1016/j.biomaterials.2014.05.084.

Rejc, E., Angeli, C. A., Atkinson, D., and Harkema, S. J. (2017). Motor recovery after activity-based training with spinal cord epidural stimulation in a chronic motor complete paraplegic. Sci. Rep. 7: 13476. doi:10.1038/s41598-017-14003-w.

Rejmontová, P., Capáková, Z., Mikušová, N., Maráková, N., Kašpárková, V., Lehocký, M., et al. (2016). Adhesion, proliferation and migration of NIH/3T3 cells on modified polyaniline surfaces. Int. J. Mol. Sci. 17, E1439. doi:10.3390/ijms17091439.

Revell, M. A. (2015). Deep Brain Stimulation for Movement Disorders. Nurs Clin North Am 50, 691–701. doi:10.1016/j.cnur.2015.07.014.

Rocha, D. N., Carvalho, E. D., and Pègo, A. P. (2016). High-throughput platforms for the screening of new therapeutic targets for neurodegenerative diseases. Drug Discov. Today 21, 1355–1366. doi:10.1016/j.drudis.2016.05.005.

Rocha, D. N., Ferraz-Nogueira, J. P., Barrias, C. C., Relvas, J. B., and Pêgo, A. P. (2015). Extracellular environment contribution to astrogliosis—lessons learned from a tissue engineered 3D model of the glial scar. Front. Cell. Neurosci. 9:377. doi:10.3389/fncel.2015.00377.

Salanova, V. (2018). Deep brain stimulation for epilepsy. Epilepsy Behav. 88, 21–24. doi:10.1016/j.yebeh.2018.06.041.

Salatino, J. W., Kale, A. P., and Purcell, E. K. (2019). Alterations in ion channel expression surrounding implanted microelectrode arrays in the brain. bioRxiv, 518811. doi:10.1101/518811.

Salatino, J. W., Ludwig, K. A., Kozai, T. D. Y., and Purcell, E. K. (2018). Glial responses to implanted electrodes in the brain. Nat Biomed Eng. 1, 862–877. doi:10.1038/s41551-017-0154-1.Glial.

Samba, R., Herrmann, T., and Zeck, G. (2015). PEDOT–CNT coated electrodes stimulate retinal neurons at low voltage amplitudes and low charge densities. J. Neural Eng. 12: 016014. doi:10.1088/1741-2560/12/1/016014.

Saryyeva, A., Nakamura, M., Krauss, J. K., and Schwabe, K. (2011). C-Fos expression after deep brain stimulation of the pedunculopontine tegmental nucleus in the rat 6-hydroxydopamine Parkinson model. J. Chem. Neuroanat. 42, 210–217. doi:10.1016/j.jchemneu.2011.08.003.

Sawyer, A. J., Tian, W., Saucier-sawyer, J. K., Rizk, P. J., Saltzman, W. M., Bellamkonda, R. V, et al. (2014). The effect of inflammatory cell-derived MCP-1 loss on neuronal survival during chronic neuroinflammation. Biomaterials 35, 6698–6706. doi:10.1016/j.biomaterials.2014.05.008.

Saxena, T., Karumbaiah, L., Gaupp, E. A., Patkar, R., Patil, K., Betancur, M., et al. (2013). The impact of chronic blood-brain barrier breach on intracortical electrode function. Biomaterials 34, 4703–4713. doi:10.1016/j.biomaterials.2013.03.007.

Schmidt, A. C., Wang, X., Zhu, Y., and Sombers, L. A. (2013). Carbon Nanotube Yarn Electrodes for Enhanced Detection of Neurotransmitter Dynamics in Live Brain Tissue. ACS Nano 24, 7864–7873. doi:10.1021/nn402857u.

Schoeler, M., Loetscher, P. D., Rossaint, R., Fahlenkamp, A. V, Eberhardt, G., Rex, S., et al. (2012). Dexmedetomidine is neuroprotective in an in vitro model for traumatic brain injury. BMC Neurol. 12, 20. doi:10.1186/1471-2377-12-20.

Seyock, S., Maybeck, V., Scorsone, E., Rousseau, L., Bergonzo, P., and Offenhhausser, A. (2017). Interfacing neurons on carbon nanotubes covered with diamond. RSC Adv 7, 153–160. doi:10.1039/C6RA20207A.

Shen, W., Das, S., Vitale, F., Richardson, A., Ananthakrishnan, A., Struzyna, L. A., et al. (2018). Microfabricated intracortical extracellular matrix-microelectrodes for improving neural interfaces. Microsystems Nanoeng. 4. doi:10.1038/s41378-018-0030-5.

Shepherd, R. K., Villalobos, J., Burns, O., and Nayagam, D. A. X. (2018). The development of neural stimulators: A review of preclinical safety and efficacy studies. J. Neural Eng. 15. doi:10.1088/1741-2552/aac43c.

Shoffstall, A. J., Ecker, M., Danda, V., Joshi-imre, A., Stiller, A., Yu, M., et al. (2018a). Characterization of the Neuroinflammatory Response to Thiol-ene Shape Memory Polymer Coated Intracortical Microelectrodes. Micromachines 9:486. doi:10.3390/mi9100486.

Shoffstall, A. J., Srinivasan, S., Willis, M., Stiller, A. M., Ecker, M., Voit, W. E., et al. (2018b). A Mosquito Inspired Strategy to Implant Microprobes into the Brain. Sci. Rep. 8:122. doi:10.1038/s41598-017-18522-4.

Smith, I., Haag, M., Ugbode, C., Tams, D., Rattray, M., Przyborski, S., et al. (2015). Neuronal-glial populations form functional networks in a biocompatible 3D scaffold. Neurosci. Lett. 609, 198–202. doi:10.1016/j.neulet.2015.10.044.

Sommakia, S., Rickus, J. L., and Otto, K. J. (2014). Glial cells, but not neurons, exhibit a controllable response to a localized inflammatory microenvironment in vitro. Front. Neuroeng. 7:41. doi:10.3389/fneng.2014.00041.

Song, J. J., Popescu, A., and Bell, R. L. (2014). Present and potential use of spinal cord stimulation to control chronic pain. Pain Physician 17, 235–246.

Song, L., Wang, K., Li, Y., and Yang, Y. (2016). Nanotopography promoted neuronal differentiation of human induced pluripotent stem cells. Colloids Surfaces B Biointerfaces 148, 49–58. doi:10.1016/j.colsurfb.2016.08.041.

Spencer, K. C., Sy, J. C., Falcòn-Banchs, R., and Cima, M. J. (2017a). Three Dimensional In Vitro Glial Scar Model to Investigate Local Strain Effects from Micromotion around Neural Implants. Lab Chip 17, 795–804. doi:10.1039/c6lc01411a.

Spencer, K. C., Sy, J. C., Ramadi, K. B., Graybiel, A. M., Langer, R., and Cima, M. J. (2017b). Characterization of Mechanically Matched Hydrogel Coatings to Improve the Biocompatibility of Neural Implants. Sci. Rep. 7:1952. doi:10.1038/s41598-017-02107-2.

Stahl, K., Mylonakou, M. N., Skare, Amiry-Moghaddam, M., and Torp, R. (2011). Cytoprotective effects of growth factors: BDNF more potent than GDNF in an organotypic culture model of Parkinson's disease. Brain Res. 1378, 105–118. doi:10.1016/j.brainres.2010.12.090.

Sun, A. X., Ng, H. H., and Tan, E. K. (2018). Translational potential of human brain organoids. Ann. Clin. Transl. Neurol. 5, 226–235. doi:10.1002/acn3.505.

Sunshine, M. D., Streeter, K. A., Gaire, J., Otto, K. J., and Fuller, D. D. (2018). Cervical spinal cord injury in a transgenic mouse expressing fluorophores in neurons, microglia, astrocytes, and oligodendrocytes. FASEB J. 32, 625.9-625.9. doi:10.1096/fasebj.2018.32.1_supplement.625.9.

Svensson, M., and Chen, P. (2018). "Novel Models to Study Stromal Cell-Leukocyte Interactions in Health and Disease," in Adv Exp Med Biol. 1060, 131–146. doi:10.1007/978-3-319-78127-3.

Szostak, K. M., Grand, L., and Constandinou, T. G. (2017). Neural Interfaces for Intracortical Recording: Requirements, Fabrication Methods, and Characteristics. Front. Neurosci. 11:665. doi:10.3389/fnins.2017.00665.

Tan, G. A., Furber, K. L., Thangaraj, M. P., Sobchishin, L., Doucette, J. R., and Nazarali, A. J. (2017). Organotypic Cultures from the Adult CNS: A Novel Model to Study Demyelination and Remyelination Ex Vivo. Cell. Mol. Neurobiol. 38, 317–328. doi:10.1007/s10571-017-0529-6.

Tang, J., Qin, N., Chong, Y., Diao, Y., Yiliguma, Wang, Z., et al. (2018). Nanowire arrays restore vision in blind mice. Nat. Commun. 9:786. doi:10.1038/s41467-018-03212-0.

Tasnim, N., Kumar, A., and Joddar, B. (2018). Attenuation of the In Vitro Neurotoxicity of 316L SS by Graphene Oxide Surface Coating. Mater Sci Eng C Mater Biol Appl. 73, 788–797. doi:10.1016/j.msec.2016.12.123.

Tawakol, O., Bredeson, S. D., and Troyk, P. R. (2016). Preparation of a neural electrode implantation device for in-vivo surgical use. Proc. Annu. Int. Conf. IEEE Eng. Med. Biol. Soc. EMBS 2016–Octob, 4507–4510. doi:10.1109/EMBC.2016.7591729.

Tekin, H., Simmons, S., Cummings, B., Gao, L., Adiconis, X., Hession, C. C., et al. (2018). Effects of 3D culturing conditions on the transcriptomic profile of stem-cell-derived neurons. Nat. Biomed. Eng. 2, 540–554. doi:10.1038/s41551-018-0219-9.

Trevathan, J. K., Baumgart, I. W., Nicolai, E. N., Gosink, B. A., Asp, A. J., Settell, M. L., et al. (2019). A Truly Injectable Neural Stimulation Electrode Made from an In-Body Curing Polymer/Metal Composite. bioRxiv, 584995. doi:10.1101/584995.

Ullrich, C., and Humpel, C. (2009). Rotenone Induces Cell Death of Cholinergic Neurons in an Organotypic Co-Culture Brain Slice Model. Neurochem Res. 34, 2147–2153. doi:10.1007/s11064-009-0014-9.

Usmani, S., Aurand, E. R., Medelin, M., Fabbro, A., Scaini, D., Laishram, J., et al. (2016). 3D meshes of carbon nanotubes guide functional reconnection of segregated spinal explants. Sci. Adv. 2, e1600087. doi:10.1126/sciadv.1600087.

Uysal, O., Sevimli, T., Sevimli, M., Gunes, S., and Sariboyaci, A. E. (2018). “Chapter 17 - Cell and Tissue Culture: The Base of Biotechnology,” in Omics Technologies and Bio-Engineering, eds. D. Barh and V. Azevedo (Academic Press), 391–429. doi: 10.1016/B978-0-12-804659-3.00017-8.

Verpelli, C., Carlessi, L., Bechi, G., Poli, E. F., Orellana, D., Heise, C., et al. (2013). Comparative neuronal differentiation of self-renewing neural progenitor cell lines obtained from human induced pluripotent stem cells. Front. Cell. Neurosci. 7:175. doi:10.3389/fncel.2013.00175.

Vitale, F., Shen, W., Driscoll, N., Burrell, J. C., Richardson, A. G., Adewole, O., et al. (2018). Biomimetic extracellular matrix coatings improve the chronic biocompatibility of microfabricated subdural microelectrode arrays. PLoS One 13, e0206137. doi:10.1371/journal.pone.0206137.

Vitale, F., Summerson, S. R., Aazhang, B., Kemere, C., and Pasquali, M. (2015). Neural Stimulation and Recording With Bidirectional, Soft Carbon Nanotube Fiber Microelectrodes. ACS Nano 9, 4465–4474. doi:10.1021/acsnano.5b01060.

Wandiyanto, J. V, Linklater, D., Perera, P. G. T., Orlowska, A., Truong, V. K., Thissen, H., et al. (2018). Pheochromocytoma (PC12) Cell Response on Mechanobactericidal Titanium Surfaces. Mater. 11, E605. doi:10.3390/ma11040605.

Wang, H. (2018). Modeling Neurological Diseases With Human Brain Organoids. Front Synaptic Neurosci 10, 15. doi:10.3389/fnsyn.2018.00015.

Wang, J. K. T., Portbury, S., Thomas, M. B., Barney, S., Ricca, D. J., Morris, D. L., et al. (2006). Cardiac glycosides provide neuroprotection against ischemic stroke: Discovery by a brain slice-based compound screening platform. Proc. Natl. Acad. Sci. 103, 10461–10466. doi:10.1073/pnas.0600930103.

Wang, J., Loye, A. M., Ketkaew, J., Schroers, J., and Kyriakides, T. R. (2018a). Hierarchical Micro- and Nano-Patterning of Metallic Glass to Engineer Cellular Responses. ACS Appl. Bio Mater 1, 51–58. doi:10.1021/acsabm.8b00007.

Wang, K., Frewin, C. L., Esrafilzadeh, D., Yu, C., Wang, C., Pancrazio, J. J., et al. (2019). High-Performance Graphene-Fiber-Based Neural Recording Microelectrodes. Adv. Mater. 31, 180586. doi:10.1002/adma.201805867.

Wang, Y., Wang, L., Guo, Y., Zhu, Y., and Qin, J. (2018b). Engineering stem cell-derived 3D brain organoids in a perfusable organ-on-a-chip system. RSC Adv. 8, 1677–1685. doi:10.1039/c7ra11714k.

Wellman, S. M., Cambi, F., and Kozai, T. D. (2018a). The role of oligodendrocytes and their progenitors on neural interface technology: A novel perspective on tissue regeneration and repair. Biomaterials 183, 200–217. doi:10.1016/j.biomaterials.2018.08.046.

Wellman, S. M., Eles, J. R., Ludwig, K. A., Seymour, J. P., Michelson, N. J., McFadden, W. E., et al. (2018b). A Materials Roadmap to Functional Neural Interface Design. Adv. Funct. Mater. 28, 1701269. doi:10.1002/adfm.201701269.

Wellman, S. M., and Kozai, T. D. Y. (2017). Understanding the Inflammatory Tissue Reaction to Brain Implants to Improve Neurochemical Sensing Performance. ACS Chem. Neurosci. 8, 2578–2582. doi:10.1021/acschemneuro.7b00403.

Wellman, S. M., and Kozai, T. D. Y. (2018). In vivo spatiotemporal dynamics of NG2 glia activity caused by neural electrode implantation. Biomaterials 164, 121–133. doi:10.1016/j.biomaterials.2018.02.037.

Weltman, A., Yoo, J., and Meng, E. (2016). Flexible, penetrating brain probes enabled by advances in polymer microfabrication. Micromachines 7:180. doi:10.3390/mi7100180.

Wendelken, S., Page, D. M., Davis, T., Wark, H. A. C., Kluger, D. T., Duncan, C., et al. (2017). Restoration of motor control and proprioceptive and cutaneous sensation in humans with prior upper-limb amputation via multiple Utah Slanted Electrode Arrays (USEAs) implanted in residual peripheral arm nerves. J Neuroeng Rehabil. 14:121. doi:10.1186/s12984-017-0320-4.

Wevers, N. R., VanVught, R., Wilschut, K. J., Nicolas, A., Chiang, C., Lanz, H. L., et al. (2016). High-throughput compound evaluation on 3D networks of neurons and glia in a microfluidic platform. Sci. Rep. 6, 38856. doi:10.1038/srep38856.

Williams, D. F. (2008). On the mechanisms of biocompatibility. Biomacromolecules 29, 2941–2953. doi:10.1016/j.biomaterials.2008.04.023.

Williams, D. F. (2009). On the nature of biomaterials. Biomaterials 30, 5897–5909. doi:10.1016/j.biomaterials.2009.07.027.

Woolley, A. J., Desai, H. A., and Otto, K. J. (2013). Chronic intracortical microelectrode arrays induce non-uniform, depth-related tissue responses. J. Neural Eng. 10:026007. doi:10.1088/1741-2560/10/2/026007.

Xicoy, H., Wieringa, B., and Martens, G. J. M. (2017). The SH-SY5Y cell line in Parkinson's disease research: a systematic review. Mol. Neurodegener. 12:10. doi:10.1186/s13024-017-0149-0.

Xu, H., Li, Z., Yu, Y., Sizdahkhani, S., Ho, W. S., Yin, F., et al. (2016). A dynamic in vivo-like organotypic blood-brain barrier model to probe metastatic brain tumors. Sci. Rep. 6, 36670. doi: 10.1038/srep36670.

Xu, J., Guo, H., Nguyen, A. T., Lim, H., and Yang, Z. (2018). A Bidirectional Neuromodulation Technology for Nerve Recording and Stimulation. Micromachines 9, E538. doi:10.3390/mi9110538.

Yang, J., Liu, L., Li, T., and Li, C. (2017). Array Focal Cortical Stimulation Enhances Motor Function Recovery and Brain Remodeling in a Rat Model of Ischemia. J. Stroke Cerebrovasc. Dis. 26, 658–665. doi:10.1016/j.jstrokecerebrovasdis.2016.11.009.

Yi, W., Chen, C., Feng, Z., Xu, Y., Zhou, C., Masurkar, N., et al. (2015). A flexible and implantable microelectrode arrays using high-temperature grown vertical carbon nanotubes and a biocompatible polymer substrate. Nanotechnology 26: 125301. doi:10.1088/0957-4484/26/12/125301.

Yin, F., Zhu, Y., Wang, Y., and Qin, J. (2018). Engineering brain organoids to probe impaired neurogenesis induced by cadmium. ACS Biomater. Sci. Eng 4, 1908–1915. doi:10.1021/acsbiomaterials.8b00160.

Zach, S., Bueler, H., Hengerer, B., and Gillardon, F. (2007). Predominant Neuritic Pathology Induced by Viral Overexpression of α-Synuclein in Cell Culture. Cell. Mol. Neurobiol. 27, 505–515. doi:10.1007/s10571-007-9141-5.

Zhou, H., Cheng, X., Rao, L., Li, T., and Duan, Y. Y. (2013). Poly(3,4-ethylenedioxythiophene)/multiwall carbon nanotube composite coatings for improving the stability of microelectrodes in neural prostheses applications. Acta Biomater. 9, 6439–6449. doi:10.1016/j.actbio.2013.01.042.

Zöndör, K., and Thoumine, O. (2017). Synaptogenic Assays Using Neurons Cultured on Micropatterned Substrates. Methods Mol Bio 1538, 29–44. doi:10.1007/978-1-4939-6688-2_3.

Zuidema, J. M., Desmond, G. P., Rivet, C. J., Kearns, K. R., Thompson, D. M., and Gilbert, R. J. (2015). Nebulized solvent ablation of aligned PLLA fibers for the study of neurite response to anisotropic-to-isotropic fiber/film transition (AFFT) boundaries in astrocyteeneuron co-cultures. Biomaterials 46, 82–94. doi:10.1016/j.biomaterials.2014.12.046.

Chapter 3

BIOCOMPATIBILITY OF PLATINUM NANOPARTICLES IN BRAIN EX-VIVO MODELS IN PHYSIOLOGICAL AND PATHOLOGICAL CONDITIONS

Maurizio Gulino[1,2,3], Sofia Duque Santos[1,2], Ana Paula Pêgo[1,2,3,4]

[1]i3S - Instituto de Investigação e Inovação em Saúde, Universidade do Porto, Porto, Portugal
[2]INEB - Instituto de Engenharia Biomédica, Universidade do Porto, Porto, Portugal
[3]FEUP - Faculdade de Engenharia, Universidade do Porto, Porto, Portugal
[4]ICBAS - Instituto de Ciências Biomédicas Abel Salazar, Universidade do Porto, Porto, Portugal

Published in Frontiers in Neuroscience, Volume 15 - 2021

ABSTRACT

Platinum nanoparticles (PtNPs) have unique physico-chemical properties that led to their use in many branches of medicine. Recently, PtNPs gathered growing interest as delivery vectors for drugs, biosensors and as surface coating on chronically implanted biomedical devices for improving electrochemical properties. However, there are contradictory statements about their biocompatibility and impact on target organs such as the brain tissue, where these NPs are finding many applications. Furthermore, many of the reported studies are conducted in homeostasis conditions and, consequently, neglect the impact of the pathologic conditions on the tissue response. To expand our knowledge on the effects of PtNPs on neuronal and glial cells, we investigated the acute effects of monodisperse sodium citrate-coated PtNPs on rat organotypic hippocampal cultures in physiological or neuronal excitotoxic conditions induced by kainic acid (KA).

The cellular responses of the PtNPs were evaluated through cytotoxic assays and confocal microscopy analysis. To mimic a pathologic scenario, 7-day organotypic hippocampal cultures were exposed to KA for 24 hours. Subsequently, PtNPs were added to each slice. We show that incubation of the slices with PtNPs for 24 hours, does not severely impact cell viability in normal conditions, with no significant differences when comparing the dentate gyrus (DG), as well as CA3 and CA1 pyramidal cell layers. Such effects are not exacerbated in KA-treated slices, where the presence of PtNPs does not cause additional neuronal PI uptake in CA3 and CA1 pyramidal cell layers. However, PtNPs cause microglial cell activation and morphological alterations in CA3 and DG regions indicating the establishment of an inflammatory reaction. Morphological analysis revealed that microglia acquire activated ameboid morphology with loss of ramifications, as a result of their response to PtNPs contact. Surprisingly, this effect is not increased in pathological conditions. Taken together, these results show that PtNPs cause microglia alterations in short-term studies. Additionally, there is no worsening of the tissue response in a neuropathological induced scenario. This work highlights the need of further research to allow for the safe use of PtNPs. Also, it supports the demand of the development of novel and more biocompatible NPs to be applied in the brain.

1. INTRODUCTION

For many decades, platinum has been employed in many branches of nanobiomedicine (Jeyaraj et al., 2019).

This metal presents prodigious physico-chemical characteristics such as good electrical conductivity, chemical stability and surface functionalization, that makes it unique among all the noble metals and suitable for several biomedical applications (Fahmy et al., 2020).

PtNps have recently gained growing interest over Pt derived compounds for the treatment of several types of cancers, thanks to their ability to induce apoptosis and cell cycle arrest, genotoxicity, oxidative stress and morphological changes in the structure of the tumor tissue. In accordance, PtNps have been shown to inhibit proliferation of human lung cancer cells (Bendale et al., 2016), breast cancer cells (Şahin et al., 2018) glioblastoma and neuroblastoma cancer cells (Asharani et al., 2010; Kutwin et al., 2017b, 2017a; Gurunathan et al., 2020), among others.

PtNps have been also proposed for photothermal treatment of certain types of tumours, as they can adsorb light and convert it into heat energy causing apoptosis of cancer cells and tumour regression (Manikandan et al., 2013; Samadi et al., 2018; Chang et al., 2019; Depciuch et al., 2020). By means of their surface functionalization, PtNps have been further explored as promising materials for drug delivery applications (Shim et al., 2017; Cao et al., 2018; Mukherjee et al., 2020). Moreover, substantial research has been conducted on the development of surface functionalized PtNps to confer enzymatic activity as well as for improving biocompatibility, bioavailability and stability in the context of their medical use (He et al., 2014; Deng et al., 2017; Franco-Ulloa et al., 2020). Remarkable attention has also been gathered by the employment of PtNPs in microelectrode design thanks to their adaptive electrochemical and mechanical properties that make them suitable for a variety of new design approaches of microelectrodes with superior properties (Islam and Islam, 2013; Aggas et al., 2019; Jeyaraj et al., 2019; Moeini et al., 2021). Overall, PtNPs have proven to be innovative tools to meet the requirements of sensitivity, target specificity and miniaturization of new designed microelectrodes. Despite the promising results obtained from early preclinical studies, there is still uncertainty in the scientific community regarding Pt toxicity and accumulation in organs and tissues (Kovach et al., 2016; Labrador-Rached et al., 2018).Conflicting findings are present in the literature about their impact in terms of safety (Wissel et al., 2018; Czubacka and Czerczak, 2019; Zeng et al., 2020; Shepherd et al., 2021). In vivo studies conducted on rats reported inflammation, cellular alterations in organs and negative effects on post-natal development (Adeyemi et al., 2016; Park et al., 2016). On the other hand, no adverse effects such as increased reactive gliosis or altered neuronal counts were observed 3 weeks after neural implants of nano-coated electrodes with PtNPs (Angelov

et al., 2016). However, few studies have focused on the PtNPs impact on the brain tissue in a pathological scenario (Prasek et al., 2013; Adeyemi et al., 2018). Considering the increasing number of applications of PtNPs for implantable microelectrode design, it is paramount to investigate their impact on neuronal and glial cells, and to conduct biocompatibility tests not only in homeostatic conditions, but also under induced pathological conditions to mimic the clinical scenario, where these materials are mainly employed. A compromised brain tissue unavoidably displays structural and cellular alterations that could lead to a different response compared to a brain tissue under physiological conditions. In this study, we selected hippocampal cultures as a model to investigate the biocompatibility of PtNPs and assess the acute response of the brain tissue in terms of cytotoxicity and cellular response. These cultures were incubated with monodispersed citrate-coated PtNPs under normal and pathological excitotoxic conditions induced by kainic acid treatment (Routbort et al., 1999). These stabilized PtNPs were assessed for the cellular responses induced after contact with brain tissue after short-time contact with brain tissue through cytotoxic and microscopy analysis, focusing on the morphological alterations of neurons, microglia, and astrocytes.

2. MATERIALS AND METHODS

2.1 ANIMALS

All the experiments were performed according to National and European Union guidelines (EU Directive 2010/63/EU for animal experiments) and with the utmost care to minimize animal suffering as well as the number of animals used. All the procedures using animals were approved by the i3S Ethics Committee (CEA, i3S). Animals were kept in an enriched housing environment with ad libitum feed and water supply. They were kept under a 12 h light/12 h dark cycle in the i3S animal facility with controlled ambient temperature and humidity. Wistar Han rat pups, males and females, 6-8 days old were used to prepare the hippocampal slice cultures.

2.2 ORGANOTYPIC HIPPOCAMPAL SLICE CULTURES

Hippocampal slice cultures were prepared as previously described (Stoppini et al., 1991). Briefly, rat pups were sacrificed by decapitation. The brain was extracted and immediately immersed in sterile ice-cold low Na^+ artificial cerebrospinal fluid (aCSF) solution containing 1 mM $CaCl_2$, 10 mM D-glucose, 4 mM KCl, 5 mM $MgCl_2$, 26 mM $NaHCO_3$ and 234 mM sucrose, previously bubbled for 15-20 minutes with 95% O_2 and 5%CO_2, as described by Optiz-Araya and Barria (Opitz-Araya and

Barria, 2011). The brain was cut longitudinally, and both hippocampi extracted, and transversally cut using a MCIlwain Tissue chopper (EC 350, Campden Instruments). 400 μm slices were obtained and gently separated using small spatulas under a Stereomicroscope (Leica S8APO). Only intact slices were selected and transferred into a 0.4 mm Millicell® PTFE culture inserts (Merk-Millipore), placed in multi-6 well plates (Corning). Each well contained 1 ml of incubation medium composed of Opti-MEM™ (Gibco) based medium supplemented with 25% (v/v) heat inactivated horse serum (Gibco), 25% (w/v) Hank's balanced salt solution (Gibco), glucose 25 mM (Sigma Aldrich) and penicillin/ streptomycin (Gibco, 100 μg/ml). Slices were maintained at 37 °C with 5% CO_2 and 95% atmospheric air for 7 days. Medium was changed 24 hours after the plating and then after every 2 days. From each animal, 25-30 hippocampal slices were selected and used for one set of experiments.

2.3 KAINIC ACID-INDUCED EXCITOTOXICITY AND PLATINUM NANOPARTICLES ADMINISTRATION

At day 7 of culture, excitotoxicity was induced by incubation of the slices with kainic acid (KA) at a concentration of 7 mM (Abcam) diluted in 1 ml of fresh incubation medium for 24 hours, in an adaptation of an experimental protocol from (Järvelä et al., 2011). Subsequently, mono-disperse citrate coated PtNPs (Nanocomposix, 50 nm) were added, as received, on the top of each slice and incubated for 24 hours. The experimental plan is shown in **Fig.1A**. PtNPs administration was carried out using a Narishige Pneumatic Microinjector (Model IM-300) connected to a nitrogen cylinder. Each insert was transferred to a petri dish, containing 2 ml of warm incubation medium. 200 ng of PtNPs suspended in aqueous 2 mM sodium citrate buffer, at a concentration of 1mg/ml were loaded into glass microcapillaries (WPI 1B200F-4, with Filament) inserted in a three-dimensional manipulator. 12-15 drops were deposited on the CA3, CA1 and DG areas, without touching the tissue. In control slice cultures, sodium citrate buffer was deposited in the same way. All the procedures were carried out in sterile conditions inside a laminar flow hood equipped with a stereomicroscope. After the procedure, the medium was replaced with fresh pre-heated medium.

2.4 PROPIDIUM IODIDE UPTAKE

Cell viability was assessed by propidium iodide (PI) exclusion, to evaluate the impact of PtNPs on the slices under normal and excitotoxic conditions. 24 hours after NPs administration, PI (Gibco) was added to the culture medium for 1h at 4 μg/ml. Slices treated with Triton X-100 0.1% (v/v) (Sigma Aldrich) in phosphate buffered saline (PBS) for 1 hour prior to PI incubation were used as positive

controls. For visualization, each membrane insert was gently cut out and placed inside a 35 mm imaging m-dish (ibidi) as previously described (Seidl and Rubel, 2010).

2.5 FLUORO-JADE STAINING

Fluoro-jade C staining was used to assess the neuronal degeneration caused by excitotoxicity induced with KA. After KA incubation for 24 hours, the membrane inserts were fixed in 4% (w/v) paraformaldehyde (PFA, Sigma Aldrich) for 1 hour with gentle shaking at room temperature (RT). After fixation, the membranes with slices were incubated in 0.06% (w/v) $KMnO_4$ for 5 minutes (Sigma Aldrich) prior to staining with 0.001% (w/v) Fluoro-Jade C solution for 30 minutes (Merk Millipore). Subsequently, the membranes were transferred onto glass slides and dried at RT for 5-10 minutes. Finally, slices were cleared in xylene (Sigma Aldrich) and coverslipped with DPX mounting medium (Merk).

2.6 IMMUNOFLUORESCENCE

At the end of the incubation period with PtNPs, slices were fixed in 4% (w/v) PFA for 1 hour with gentle shaking at room temperature. Slices were incubated in permeabilization/blocking buffer composed of 1% (w/v) bovine serum albumin (BSA, Sigma Aldrich), 5% (v/v) heat-inactivated fetal bovine serum (FBS, Gibco) and 1% (v/v) Triton X-100 in PBS overnight at 4°C with gentle shaking. After PBS washing, slices were incubated with rabbit anti-Iba-1 (1:800, Wako Chemicals), mouse anti-β3-tubulin (1:500, Promega) and rabbit anti-GFAP (1:500, Abcam) for 48 hours at 4°C with gentle shaking diluted in blocking buffer containing 1% (w/v) BSA, 5% (v/v) FBS, 0.3% (v/v) Triton X-100 in PBS for 48 hours at 4°C with gentle shaking. Slices were washed again with 0.05% (v/v) Triton X-100 in PBS at RT with gentle shaking. After primary antibody incubation, slices were incubated with Alexa Fluor 488 rabbit anti-goat IgG (H+L) secondary antibody (Invitrogen) and Alexa Fluor 647 donkey anti-mouse IgG (H+L) secondary antibody (Invitrogen) for 3 hours at RT with gentle shaking and then washed again with 0.05% Triton-100 in PBS at RT with gentle shaking. To stain the nuclei, slices were incubated in Hoechst 33342 solution (1 mg/ml, Thermofisher) in PBS for 30 minutes. Slices were placed on glass slides for mounting, as previously described (Yoon et al., 2011), using a bridge mounting technique to preserve integrity of the slices. Briefly, two 22 mm x 22 mm coverslips were glued on the glass slides to create a chamber in which to place the slices. The space created was filled with Mowiol/glycerol (3:1, Sigma Aldrich) mounting medium and gently

covered with a 40 mm x 22 mm coverslip to close the gap between the two slides. The coverslip was glued with nail varnish and stored in the dark at 4°C, till further use.

2.7 IMAGE ANALYSIS AND QUANTIFICATION

For image acquisition of PI uptake, a Zeiss Axiovert 200M inverted fluorescence microscope equipped with a 565 nm filter was used. Images were acquired using a 5X objective. Analysis and quantification of PI uptake was performed in CA3, CA1 and DG regions of each brain slice using Image J software (version 1.53; National Institutes of Health, United States).

Fluoro-jade C and immunofluorescence image acquisition was performed using a Leica Scanning Confocal SP8 equipped with 405, 488, 633 filters (Leica Microsystems, Germany) composed of an inverted microscope Leica DMI8 (Leica Microsystems, Germany) and LAS X software (Leica Microsystems, Germany). For fluorescence intensity quantification, images were acquired using 10X objective. Confocal image stacks of 512 × 512 (16-bit depth, pixel size 3 μm, zoom 0.75). Quantification of Iba-1, GFAP, β3-tubulin and PI intensity in the CA3, CA1, and DG regions was performed using Image J software. 80-100 μm stacks were acquired from each slice starting from the top of the tissue.

For the image acquisition of Iba-1, GFAP and β3-tubulin densities in CA3 region, images were acquired using a 40X objective, with confocal image stacks of 1024 × 1024 pixel, 16-bit depth, pixel size 0.63 μm, zoom 1.0. Quantification was performed using the surface analysis tool on Imaris Software (version 9.5; Oxford Instruments, United Kingdom).

For the of 3D- reconstruction of microglial cell morphology, images were acquired more in detail using 63X objective, with confocal 16-bit depth image stacks of 1024 × 1024 pixels, with pixel size of 0.334 μm and zoom set at 3.0. Single cells with complete and defined processes were selected and imaged for analysis. Quantification of morphology was performed using the filament tool tracer on Imaris software. Cell processes were automatically created from the cell soma using AutoPath (no loops) algorithm and manually adjusted for a proper tracing. The number of processes as well as the number of terminal points and branching points was calculated per each cell. To quantify the degree of arborization, the total number of Sholl intersections and the filament full branch depth (the maximum number of branches between a starting point and a terminal point) was also calculated (Salois and Smith, 2016).

2.8 STATISTICS

Data from three independent experiments were presented as the mean ± standard error of the mean (SEM). Tukey's test after one-way analysis of variance (ANOVA) was used for statistical analysis. Analysis and visualization of data was carried out using GraphPad Prism 9 (GraphPad Software, San Diego, CA).

3. RESULTS

3.1 ORGANOTYPIC HIPPOCAMPAL SLICES ARE RESPONSIVE TO THE PATHOLOGICAL STIMULUS

To determine the response of the organotypic hippocampal slice cultures to excitotoxic damage induced by KA, we first quantified the uptake of PI to assess cell viability after the treatment. As previously reported (Holopainen et al., 2004; Järvelä et al., 2011; Jung et al., 2013a; Kim et al., 2015a), treatment with KA at low concentrations (7μM) for 24 hours caused significant neural cell viability impairment in CA3 and, to a lower extent, in CA1 and DG regions compared to untreated cultures (**Fig.2A**). To confirm that the cell population that was impacted the most, we performed Fluoro-jade C staining to assess neuronal degeneration. Imaging of organotypic hippocampal slices showed staining of degenerating neurons in the CA3 region, with the same staining pattern described in previous works (**Fig.1B**) (Jung et al., 2013b). These results confirmed the expected response of the organotypic hippocampal slices ex vivo, in an epileptic/ pathological scenario as observed in vivo.

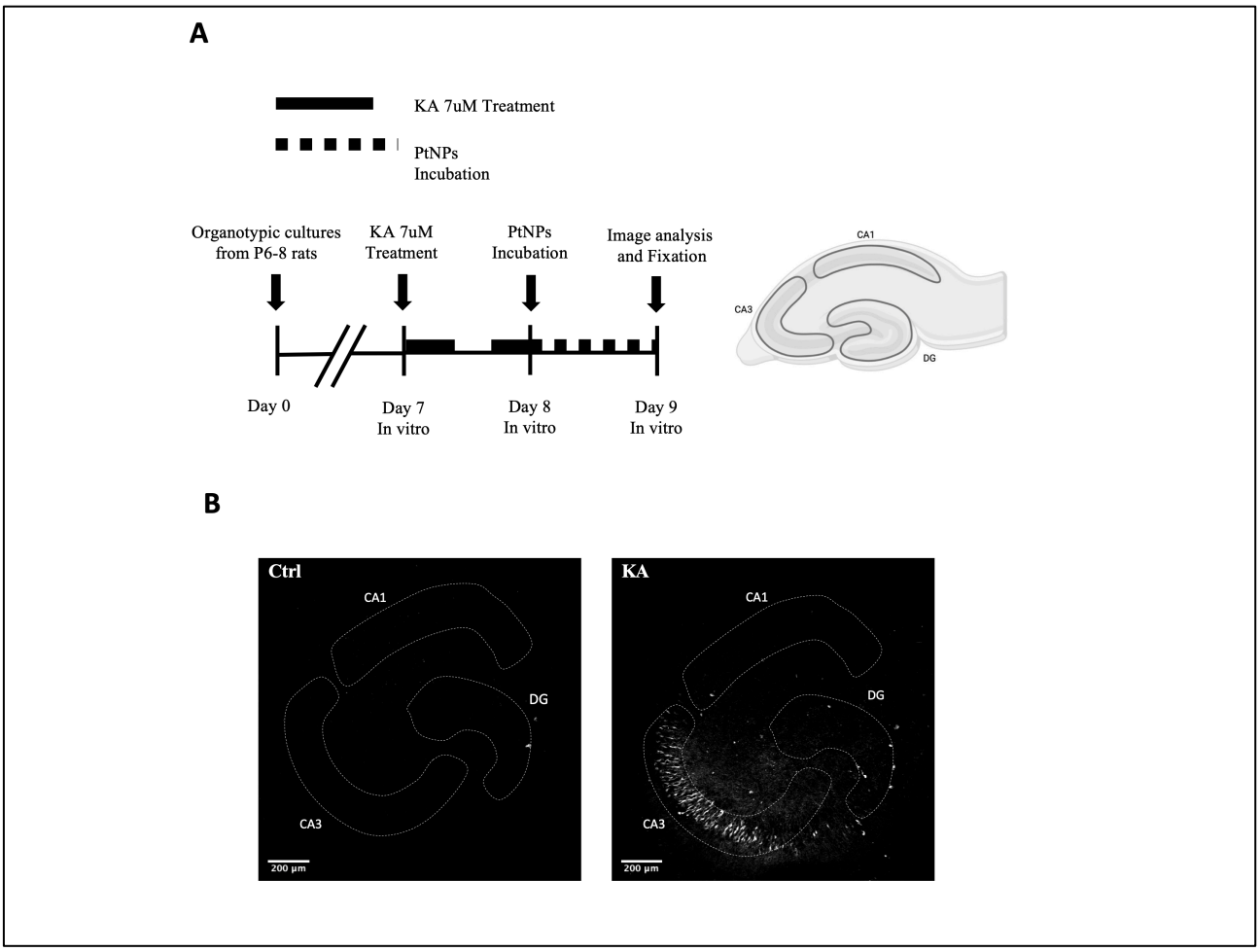


***Figure 1**. Establishment of rat hippocampal organotypic cultures as a 3D model to study the biocompatibility of PtNPs both in normal and pathological conditions. (A) Experimental scheme for inducing the pathological state and assessing the biocompatibility of PtNPs in the organotypic hippocampal slices. After 7 days in culture, slices are treated with KA for 24 hours followed by a 24-hour incubation period with PtNps. (B) Representative Fluorojade C staining of degenerating neurons in organotypic hippocampal slices under control condition and KA 7uM at day 8 in vitro.*

3.2 PLATINUM NANOPARTICLES DO NOT NEGATIVELY IMPACT CELL VIABILITY IN NORMAL OR PATHOLOGICAL CONDITIONS

Neural cell viability and neuronal cell integrity upon incubation with PtNPs were evaluated thorough PI uptake and β3-tubulin immunofluorescence, respectively, in normal and pathological conditions. Before NPs incubation, a subset of slices was first challenged with KA for 24 hours, as previously assessed to induce neurodegeneration, especially in the CA3 region. Application of PtNPs drop by drop on each slice was carried out to provide a homogeneous and direct deposition throughout the

whole tissue surface to assess the different regional responses to a known NP concentration. After, slices were incubated with PtNPs for an additional 24-hour period (**Fig.1A**). Image analysis and quantification of PI uptake was carried out in the whole slice (data not shown) and in the CA3, CA1 and DG regions. Our results show that PtNPs do not reduce cell viability in normal conditions (**Fig.2A**), as no significant differences were observed when compared to control cultures. In KA-treated slices, as already described above, KA at low concentrations (7μM) for 24 hours caused visible neuronal cell death in CA3 and, to a lower extent, in CA1 and DG regions compared to untreated cultures (**Fig.2A**). Despite this evident compromised tissue, no significant PI uptake was observed in KA-treated slices incubated with PtNPs in all the three regions (**Fig.2B**).

To further characterize the impact of PtNPs on neuronal cells, we performed immunofluorescence analysis using β3-tubulin staining. Fluorescence intensity analysis of CA3, CA1 and DG areas was first performed to assess the effects of PtNPs on neuronal cells (**Fig.3A**). Our results show that PtNPs did not cause significant neuronal cell loss in normal conditions. Furthermore, we did not observe alterations in β3-tubulin fluorescence intensity in KA-treated slices in all the three regions (**Fig.3A**). In addition, we performed the analysis of β3-tubulin density at the level of the CA3 region. This region was selected as the area mainly susceptible to cellular alterations in vivo and ex vivo (Yu et al., 2016; Neville et al., 2018). Our results show that no significant alterations occurred in neuronal density, indicating that PtNPs do not impair neuronal integrity in normal conditions. Even though in KA-treated slices we observed evident impairment in neuronal integrity and the presence of aberrating pyramidal neurons at the level of the CA3 region due to the KA treatment, we do not report any significant difference in β3-tubulin density regardless of the PtNPs incubation (**Fig.3B**).

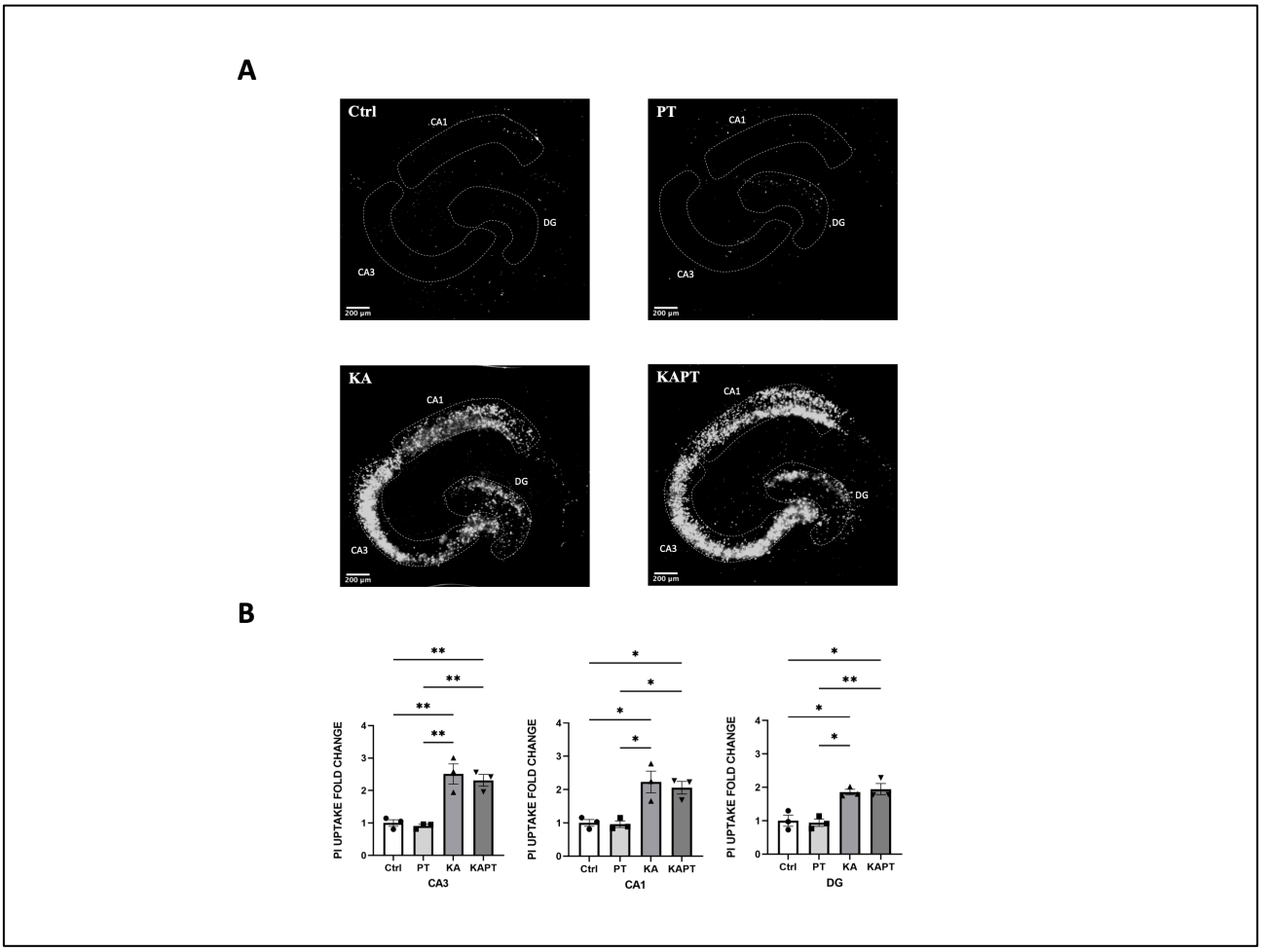


Figure 2. *Platinum nanoparticles do not impact cell viability in normal and pathological conditions after 24 hours of contact. (A) Representative PI staining of dead cells in organotypic hippocampal slices under control conditions (CTRL; untreated slices), PtNPs (PT), KA treatment (KA) and KA treatment + PtNPs (KAPT). (B) Quantitative analysis of PI uptake in CA3, CA1 and DG in normal and pathological conditions. Data are expressed as integrated density fold change from the basal value of control slices and presented as mean ± SEM (n = 3 independent experiments; 4-6 slices analyzed per group/experiment). Tukey's test after one-way analysis of variance (ANOVA) was used for statistical analysis. *p < 0.05; **p < 0.01.*

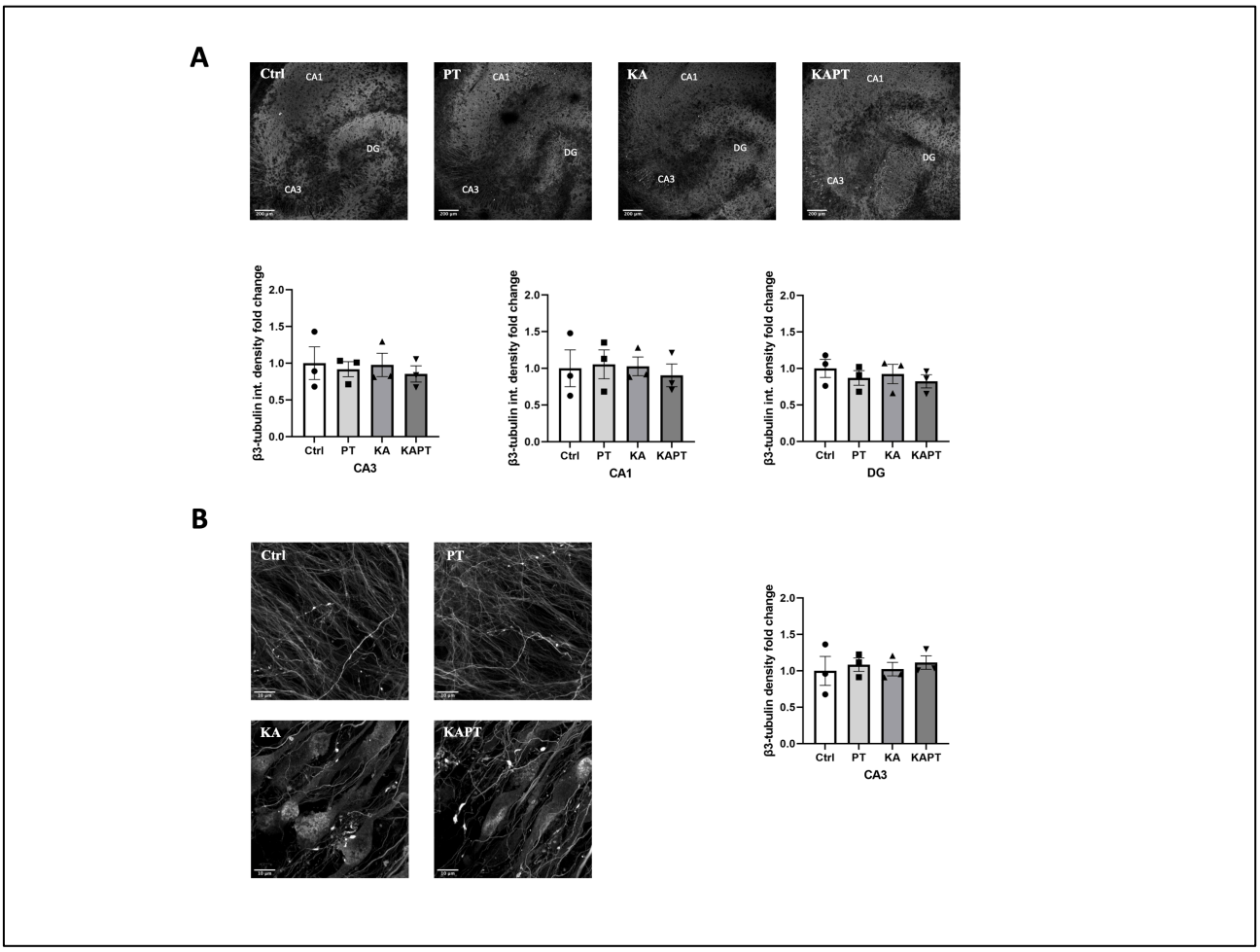


Figure 3. *Platinum nanoparticles do not further impact neuronal integrity in normal and pathological conditions after 24 hours of contact. (A) Representative beta-3 tubulin immunostaining of organotypic hippocampal slices under control conditions (untreated), PtNPs, KA treatment and KA treatment + PtNPs. Bottom charts represent the quantitative analysis of beta-3 tubulin fluorescence intensity in CA3, CA1 and DG. (B) Magnified images of CA3 region showing alterations in microtubule morphology only in KA-treated slices compared to controls, regardless of PtNPs incubation. Right chart represents the quantification of the b3-tubulin immunostaining in the high magnification CA3 area for the different slices. Data are expressed as integrated density fold change from the basal value of control slices and presented as mean ± SEM (n = 3 independent experiments; 4-6 slices analyzed per group/experiment). Tukey's test after one-way analysis of variance (ANOVA) was used for statistical analysis.*

3.3 PLATINUM NANOPARTICLES CAUSE MICROGLIA ACTIVATION IN ORGANOTYPIC HIPPOCAMPAL SLICES

To investigate the impact of PtNPs on glial cells, we performed immunofluorescence analysis on microglia and astrocytes.

Iba-1 fluorescence intensity measurements were performed on CA3, CA1 and DG regions. Interestingly, we observed a significant increase in Iba-1 fluorescence intensity in slices incubated with PtNPs in all the three regions. In more detail, we report a significant 1.4-fold increase in Iba-1 fluorescence intensity in CA1 region, 2-fold increase in CA3 and 1.5-fold increase in DG area. (**Fig.4A**). In KA-treated cultures, we reported higher Iba-1 intensity levels in CA3 (2-fold increase) and, to a lower extent, in CA1 area (1.4-fold increase) (**Fig.4A**). Incubation of PtNPs in KA treated slices led to the same increase in Iba-1 as in the slices only subjected to KA treatment. Further analysis on microglia density was carried out in the CA3 area in all experimental groups. In normal conditions, we observed a significant 2-fold increase in microglial density after PtNPs incubation, as a result of cell activation towards a reactive phenotype (**Fig.4B**). As already reported in the literature, a higher increase in microglial density was observed in KA treated slices (Araki et al., 2020). However, consistent with the above-described data, incubation with PtNPs did not cause any exacerbation of the effect already induced by KA.

To investigate the reactivity of astrocytes to PtNPs, we performed GFAP immunofluorescence staining. GFAP fluorescence intensity measurements in CA3, CA1 and DG regions revealed non-significant alterations in astrocyte states in all the conditions tested (**Fig.5A** and **5B**). Analysis of GFAP density was carried out at higher magnification in CA1 region as the most susceptible region to GFAP alteration in KA animal models of epilepsy (Vargas et al., 2013; Wu et al., 2021). In accordance with the measurements of GFAP fluorescence intensity, no significant differences were observed in astrocytes density (**Fig.5C**) in all the treatment groups. These data indicate that, despite having observed microglial activation after PtNPs administration in all the hippocampal regions, astrocytes density and integrity remained preserved after 24 hours of contact with PtNPs.

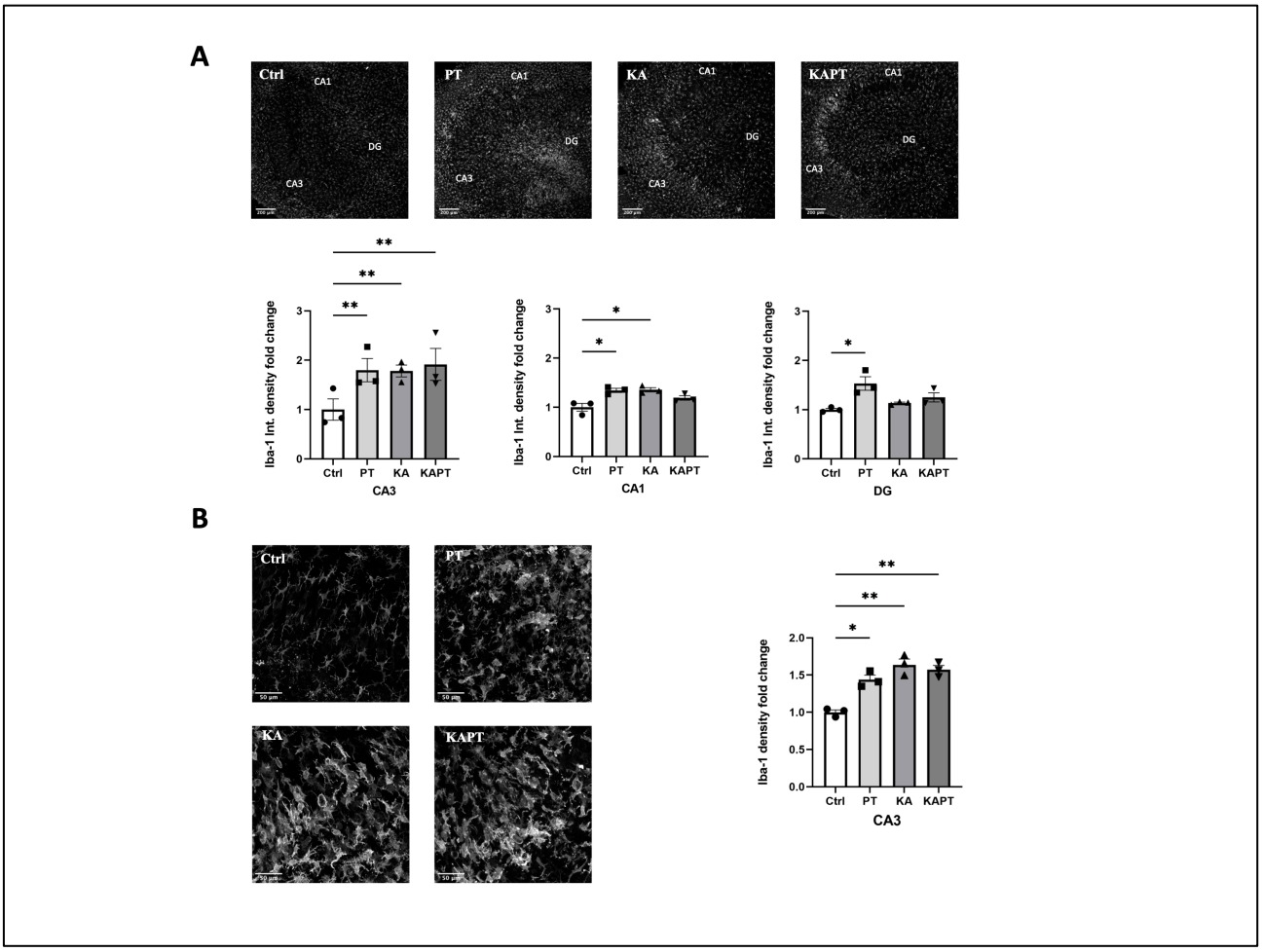


Figure 4. *Platinum nanoparticles cause microglia activation in organotypic hippocampal slices after 24 hours of contact. (A) Representative Iba-1 immunostaining of organotypic hippocampal slices under control conditions, PtNPs, KA treatment and KA treatment + PtNPs. Bottom charts represent the quantitative analysis of Iba-1 fluorescence intensity in CA3, CA1 and DG. (B) Magnified images of Iba-1 stained microglia at the level of the CA3 region, showing altered morphology of cells in all the treatment groups compared to the control. Right chart represents Iba-1 density quantification at the CA3 region for all experimental groups. Data are expressed as Iba-1 fluorescence intensity and density fold change from the value of control slices and presented as means ± SEM (n = 3 independent experiments; 4-6 slices analyzed per group/experiment). Tukey's test after one-way analysis of variance. (ANOVA) was used for statistical analysis. *p < 0.05; **p< 0.01.*

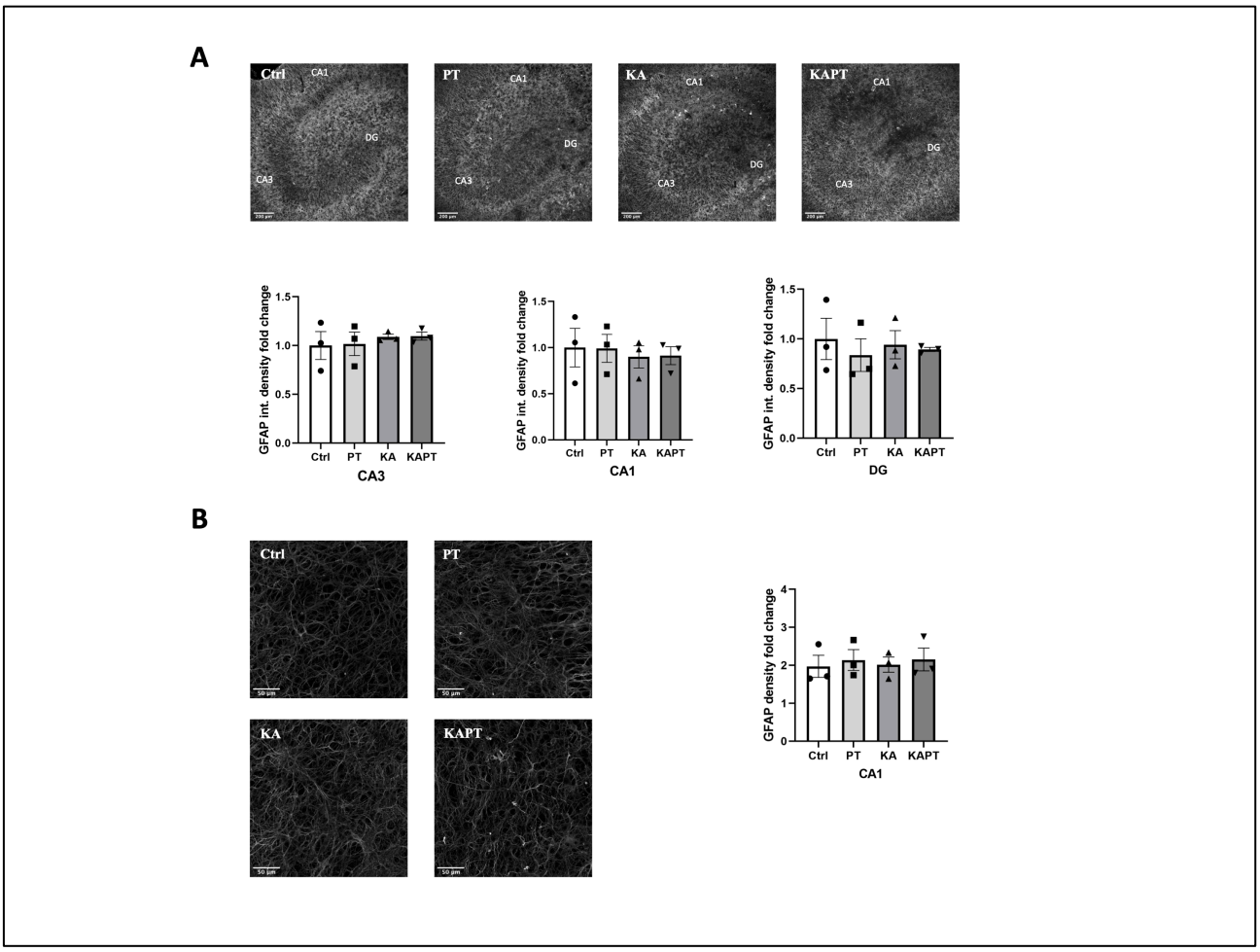


Figure 5. *Platinum nanoparticles do not cause astrogliosis in organotypic hippocampal slices after 24 hours of contact (A) Representative GFAP immunostaining of organotypic hippocampal slices under control condition, PtNPs, KA treatment and KA treatment with PtNps. Bottom charts represent the quantitative analysis of GFAP fluorescence intensity in CA3, CA1 and DG. (B) Magnified images of GFAP stained astrocytes at the level of the CA1 region. Right chart represents GFAP density quantification at the CA1 region showing non-significant differences in all the treatment groups. Data are expressed as integrated density and density fold change from the value of control slices and presented as means ± SEM (n = 3 independent experiments; 4-6 slices analyzed per group/experiment). Tukey's test after one-way analysis of variance (ANOVA) was used for statistical analysis.*

3.4 PLATINUM NANOPARTICLES CAUSE MORPHOLOGICAL ALTERATIONS OF MICROGLIA

Further image analysis was carried out to study the impact of PtNPs on microglia morphology. Iba-1-stained microglia from CA3 region were imaged and analyzed using the filament tool on Imaris software. In both normal and pathological conditions, a significant reduction in the number of processes was observed in slices incubated with PtNPs ($p<0.01$), accompanied by a reduction of the number of branching points ($p<0.001$) and terminal points ($p<0.01$) (**Fig.6A**). To analyze the degree of arborization of microglia, we also quantified the filament full branch depth (the highest value of bifurcations of the processes for each cell) and performed automated Sholl analysis in imaris. We observe a significant decrease in the level of bifurcation in slices treated with PtNPs, indicating that microglia underwent morphological alterations from ramified state to a reactive ameboid state as result of cell activation. Moreover, we identified internalization of PtNPs by microglia and this could explain the reactive phenotype that was observed (**Fig.6B**). In KA-treated slices we reported a similar behavior of microglia in response to the induced neuronal cell death and neurodegeneration. It has been already reported in vivo, in vivo and ex vivo that microglia migrate at the level of the CA3 region in response to the neurodegeneration induced by KA acquiring a reactive ameboid shape (Araki et al., 2020). In line with the previous quantifications, we did not observe any amplification of the inflammatory response in KA-treated slices incubated with PtNPs.

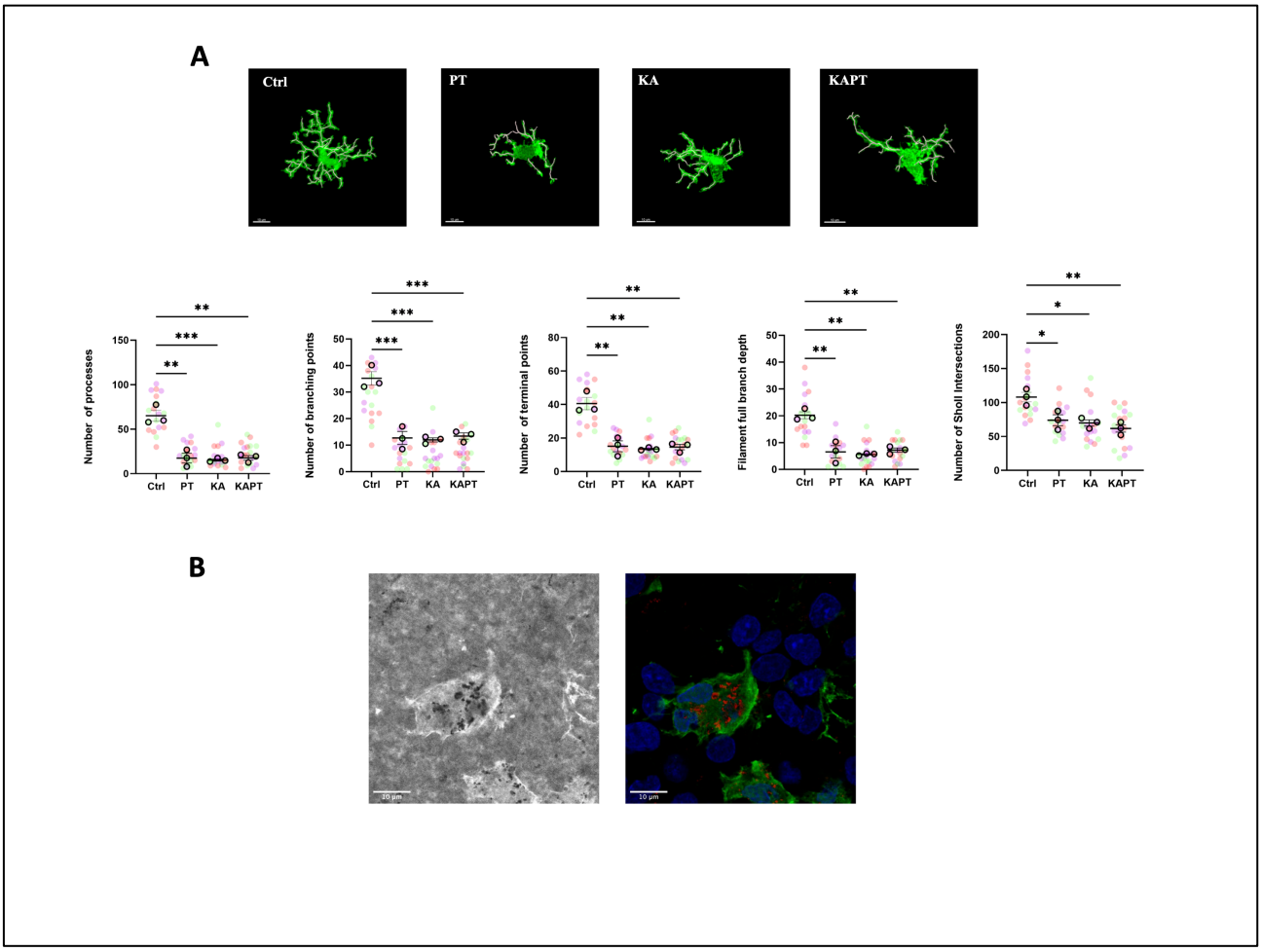


Figure 6. *Platinum nanoparticles cause morphological alterations of microglia after 24 hours of contact. (A) Representative Iba-1 immunostaining of microglia at 63X magnification, showing alteration in microglia morphology in all the treatment groups compared to controls. White cylinders highlight branch complexity. Bottom charts represent microglia morphology quantification showing significant differences in the number of processes, branching and terminal points, as well as the branch complexity and ramification in all the treatment groups compared to controls. (B) Left: representative brightfield image showing PtNPs internalization by microglia. Right: merge of the brightfield image with PtNPs colored in red with the fluorescent image showing microglia in green and nuclei in blue. Dots in the dot plots represent individual cells. Data are presented as means ± SEM (n = 3 independent experiments; 5-8 cells analyzed per group/experiment). Tukey's test after one-way analysis of variance (ANOVA) was used for statistical analysis. *p < 0.05; **p< 0.01; ***p<0.001.*

4. DISCUSSION

Despite the improvements in nanobiomedicine and biomedical device fabrication, there are still significant limitations on biocompatibility and electrochemical performance of materials and coatings used for microelectrode design. Therefore, one of the current challenges in the field has been uncovering the most effective intervention strategies to overcome adverse biocompatibility and durability issues and to promote material homeostatic integration in the central nervous system. Toward this end, the use of appropriate experimental models can provide significant advantages in the development and testing of biocompatible smart materials for microelectrode design.

The main goal of this work was to test the biocompatibility and the acute cellular response to metal NPs, by exploring rodent brain organotypic cultures as ex-vivo models. Among the great variety of in vitro biological models available, organotypic cultures represent one of the best biological tools for this purpose because they offer the possibility to mimic several pathological conditions and to isolate specific cerebral regions, ensuring the preservation of tissue architecture and synaptic organization (Gulino et al., 2019). Moreover, the tunability of the experimental conditions make them a relevant alternative for testing diverse new materials and designs at the preclinical level resulting in a refinement of subsequent in vivo studies and a reduction on the use of animal models.

We, in fact, showed through this work, the organotypic cultures versatility for the assessment of biocompatibility of materials such as Pt in physiological and induced pathological conditions. Considering the increasing number of biomedical applications of PtNPs, it is paramount to unravel their biocompatibility and toxicological potential while envisaging its safe clinical use. To the best of our knowledge, this is the first time that such organotypic based disease model has been explored to assess the biological performance of PtNPs. Such 3D complex models can serve as promising alternatives to animal studies used for investigation on the impact of metallic nanoparticles and devices on neural tissue. Additionally, glial cells, the effective determinants of the nervous tissue response to materials can be studied in detail in their 3D environment. Microglia are the key-regulators of brain inflammation and play a double edged-sword role in many pathophysiological processes. In the process of nervous tissue response, they act as first mediators of the acute phase of the response and become activated in the first hours after material contact. They reach the vicinity of the injury site and secrete pro-inflammatory cytokines which in turn lead to astrocyte and oligodendrocyte activation along with progressive neuronal cell loss at the level of the tissue-material interface (Gulino et al., 2019; Wellman et al., 2019; Huang et al., 2020).

In this study, we report that short time (24h) incubation of organotypic cultures with monodispersed citrate-coated PtNPs did not hamper neuronal viability and integrity. PI uptake analysis revealed

absence of cell viability impairment, as well as similar β3-tubulin fluorescence expression, density and morphology indicating the absence of neuronal cell loss. However, we reported a significant increase in Iba-1 fluorescence expression and density in CA3, CA1 and DG areas as consequence of microglial cell activation (Kozai et al., 2012; Yang et al., 2021). Morphological analysis revealed that microglia displayed a unramified morphology, with reduced number of branches and process length, indicating the acquisition of a reactive ameboid phenotype.

The impact of PtNPs was also investigated in organotypic cultures under excitotoxic conditions induced by KA. It is widely described in the literature that KA in vivo and ex vivo induces neuronal cell loss, hippocampal neurodegeneration, glial activation and oxidative stress. To mimic the same pathological scenario, typical of neurological conditions like for example epilepsy, we confirmed through microscopic analysis the induction of neural cell cytotoxicity, neuronal degeneration and microglia activation mainly at the level of the CA3 region. Surprisingly, we did not report any exacerbation of the response of KA-treated slices to PtNPs incubation for 24 hours. Such finding may be explained by the considerable cytotoxic effect induced by KA that could not be significantly added up by the PtNPs action, as observed in non-pathological conditions. Another hypothesis that can explain the non-observation of an additive effect could result from neuroprotection elicited by microglia in the pathological tissue explant. So, when the addition of the PtNPs occurs, the inflammatory response triggered by the KA treatment is already ongoing and, therefore, the tissue reaction to the PtNPs is distinct from the one observed in the physiological tissue explant. In fact, it has been previously described that microglia can play a neuroprotective role in hippocampal excitotoxicity (Vinet et al., 2012). In particular, it has been reported an increase in neuronal survival rate in vitro (Yu et al., 2019; Wang et al., 2021), as well as upregulation of pro- and anti-inflammatory genes after intranasal administration of KA in vivo (Sabilallah et al., 2016). In light of these observations, our findings may support the hypothesis of a non-detectable effect and/or a neuroprotective effect exerted by microglia after 24 hours of incubation of KA and could explain the absence of an additive effect in the response to PtNPs as observed in normal conditions. Finally, our experiments demonstrated the importance of screening materials in biological models with increased complexity that closely mimic the in vivo scenario and strongly point to the importance of the choice of relevant based disease models for a proper material characterization in homeostatic and non-homeostatic conditions.

In this work we employed rodent brain organotypic cultures as ex-vivo models to study the biocompatibility of new classes of smart materials and coatings for microelectrode design to be applied in disease context. We in fact showed, through our work, their ability for the assessment of biocompatibility of PtNPs and the possibility to evaluate the glial and neuronal acute cell response

under reproducible and controlled experimental conditions. Nevertheless, due to the possibility to maintain organotypic cultures for extended periods of time, one can also envisage the investigation of the implications of PtNPs in the brain tissue in the long term, what will be the focus of future studies in the group.

5. ACKNOWLEDGMENTS

The authors acknowledge the funding from the European Union's Horizon 2020 Research and Innovation Programme under the Marie Skłodowska-Curie grant agreement No. 764977, in the framework of the mCBEEs project (Advanced integrative solutions to corrosion problems beyond micro-scale: towards long-term durability of miniaturized biomedical, electronic and energy systems). The work was also financed by Portuguese funds through FCT/MCTES in the framework of the project "Institute for Research and Innovation in Health Sciences" - UIDB/04293/2020.
The authors thank the support of the i3S Scientific Platforms Bioimaging and Advanced Light microscopy (ALM), members of the national infrastructure PPBI - Portuguese Platform of Bioimaging (PPBI-POCI-01-0145-FEDER-022122). Santos SD acknowledges FCT for her contract under the Norma Transitória–DL57/2016/CP/CP1360/CT0013.

REFERENCES

Adeyemi, O., Olajide, I., Adeyanju, A., Awakan, O., and Otohinoyi, D. (2018). Modulation of rat plasma kynurenine level by platinum nanoparticles and likely association with oxidative stress. Biointerface Res. Appl. Chem. 8.

Adeyemi, O. S., Sulaiman, F. A., Akanji, M. A., Oloyede, H. O. B., Sulaiman, A. A., Olatunde, A., et al. (2016). Biochemical and morphological changes in rats exposed to platinum nanoparticles. Comp. Clin. Path. 25, 855–864. doi:10.1007/s00580-016-2274-5.

Aggas, J. R., Bhat, A., Walther, B. K., and Guiseppi-Elie, A. (2019). Nano-Pt ennobling of stainless steel for biomedical applications. Electrochim. Acta 301, 153–161. doi: 10.1016/j.electacta.2019.01.177.

Angelov, S. D., Koenen, S., Jakobi, J., Heissler, H. E., Alam, M., Schwabe, K., et al. (2016). Electrophoretic deposition of ligand-free platinum nanoparticles on neural electrodes affects their impedance in vitro and in vivo with no negative effect on reactive gliosis. J. Nanobiotechnology 14, 3. doi:10.1186/s12951-015-0154-9.

Araki, T., Ikegaya, Y., and Koyama, R. (2020). Microglia attenuate the kainic acid-induced death of hippocampal neurons in slice cultures. Neuropsychopharmacol. Reports 40, 85–91. doi: 10.1002/npr2.12086.

Asharani, P. V, Xinyi, N., Hande, M. P., and Valiyaveettil, S. (2010). DNA damage and p53-mediated growth arrest in human cells treated with platinum nanoparticles. Nanomedicine (Lond). 5, 51–64. doi:10.2217/nnm.09.85.

Bendale, Y., Bendale, V., Natu, R., and Paul, S. (2016). Biosynthesized Platinum Nanoparticles Inhibit the Proliferation of Human Lung-Cancer Cells in vitro and Delay the Growth of a Human Lung-Tumor Xenograft in vivo: -In vitro and in vivo Anticancer Activity of bio-Pt NPs. J. pharmacopuncture 19, 114–121. doi:10.3831/KPI.2016.19.012.

Cao, G.-J., Fisher, C. M., Jiang, X., Chong, Y., Zhang, H., Guo, H., et al. (2018). Platinum nanoparticles: an avenue for enhancing the release of nitric oxide from S-nitroso-N-acetylpenicillamine and S-nitrosoglutathione. Nanoscale 10, 11176–11185. doi:10.1039/C8NR03874K.

Chang, C., Wang, C., Zhang, C., Li, L., Zhang, Q., and Huang, Q. (2019). Albumin-Encapsulated Platinum Nanoparticles for Targeted Photothermal Treatment of Glioma. J. Biomed. Nanotechnol. 15, 1744–1753. doi:10.1166/jbn.2019.2803.

Czubacka, E., and Czerczak, S. (2019). Are platinum nanoparticles safe to human health? Med. Pr. 70, 487–495. doi:10.13075/mp.5893.00847.

Deng, H.-H., Lin, X.-L., Liu, Y.-H., Li, K.-L., Zhuang, Q.-Q., Peng, H.-P., et al. (2017). Chitosan-stabilized platinum nanoparticles as effective oxidase mimics for colorimetric detection of acid phosphatase. Nanoscale 9, 10292–10300. doi:10.1039/C7NR03399K.

Depciuch, J., Steć, M., Maximenko, A., DrzymbBa, E., Pawlyta, M., Baran, J., et al. (2020). Synthesis method-dependent photothermal effects of colloidal solutions of platinum nanoparticles used in photothermal anticancer therapy. Appl. Organomet. Chem. 34. doi: 10.1002/aoc.5401.

Fahmy, S. A., Preis, E., Bakowsky, U., and Azzazy, H. M. E.-S. (2020). Platinum Nanoparticles: Green Synthesis and Biomedical Applications. Molecules 25, 4981. doi:10.3390/molecules25214981.

Franco-Ulloa, S., Tatulli, G., Bore, S. L., Moglianetti, M., Pompa, P. P., Cascella, M., et al. (2020). Dispersion state phase diagram of citrate-coated metallic nanoparticles in saline solutions. Nat. Commun. 11, 5422. doi:10.1038/s41467-020-19164-3.

Gulino, M., Kim, D., Pané, S., Santos, S. D., and Pêgo, A. P. (2019). Tissue Response to Neural Implants: The Use of Model Systems Toward New Design Solutions of Implantable Microelectrodes. Front. Neurosci. 13, 689. doi:10.3389/fnins.2019.00689.

Gurunathan, S., Jeyaraj, M., Kang, M.-H., and Kim, J.-H. (2020). Anticancer Properties of Platinum Nanoparticles and Retinoic Acid: Combination Therapy for the Treatment of Human Neuroblastoma Cancer. Int. J. Mol. Sci. 21. doi:10.3390/ijms21186792.

He, S., Deng, H.-H., Liu, A., Li, G., Lin, X., Chen, W., et al. (2014). Synthesis and Peroxidase-Like Activity of Salt-Resistant Platinum Nanoparticles by Using Bovine Serum Albumin as the Scaffold. ChemCatChem 6. doi:10.1002/cctc.201400011.

Holopainen, I. E., Järvelä, J., Lopez-Picon, F. R., Pelliniemi, L. J., and Kukko-Lukjanov, T.-K. (2004). Mechanisms of kainate-induced region-specific neuronal death in immature organotypic hippocampal slice cultures. Neurochem. Int. 45, 1–10. doi: 10.1016/j.neuint.2004.01.005.

Huang, S.-H., Shmoel, N., Jankowski, M. M., Erez, H., Sharon, A., Abu-Salah, W., et al. (2020). Immunohistological and Ultrastructural Study of the Inflammatory Response to Perforated Polyimide Cortical Implants: Mechanisms Underlying Deterioration of Electrophysiological Recording Quality. Front. Neurosci. 14, 926. doi:10.3389/fnins.2020.00926.

Islam, M., and Islam, M. (2013). Electro-deposition Method for Platinum Nano-particles Synthesis. Eng. Int. 1. doi:10.18034/ei.v1i2.120.

Järvelä, J. T., Ruohonen, S., Kukko-Lukjanov, T. K., Plysjuk, A., Lopez-Picon, F. R., and Holopainen, I. E. (2011). Kainic acid-induced neurodegeneration and activation of inflammatory processes in organotypic hippocampal slice cultures: Treatment with cyclooxygenase-2 inhibitor does not prevent neuronal death. Neuropharmacology 60, 1116–1125. doi:10.1016/j.neuropharm.2010.09.024.

Jeyaraj, M., Gurunathan, S., Qasim, M., Kang, M.-H., and Kim, J.-H. (2019). A Comprehensive Review on the Synthesis, Characterization, and Biomedical Application of Platinum Nanoparticles. Nanomater. (Basel, Switzerland) 9, 1719. doi:10.3390/nano9121719.

Jung, N. Y., Lee, K. H., Won, R., and Lee, B. H. (2013a). Neuroprotective effects of α-tocotrienol on kainic acid-induced neurotoxicity in organotypic hippocampal slice cultures. Int. J. Mol. Sci. 14, 18256–18268. doi:10.3390/ijms140918256.

Jung, N. Y., Lee, K. H., Won, R., and Lee, B. H. (2013b). Neuroprotective effects of α-tocotrienol on kainic acid-induced neurotoxicity in organotypic hippocampal slice cultures. Int. J. Mol. Sci. 14, 18256–18268. doi:10.3390/ijms140918256.

Kim, H. G., Jeong, H. U., Hong, S. I., and Oh, M. S. (2015). Houttuyniae Herba Attenuates Kainic Acid-Induced Neurotoxicity via Calcium Response Modulation in the Mouse Hippocampus. Planta Med. 81, 1697–1704. doi:10.1055/s-0035-1557832.

Kovach, K. M., Kumsa, D. W., Srivastava, V., Hudak, E. M., Untereker, D. F., Kelley, S. C., et al. (2016). High-throughput in vitro assay to evaluate the cytotoxicity of liberated platinum compounds for stimulating neural electrodes. J. Neurosci. Methods 273, 1–9. doi:10.1016/j.jneumeth.2016.07.018.

Kozai, T., Vazquez, A., Weaver, C. L., Kim, S.-G., and Cui, X. (2012). In vivo two-photon microscopy reveals immediate microglial reaction to implantation of microelectrode through extension of processes. J. Neural Eng. 9 6, 66001. doi:10.1088/1741-2560/9/6/066001.

Kutwin, M., Sawosz, E., Jaworski, S., Hinzmann, M., Wierzbicki, M., Hotowy, A., et al. (2017a). Investigation of platinum nanoparticle properties against U87 glioblastoma multiforme. Arch. Med. Sci. 13, 1322–1334. doi:10.5114/aoms.2016.58925.

Kutwin, M., Sawosz, E., Jaworski, S., Wierzbicki, M., Strojny, B., Grodzik, M., et al. (2017b). Assessment of the proliferation status of glioblastoma cell and tumour tissue after nanoplatinum treatment. PLoS One 12, e0178277. doi:10.1371/journal.pone.0178277.

Labrador-Rached, C. J., Browning, R. T., Braydich-Stolle, L. K., and Comfort, K. K. (2018). Toxicological Implications of Platinum Nanoparticle Exposure: Stimulation of Intracellular Stress, Inflammatory Response, and Akt Signaling In Vitro. J. Toxicol. 2018, 1367801. doi:10.1155/2018/1367801.

Manikandan, M., Hasan, N., and Wu, H.-F. (2013). Platinum nanoparticles for the photothermal treatment of Neuro 2A cancer cells. Biomaterials 34, 5833–5842. doi: 10.1016/j.biomaterials.2013.03.077.

Moeini, B., Avval, T. G., Linford, M. R., Ghalkhani, M., Kaykhaii, M., and Abdullah Mirzaie, R. (2021). Surface-orientated platinum nanoparticles electrodeposited on a carbon substrate as a high performance electrocatalyst for glucose oxidation reaction in alkaline media. Mater. Sci. Eng. B 268, 115147. doi: 10.1016/j.mseb.2021.115147.

Mukherjee, S., Kotcherlakota, R., Haque, S., Bhattacharya, D., Kumar, J. M., Chakravarty, S., et al. (2020). Improved delivery of doxorubicin using rationally designed PEGylated platinum nanoparticles for the treatment of melanoma. Mater. Sci. Eng. C 108, 110375. doi: 10.1016/j.msec.2019.110375.

Neville, K. E., Bosse, T. L., Klekos, M., Mills, J. F., Weicksel, S. E., Waters, J. S., et al. (2018). A novel ex vivo method for measuring whole brain metabolism in model systems. J. Neurosci. Methods 296, 32–43. doi:10.1016/j.jneumeth.2017.12.020.

Opitz-Araya, X., and Barria, A. (2011). Organotypic hippocampal slice cultures. J. Vis. Exp., 2462. doi:10.3791/2462.

Park, E. Y., Woo, Y., Kim, S. J., Kim, D. H., Lee, E. K., De, U., et al. (2016). Anticancer effects of a new SIRT inhibitor, MHY2256, against human breast cancer MCF-7 cells via regulation of MDM2-p53 binding. Int. J. Biol. Sci. 12, 1555–1567. doi:10.7150/ijbs.13833.

Prasek, M., Sawosz, E., Jaworski, S., Grodzik, M., Ostaszewska, T., Kamaszewski, M., et al. (2013). Influence of nanoparticles of platinum on chicken embryo development and brain morphology. Nanoscale Res. Lett. 8, 251. doi:10.1186/1556-276X-8-251.

Routbort, M. J., Bausch, S. B., and McNamara, J. O. (1999). Seizures, cell death, and mossy fiber sprouting in kainic acid-treated organotypic hippocampal cultures. Neuroscience 94, 755–765. doi: 10.1016/S0306-4522(99)00358-9.

Sabilallah, M., Fontanaud, P., Linck, N., Boussadia, B., Peyroutou, R., Lasgouzes, T., et al. (2016). Evidence for Status Epilepticus and Pro-Inflammatory Changes after Intranasal Kainic Acid Administration in Mice. PLoS One 11, e0150793. doi: 10.1371/journal.pone.0150793.

Şahin, B., Aygün, A., Gündüz, H., Şahin, K., Demir, E., Akocak, S., et al. (2018). Cytotoxic effects of platinum nanoparticles obtained from pomegranate extract by the green synthesis method on the MCF-7 cell line. Colloids Surf. B. Biointerfaces 163, 119—124. doi:10.1016/j.colsurfb.2017.12.042.

Salois, G., and Smith, J. S. (2016). Housing Complexity Alters GFAP-Immunoreactive Astrocyte Morphology in the Rat Dentate Gyrus. Neural Plast. 2016, 3928726. doi:10.1155/2016/3928726.

Samadi, A., Klingberg, H., Jauffred, L., Kjær, A., Bendix, P. M., and Oddershede, L. B. (2018). Platinum nanoparticles: a non-toxic, effective and thermally stable alternative plasmonic material for cancer therapy and bioengineering. Nanoscale 10, 9097–9107. doi:10.1039/C8NR02275E.

Seidl, A. H., and Rubel, E. W. (2010). A simple method for multiday imaging of slice cultures. Microsc. Res. Tech. 73, 37–44. doi:10.1002/jemt.20750.

Shepherd, R. K., Carter, P. M., Dalrymple, A. N., Enke, Y. L., Wise, A. K., Nguyen, T., et al. (2021). Platinum dissolution and tissue response following long-term electrical stimulation at high charge densities. J. Neural Eng. 18, 36021. doi:10.1088/1741-2552/abe5ba.

Shim, K., Kim, J., Heo, Y.-U., Jiang, B., Li, C., Shahabuddin, M., et al. (2017). Synthesis and Cytotoxicity of Dendritic Platinum Nanoparticles with HEK-293 Cells. Chem. Asian J. 12, 21–26. doi:10.1002/asia.201601239.

Stoppini, L., Buchs, P. A., and Muller, D. (1991). A simple method for organotypic cultures of nervous tissue. J. Neurosci. Methods 37, 173–182. doi:10.1016/0165-0270(91)90128-m.

Vargas, J. R., Takahashi, D. K., Thomson, K. E., and Wilcox, K. S. (2013). The expression of kainate receptor subunits in hippocampal astrocytes after experimentally induced status epilepticus. J. Neuropathol. Exp. Neurol. 72, 919–932. doi:10.1097/NEN.0b013e3182a4b266.

Vinet, J., van Weering, H. R. J., Heinrich, A., Kälin, R. E., Wegner, A., Brouwer, N., et al. (2012). Neuroprotective function for ramified microglia in hippocampal excitotoxicity. J. Neuroinflammation 9, 27. doi:10.1186/1742-2094-9-27.

Wang, D., Zhou, Z., Zhang, B., and Zhu, J. (2021). Regulatory effect of kainic acid on microglia in different inflammatory states. Res. Sq. doi:10.21203/rs.3.rs-417620/v1.

Wellman, S. M., Li, L., Yaxiaer, Y., McNamara, I., and Kozai, T. D. Y. (2019). Revealing Spatial and Temporal Patterns of Cell Death, Glial Proliferation, and Blood-Brain Barrier Dysfunction Around Implanted Intracortical Neural Interfaces. Front. Neurosci. 13, 493. doi:10.3389/fnins.2019.00493.

Wissel, K., Brandes, G., Pütz, N., Angrisani, G. L., Thieleke, J., Lenarz, T., et al. (2018). Platinum corrosion products from electrode contacts of human cochlear implants induce cell death in cell culture models. PLoS One 13, e0196649. doi: 10.1371/journal.pone.0196649.

Wu, Z., Deshpande, T., Henning, L., Bedner, P., Seifert, G., and Steinhäuser, C. (2021). Cell death of hippocampal CA1 astrocytes during early epileptogenesis. Epilepsia 62, 1569–1583. doi: 10.1111/epi.16910.

Yang, Q., Vazquez, A. L., and Cui, X. T. (2021). Long-term in vivo two-photon imaging of the neuroinflammatory response to intracortical implants and micro-vessel disruptions in awake mice. Biomaterials 276, 121060. doi: 10.1016/j.biomaterials.2021.121060.

Yoon, J. J., Suri, V., Nicholson, L. F. B., and Green, C. (2011). Improved Immunohistochemical Protocol for Organotypic Brain Slice Cultures. Microsc. Anal. 25, 5–7.

Yu, L. M. Y., Polygalov, D., Wintzer, M. E., Chiang, M.-C., and McHugh, T. J. (2016). CA3 Synaptic Silencing Attenuates Kainic Acid-Induced Seizures and Hippocampal Network Oscillations. eNeuro 3, ENEURO.0003-16.2016. doi:10.1523/ENEURO.0003-16.2016.

Yu, T., Yu, H., Zhang, B., Wang, D., Li, B., Zhu, J., et al. (2019). Promising Neuroprotective Function for M2 Microglia in Kainic Acid-Induced Neurotoxicity Via the Down-Regulation of NF-κB and Caspase 3 Signaling Pathways. Neuroscience 406, 86–96. doi:10.1016/j.neuroscience.2019.03.002.

Zeng, X., Sun, J., Li, S., Shi, J., Gao, H., Sun Leong, W., et al. (2020). Blood-triggered generation of platinum nanoparticle functions as an anti-cancer agent. Nat. Commun. 11, 567. doi:10.1038/s41467-019-14131-z

Chapter 4

NOVEL MULTIFERROIC CORE-SHELL NANOPARTICLES DISPLAYING MAGNETOELECTRIC FEATURES FOR BRAIN STIMULATION: BIOCOMPATIBILITY AND ORGANOTYPIC CULTURES APPLICATION

M. Gulino[1, 2, 3], D. Kim[4], T. Qiao[4], X. Chen[4], S. D. Santos[1, 2], S. Pané[4], A. P. Pêgo[1, 2, 3, 5]

[1]i3S - Instituto de Investigação e Inovação em Saúde, Universidade do Porto, Porto, Portugal

[2]INEB - Instituto de Engenharia Biomédica, Universidade do Porto, Porto, Portugal

[3]FEUP - Faculdade de Engenharia, Universidade do Porto, Porto, Portugal

[4]Multi-scale Robotics Lab (MSRL), Institute of Robotics and Intelligent Systems (IRIS), ETH Zurich, Zurich, Switzerland

[5]ICBAS - Instituto de Ciências Biomédicas Abel Salazar, Universidade do Porto, Porto, Portugal

Research article under preparation for submission

ABSTRACT

In the present work, novel multiferroic cobalt ferrite-based nanoparticles (CFO NPs) coated with calcium/zirconium-doped barium titanate (CFO-BCZT) with excellent magnetoelectric coupling properties and biocompatibility for neural applications are presented. The synthesis of the core-shell structure was carried out through hydrothermal and sol-gel processes. Uncoated CFO NPs and CFO NPs coated with bismuth ferrite (CFO-BFO), as the most widely studied multiferroic coating material, were used for comparison with the corresponding coated sample.

X-ray diffraction studies revealed cubic space group of CFO core and tetragonal BCZT shell without any secondary phase, nor impurities. Excellent magnetoelectric coupling effect of CFO-BCZT NPs was revealed through piezoresponse force microscopy.

Cellular responses to CFO-BCZT NPs were evaluated through cytotoxicity assays, microscopy analysis and cellular uptake on in vitro primary cultures of neurons, astrocytes and microglia. Additionally, ex vivo rodent organotypic hippocampal cultures were employed to investigate the long-term response of the tissue and the impact of NP motion upon the application of a magnetic field. Finally, the ability of CFO-BCZT NPs to induce neural stimulation and differentiation was assessed in vitro on SH-SY5Y neuronal cell lines under magnetic stimulation.

The results herein presented showed excellent biocompatibility of CFO-BCZT NPs both in vitro and ex vivo. The motion of CFO-BCZT NPs through magnetic attraction was successfully achieved on organotypic hippocampal cultures using a magnetic plate for 30 minutes, without causing neither cell damage nor disruption of neural connections.

With the tested stimulation parameters, a trend toward neural differentiation induced by CFO-BCZT NPs under magnetic stimulation was observed in SH-SY5Y cells.

The results herein presented show the excellent biocompatibility of CFO-BCZT NPs both in vitro and ex vivo. Conversely, CFO-BFO NPs caused a decrease in viability of primary microglia in vitro at the highest concentration tested after 24 h of contact, as well as an increase in IBA-1 fluorescence intensity after 14 days of contact and morphological alterations of microglia towards an ameboid shape, as an indication of cell activation towards an inflammatory state.

In conclusion, these data indicate that CFO-BCZT NPs not only exhibit a magnetoelectric coupling effect, but they are also more biocompatible compared to CFO-BFO and uncoated CFO NPs. This sets the exploration of CFO-BCZT NPs as promising composite materials for neural applications.

1. INTRODUCTION

Transcranial magnetic stimulation (TMS) represents an effective minimally invasive approach for the treatment of several neurological dysfunctions (Attal et al., 2021; Fitzgerald, 2021). Even though already translated to the clinics and considered safe for long-term applications, this technology presents some limitations such as the impossibility to stimulate deep brain areas (Deng et al., 2014).
Magnetoelectric nanoparticles (MENPs) are an emerging class of materials with distinctive physicochemical properties that allow them to be employed in a vast number of biomedical applications, including in the context of the central nervous system (Kopyl et al., 2021). MENPs are core-shell structures composed of a traditionally ferromagnetic core and a piezoelectric shell, whose combination leads to the magnetoelectric coupling effect, enabling their manipulation and navigation through the body, even at deeper levels, using external magnetic field gradients (Chen et al., 2019). Among the multitude of applications of MENPs, relevant studies have been focusing on their use as drug nanocarriers for cancer therapy (Stewart et al., 2018; Shahzad et al., 2021), for targeted delivery of drugs across the blood-brain barrier (BBB) and controlled release in the brain parenchyma. Recent in vivo studies showed successful non-invasive delivery of MENPs in the brain in rodent and non-human primate models (Kaushik et al., 2019; Pardo et al., 2021). Nevertheless, one of the most promising applications of MENPs is in the context of deep brain stimulation (DBS), thanks to the possibility to generate localized electric fields by external magnetic stimuli. MENPs can represent the new generation of neurostimulators for DBS with several advantages over traditional implantable microelectrodes and TMS such as the modulation of deep brain areas while providing minimal invasiveness and target specificity. In vivo studies on rodent animal models reported remote electrical polarization of MENPs with external magnetic fields and subsequent local modulation of neural activity in deep brain targets (Jahanshahi et al., 2021; Nguyen et al., 2021).
Unfortunately, nowadays, the use of MENPs is only limited to the preclinical level. To speed their translation from bench to bedside, it is paramount to establish their safety and reliability for clinical use. But studies conducted to determine the response of neuronal and glial cells when in contact with the proposed MENPs, as well as the impact of their motion through the brain tissue is scarce or inexistent. Moreover, very limited knowledge is available regarding the potential long-term toxicity of the most widely employed materials for MENPs design, and rigorous diagnostic assessments are necessary before their broad employment in the clinic.

With this purpose, the use of functional and biocompatible coatings, or the use of coatings with improved properties at the physical and biological level for MENPs design is essential to meet the biomedical requirements for successful biomaterials.

CFO represents a potential core material for MENPs thanks to its physical characteristics such as chemical and thermal stability, good saturation magnetization and magnetostriction (Amiri and Shokrollahi, 2013; Srinivasan et al., 2018). BFO is one of the most widely studied multiferroic materials thanks to its attractive electrical, magnetic and piezoelectric properties. Thanks to its large piezoelectric coefficient, BFO has been also employed as coating for magnetostrictive CFO for the production of MENPs and nanomaterials for tissue electrical stimulation (Mushtaq et al., 2019b; Dong et al., 2020). However, pre-clinical and clinical studies in the literature have reported toxicity of BFO and bismuth compounds (Song et al., 2014; Gao et al., 2015; Staedler et al., 2015; Sampognaro et al., 2017; Borbinha et al., 2019).

Likewise, BCZT represents a potential candidate coating for CFO NPs thanks to its enhanced piezoelectric properties (Kumar et al., 2016; Praveen et al., 2018). However, BCZT had already shown to be an attractive biocompatible and stable material for biomedical implants and devices (Scarisoreanu et al., 2017; Poon et al., 2020).

Here, novel functional multiferroic core-shell NPs of cobalt ferrite (CFO) coated with calcium, zirconium-doped barium titanate (CFO-BCZT) are presented. The proposed BCZT coating is compared with BFO as shell for CFO core towards the design of MENPs with ideal magnetoelectric coupling effect and biocompatibility for neural applications. The synthesis of CFO-BCZT and CFO-BFO NPs by means of hydrothermal and sol-gel processes, their characterization in terms of structure and magnetoelectric performance, are described.

Besides performing the traditional short-term in vitro primary cell cultures, we have also assessed long-term biocompatibility, which was evaluated on more complex and relevant systems - the rodent organotypic hippocampal cultures (Gulino et al., 2019, 2021b).

In the literature, studies conducted to evaluate MENPs motion have been limited on assessing their crossing through the BBB and presence in the central nervous system and other organs. One study has been conducted to assess the impact of MENPs motion on brain tissue (Ramaswamy et al., 2015). To the best of our knowledge, we here employ for the first time, organotypic hippocampal cultures to explore the impact of MENPs motion in terms of tissue viability and neuronal network integrity, 24 h after external magnetic field application.

Finally, the potential of CFO-BCZT NPs on inducing neural differentiation under magnetic stimulation is investigated in vitro on human neuronal cells.

2. MATERIALS AND METHODS

Unless mentioned otherwise all reagents were acquired from Sigma Aldrich with chemical grade.

2.1 SYNTHESIS OF CFO CORE NPS

Single crystalline CFO core NPs were synthesized using co-precipitation and hydrothermal methods, as previously described (Mushtaq et al., 2019a; Kim et al., 2022). 2 g of acetyltrimethylammonium bromide was dissolved in 30 mL of deionized (DI) water and then 1 g of iron(III) chloride hexahydrate and 0.24 g of cobalt(II) chloride anhydrous powders were dissolved. Subsequently, 6 M of an aqueous sodium hydroxide solution was mixed with the previous solution (co-precipitation). Synthesized CFO NPs were collected and washed with DI water, acetone, and ethanol.

2.2 SYNTHESIS OF CFO-BFO CORE-SHELL NPS

BFO shell was synthesized by sol-gel process as previously described (Mushtaq et al., 2019a; Kim et al., 2022). 0.243 g of iron(III) nitrate nonahydrate and 0.322 g of bismuth(III) nitrate pentahydrate were dissolved in 60 mL of ethylene glycol solution and mixed with 0.1 g of CFO NPs. The solvent was evaporated overnight at 80 ℃ and the dried powder annealed at 600 ℃ for 2 h

2.3 SYNTHESIS OF CFO-BCZT CORE-SHELL NPS

BCZT shell was synthesized by a sol-gel process. Firstly, 2.45 mL of titanium(IV) butoxide (97 wt. %, and 0.37 mL of zirconium(IV) butoxide solution (80 wt.) were added dropwise to a solution of 10 mL 2-methoxyethanol and 1 mL acetylacetone (solution A). 1.736 g of barium acetate and 0.211 g of calcium acetate were dissolved in 5 mL of glacial acetic acid at 60 °C and mixed with solution A after natural cooling to room temperature (solution B). 75 mg of CFO NPs dispersed in 0.33 mL of DI water was then added into 3.3 mL of solution B. After stirring for 1 h, solvent evaporated overnight at 80 °C and then the resulting particles annealed at 900 °C for 2 h.

2.4 CHARACTERIZATION OF MENPS

The crystallinity of CFO-BCZT and CFO-BFO NPs was analyzed with an X-ray diffractometer (Bruker AXS D8 Advance). Transmission electron microscopy (TEM), high-angle annular dark-field scanning transmission electron microscopy (HAADF-STEM), and energy dispersive X-ray spectroscopy (EDX) were performed with FEI Talos F200X. To analyze piezoelectric and magnetoelectric properties of core-shell NPs, piezoresponse force microscopy (NT-MDT) equipped with an in-plane DC magnetic field setup was employed. The local piezoelectric hysteresis loop was measured by applying DC voltage superimposed with small AC voltage between the Au-coated conductive tip and the Au-coated substrate. The local hysteresis loops were measured and averaged over 5 times.

2.5 ANIMALS

All the procedures using animals were pre-approved by the i3S Ethics Committee (CEA, i3S). All the experiments were performed according to institutional ethical guidelines (i3S), the National law (DL 113/2013) and European Union guidelines (EU Directive 2010/63/EU for animal experiments) with maximal care to minimize animal suffering, as well as the number of animals used. Only authorized and experienced researchers performed animal experimentation. The rats or mice were kept in an enriched housing environment with ad libitum feed and water supply. They were kept under a 12h light/12h dark cycle at the i3S animal facility, with controlled ambient temperature and humidity.

Wistar Han rat pups, males and females, 0-2 days old were used to obtain primary microglia and astrocytes isolated from brains. Wistar Han rat pups, males and females, 6–8 days old were used to prepare the hippocampal slice cultures. C57BL/6 mice embryos (E16.5) were used to obtain primary mouse neuronal cortical cell cultures (NCCC).

2.6 PRIMARY MICROGLIA AND ASTROCYTE CULTURES

Primary cultures of microglia and astrocytes were obtained from P0-P2 rat pups, as previously described, with some modifications (Lian et al., 2016). Briefly, cortices were isolated and digested in Hank's Balanced Salt Solution (HBSS, Gibco, Life Technologies) without Ca^{2+}, Mg^{2+} and supplemented with trypsin (0.0025% (w/v), Gibco, Life Technologies) and 0.001 mg/mL DNAse I (Applichem LifeSciences) for 15 minutes at 37ºC. Dissociated cortices were cultured in 10 µg/mL

poly(L-lysine) (PLL) coated 75 cm^2 flasks (BioLite) and maintained in Dulbecco's Modified Eagle Medium (DMEM, Gibco, Life Technologies) supplemented with 10% (v/v) heat-inactivated (30 min, 56ºC) fetal bovine serum (FBS, Gibco, Life Technologies) and 1% (v/v) penicillin-streptomycin (P/S, Biowest). When confluence was reached (~12 days) the flasks were shaken for 2 h (200 rpm, 37ºC, 5% CO_2) on an orbital shaker to obtain the cells that detach - microglia. Subsequently, an additional overnight shake (220 rpm, 37ºC, 5% CO_2) was carried out to remove other more loosely attached cells - microglia and oligodendrocyte progenitor cells. This process was repeated once a week for three weeks. The remaining cells were mainly astrocytes that were then further trypsinized (0.025% (w/v) trypsin-EDTA, Gibco, Life Technologies) at 37ºC for 5 min to increase cell purity.
Primary microglia were incubated in DMEM Nutrient Mixture F-12 (Gibco, Life Technologies) supplemented with 10% (v/v) heat inactivated FBS and 1% (v/v) PS antibiotics and plated in poly(D-lysine) (PDL) coated CellCarrier Ultra 96-well microplates (Perkin-Elmer) at a concentration of 30,000 viable cells (trypan blue assay) per well in 100 mL. Similarly, primary astrocytes (90% purity) were plated into uncoated 96-well microplates at a concentration of 9,600 viable cells per well in 100 mL of DMEM supplemented with 10% (v/v) heat inactivated FBS and 1% (v/v) PS. Both cell types were maintained at 37ºC with 95% O_2 and 5% CO_2 for 24h until further use.

2.7 CORTICAL NEURON CULTURES

Primary mouse neuronal cortical cell cultures (NCCC) were prepared from E16.5 C57BL/6 mice embryos. Briefly, cortices were digested with trypsin (1.5 mg/mL), washed with HBSS containing 10% (v/v) FBS and then washed only with HBSS to remove FBS. The tissue was then mechanically dissociated in Neurobasal medium (NBM; Gibco, Life Technologies) using a pipette, and cells were filtered and counted (95% purity). Cells were then plated in PDL coated 96-well microplates at a concentration of $15x10^4$ viable cells per well in a total volume of 300 µL of NBM supplemented with 2% (v/v) NeuroCult™ SM1 Neuronal Supplement (StemCell Technologies), L-glutamine (0.5 mM), L-glutamic acid monosodium salt hydrate (0.025 mM) and gentamycin (50 µg/mL, Gibco, Life Technologies) at 37°C with 5% CO_2, for 7 days until further use.

2.8 LIVE-DEAD ASSAY

Primary cortical neurons, microglia and astrocytes were incubated with the MENPs at a concentration of 10 and 100 µg/mL for 24h (**Fig.1A**). Subsequently, Calcein AM cell permeant (Molecular Probes) and Hoechst 33342 (Anaspec) were added in the medium in each well at a final concentration of 1

μM and 20 μM, respectively, for 20 min. Finally, cells were incubated with propidium iodide (PI) at a concentration of 1.5 μM for additional 5 min. As positive controls for all the cells, 0.01% (v/v) Triton X-100 was added in the medium to induce cell death, 10 min before incubation with the fluorescent dyes. Finally, cells were immediately imaged using an INCell Analyzer 2000 (GE Healthcare) for high-throughput analysis.

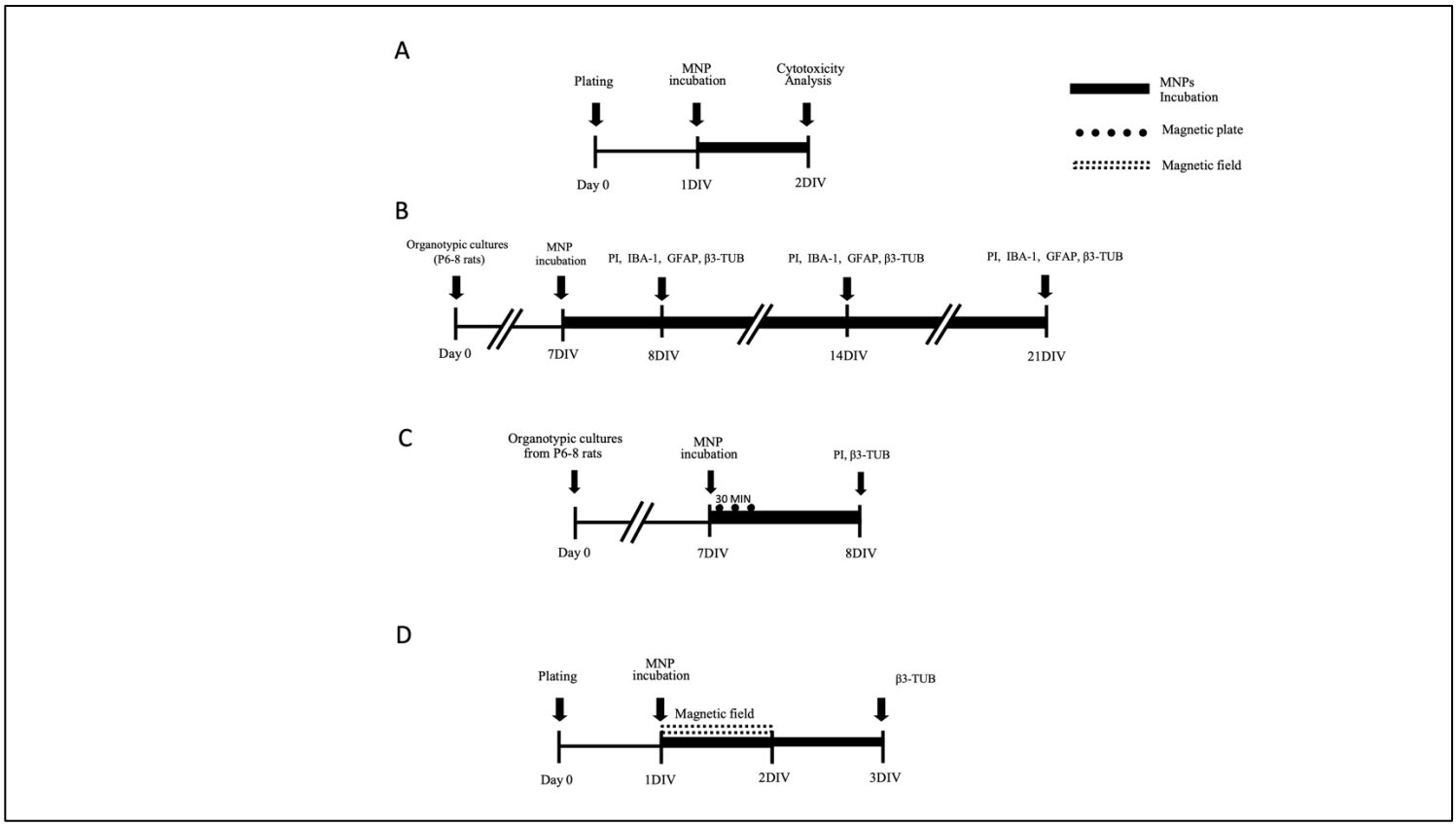


Figure 1. *Experimental set-up of the in vitro primary neural cell and ex vivo rat hippocampal organotypic cultures to study the safety and biocompatibility of MENPs. (A) Experimental scheme for investigating the biocompatibility of MENPs in in vitro primary neuronal and glial cells. (B) Experimental scheme for investigation of the biocompatibility of MENPs in the organotypic hippocampal slices. After 7 days in culture, slices were incubated with MENPs for additional 14 days. (C) Experimental scheme for studying the impact of MENP motion on rat hippocampal organotypic cultures. (D) Experimental scheme for assessing the induction of neural differentiation by MENPs after magnetic stimulation on SH-SY5Y cells.*

2.9 REACTIVE OXYGEN SPECIES (ROS) AND NITRITE OXIDE (NO) QUANTIFICATION

CellROX^{TM} Deep Red Reagent (Invitrogen) was employed for the detection of ROS production by primary microglia, according to manufacturer's instructions. Briefly, after 24h incubation with MENPs, CellROX Deep Red Reagent was added in the incubation medium at a final concentration of 5 μM for 30 min. Then, cells were immediately imaged using an INCell Analyzer 2000. Cells incubated for 3 h with 100 μM menadione diluted in the cell culture medium prior ROS quantification were used as positive control.

NO production by microglia was measured using the Griess Reagent detection method as previously described (Cho et al., 2016). After the incubation with MENPs for 24h, 100 mL of supernatant was transferred into a 96 well plate and mixed with equal volumes of Griess reagent for 1 h at room temperature (RT). Subsequently absorbance was measured with a BioTek Synergy Mx Monochromator-Based Multi-Mode Reader (Agilent) at a wavelength of 550 nm. Lipopolysaccharide (LPS) at a concentration of 200 ng/mL in PBS for 24 h in the incubation medium was used as positive control.

2.10 PRUSSIAN BLUE STAINING

To assess and quantify MENPs internalization in microglia, we employed the Prussian blue staining as previously described(Neubert J et al., 2015). Briefly, after incubation with MENPs at 10 μg/mL for 24 h, cells were washed twice with 0.1M phosphate-buffered saline (PBS) and fixed in 4% (w/v) paraformaldehyde (PFA) in PBS for 15 min. After PFA removal, cells were incubated with Perl's reagent composed with equal amounts (1:1, v/v) of 4% (w/v) potassium ferrocyanide in DI water and 12% (w/w) aqueous hydrochloric acid solution (HCl) for 30 min. Subsequently, cells were washed three times with DI water, counterstained with 0.1% (w/v) Nuclear Fast Red solution in DI water for 5 min, followed by three washes with DI water and immediately imaged.

2.11 ORGANOTYPIC HIPPOCAMPAL SLICE CULTURES

Rodent Organotypic hippocampal slice cultures were established with the interface method as previously described (Gulino et al., 2021). Briefly, 400 μm slices obtained from hippocampus of rat pups' brain, were placed into 0.4 μm Millicell® PTFE culture inserts (Merck-Millipore) in multi-6 well plates (Corning) and maintained at 37°C with 5% CO_2 and 95% atmospheric air for 7 days. 1

mL of incubation medium composed of Opti-MEM™ (Gibco, Life Technologies) based medium supplemented with 25% (v/v) heat inactivated horse serum (HS, Gibco, Life Technologies), 25% (v/v) HBSS, D-(+)-glucose 25 mM and 1% (v/v) PS was placed in each well. Medium was changed 24 h after the plating and then every 2 days.

MENPs administration was carried out at 7 days in vitro (DIV) using a Narishige Pneumatic Microinjector (Model IM-300) connected to a nitrogen cylinder as previously described (Gulino et al., 2021). Inserts with the brain slices were transferred into a petri dish with 3 mL of warm incubation medium. 400 ng of MENPs suspended in 1M HEPES buffer (Gibco, Life Technologies), at a concentration of 2 mg/mL were first sonicated for 1 minute in a sonication bath, then loaded into glass microcapillaries (WPI 1B200F-4, with Filament) and inserted in a three-dimensional manipulator. 12–15 drops were deposited on the cornu Ammonis (CA) 3, CA1, and dentate gyrus (DG) areas, without damaging the tissue. In control slice cultures, HEPES buffer was deposited in the same way. The procedure was carried out in sterile conditions inside a laminar flow hood equipped with a KL300 stereomicroscope (Leica). After MENPs administration, inserts were placed in the well plates with fresh pre-heated medium.

Subsets of slice cultures were analyzed at 8 DIV, 14 DIV and 21 DIV (**Fig.1B**).

2.12 MOTION EXPERIMENTS OF MENPS IN ORGANOTYPIC HIPPOCAMPAL SLICE CULTURES

The impact of CFO-BCZT NPs motion was assessed on organotypic hippocampal slice cultures. Briefly, 400 ng of CFO-BCZT were administered on a sub-set of cultures at 7 days after plating. Then, a magnetic plate for magnetofection (10000 Oe, OZ Biosciences) was placed at the bottom of the 6 well plate containing the insert and left in the incubator for 30 minutes to allow motion of the MENPs from the top of the slices inwards. Subsequently, the magnetic plate was removed, and slices were kept in the incubator for additional 24 h (**Fig.1C**). The impact of MENPs motion in the brain tissue was assessed by PI uptake and β3-tubulin immunofluorescence. Moreover, MENPs penetration and tissue integrity were also evaluated on slice cryosections by confocal and TEM imaging.

2.13 PROPIDIUM IODIDE ASSAY IN ORGANOTYPIC HIPPOCAMPAL SLICE CULTURES

PI uptake was performed to assess the impact of MENPs on organotypic hippocampal slice cultures as previously described (Gulino et al., 2021). The assay was performed at 8 DIV, 14 DIV and 21 DIV after MENPs administration (DIV7). PI was added to the culture medium for 1 h at a concentration

of 6 μM. Slices treated with 0.1% (v/v) Triton X-100 in PBS for 1 h prior to PI administration were used as positive controls. For visualization, each membrane insert was gently cut out and placed inside a 35 mm imaging μ-dish (ibidi).

2.14 IMMUNOFLUORESCENCE

In organotypic hippocampal slice cultures, at the end of the 3 above-described time points (**Fig.1B**), the medium was removed from each well and inserts were washed with pre-warmed PBS for 2 times, followed by fixation of the slices with 4% (w/v) PFA at room temperature (RT) for 1 h. Slices still attached to the membrane were individually cut out and incubated in permeabilization/blocking buffer composed of 1% (w/v) BSA, 5% (v/v) heat-inactivated FBS and 1% (v/v) Triton X-100 in PBS overnight at 4°C with gentle shaking. After PBS washing, slices were incubated with rabbit anti-ionized calcium binding adaptor molecule 1 (Iba-1, 1:800, Wako Chemicals), mouse anti-β3-tubulin (1:500, Promega) and rabbit anti-glial fibrillary acidic protein (GFAP, 1:500, Abcam) diluted in blocking buffer containing 1% (w/v) BSA, 5% (v/v) FBS, and 0.3% (v/v) Triton X-100 in PBS for 48 h at 4°C with gentle shaking. Slices were washed again with 0.05% (v/v) Triton X-100 in PBS at RT with gentle shaking. After primary antibody incubation, slices were incubated with Alexa Fluor 488 rabbit anti-goat IgG (H + L) secondary antibody (1:1000, Invitrogen) and Alexa Fluor 647 donkey anti-mouse IgG (H + L) secondary antibody (1:1000, Invitrogen) in blocking buffer for 3 h at RT with gentle shaking and then washed again with 0.05% Triton-100 in PBS at RT with gentle shaking.

Nuclei were stained with Hoechst 33342 solution (1 μg/mL, Thermo Fisher Scientific) in PBS for 30 min. Slices were placed on glass slides for mounting, as previously described using a bridge mounting technique to preserve integrity of the slices (Gulino et al., 2021). The samples were mounted with homemade Mowiol/glycerol (3:1), cover slipped and stored in the dark at 4°C, till further use.

To prepare cryosections, after PFA fixation slices were incubated at 4°C overnight in 30% (w/v) sucrose solution in PBS. Then, slices were immersed in optimal cutting temperature embedding matrix (OCT, Fisher Scientific), frozen in liquid nitrogen and immediately stored at -20°C till further use. 20 μM transversal Cryosections were obtained using a CM1900 1 1 cryostat (Leica) and placed on glass slides. Nuclei were counterstained with 1% fast nuclear red solution for 5 min and mounted using homemade Mowiol/glycerol mounting medium as described above.

2.15 TEM IMAGE ANALYSIS

For the ultrastructure analysis of the tissue and MENPs, organotypic hippocampal slice cultures were fixed in a solution of 2.5% (w/v) glutaraldehyde (Electron Microscopy sciences) with 2% (w/v) formaldehyde (Electron Microscopy sciences) in 0.1 M sodium cacodylate buffer at pH 7.4 for 1 h, at RT, and post fixed in 1% w/v osmium tetroxide (Electron Microscopy Sciences) diluted in 0.1 M sodium cacodylate buffer. Slices were resuspended in HistogelTM (Thermo, HG-4000-012) and then stained with aqueous 1% (w/v) uranyl acetated solution overnight, dehydrated and embedded in Embed-812 resin (Electron Microscopy sciences). Ultra-thin longitudinal hippocampal slice sections (50 nm thickness) were cut on an RMC Ultramicrotome (PowerTome, USA) using Diatome diamond knifes. Sections were then mounted on mesh copper grids (Electron Microscopy Sciences) and stained with uranyl acetate substitute (Electron Microscopy Sciences) and lead citrate (Electron Microscopy Sciences) for 5 min each.

2.16 NEURAL STIMULATION EXPERIMENTS USING MENPS ON IN VITRO SH-SY5Y CELLS

To investigate the potential of MENPs on inducing neural differentiation, we employed immortalized SH-SY5Y cells.

For this experiment, CFO core shell NPs with thicker BCZT coating (15±5 nm) were employed to provide efficient electric field generation upon magnetic stimulation.

SH-SY5Y neuroblastoma cells were obtained from The American Type Culture Collection (ATCC). Cells were cultured in t75 flasks with DMEM GlutaMAX™ Supplement (Gibco, Life Technologies) with 15% (v/v) FBS and 1% (v/v) PS. The cells were maintained in culture for up to 5 passages at 37 °C with 95% Oxygen and 5% CO_2 until experiments.

Cells were plated in CellCarrier Ultra 96 well microplates at a concentration of $1{,}2x10^4$ cells per well in 200 mL of high glucose GlutaMAX™ Supplement with 15% (v/v) FBS, 1% (v/v) PS and 10uM Retinoic acid. After 24h, cells were incubated with MENPs diluted in the medium at 10 μg/mL. The plate was inserted in a custom-built electrical setup generating the AC signal for magnetic stimulation (**Fig.2**) as previously described (Mushtaq et al., 2019c). The magnetic field strength employed was 17,7 mT (1.5Khz). Cells were stimulated for 24h at 37 °C with 95% Oxygen and 5% CO_2, followed by additional 24h without magnetic stimulation for additional 24h.

To assess the induction of neural differentiation by MENPs after magnetic stimulation (**Fig.1D**), cells were fixed as described above for in vitro cell cultures. Subsequently, cells were first permeabilized with 0.2% (v/v) Triton X-100 in PBS for 15 min at RT, followed by incubation with blocking buffer composed of 5% (w/v) BSA in PBS for 1 h at RT. After PBS washing, cells were incubated with mouse anti-β3-tubulin (1:500, Promega) diluted in blocking buffer containing 2% (w/v) BSA, in PBS for 24 h at 4°C with gentle shaking. After 2 washes in PBS at RT with gentle shaking, cells were incubated with Alexa Fluor 488 donkey anti-mouse IgG (H + L) secondary antibody (1:1000, Invitrogen) in blocking buffer for 1 h at RT with gentle shaking. After 2 washes in PBS at RT for 5 min, one drop of Fluoromount^{TM} mounting medium was added to each well.

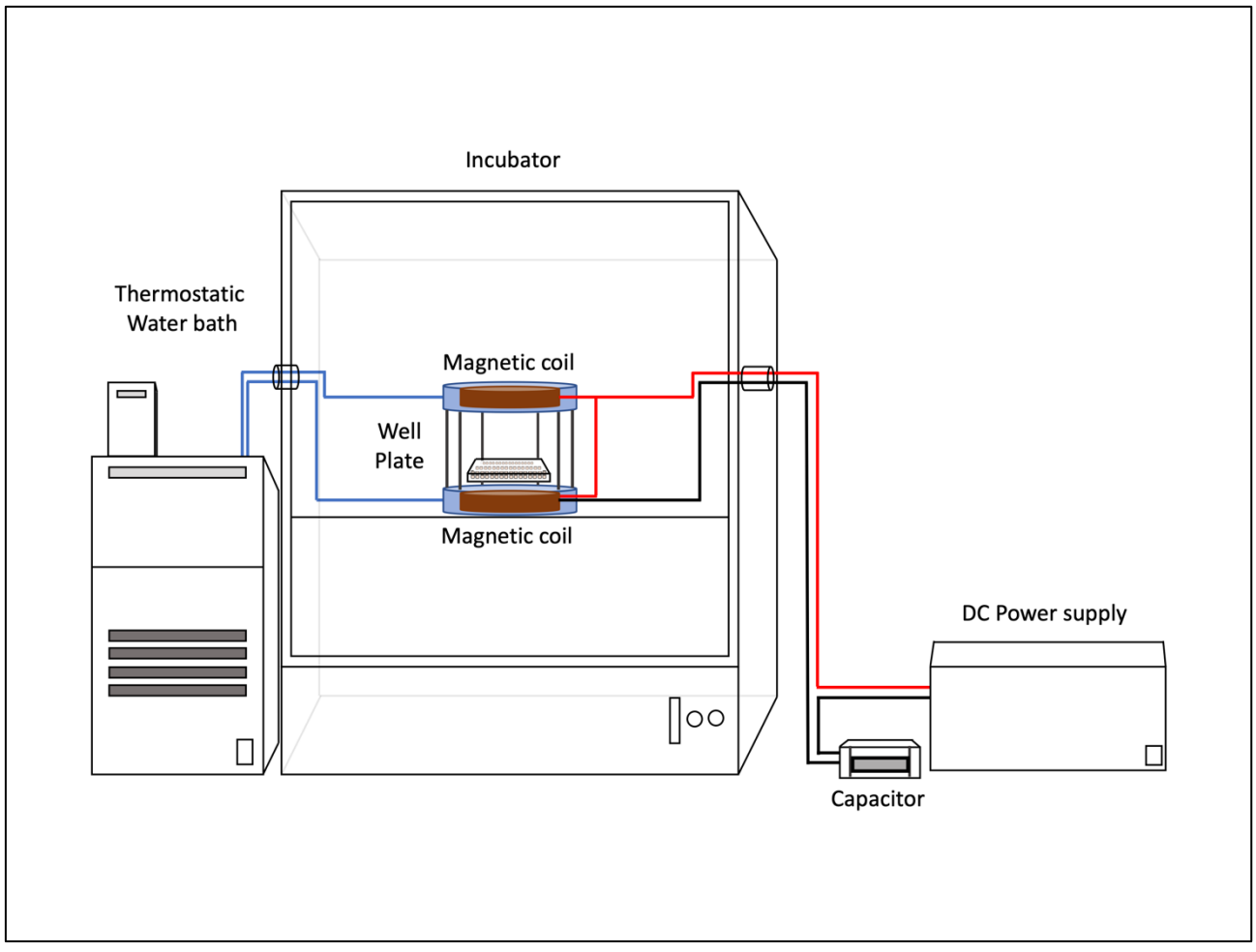


Figure 2.. *Custom built setup for Magnetic Stimulation. The power supply produces AC current at 4,5 A which flows through the magnetic coils, generating an AC magnetic field of 17,7 mT at 1,5 Khz. The thermostatic Water bath is employed to avoid overheating of the magnetic coils and keep the temperature of 37°C. The well plate containing cells incubated with MENPs is placed in the middle of the 2 coils for 24 h.*

2.17 IMAGE ANALYSIS AND QUANTIFICATION

High throughput live/dead analysis of microglia, astrocytes and neurons incubated with MENPs at 10 and 100 μg/mL for 24h was carried out with the INCell Analyzer 2000 platform (GE Healthcare) using a 20X objective. Quantification of dead cells, total cell number and area was performed using the INCELL developer toolbox software (version 1.9, GE Healthcare).

For the quantification of MENPs internalization by microglia, a Zeiss Axiovert 200M inverted fluorescence microscope with brightfield and 40X objective was used. Quantification of cell content of MENPs in every cell was performed using ilastik software (version 1.3.3) and Image J software (version 1.53; National Institutes of Health, United States).

For image acquisition of PI uptake and immunofluorescence intensity quantification of Iba-1, GFAP and β3-tubulin a Zeiss Axiovert 200M inverted fluorescence microscope equipped with a 488, 565 and 647 nm filters was used. Images were acquired using a 5x objective. Analysis and quantification of fluorescence intensity was performed on consistently selected regions of interest in CA3, CA1, and DG districts of each brain slice using Image J software.

Immunofluorescence image acquisition of Hoechst, Iba-1, GFAP and β3-tubulin in the organotypic hippocampal cultures was performed using a Leica Scanning Confocal SP8 equipped with 405, 488, and 633 filters (Leica Microsystems, Germany) composed of an inverted microscope Leica DMI8 (Leica Microsystems, Germany) and LAS X software (Leica Microsystems, Germany).

For the image acquisition of GFAP and β3-tubulin structures in the organotypic hippocampal cultures, images were acquired using a 63X objective, with confocal image stacks of 512x512 pixel, 16-bit depth, pixel size 0.63 μm, and zoom 0.75. Quantification was performed using the skeletonization tool on Image J Software.

For the reconstruction of microglial cell morphology, images were acquired using 63x objective, with confocal 16-bit depth image stacks of 1024 × 1024 pixels, with pixel size of 0.334 μm and zoom set at 0.75. Single cells with complete and defined processes were selected and imaged for analysis. Quantification of morphology was performed using skeletonization tool on ImageJ Software. The cell soma area, the number of processes as well as the number of end points and junctions were calculated per each cell.

For the quantification of MENPs motion and penetration into the brain tissue after the application of the magnetic field, images of tissue cryosections were acquired with a Zeiss Axiovert 200M inverted fluorescence microscope with 63X objective equipped with a digital camera. Quantification was

performed using Image J software by drawing a line from the detected MENPs into the tissue to the top side of the brain slice. To further confirm the differences between control groups, confocal images of Hoechst-stained brain slices with MENPs were acquired with a Leica Scanning Confocal SP8 equipped with 405 and brightfield filters.

For the ultrastructure analysis of brain tissue and MENPs, images were viewed on a JEOL JEM 1400 transmission electron microscope (JEOL, Tokyo, Japan) and images were digitally recorded using a CCD digital camera Orius 1100W (Tokyo, Japan).

For the high-throughput analysis of neural differentiation on SH SY5Y cells, images were acquired with the INCell Analyzer 2000 platform using a 20X objective and subsequently pre-processed using Ilastik software. Finally, the maximum neurite length, number of endpoints, the total number of cells per well and the area of the network per cell were calculated using image J software.

2.18 STATISTICS

Data from three independent experiments were presented as the mean ± standard error of the mean (SEM). Tukey's test after one-way analysis of variance (ANOVA) was used for statistical analysis. Analysis and visualization of data was carried out using GraphPad Prism 9 (GraphPad Software, San Diego, CA, United States).

3. RESULTS

3.1 CFO-BCZT NPS DISPLAY APPROPRIATE MAGNETOELECTRIC PROPERTIES

Magnetoelectric CFO-BCZT core-shell NPs are here proposed as novel multiferroic core-shell NPs. These were prepared using hydrothermal and sol-gel methods. CFO NPs coated with BFO (CFO-BFO NPs) as one of the most widely studied multiferroic coating materials (Hojo et al., 2018), were used for comparison with the corresponding coated sample.

Since CFO has a large magnetostriction coefficient (max. 600 ppm) (Bozorth et al., 1955; Venkata Siva et al., 2020), this material was chosen as the magnetostrictive core material and synthesized using co-precipitation and hydrothermal methods. Piezoelectric BCZT and BFO shell materials were then coated over the CFO core NPs by sol-gel processes. The crystalline structures of CFO-BFO and CFO-BCZT core-shell NPs were analyzed by X-ray diffraction (**Fig.3A, B**), which confirmed cubic Fd-3m space group of CFO core particles, hexagonal R3c BFO shell, and tetragonal P4mm BCZT

shell without any secondary phase nor impurities. HAADF-STEM and EDX images further prove core-shell structure of CFO-BFO **(Fig.3A, (a-e))** and CFO-BCZT **(Fig.3B, (a-h))** NPs with core particles containing Co, Fe and shells containing Bi, Fe for BFO and Ba, Zr, Ca, Ti for BCZT. The size of the CFO core NPs is 35 ± 8 nm, the thickness of BFO shell is around 2 ± 1 nm, thin and thick BCZT shells are around 2 ± 1 nm and 15 ± 5 nm, respectively, as determined by HAADF-STEM images.

Magnetoelectric properties of both core-shell NPs were characterized by local piezoelectric hysteresis loops measured by the PFM with or without magnetic fields (**Fig.4A, B**). Under a 500 Oe DC in-plane magnetic field, both CFO-BFO and CFO-BCZT NPs showed noticeable shifts in their coercive voltages. For CFO-BFO NPs, positive and negative coercive voltages shifted from 3.18 V to 2.33 V and -1.34 V to -1.91 V, respectively, and for CFO-BCZT NPs, positive and negative coercive voltages shifted from 1.21 V to 1.76 V and -3.04 V to -3.32 V, respectively, which indicates clear magnetoelectric coupling in both core-shell MENPs.

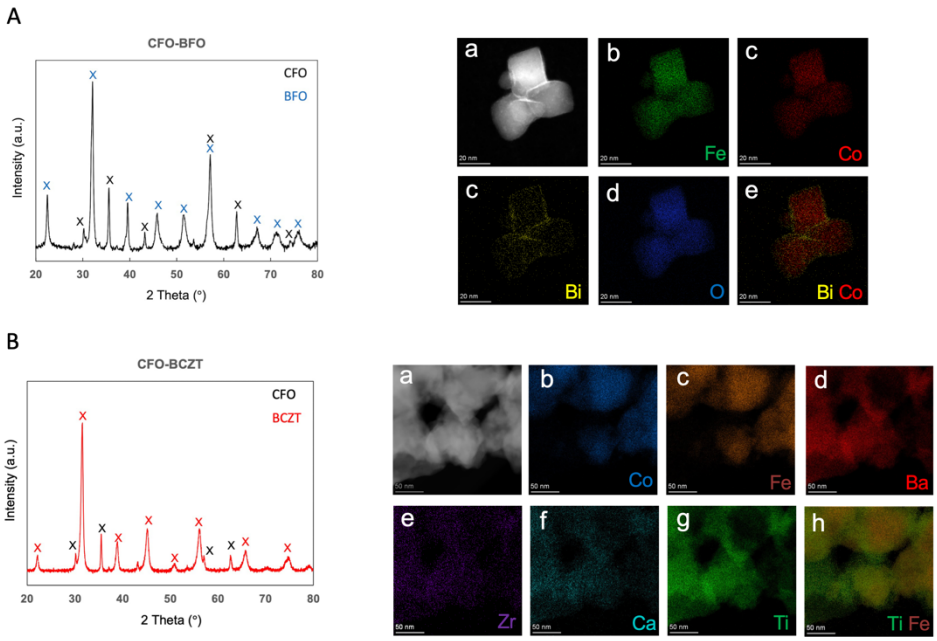


***Figure 3**. MENPs characterization. (A) X-ray diffractions of CFO-BFO core-shell NPs. Right images showing CF-BFO (a) HAADF-STEM and (b-e) EDX. (B) X-ray diffractions of CFO-BCZT core-shell NPs. Right images showing CFO-BCZT (a) HAADF-STEM and (b-h) EDX.*

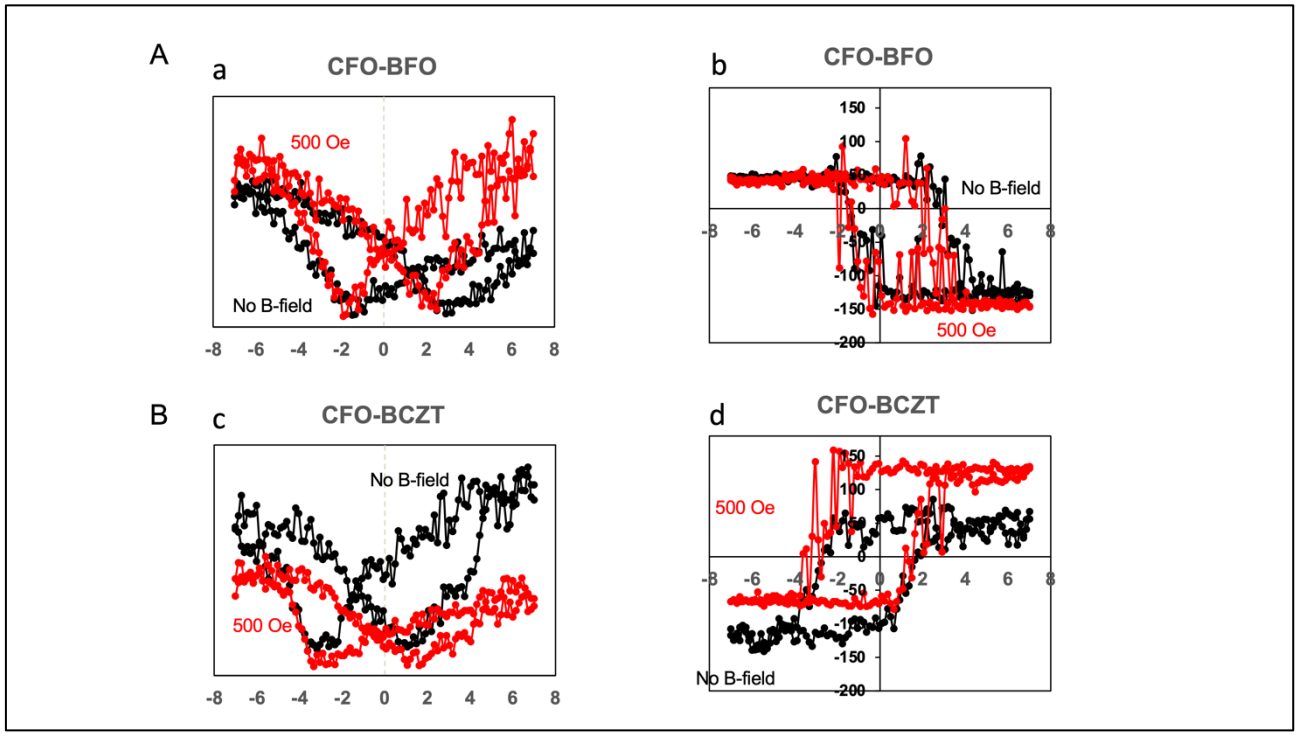


***Figure 4**. PFM local hysteresis loops of core-shell nanoparticles. (A) (a) Amplitude and (b) phase of CFO-BFO NPs. (B) (c) Amplitude and (d) phase of CFO-BCZT NPs.*

3.2 CFO-BCZT NPS DO NOT IMPACT NEURAL CELL VIABILITY EVEN AT HIGH CONCENTRATIONS

MENPs cytotoxicity was first evaluated by exploring different neural cell cultures – cortical neurons, astrocytes and microglia, with a high throughput live/dead assay using the INCELL analyzer. These cells were selected to mimic the main cell types the particles would encounter when administered in the brain. After incubation CFO-BCZT, uncoated CFO and CFO-BFO NPs at 10 and 100 µg/mL for 24h (**Fig.1A**), we observed that while neuronal and astrocytes' viabilities were not affected (**Fig.5**), primary microglia viability was significantly compromised by CFO-BFO NPs at 100 µg/mL (**Fig. 6A**). Moreover, we observed significant microglia cell shrinkage and decrease in cell adhesion (**Fig. 6B and C**) in cells incubated with uncoated CFO NPs at 100 µg/mL. Despite these findings, we did not observe any increase in ROS and NO production at the above-described conditions in all the NPs

tested (**Fig.7A and B**). Prussian blue staining revealed that CFO-BCZT and CFO-BFO NPs are less internalized by microglia when compared to CFO NPs (**Fig.7C**). These data suggest that the BFO and BCZT shells make the NPs less prone to microglia phagocytic activity. Nevertheless, as stated above, BFO shell showed to be more toxic at high concentrations compared to BCZT regardless of the internalization by microglia.

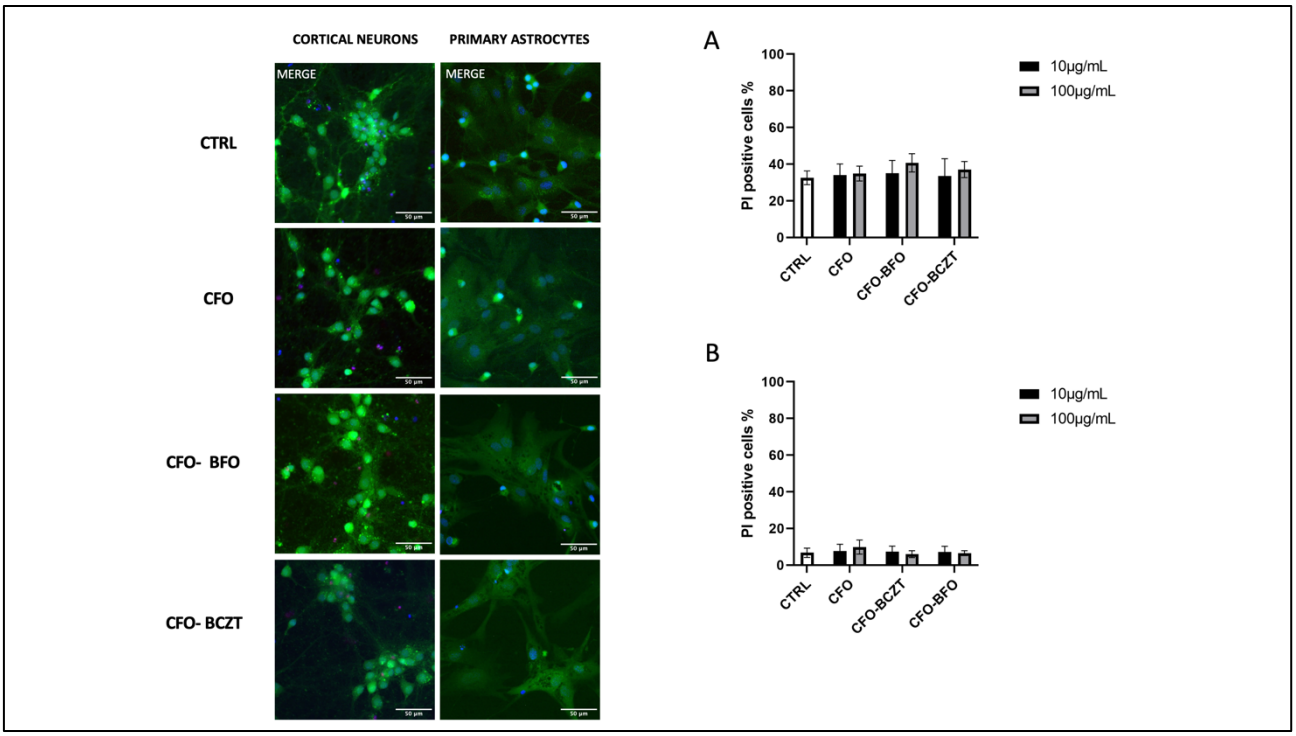


***Figure 5**. CFO, CFO-BCZT AND CFO-BFO NPs do not impact primary cortical neuron and astrocyte viability after 24 h of incubation at low and high concentrations. Representative propidium iodide (red), Calcein (green) Hoechst (blue) staining of cortical neurons and primary astrocytes under control conditions (CTRL; untreated cells), CFO NPs 100 µg/mL, CFO-BCZT NPs 100 µg/mL and CFO-BFO NPs 100 µg/mL. (A) Chart representing the quantification of PI-positive neuron percentage in control and treatment groups. (B) Chart representing the quantification of PI-positive astrocytes percentage in control and treatment groups.*

Data are expressed as the percentage of PI-positive cells on the total of cells and presented as mean ± standard error of the mean (SEM) (n = 3 independent experiments: 24 images per group/experiment). Tukey's test after one–way analysis of variance (ANOVA) was used for statistical analysis.

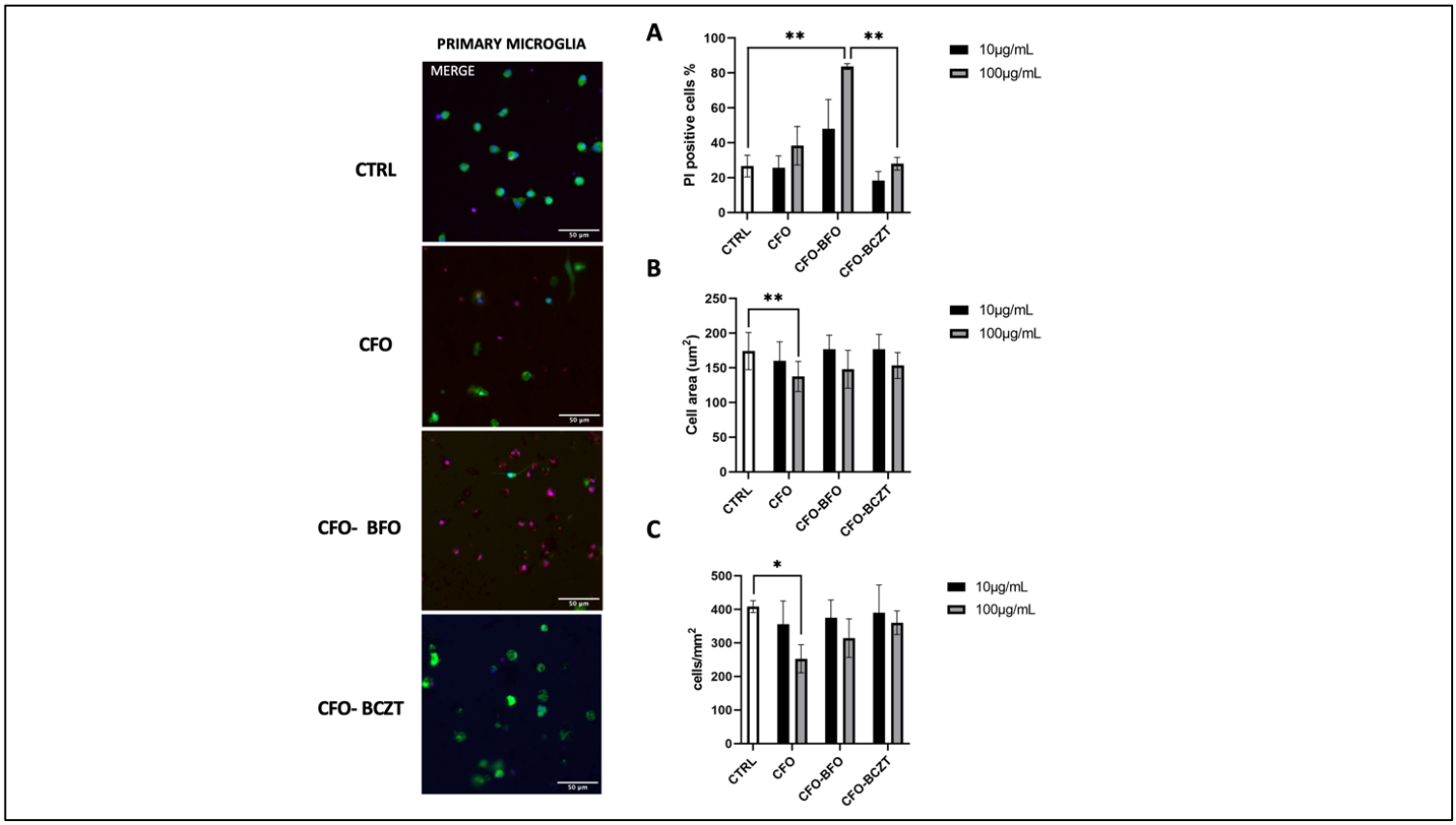


Figure 6. *CFO-BFO NPS impact microglial cells viability after 24 h of incubation at high concentrations (A) Representative propidium iodide (red), Calcein (green) Hoechst (blue) staining primary microglia under control conditions (CTRL; untreated cells), CFO NPs 100 µg/mL, CFO-BCZT NPs 100 µg/mL and CFO-BFO NPs 100 µg/mL. Right charts representing the quantification of PI-positive cells percentage (B), cell area (C) and cell detachment (D) in control and treatment groups. Data are expressed as the percentage PI-positive cells on the total of cells, cell area in um2 and cell density in mm2 and presented as mean ± standard error of the mean (SEM) (n = 3 independent experiments: 24 images per group/experiment). Tukey's test after one–way analysis of variance (ANOVA) was used for statistical analysis. *p < 0.05; **p < 0.01.*

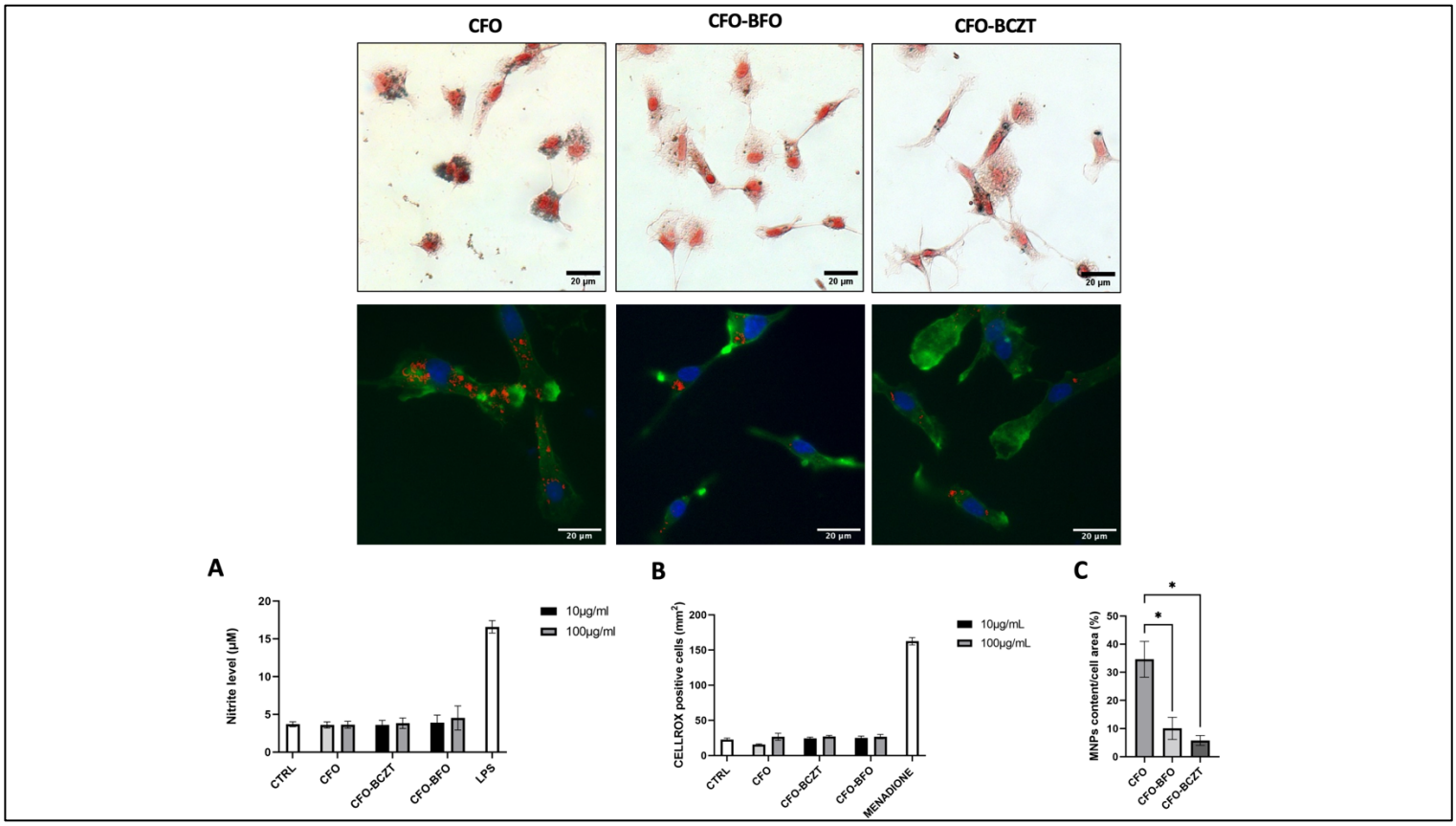


***Figure** 7. CFO-BCZT AND CFO-BFO NPs are less internalized than CFO NPs by microglia and do not cause any changes in ROS and NO levels after 24 h of incubation at low and high concentrations. Representative fast nuclear red/Prussian blue-stained microglial cells under control conditions (CTRL; untreated cells), CFO, CFO-BFO and CFO-BCZT NPs at 10 µg/mL. Bottom images showing phalloidin (green) and hoechst (blue) stained microglia merged with brightfield showing internalization of MENPs (red). Bottom charts showing (A) the quantification of nitrite levels, (B) ROS levels, and (C) MENPs content in control and treatment groups. Data are expressed as nitrite levels in uM, Cell ROX positive cells/mm2, % of intracellular NPs area divided by the total cell area and presented as mean ± standard error of the mean (SEM) (n = 3 independent experiments: 24 images per group/experiment). Tukey's test after one–way analysis of variance (ANOVA) was used for statistical analysis. *p < 0.05.*

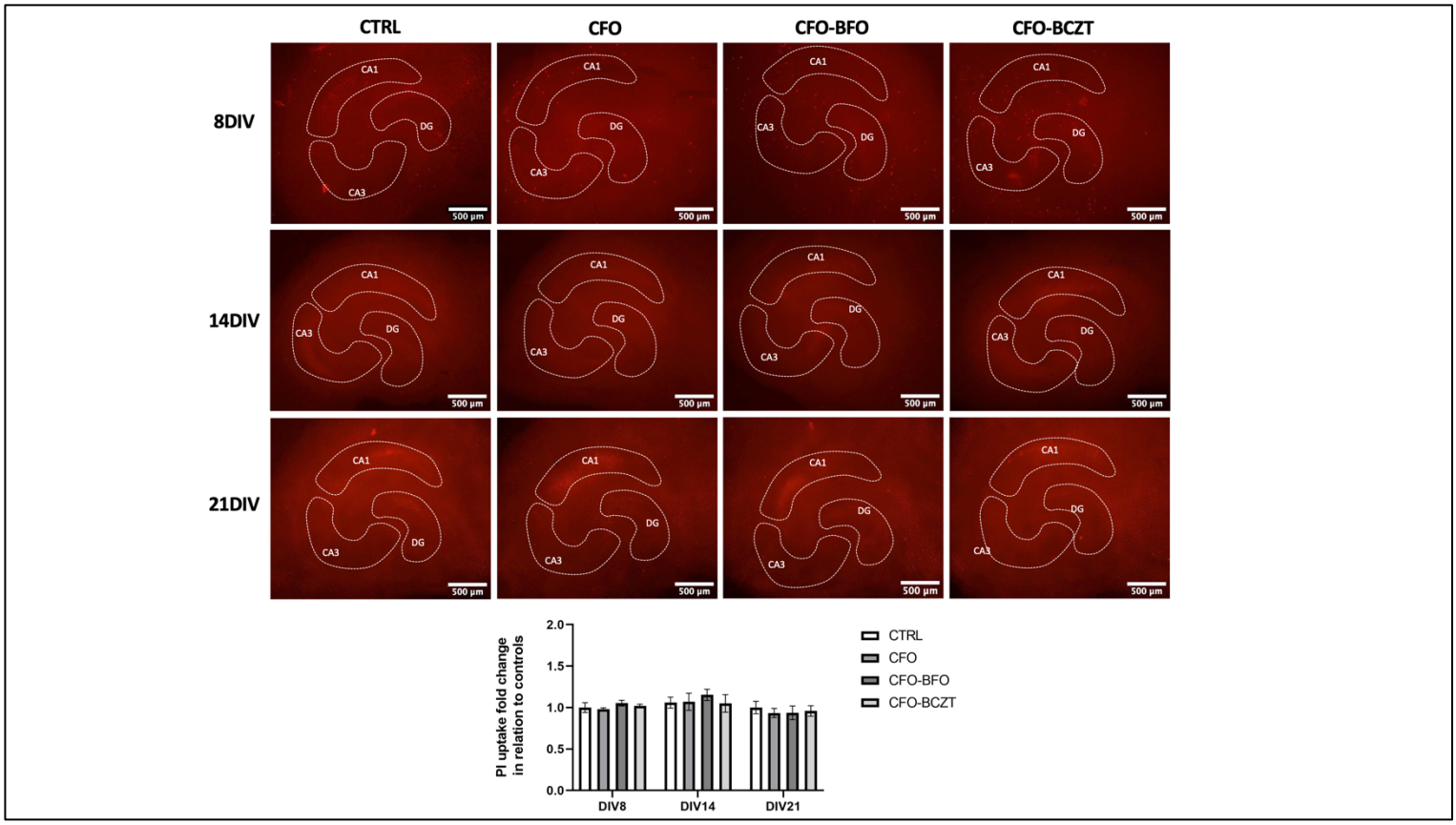
3.3 CFO-BCZT NPS DO NOT COMPROMISE CELL VIABILITY AND NEURONAL CELL INTEGRITY IN ORGANOTYPIC HIPPOCAMPAL SLICE CULTURES

We have tested the biocompatibility of the CFO-BCZT NPs in an in vitro model of higher complexity – the brain slices. Once again, CFO and CFO-BFO particles were tested for comparison. Cell viability upon incubation with MENPs was evaluated through PI uptake and neuronal cell integrity through β3-tubulin immunofluorescence and bioimaging, as previously described (Gulino et al., 2021). MENPs were applied at 7 DIV drop by drop on the top of each slice at the same concentration (400ng/slice) and incubated for additional 14 days **(Fig.1B)**. Image analysis and quantification of PI uptake was carried out in the whole slice at 8, 14 and 21 DIV (**Supplementary Fig.1**). At these time points, we did not observe significant differences in slices treated with the different MENPs when compared to control slices. In accordance with the in vitro tests conducted in primary cultures of cortical neurons, no significant differences were observed in β3-tubulin fluorescence intensity at all the three time points analyzed (**Supplementary Fig.2**). Additional structural analysis of β3-tubulin revealed non-significant neuronal alterations in slices treated with MENPs compared to untreated cultures (**Fig.8A**).

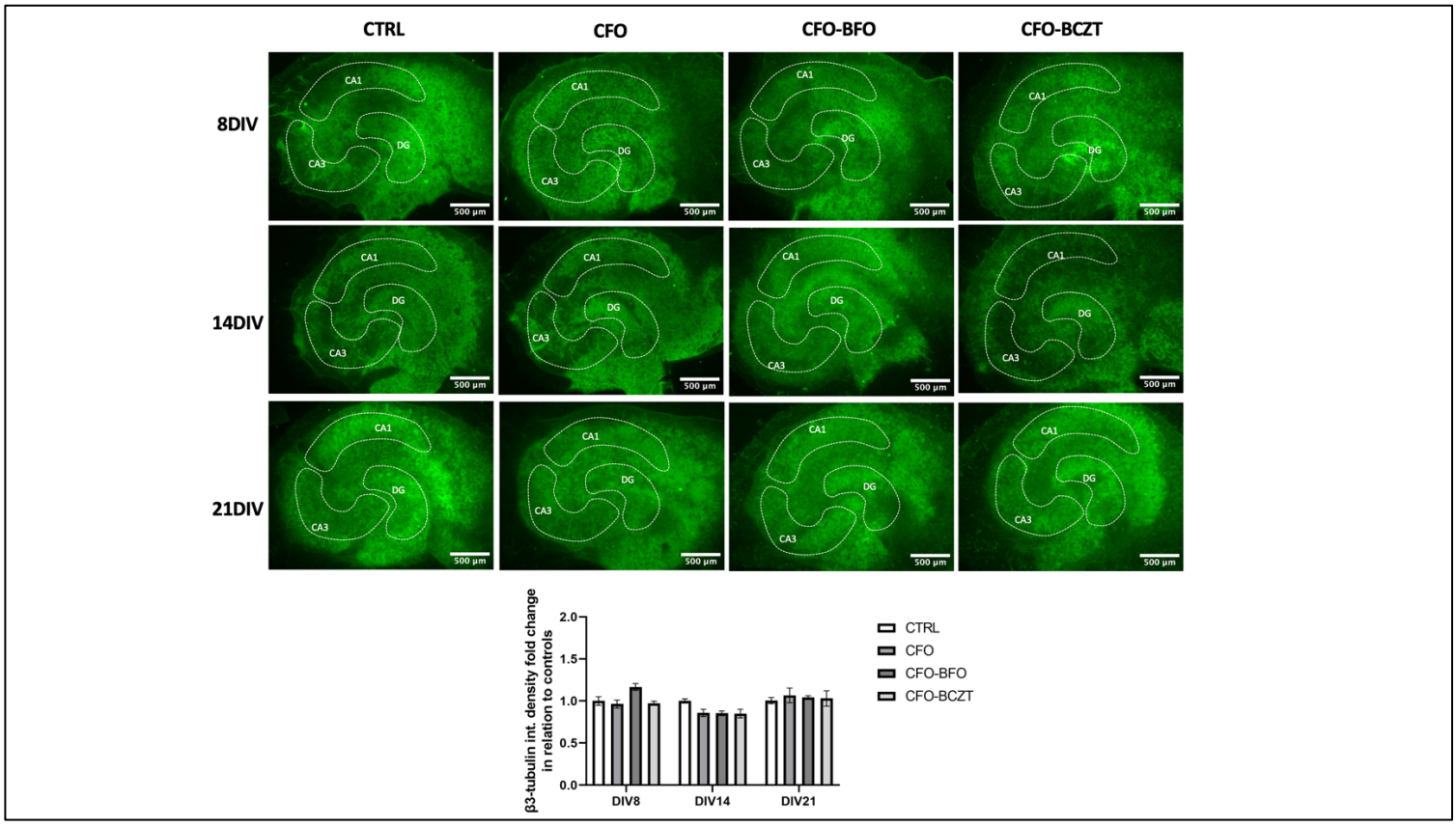
Immunofluorescence analysis on microglia and astrocytes was performed to investigate the response of glial cells on MENPs. When investigating astrocyte reactivity with GFAP immunofluorescence, we did not observe any significant increase in GFAP fluorescence intensities in all the time points and treatment groups (**Supplementary Fig.3**), as well as non-significant alterations in GFAP area (**Fig.8B**). In conformity with in vitro experiments, these data indicate that astrocyte integrity remained unaltered after 14 days of contact with the examined MENPs.

Subsequently, we performed Iba-1 fluorescence intensity measurements to investigate the impact of MENPs on microglia. Differently from what we observed for astrocytes, our results showed a significant increase (1.3-fold) in Iba-1 fluorescence intensity in slices treated with CFO-BFO NPs at 21 DIV, while non-significant effects were observed with uncoated CFO and CFO-BCZT NPs (**Supplementary Fig.4**). However, structural analysis of microglia morphology showed significant alterations also at 14 DIV in slices treated with CFO and CFO-BFO NPs. In particular, we observed significant decrease in the number of microglial branches in CFO-BFO treated slices at 14 and 21 DIV, as well as the number of endpoints, junctions and increase in cell body areas (**Fig.9**). In line with the in vitro cell culture experiments, we observed morphological alterations also in slices treated with uncoated CFO NPs, such as significant decrease in the number of endpoints already at 14 DIV as well as in the number of junctions at 21 DIV. Conversely, non-significant morphological

alterations were observed in all the time points in slices treated with CFO-BCZT NPs, implying that the BCZT coating displays better biocompatibility compared to uncoated CFO and CFO-BFO NPs.



Supplementary Figure 1*. CFO-BCZT NPs do not impact cell viability in organotypic hippocampal slices after 14 days of contact. Representative PI staining of organotypic hippocampal slices under control conditions (CTRL; untreated slices), CFO, CFO-BFO and CFO-BCZT NPs. Bottom chart represents the quantitative analysis of PI fluorescence intensity at 8DIV, 14 DIV and 21DIV. Data are expressed as PI fluorescence intensity fold change from the value of control slices and presented as means ± standard error of the mean (SEM) (n = 3 independent experiments; 4–6 slices analyzed per group/experiment). Tukey's test after one–way analysis of variance (ANOVA) was used for statistical analysis.*



Supplementary Figure 2. *CFO-BCZT NPs do not impact neuronal integrity and do not cause astrogliosis in organotypic hippocampal slices after 14 days of contact. Representative β3-tubulin staining of organotypic hippocampal slices under control conditions (CTRL; untreated slices), CFO, CFO-BFO and CFO-BCZT NPs. Bottom chart represents the quantitative analysis of β3-tubulin fluorescence intensity at 8DIV, 14 DIV and 21DIV. Data are expressed as β3-tubulin fluorescence intensity fold change from the value of control slices and presented as means ± standard error of the mean (SEM) (n = 3 independent experiments; 4–6 slices analyzed per group/experiment). Tukey's test after one–way analysis of variance (ANOVA) was used for statistical analysis.*

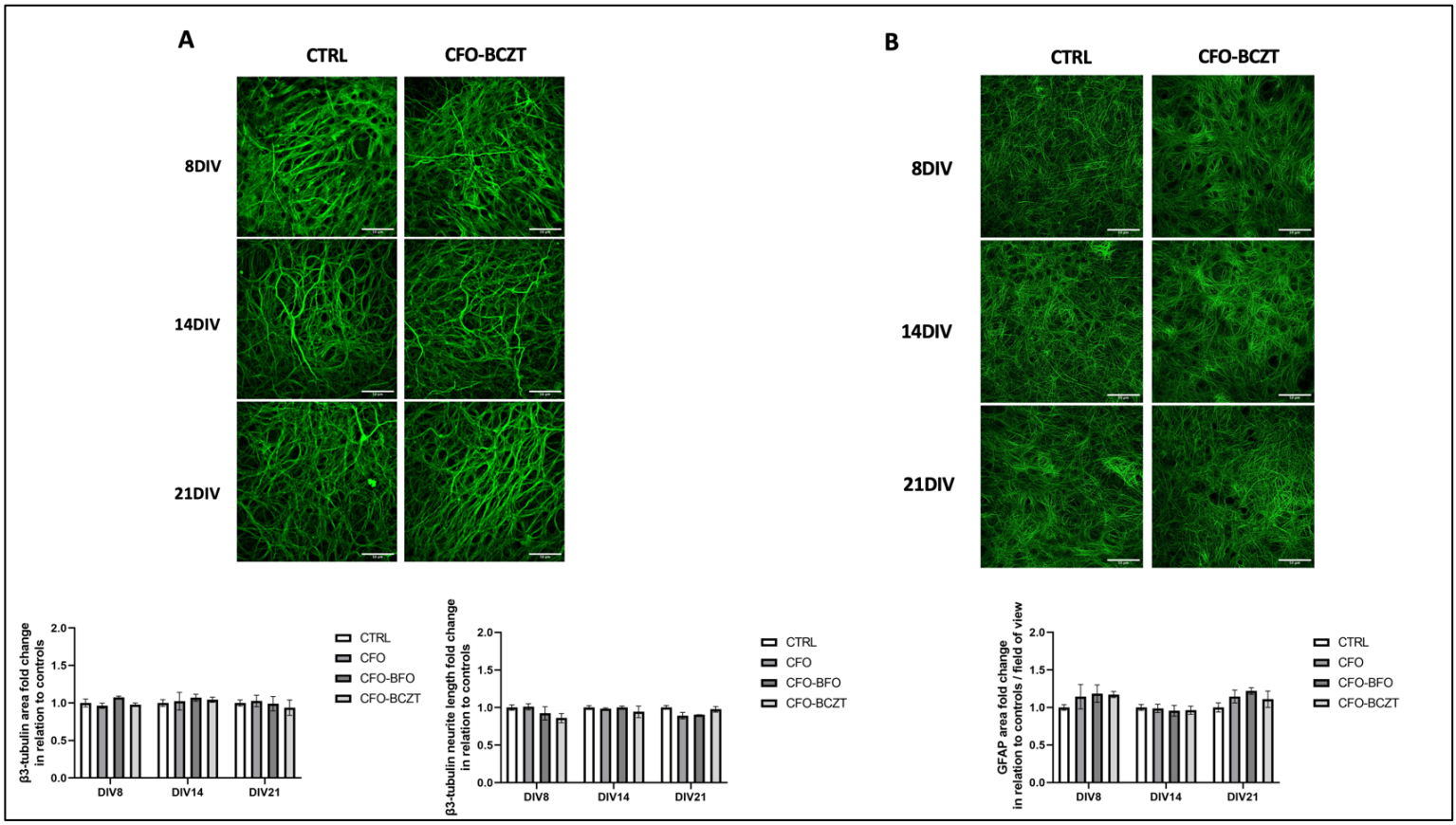
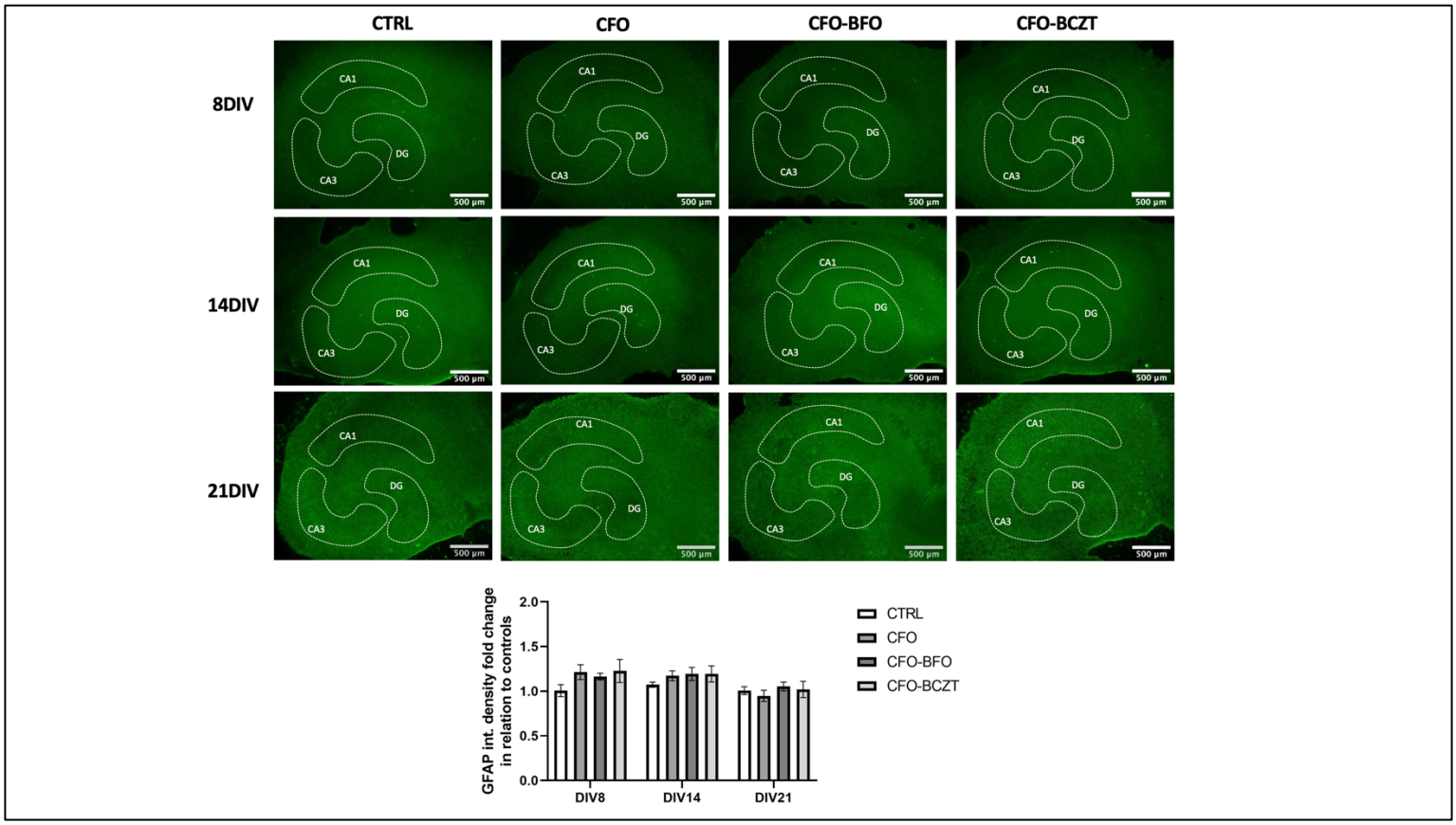
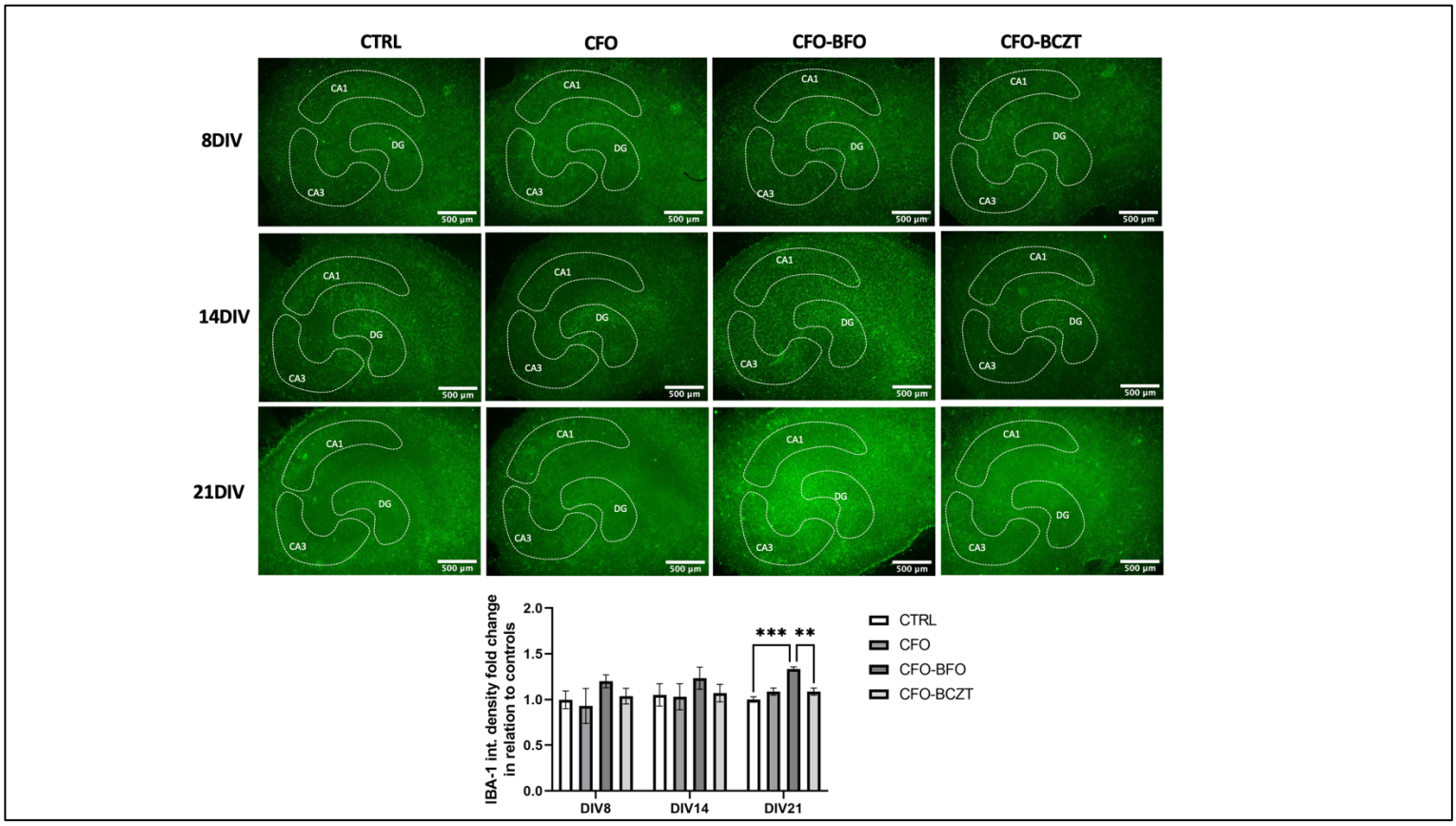


Figure 8. *CFO-BCZT NPs did not cause morphological alterations of β3-tubulin in Organotypic Hippocampal Slice cultures at 8DIV, 14DIV and 21DIV. (A) Representative β3-tubulin immunostaining of neurons under control conditions (CTRL; untreated cells) and CFO-BCZT NPs. Bottom charts representing β3-tubulin morphology quantification showing non-significant differences in the area as well as the total neurite length per field of view in all the treatment groups compared to controls. (B) Representative GFAP immunostaining of organotypic hippocampal slices under control conditions (CTRL; untreated slices), and CFO-BCZT NPs. Bottom chart represents GFAP area quantification showing non-significant differences in GFAP area in all treatment groups compared to controls. Data are expressed as the β3-tubulin area, total β3-tubulin neurite length fold changes and GFAP area fold change per field of view from the value of control slices and presented as mean ± standard error of the mean (SEM) (n = 3 independent experiments: 4–6 slices analyzed per group/experiment). Tukey's test after one–way analysis of variance (ANOVA) was used for statistical analysis.*



Supplementary Figure 3. *CFO@BCZT NPs did not cause astrogliosis in organotypic hippocampal slices at 8DIV, 14DIV and 21DIV. Representative GFAP immunostaining of organotypic hippocampal slices under control conditions (CTRL; untreated slices), CFO, CFO@BFO and CFO@BCZT NPs. Bottom chart represents the quantitative analysis of GFAP fluorescence intensity. Data are expressed as GFAP fluorescence intensity fold change from the value of control slices and presented as means ± standard error of the mean (SEM) (n = 3 independent experiments; 4–6 slices analyzed per group/experiment). Tukey's test after one–way analysis of variance (ANOVA) was used for statistical analysis.*



Supplementary Figure 4. *CFO-BCZT NPs did not cause microglia activation in organotypic hippocampal slices at 8DIV, 14DIV and 21DIV. Representative Iba-1 immunostaining of organotypic hippocampal slices under control conditions (CTRL; untreated slices), CFO, CFO-BFO and CFO-BCZT NPs. Bottom chart represents the quantitative analysis of Iba-1 fluorescence intensity at 8DIV, 14 DIV and 21DIV. Data are expressed as Iba-1 fluorescence intensity fold change from the value of control slices and presented as means ± standard error of the mean (SEM) (n = 3 independent experiments; 4–6 slices analyzed per group/experiment). Tukey's test after one–way analysis of variance (ANOVA) was used for statistical analysis. **p < 0.01; ***p < 0.001.*

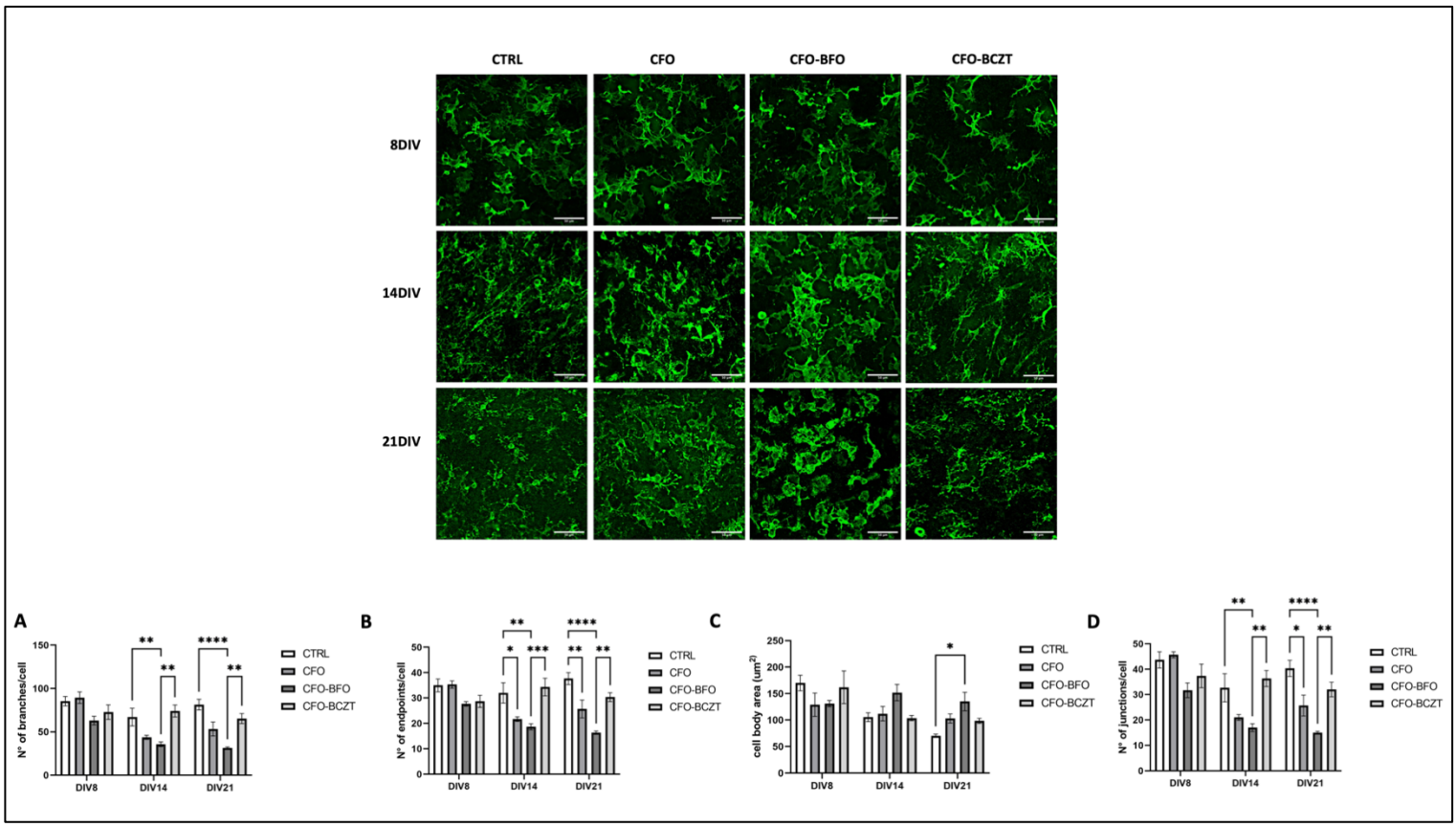


Figure 9. *CFO-BCZT NPs did not cause microglia activation and morphological alterations in organotypic hippocampal slice cultures. Representative Iba-1 staining of microglial cells under control conditions (CTRL; untreated cells), CFO, CFO-BFO and CFO-BCZT NPs. Bottom charts representing microglia morphology quantification showing significant differences in the number of branches at 14DIV and 21DIV, cell body area, as well as the number of endpoints and junctions compared to controls. Data are presented as means ± standard error of the mean (SEM) (n = 3 independent experiments; 5–8 cells analyzed per group/experiment). Tukey's test after one–way analysis of variance (ANOVA) was used for statistical analysis. *p < 0.05; **p < 0.01; ***p < 0.001; **** p <0.0009.*

3.4 CFO-BCZT NPS MOTION DOES NOT IMPACT BRAIN TISSUE VIABILITY AND INTEGRITY

The impact of CFO-BCZT NPs motion was assessed in organotypic hippocampal slice cultures. MENPs penetration in the brain tissue imposed by the magnetic field was confirmed by the identification of CFO-BCZT NPs in transversal cryosections of the brain slices analyzed by TEM and confocal microscopy. After staining with Prussian blue and fast nuclear red, which stain iron and nuclei respectively, we identified the presence of CFO-BCZT NPs in depth in the brain tissue. The application of the magnetic plate at the bottom of the inserts for 30 min led to a penetration of around 40 µm from the top of each slice (**Fig.10A**). Complementarily, confocal imaging and 3D reconstruction with Imaris software (**Fig.10B**) confirmed the presence of MENPs in deep areas compared to control cultures.

Such findings are also confirmed by TEM images, where it was also possible to observe the preservation of cellular compartments such as the cytoskeleton, synapses, and mitochondria in the surrounding of MENPs aggregates, regardless of their motion through the tissue (**Fig.10C and D**).

To further determine the impact of motion on the brain tissue, we performed a PI assay after 24h, followed by the analysis of tissue integrity by β3-tubulin immunofluorescence. In **Fig.11A** we show that motion of CFO-BCZT NPs did not hamper tissue viability 24h post-treatment. The quantification of the number of β3-tubulin junctions and processes' length showed non-significant differences when comparing control slices and slices where the magnetic field was applied (**Fig.11B**) indicating that the MENPs movement did not compromise neuronal integrity.

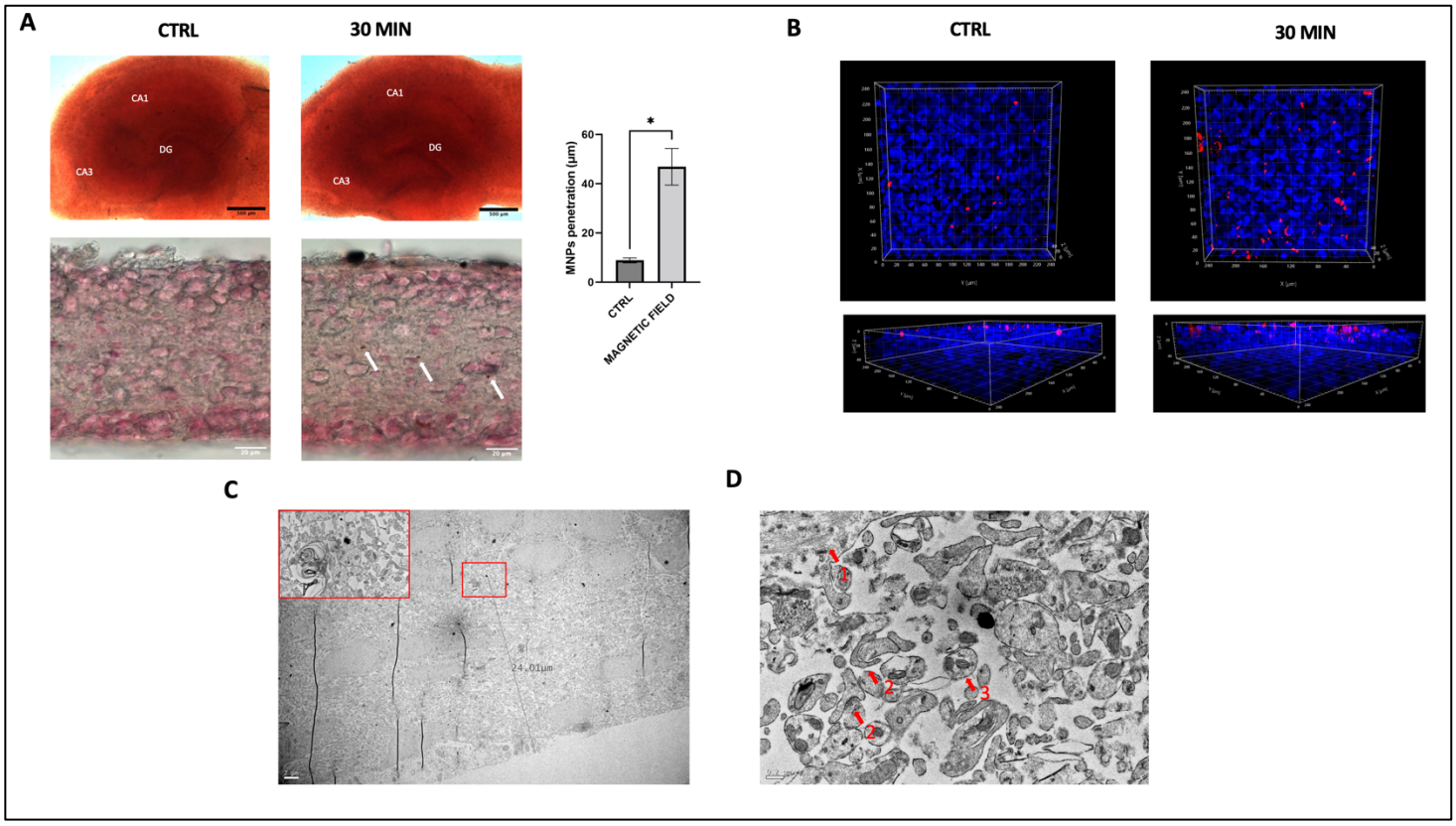


Figure 10. *CFO-BCZT NPs can penetrate in the brain tissue after application of a magnetic field for 30 minutes using the magnetic plate. (A) Representative Prussian blue/ fast nuclear red-stained organotypic hippocampal slices under control conditions (CTRL slices treated with CFO-BCZT), and after 30 min of the application of the magnetic field with the magnetic plate (MAGNETIC FIELD). Bottom images showing stained 20 µm organotypic hippocampal cryosections showing penetration of CFO-BCZT NPs in the tissue. White arrows indicate CFO-BCZT NPs. Right chart represents the quantification of CFO-BCZT NPs penetration in both groups. (B) Representative 3D hoechst-stained organotypic hippocampal slices merged with brightfield showing penetration of CFO-BCZT NPs (in red) through the tissue. (C) Representative TEM image showing penetration of CFO-BCZT NPs into the brain tissue. Red square representing higher magnification ROI showing the NPs. (D) TEM image of brain section showing integrity of the brain tissue surrounding a CFO-BCZT NPs aggregate. Red arrows indicate (1) cell cytoskeleton, (2) synapses and (3) mitochondria. Data are expressed as distance of NPs from the surface of the slice in µm and presented as means ± standard error of the mean (SEM) (n = 3 independent experiments; 3 slices analyzed per group/experiment). Tukey's test after one–way analysis of variance (ANOVA) was used for statistical analysis. *$p < 0.05$.*

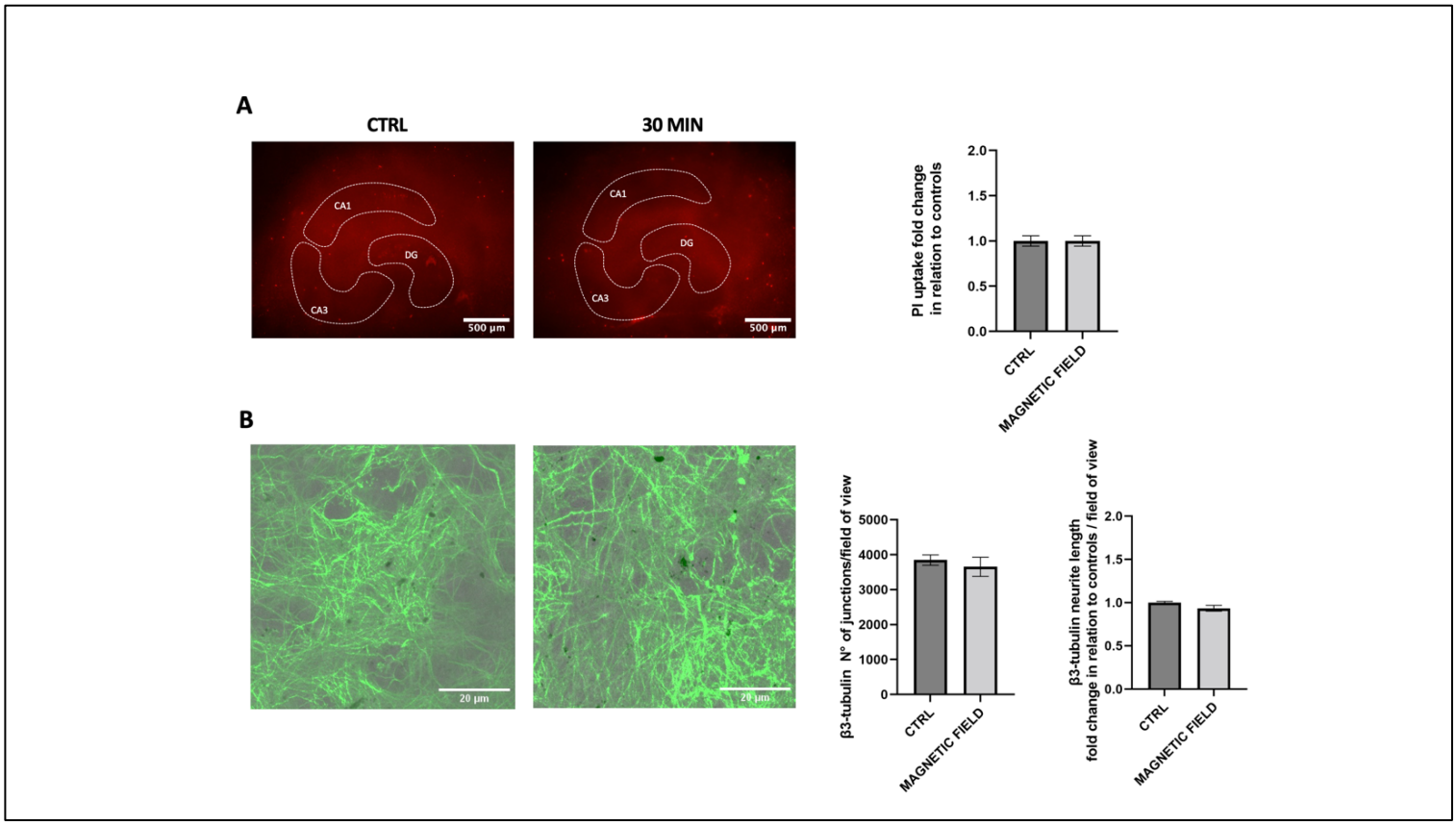


Figure 11. *CFO-BCZT NPs penetration into the brain tissue did not hamper viability and tissue integrity after 24 h of contact. (A) Representative PI staining of organotypic hippocampal slices under control conditions (CTRL; slices treated with CFO-BCZT), and after 30 min of the application of the magnetic field with the magnetic plate, followed by 24 h in normal conditions. Right chart represents the quantitative analysis of PI fluorescence intensity after 24 h. (B) Representative B3tubuline-stained organotypic hippocampal slices merged with brightfield showing that penetration of CFO-BCZT NPs does not hamper tissue integrity after 24 h. Right charts represent the quantifications of the number of β3-tubulin junctions and the total β3-tubulin neurite length fold change. Data are expressed as distance of NPs from the surface of the slice in µm, number of β3-tubulin junctions per field and total β3-tubulin neurite length fold change per field from the value of control slice and presented as means ± standard error of the mean (SEM) (n = 3 independent experiments; 3 slices analyzed per group/experiment). Tukey's test after one–way analysis of variance (ANOVA) was used for statistical analysis. *p < 0.05.*

3.5 UNDER A MAGNETIC FIELD CFO-BCZT NPS INDUCE CELLULAR DIFFERENTIATION IN SH-SY5Y CELLS

Preliminary in vitro experiments on the stimulation of the SH-SY5Y neuronal cell line were conducted to assess the impact of electrical stimulation on the induction of neural differentiation by the proposed CFO-BCZT NPs. Cells were incubated with CFO-BCZT and CFO-BFO NPs at a concentration of 10 µg/mL and placed inside the incubator under constant magnetic field (4.5A) for 24 h, followed by 24 h in normal conditions. High-throughput image analysis and quantification revealed that magnetic stimulation of both core-shell MENPs led to an increase in neurite extension, number of endpoints and a decrease in cell growth compared to control cultures. These data indicate that 24 h of magnetic field is enough to trigger the electrical stimulation of cells by both CFO-BCZT and CFO-BFO NPs, leading to a small change toward a differentiated phenotype (**Fig.12**).

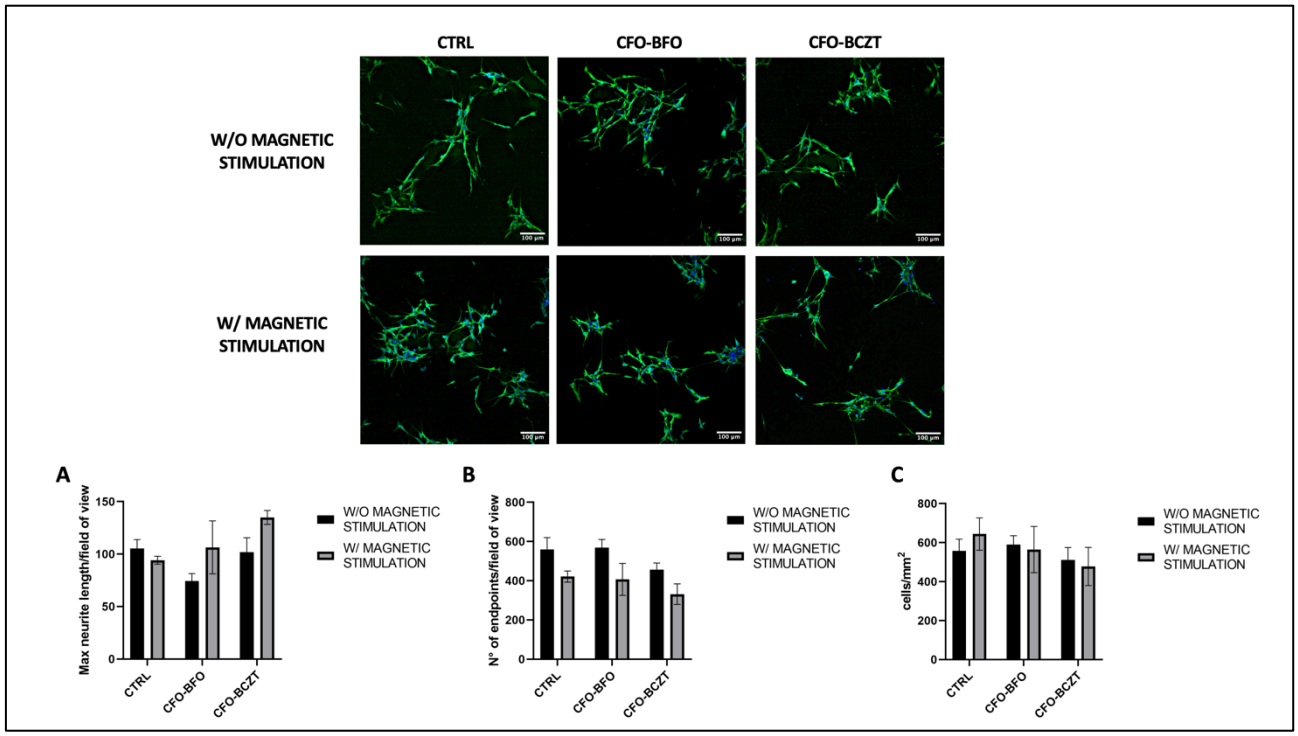


***Figure 12**. CFO-BCZT NPs and CFO-BFO NPs induce neural differentiation on SH-SY5Y cells after magnetic stimulation (4.5A) for 24h. Representative β3-tubulin and Hoechst staining of SH-SY5Y cells under control conditions (CTRL), CFO-BFO and CFO-BCZT NPs at 10 µg/mL. Bottom charts represent the quantifications of (A) the maximum β3-tubulin neurite length per field of view, (B) the number of endpoints per field of view and (C) the number of Hoechst positive cells per mm2.*

Data are expressed as maximum neurite length in µm, number of endpoints per field of view and number of Hoechst positive cells per mm2 and presented as means ± standard deviation (n = 1 independent experiment; 30 images analyzed per group/experiment).

4. DISCUSSION

The potential of MENPs as smart nanodevices for drug delivery or neurostimulation is undisputed (Guduru et al., 2015; Rodzinski et al., 2016). The evaluation of safety and biocompatibility of newly designed MENPs is paramount to enable the application of new technologies such as DBS and promote the clinical progress for new treatment strategies for neurological diseases.

In the context of the central nervous system, potential toxicity and harmful biological effects are a matter of further concern due to the very sensitive and responsive nature of these tissues. However, despite the advances in biocompatibility and promising results from recent in vivo works, there is still a long way to go before their application to human patients.

In this study, we aimed at developing and at evaluating the biocompatibility of CFO-BCZT NPs as promising multiferroic core-shell MENPs for future neural applications. We have proposed BCZT because it has been reported to display excellent biocompatibility, a higher piezoelectric coefficient than barium titanate ceramics, alongside with BCZT proven suitability for neurosciences (Scarisoreanu et al., 2017; Poon et al., 2020; Janusas et al., 2021).

We have successfully synthesized functional multiferroic core-shell cobalt ferrite (CFO) NPs coated with calcium/zirconium-doped barium titanate (CFO-BCZT) and bismuth ferrite (CFO-BFO) as a reference coating with hydrothermal and sol-gel processes. X-ray diffraction studies confirmed cubic Fd-3m space group of CFO core particles, hexagonal R3c BFO shell, and tetragonal P4mm BCZT shell. HAADF-STEM and EDX images confirmed the core-shell structure of both CFO-BFO CFO-BCZT NPs, a size of 35 ± 8 nm of CFO core, the thickness of BFO shell around 2 ± 1 nm, and thin and thick BCZT shells around 2 ± 1 nm and 15 ± 5 respectively. PFM has shown that both MENPs display magnetoelectric coupling effect. Subsequently, we evaluated their biocompatibility in vitro and ex vivo.

With our in vitro studies, employing primary cortical neurons, microglia and astrocytes, we report that the CFO-BCZT NPs display better biocompatibility over CFO-BFO NPs and uncoated CFO NPs at high concentrations, with the former having no significant impact on neural cell viability and glial cell activation. While we show that all tested MENPs did not cause significant cell death in primary

cultures of astrocytes and cortical neurons, at the two tested concentrations, the NPs behavior was different when in contact with microglia. For these cells, we observed that the treatment for 24 h with CFO-BFO NPs at the highest concentration caused a significant impairment in microglial cell viability compared to controls. Interestingly, such effects are not associated with neither an increase in NO and ROS production nor with MENPs internalization. The internalization studies showed in fact that uncoated CFO NPs are more internalized than both CFO-BCZT and CFO-BFO NPs, as both coatings make the microglia less prone to phagocytic activity. However, BFO coating caused significant impairment in microglial viability at high concentrations regardless of ROS and NO production, but this may be probably due to electrostatic interactions with the cell membranes (Staedler et al., 2015). For the CFO NPs we have observed microglial shrinkage and detachment at high concentrations after 24h of treatment, as a result of the enhanced cell engulfment and intrinsic toxicity of CFO. Such toxicity may be mitigated by the presence of the BCZT shell, possibly as a consequence of the reduction in the cobalt ions leaching out from the CFO core (Horev-Azaria et al., 2013).

Response of the brain tissue was evaluated in the ex vivo rat organotypic hippocampal slice cultures, focusing on the CA1, CA3 and DG sub-regions, as the most susceptible to cellular responses. Our results, which are commensurate with the in vitro studies, showed that, while non-significant effects were observed in neurons and astrocytes, Iba-1 fluorescence intensity was increased in slices treated with CFO-BFO NPs at 21 DIV compared to uncoated CFO NPs, CFO-BCZT NPs and control cultures, as result of microglia activation upon material contact. Moreover, the analysis of microglia morphology revealed significant alterations also from 14DIV in slices treated with uncoated CFO and, to a greater extent, with CFO-BFO NPs. Interestingly, no negative or adverse effects were observed with CFO-BCZT NPs in all the time points investigated.

Our results on BFO effects at high concentrations are in compliance with other recent in vitro studies that investigated the toxic effects of bismuth-based materials. Song and co-workers reported dose-dependent neurotoxicity in PC12 pheochromocytoma rat cell lines exposed to high levels of BFO NPs. Such effects were mainly caused by the interaction of BFO NPs with the cell membranes, resulting in a decrease in cell adhesion and proliferation (Song et al., 2014). Gao and colleagues reported a dose-dependent decrease in viability in human skin-derived cell lines treated with bismuth oxybromide NPs, namely damaging cell membrane integrity and induction of apoptosis (Gao et al., 2015). Similarly, Staedler and colleagues reported moderate cytotoxicity of human adenocarcinoma (A549), lung squamous carcinoma (NCI-H520) and, to a greater extent, acute monocytic leukemia (THP-1) cell lines exposed to BFO NPs for 72h. Interestingly, such cytotoxicity was less pronounced when the NPs were coated with polyethylene glycol, suggesting that BFO NPs interfere with the

physiology of the cell membrane (Staedler et al., 2015). Moreover, several clinical studies reported cases of bismuth intoxication in patients undergoing prolonged exposure to high levels of bismuth-based drugs (Akinci et al., 2015; Fowler et al., 2015). Two cases of bismuth neurotoxicity were reported in patients undergoing treatment with bismuth iodoform paraffin paste as an antiseptic after surgical operation in the jaws. The patients presented confusion, high levels of bismuth concentration in the blood, and one of them experienced also depression and suicidal thoughts (Atwal and Cousin, 2016). Borbinha and colleagues described a case of bismuth neurotoxicity in a patient undergoing bismuth subsalicylate supplementation for several years to treat gastroenterological complaints. The patient presented abnormal behavior, confusion, encephalopathy and myoclonus, accompanied by high levels of bismuth in urine, serum, and cerebrospinal fluid (Borbinha et al., 2019). Similar neurotoxic effects have been described in a woman after chronic ingestion bismuth subgallate to treat gastrointestinal syndrome. This patient presented progressive encephalopathy, aphasia, myoclonus and gait instability (Sampognaro et al., 2017).

Here, further studies on the impact of MENPs motion through the brain tissue were carried out in organotypic hippocampal slice cultures with CFO-BCZT NPs. We progressed with the experiments only with CFO-BCZT NPs due to their superior biological performance and because the magnetic attraction effect would mainly depend on the CFO core regardless of the type of shell. We successfully induced CFO-BCZT NPs motion through the tissue using a magnetic plate placed on the bottom of the well plate for 30 min. Additionally, we showed that such penetration from the top of the slices inwards was harmless and did not cause any effects in terms of integrity of tissue architecture or cell death after 24 h. Due to the lack of such studies in the literature, we have shown throughout this work the versatility of organotypic cultures as an excellent platform to investigate the effects of motion of the various core-shell MENPs developed, as they offer the possibility to dissect their impact at the cellular level over extended periods of time in a living 3D tissue that closely mimics the in vivo scenario.

Preliminary in vitro experiments on stimulation of SH-SY5Y cells were carried out with CFO-BCZT and CFO-BFO NPs at 10 μg/mL. This is an ideal concentration to elicit neuronal response upon electrical stimulation, taking into consideration previously reported in vitro studies (Marino et al., 2015; Kozielski et al., 2022; Zhang et al., 2022), as well as NP density at the interface with the cells. We show that under magnetic stimulation for 24h CFO-BCZT NPs can induce higher neurite extension as a result of phenotype change toward a differentiated state. Although not investigated, such effects could be explained by the generation of action potentials by membrane depolarization, enhanced expression of neuron-specific proteins, neurotrophic factors release and enhancement of

autophagy signaling in response to the localized electric fields at the nanoscale level produced by CFO-BCZT NPs under magnetic stimulation (He et al., 2021; Zhang et al., 2021, 2022b).

In conclusion, here we demonstrate the ability of the proposed BCZT coating to confer magnetoelectric coupling effect to CFO NPs and to sustain better biocompatibility compared to BFO in vitro and ex vivo. We have also shown the capability of CFO-BCZT NPs to be guided through the brain by external magnetic field application in a safe way without compromising tissue viability and neuronal integrity, and to evoke wireless neuronal electrical stimulation resulting in the promotion of cell differentiation and neurite outgrowth. In light of these observations, our findings confirmed the favorable potential of BCZT for the design of biocompatible multiferroic core-shell magnetoelectric NPs for applications in the central nervous tissue. Further, these indicate that the proposed approach can lead the field toward the direction of the successful translation of MENPs for the treatment of diverse neurological conditions.

5. ACKNOWLEDGMENTS

The authors acknowledge the funding from the European Union's Horizon 2020 Research and Innovation Programme under the Marie Skłodowska-Curie grant agreement No. 764977, in the framework of the mCBEEs project (Advanced integrative solutions to corrosion problems beyond micro-scale: toward long-term durability of miniaturized biomedical, electronic, and energy systems).

DK, TQ, XC and SP acknowledge the funding from the European Research Council Consolidator Grant "Highly Integrated Nanoscale Robots for Targeted Delivery to the Central Nervous System" (HINBOTS) under the grant no. 771565.

The authors thank the support of the i3S Scientific Platforms Bioimaging, Advanced Light Microscopy (ALM), Histology and Electron Microscopy (HEMS), members of the national infrastructure PPBI–Portuguese Platform of Bioimaging (PPBI-POCI-01-0145-FEDER-022122), as well as the i3S Scientific Platform BioSciences Screening, member of the PT-OPENSCREEN (NORTE-01-0145-FEDER-085468) and PPBI (PPBI-POCI-01-0145-FEDER-022122). The assistance of Ana Rita Malheiro and Rui Fernandes, who conducted the TEM analysis of the brain tissue is acknowledged.

SS acknowledges FCT for her contract under the Norma Transitória (DL57/2016/CP/CP1360/CT0013).

REFERENCES

Akinci, E., Köylü, R., Yortanli, M., Gümüş, H., Köylü, Ö., Altintepe, L., et al. (2015). Acute Bismuth Intoxication: Acute Renal Failure, Tonsillar Ulceration and Posterior Reversible Encephalopathy Syndrome. *Hong Kong Journal of Emergency Medicine* 22, 121–125. doi: 10.1177/102490791502200208.

Amiri, S., and Shokrollahi, H. (2013). The role of cobalt ferrite magnetic nanoparticles in medical science. *Materials Science and Engineering: C* 33, 1–8. doi: 10.1016/j.msec.2012.09.003.

Attal, N., Poindessous-Jazat, F., de Chauvigny, E., Quesada, C., Mhalla, A., Ayache, S. S., et al. (2021). Repetitive transcranial magnetic stimulation for neuropathic pain: a randomized multicentre sham-controlled trial. *Brain* 144, 3328–3339. doi: 10.1093/brain/awab208.

Atwal, A., and Cousin, G. C. S. (2016). Bismuth toxicity in patients treated with bismuth iodoform paraffin packs. *British Journal of Oral and Maxillofacial Surgery* 54, 111–112. doi: 10.1016/j.bjoms.2015.09.009.

Borbinha, C., Serrazina, F., Salavisa, M., and Viana-Baptista, M. (2019). Bismuth encephalopathy- a rare complication of long-standing use of bismuth subsalicylate. *BMC Neurol* 19, 212. doi: 10.1186/s12883-019-1437-9.

Bozorth, R. M., Tilden, E. F., and Williams, A. J. (1955). Anisotropy and Magnetostriction of Some Ferrites. *Physical Review* 99, 1788–1798. doi: 10.1103/PhysRev.99.1788.

Chen, X.-Z., Liu, J.-H., Dong, M., Müller, L., Chatzipirpiridis, G., Hu, C., et al. (2019). Magnetically driven piezoelectric soft microswimmers for neuron-like cell delivery and neuronal differentiation. *Mater Horiz* 6, 1512–1516. doi: 10.1039/C9MH00279K

Cho, N., Moon, E. H., Kim, H. W., Hong, J., Beutler, J. A., and Sung, S. H. (2016). Inhibition of Nitric Oxide Production in BV2 Microglial Cells by Triterpenes from Tetrapanax papyriferus. *Molecules* 21. doi: 10.3390/molecules21040459.

Deng, Z.-D., Lisanby, S. H., and Peterchev, A. v (2014). Coil design considerations for deep transcranial magnetic stimulation. *Clinical Neurophysiology* 125, 1202–1212. doi: 10.1016/j.clinph.2013.11.038.

Dong, M., Wang, X., Chen, X., Mushtaq, F., Deng, S., Zhu, C., et al. (2020). 3D-printed soft magnetoelectric microswimmers for delivery and differentiation of neuron-like cells. *Adv Funct Mater* 30, 1910323. doi: 10.1002/adfm.201910323

Fitzgerald, P. B. (2021). Targeting repetitive transcranial magnetic stimulation in depression: do we really know what we are stimulating and how best to do it? *Brain Stimul* 14, 730–736. doi: 10.1016/j.brs.2021.04.018.

Fowler, B. A., Sullivan, D. W., and Sexton, M. J. (2015). "Chapter 31 - Bismuth," in *Handbook on the Toxicology of Metals (Fourth Edition)*, eds. G. F. Nordberg, B. A. Fowler, and M. Nordberg (San Diego: Academic Press), 655–666. doi: 10.1016/B978-0-444-59453-2.00031-7.

Gao, X., Wang, Y., Peng, S., Yue, B., Fan, C., Chen, W., et al. (2015). Comparative toxicities of bismuth oxybromide and titanium dioxide exposure on human skin keratinocyte cells. *Chemosphere* 135, 83–93. doi: 10.1016/j.chemosphere.2015.03.075.

Guduru, R., Liang, P., Hong, J., Rodzinski, A., Hadjikhani, A., Horstmyer, J., et al. (2015). Magnetoelectric 'spin'on stimulating the brain. *Nanomedicine* 10, 2051–2061. doi: 10.2217/nnm.15.52

Gulino, M., Duque Santos, S., and Pêgo, A. P. (2021a). Biocompatibility of Platinum Nanoparticles in Brain ex vivo Models in Physiological and Pathological Conditions. *Front Neurosci* 15. doi: 10.3389/fnins.2021.787518.

Gulino, M., Kim, D., Pané, S., Santos, S. D., and Pêgo, A. P. (2019). Tissue Response to Neural Implants: The Use of Model Systems Toward New Design Solutions of Implantable Microelectrodes. *Front Neurosci* 13, 689. doi: 10.3389/fnins.2019.00689.

Gulino, M., Santos, S. D., and Pêgo, A. P. (2021b). Biocompatibility of Platinum Nanoparticles in Brain ex vivo Models in Physiological and Pathological Conditions. *Front Neurosci* 15. doi: 10.3389/fnins.2021.787518.

He, L., Sun, Z., Li, J., Zhu, R., Niu, B., Tam, K. L., et al. (2021). Electrical stimulation at nanoscale topography boosts neural stem cell neurogenesis through the enhancement of autophagy signaling. *Biomaterials* 268, 120585.

Hojo, H., Oka, K., Shimizu, K., Yamamoto, H., Kawabe, R., and Azuma, M. (2018). Development of bismuth ferrite as a piezoelectric and multiferroic material by cobalt substitution. *Advanced Materials* 30, 1705665.

Horev-Azaria, L., Baldi, G., Beno, D., Bonacchi, D., Golla-Schindler, U., Kirkpatrick, J. C., et al. (2013). Predictive Toxicology of cobalt ferrite nanoparticles: comparative in-vitro study of different cellular models using methods of knowledge discovery from data. *Part Fibre Toxicol* 10, 32. doi: 10.1186/1743-8977-10-32.

Jahanshahi, A., Kozielski, K., Temel, Y., and Sitti, M. (2021). Wireless deep brain stimulation in freely moving mice with nonresonant powering of magnetoelectric nanoparticles. *Brain Stimulation: Basic, Translational, and Clinical Research in Neuromodulation* 14, 1742. doi: 10.1016/j.brs.2021.10.514.

Janusas, T., Urbaite, S., Palevicius, A., Nasiri, S., and Janusas, G. (2021). Biologically Compatible Lead-Free Piezoelectric Composite for Acoustophoresis Based Particle Manipulation Techniques. *Sensors* 21. doi: 10.3390/s21020483.

Kaushik, A., Rodriguez, J., Rothen, D., Bhardwaj, V., Jayant, R. D., Pattany, P., et al. (2019). MRI-Guided, Noninvasive Delivery of Magneto-Electric Drug Nanocarriers to the Brain in a Nonhuman Primate. *ACS Appl Bio Mater* 2, 4826–4836. doi: 10.1021/acsabm.9b00592.

Kim, D., Efe, I., Torlakcik, H., Terzopoulou, A., Veciana, A., Siringil, E., et al. (2022). Magnetoelectric Effect in Hydrogen Harvesting: Magnetic Field as a Trigger of Catalytic Reactions. *Advanced Materials* 34, 2110612. doi: 10.1002/adma.202110612.

Kopyl, S., Surmenev, R., Surmeneva, M., Fetisov, Y., and Kholkin, A. (2021). Magnetoelectric effect: principles and applications in biology and medicine– a review. *Mater Today Bio* 12, 100149. doi: 10.1016/j.mtbio.2021.100149.

Kozielski, K. L., Jahanshahi, A., Gilbert, H. B., Yu, Y., Erin, Ö., Francisco, D., et al. (2022). Nonresonant powering of injectable nanoelectrodes enables wireless deep brain stimulation in freely moving mice. *Sci Adv* 7, eabc4189. doi: 10.1126/sciadv.abc4189.

Kumar, A. S., Lekha, C. S. C., Vivek, S., Saravanan, V., Nandakumar, K., and Nair, S. S. (2016). Multiferroic and magnetoelectric properties of Ba0.85Ca0.15Zr0.1Ti0.9O3–CoFe2O4 core–shell nanocomposite. *J Magn Magn Mater* 418, 294–299. doi: 10.1016/j.jmmm.2016.02.065.

Lian, H., Roy, E., and Zheng, H. (2016). Protocol for primary microglial culture preparation. *Bio Protoc* 6, e1989–e1989.

Marino, A., Arai, S., Hou, Y., Sinibaldi, E., Pellegrino, M., Chang, Y.-T., et al. (2015). Piezoelectric Nanoparticle-Assisted Wireless Neuronal Stimulation. *ACS Nano* 9, 7678–7689. doi: 10.1021/acsnano.5b03162.

Mushtaq, F., Chen, X., Torlakcik, H., Steuer, C., Hoop, M., Siringil, E. C., et al. (2019a). Magnetoelectrically Driven Catalytic Degradation of Organics. *Advanced Materials* 31, 1901378. doi: 10.1002/adma.201901378.

Mushtaq, F., Torlakcik, H., Vallmajo-Martin, Q., Siringil, E. C., Zhang, J., Röhrig, C., et al. (2019b). Magnetoelectric 3D scaffolds for enhanced bone cell proliferation. *Appl Mater Today* 16, 290–300. doi: 10.1016/j.apmt.2019.06.004.

Mushtaq, F., Torlakcik, H., Vallmajo-Martin, Q., Siringil, E. C., Zhang, J., Röhrig, C., et al. (2019c). Magnetoelectric 3D scaffolds for enhanced bone cell proliferation. *Appl Mater Today* 16, 290–300.

Neubert J, Wagner S, Kiwit J, Bräuer AU, and Glumm J (2015). New findings about iron oxide nanoparticles and their different effects on murine primary brain cells. *Int J Nanomedicine* 10, 2033–2049. Available at: https://doi.org/10.2147/IJN.S74404 [Accessed August 18, 2022].

Nguyen, T., Gao, J., Wang, P., Nagesetti, A., Andrews, P., Masood, S., et al. (2021). In Vivo Wireless Brain Stimulation via Non-invasive and Targeted Delivery of Magnetoelectric Nanoparticles. *Neurotherapeutics* 18, 2091–2106. doi: 10.1007/s13311-021-01071-0.

Pardo, M., Roberts, E. R., Pimentel, K., Yildirim, Y. A., Navarrete, B., Wang, P., et al. (2021). Size-dependent intranasal administration of magnetoelectric nanoparticles for targeted brain localization. *Nanomedicine* 32, 102337. doi: 10.1016/j.nano.2020.102337.

Poon, K. K., Wurm, M. C., Evans, D. M., Einarsrud, M.-A., Lutz, R., and Glaum, J. (2020). Biocompatibility of (Ba,Ca)(Zr,Ti)O3 piezoelectric ceramics for bone replacement materials. *J Biomed Mater Res B Appl Biomater* 108, 1295–1303. doi: 10.1002/jbm.b.3477.

Praveen, P., Monaji, V., Chandrakala, E., Indla, S., Kumar, D., V, S., et al. (2018). Enhanced magnetoelectric coupling in Ti and Ce substituted lead free CFO-BCZT laminate composites. *J Alloys Compd* 750. doi: 10.1016/j.jallcom.2018.04.026.

Ramaswamy, B., Kulkarni, S. D., Villar, P. S., Smith, R. S., Eberly, C., Araneda, R. C., et al. (2015). Movement of magnetic nanoparticles in brain tissue: mechanisms and impact on normal neuronal function. *Nanomedicine* 11, 1821–1829. doi: 10.1016/j.nano.2015.06.003.

Rodzinski, A., Guduru, R., Liang, P., Hadjikhani, A., Stewart, T., Stimphil, E., et al. (2016). Targeted and controlled anticancer drug delivery and release with magnetoelectric nanoparticles. *Sci Rep* 6, 20867. doi: 10.1038/srep20867.

Sampognaro, P. J., Vo, K. T., Richie, M. B., Blanc, P. D., and Keenan, K. J. (2017). Bismuth Subgallate Toxicity in the Age of Online Supplement Use. *Neurologist* 22, 237–240. doi: 10.1097/NRL.0000000000000144.

Scarisoreanu, N. D., Craciun, F., Ion, V., Birjega, R., Bercea, A., Dinca, V., et al. (2017a). Lead-Free Piezoelectric (Ba,Ca)(Zr,Ti)O3 Thin Films for Biocompatible and Flexible Devices. *ACS Appl Mater Interfaces* 9, 266–278. doi: 10.1021/acsami.6b14774.

Shahzad, K., Mushtaq, S., Rizwan, M., Khalid, W., Atif, M., Din, F. U., et al. (2021). Field-controlled magnetoelectric core-shell CoFe2O4@BaTiO3 nanoparticles as effective drug carriers and drug release in vitro. *Materials Science and Engineering: C* 119, 111444. doi:10.1016/j.msec.2020.111444.

Song, Q., Liu, Y., Jiang, Z., Tang, M., Li, N., Wei, F., et al. (2014). The acute cytotoxicity of bismuth ferrite nanoparticles on PC12 cells. *Journal of Nanoparticle Research* 16, 2408. doi: 10.1007/s11051-014-2408-0.

Srinivasan, S. Y., Paknikar, K. M., Bodas, D., and Gajbhiye, V. (2018). Applications of cobalt ferrite nanoparticles in biomedical nanotechnology. *Nanomedicine* 13, 1221–1238. doi: 10.2217/nnm-2017-0379.

Staedler, D., Passemard, S., Magouroux, T., Rogov, A., Maguire, C. M., Mohamed, B. M., et al. (2015). Cellular uptake and biocompatibility of bismuth ferrite harmonic advanced nanoparticles. *Nanomedicine* 11, 815–824. doi: 10.1016/j.nano.2014.12.018.

Stewart, T. S., Nagesetti, A., Guduru, R., Liang, P., Stimphil, E., Hadjikhani, A., et al. (2018). Magnetoelectric nanoparticles for delivery of antitumor peptides into glioblastoma cells by magnetic fields. *Nanomedicine* 13, 423–438. doi: 10.2217/nnm-2017-0300.

Venkata Siva, K., Sudersan, S., and Arockiarajan, A. (2020). Bipolar magnetostriction in CoFe2O4: Effect of sintering, measurement temperature, and prestress. *J Appl Phys* 128, 103904. doi: 10.1063/5.0021796.

Zhang, E., Abdel-Mottaleb, M., Liang, P., Navarrete, B., Yildirim, Y. A., Campos, M. A., et al. (2022). Magnetic-field-synchronized wireless modulation of neural activity by magnetoelectric nanoparticles. *Brain Stimul* 15, 1451–1462. doi: 10.1016/j.brs.2022.10.004

Zhang, Y., Chen, S., Xiao, Z., Liu, X., Wu, C., Wu, K., et al. (2021). Magnetoelectric nanoparticles incorporated biomimetic matrix for wireless electrical stimulation and nerve regeneration. *Adv Healthc Mater* 10, 2100695. doi: 10.1002/adhm.202100695.

CHAPTER 5

CONCLUSIONS AND FUTURE DIRECTIONS

In recent years, we assisted in the explosive growth of bioengineering and material sciences fields, complemented by a unique development of new technologies for a multitude of biomedical applications. This technological progress has led to an unprecedented evolution of the neurostimulation therapy field, and this is confirmed by the growth of its global market, which is expected to reach 8.7 billion dollars in 2028 (globenewswire.com; September 27, 2022, 05:17 ET; source: Vantage Market Research). DBS electrodes are the real key to the success reached in the clinics in terms of treatment efficacy and treatment options for a variety of neurologic and neuropsychiatric dysfunctions. At the beginning of their application in the clinics, their efficacy was counteracted by the invasiveness of the surgical procedure with frequent side effects to the patients as well as the poor durability of the material itself. What emerged was that the electrode should have not only better electrical performance but also better biocompatibility for long-term applications. This has led to the need for a multidisciplinary approach to research, where it is required the collaborative work of clinicians, bioengineers and material scientists to surmount these limitations. Nowadays, the new generation of microelectrodes has dramatically improved. The size and stiffness were reduced to minimize nervous tissue response while keeping the ability to deliver electrical impulses.

New approaches involving the use of softer materials, CPs, CHs, CNTs, biocompatible and bioactive coatings as well as minimally invasive strategies have been proposed to design microelectrodes with superior electrochemical and biological performance for their translation for clinical use.

The challenges that still must be solved reside at the micro and nanoscale, namely at the tissue-electrode interface. It is not completely clear how the process of nervous tissue response and glial scar formation to foreign materials works. The sequence of physical and biochemical events and the role of the various cell types must be investigated in the preclinical phase to develop materials and coatings that can modulate tissue response while promoting neuronal communication.

This Ph.D. thesis highlights the use of consistent biological models with increased complexity and reproducibility as an advantageous tool for the testing of an increasing number of new materials and coatings for microelectrode design. This aspect acquires much more significance when considering that in vivo animal studies are not suitable for high throughput material testing due to ethical constraints and costs. In this context, we proposed brain organotypic cultures as the best biological model with the compromise to provide high complexity and reproducibility, while with a reduced need for animals.

Brain organotypic cultures have been widely employed as excellent 3D platforms for the study of the pathophysiology of neurological diseases and the screening of new drugs. This model presents a great number of advantages over traditional 2D in vitro biological models such as the preservation of the 3D tissue architecture of the native tissue and the possibility to mimic the hallmark of disease by external treatment. However, very few works have employed organotypic cultures to assess the biocompatibility and performance of materials for microelectrode fabrication and the opportunity to study molecular interactions occurring in the immediate vicinity of the tissue-material interface.

In our studies, these cultures allowed us to shed light on the impact of PtNPs, a material of increasing interest for biomedicine, on the viability and inflammatory status of neural tissue in the acute phase of the response. Moreover, we had the possibility to assess their impact under physiological and neuronal excitotoxic conditions induced by kainic acid, a potent neurodegenerative drug employed to induce epileptic seizures on in vivo animal models and to recapitulate an epileptic environment in vitro and ex vivo. We found that, while the NPs did not compromise cell viability, they induced an inflammatory response activating microglia. Moreover, we showed that such an effect was not exacerbated in the induced pathological conditions. This study corroborates previous observations on the key role of microglia in mediating innate and adaptive responses during CNS injury, inflammation and disease. We believe that this study has great relevance in the view of the need to understand the biochemical and material-related reactions at the microscale responsible for device failure during clinical applications. Fully metal microelectrodes or electrodeposited coatings can suffer alteration once implanted in the tissue due to the presence of abiotic-biotic reactions that could lead to their degradation and release of metal NPs at the site of implantation. Therefore, the selected study design can provide reliable information that can help the community to better understand the impact of Pt on the tissues and further contribute to the already promising potential of Pt for various biomedical applications, with special relevance in neurosciences. Thanks to the possibility to maintain organotypic cultures for extended periods – up to 2 months - further studies can be conducted to evaluate the long-term tissue response to Pt before proceeding to in vivo studies.

With our studies, we also showed the versatility of organotypic cultures, especially for the assessment of materials in the form of NPs. We in fact described a simple method to put in contact NPs with the brain tissue in a non-invasive way using microinjection tools under controlled and reproducible conditions. This is very important because it allowed us to evaluate the impact of materials without affecting the results by potential damage caused by implantation, keeping the integrity of the tissue.

Then, we conducted in vitro biocompatibility studies of novel multiferroic core-shell CFO-BCZT NPs, using uncoated CFO and CFO-BFO NPs for comparison, on primary cultures of neurons, astrocytes and microglia. We evaluated the cellular responses through cytotoxicity assays, microscopy analysis and cellular uptake, showing that astrocytes and neuronal viability was not affected after MNPs exposure, while primary microglia viability was compromised by CFO-BFO NPs at the highest concentration tested (100 μg/mL) after 24h of contact.

We also employed these organotypic cultures to assess the impact of CFO-BCZT NPs, uncoated CFO and CFO-BFO NPs in the same set of experiments, by taking advantage of the possibility to obtain several tissue cultures from a single animal. These experiments, whose results were in accordance with previous in vitro experiments, allowed us to show the superior biocompatibility of BCZT over BFO coating in a more complex biological model and the suitability of CFO-BCZT NPs for wireless-controlled motion, without compromising tissue viability and structural integrity. Our preliminary in vitro experiments also confirmed their potential on inducing neurite outgrowth and cell differentiation under magnetic stimulation. As a rising technology, a huge preclinical assessment is paramount to satisfy the minimal requirements for their application in the life science field.

As future directions, the aim is to confirm our early findings using complex ex vivo and in vivo models to better characterize their biocompatibility and suitability for DBS. As first objective, taking advantage of the possibility to produce organotypic cultures from different brain areas, we are planning to explore other pathological scenarios in which these systems are expected to be employed. One interesting avenue of research is the use of organotypic cultures as models of Parkinson's disease. These cultures can be obtained by the establishment of sagittal or coronal brain slices containing nigrostriatal projections and the induction of dopaminergic lesions through incubation with 6-hydroxydopamine (6-OHDA), a neurotoxic compound largely employed to destroy dopaminergic and noradrenergic neurons. Besides the biocompatibility study in physiological and pathological conditions, these cultures can also be employed to evaluate the potential of MNPs to induce wireless axonal growth and neuronal differentiation under magnetic stimulation.

Then, larger preclinical research employing in vivo animal models of disease will be paramount to fulfill the minimal requirements for their biological testing, to confirm the safety of MNPs motion and wireless neural stimulation before clinical trials.

Taken together, our results have shown that these novel nanomaterials hold promising potential for wireless DBS and may be ideal candidates to be proposed for realizing the transition from the

conventional use of implantable devices towards a new frontier of technologies and approaches for the clinical treatment of neurological pathologies. However, there is still a long way to go for their progression along the development pipeline. As previously reported, a large number of investigations are still required to guarantee their effective safety and durability for long-term applications. Considering this, our studies clearly show the utility of brain organotypic cultures as an excellent and reliable platform to uncover their characteristics in terms of biocompatibility, features and, more importantly, to speed up their testing at the preclinical phase. Finally, we believe that this work will be useful for scientists to demonstrate the great potential of these models for smart nanomaterials testing.